

**THE DESIGN, SYNTHESIS AND ENZYMATIC EVALUATION OF  
AMINOCYCLITOL INHIBITORS OF GLUCOCEREBROSIDASE**

By

Benjamin Tyler Adams

A Thesis submitted to

The Department of Chemistry

Faculty of Science and Environmental Studies

Lakehead University

In partial fulfillment of the requirements for the degree of

Master of Science

August 2013

© Benjamin Tyler Adams, 2013

## **Abstract**

Gaucher disease, the most common lysosomal storage disorder, is caused by mutations in the GBA gene which codes for the enzyme glucocerebrosidase (GCCase) resulting in its deficiency. GCCase deficiency results in the accumulation of its substrate glucosylceramide (GlcCer) within the lysosomes leading to various severities of hepatosplenomegaly, bone disease and neurodegeneration. For most forms of Gaucher disease, the mutations in the GBA gene cause the enzyme to misfold but retain catalytic activity. However, the misfolded mutant enzyme is recognized and degraded by the endoplasmic reticulum-associated degradation (ERAD) pathway prior to delivery into the lysosome. Symptoms begin to show in patients when the function of the defective enzyme drops below 10-20% residual enzyme activity.

There are currently three therapeutic approaches to treat Gaucher disease: enzyme replacement therapy (ERT), substrate reduction therapy (SRT), and a relatively recent addition, enzyme enhancement therapy (EET) through the use of pharmacological chaperones. Many pharmacological chaperones are competitive inhibitors that are capable of enhancing lysosomal GCCase activity by stabilizing the folded conformation of GCCase enabling it to bypass the ERAD pathway. Once the mutant enzyme enters the lysosome, high levels of GlcCer can outcompete the competitive inhibitor binding to the enzyme, thus partially restoring the hydrolytic pathway.

For this thesis, a series of alkylated aminocyclitol derivatives have been synthesized and evaluated as competitive inhibitors of GCCase with the intent of discovering specific and efficient pharmacological chaperones for Gaucher disease. Importantly, we have discovered that N,O-alkylated inosamines are potent inhibitors of GCCase and therefore are lead compounds as a potential new EET for the treatment of Gaucher Disease.

Based on the potency of the alkylated inosamines as reversible inhibitors, we designed and synthesized several alkylated conduritol aziridine inhibitors to be used as mechanism-based inactivators of GCCase. All three aziridine compounds synthesized were potent inhibitors of GCCase with  $k_i/K_i$  values ranging from 3.837 to 3674  $\text{mM}^{-1}\text{min}^{-1}$ . For comparison purposes, our most potent inhibitor is 37 times more effective than the best published inhibitor of GCCase. In addition, the alkylated aziridines were shown to be cell permeable and effective at inhibiting GCCase inside of living HeLa cervical cancer cells, thus demonstrating their enormous potential as activity based probes, GCCase labeling agents or potential molecular imaging agents for assessing ERT.

## Table of Contents

<b>Abstract</b> .....	<b>ii</b>
<b>List of Tables</b> .....	<b>ix</b>
<b>List of Figures</b> .....	<b>ix</b>
<b>List of Schemes</b> .....	<b>xi</b>
<b>List of Abbreviations</b> .....	<b>xii</b>
<b>Acknowledgments</b> .....	<b>xvi</b>
<b>Chapter 1: General Introduction</b> .....	<b>1</b>
1.1 Glycosidases.....	1
1.1.1 Glycosidase Mechanisms.....	2
1.1.2 Glycosidase Inhibitors.....	7
1.2 Lysosomal Storage Diseases .....	8
1.2.1 Enzyme Replacement Therapy .....	12
1.2.2 Substrate Reduction Therapy .....	12
1.2.3 Enzyme Enhancement Therapy .....	13
1.2.4 Gaucher Disease .....	15
1.2.5 Glucocerebrosidase .....	16
1.3 Research Objectives.....	18
<b>Part A: Aminocyclitol Competitive Inhibitors of Glucocerebrosidase</b> .....	<b>19</b>
<b>1.4 Introduction</b> .....	<b>19</b>
1.4.1 Non-covalent Glycosidase Inhibitors .....	19
<b>Chapter 2: Results and Discussion</b> .....	<b>22</b>
<b>2.1 Synthesis</b> .....	<b>22</b>
2.1.1 Synthesis of Substrate 2,4-dinitrophenyl- $\beta$ -D-glucopyranoside (2,4-DNP- $\beta$ -D-glc) .....	22
2.1.2 Synthesis of N-alkylated Inhibitors .....	24
2.1.3 Synthesis of O-alkylated Inhibitors and O- and N-alkylated Inhibitors .....	29
<b>2.2 Expression and Purification of a Model <math>\beta</math>-glucosidase ABG</b> .....	<b>32</b>
<b>2.3 Enzyme Inhibition Studies with ABG and GCCase</b> .....	<b>33</b>
2.3.1 Kinetic Analysis of the Inhibition of ABG and GCCase by the N-alkylated Inhibitor 3.12 .....	34
2.3.2 Kinetic Analysis of the Inhibition of ABG and GCCase by O-alkylated Inhibitors 3.19, 3.20 and 3.21 .....	37

2.3.3 Kinetic Analysis of the Inhibition of ABG and GCase by O- and N-alkylated Inhibitors 3.29-3.33	41
2.3.4 Conclusions and Future Work.....	46
2.3.5 Special Note .....	47
<b>Part B: Mechanism-based Aziridine Glucocerebroside Inhibitors .....</b>	<b>48</b>
<b>3.1 Introduction .....</b>	<b>48</b>
3.1.1 Covalent Glycosidase Inhibitors.....	48
<b>Chapter 4: Results and Discussion.....</b>	<b>52</b>
<b>4.1 Synthesis.....</b>	<b>52</b>
4.1.1 Synthesis of Aziridine Inhibitors .....	52
<b>4.2 Kinetic Analysis of the Irreversible Inhibition of ABG and GCase by Aziridine Inhibitors 3.39-3.41 .55</b>	<b>55</b>
4.2.1 Inactivation rates of ABG with Inhibitors 3.39, 3.40 and 3.41.....	57
4.2.2 Inactivation Rates of GCase with Inhibitors 3.39, 3.40 and 3.41.....	60
4.2.3 Turnover of the Inhibitor-Enzyme Covalent Intermediate .....	64
4.2.4 Kinetic Analysis of the Inactivation of GCase in Cell Lysates by Aziridine Inhibitors 3.39-3.41	65
<b>4.3 Conclusions and Future Work .....</b>	<b>68</b>
<b>Chapter 5: Experimental.....</b>	<b>69</b>
<b>5.1 General Considerations: .....</b>	<b>69</b>
3.01 1,2,3,4,6-Penta-O-acetyl- $\beta$ -D-glucopyranose .....	69
3.02 2,3,4,6-Tetra-O-acetyl- $\beta$ -D-glucopyranose.....	70
3.03 1-(2,4-dinitrophenoxy)-2,3,4,6-Tetra-O-acetyl- $\beta$ -D-glucopyranose .....	70
3.04 2,4-dinitrophenyl- $\beta$ -D-glucopyranoside .....	71
3.05 (3aR,4R,5S,6S,7R,7aS)-2,2-dimethylhexahydrobenzo[d][1,3]dioxole-4,5,6,7-tetraol.....	71
3.07 (1R,2R,3S,4R,5R,6S)-3,4,5,6-tetrakis(benzyloxy)cyclohexane-1,2-diol.....	72
3.08 (1r,2R,3S,4r,5R,6S)-2,3,4,5,6-pentakis(benzyloxy)cyclohexanol .....	73
3.09 (1R,2S,3r,4R,5S,6s)-6-azido-1,2,3,4,5-pentabenzoyloxycyclohexane.....	74
3.10 (1s,2R,3S,4r,5R,6S)-2,3,4,5,6-pentakis(benzyloxy)cyclohexanamine .....	75
3.11 (1s,2R,3S,4r,5R,6S)-2,3,4,5,6-pentakis(benzyloxy)-N-hexylcyclohexanamine .....	75
3.12 (1R,2S,3r,4R,5S,6s)-6-(hexylamino)cyclohexane-1,2,3,4,5-pentaol .....	76
3.13 (1S,2S,3R,4R,5S,6R)-2,3,4,5-tetrakis(benzyloxy)-6-(nonyloxy)cyclohexanol.....	77
3.14 (1S,2S,3R,4R,5S,6R)-2,3,4,5-tetrakis(benzyloxy)-6-(hexyloxy)cyclohexanol .....	78

3.16 (((1S,2R,3R,4S,5R,6R)-5-azido-6-(nonyloxy)cyclohexane-1,2,3,4-tetraol)tetrakis(oxy))tetrakis(methylene))tetrabenzene .....	79
3.17 (((1S,2R,3R,4S,5R,6R)-5-azido-6-(hexyloxy)cyclohexane-1,2,3,4-tetraol)tetrakis(oxy))tetrakis(methylene))tetrabenzene .....	80
3.19 (1R,2S,3R,4S,5S,6R)-5-amino-6-(nonyloxy)cyclohexane-1,2,3,4-tetraol .....	82
3.20 (1R,2S,3R,4S,5S,6R)-5-amino-6-(hexyloxy)cyclohexane-1,2,3,4-tetraol.....	83
3.21(1R,2S,3R,4S,5S,6R)-5-amino-6-butoxycyclohexane-1,2,3,4-tetraol .....	84
3.22 (1R,2S,3R,4R,5S,6R)-2,3,4,5-tetrakis(benzyloxy)-6-(nonyloxy)cyclohexanamine.....	85
3.23 (1R,2S,3R,4R,5S,6R)-2,3,4,5-tetrakis(benzyloxy)-6-(hexyloxy)cyclohexanamine .....	86
3.24 (1R,2S,3R,4R,5S,6R)-2,3,4,5-tetrakis(benzyloxy)-6-(nonyloxy)-N-octylcyclohexanamine.....	87
3.25 (1R,2S,3R,4R,5S,6R)-2,3,4,5-tetrakis(benzyloxy)-N-hexyl-6-(nonyloxy)cyclohexanamine .....	88
3.26 (1R,2S,3R,4R,5S,6R)-2,3,4,5-tetrakis(benzyloxy)-N-butyl-6-(nonyloxy)cyclohexanamine .....	89
3.27 (1R,2S,3R,4R,5S,6R)-2,3,4,5-tetrakis(benzyloxy)-6-(hexyloxy)-N-octylcyclohexanamine .....	90
3.29 (1S,2R,3S,4R,5R,6S)-5-(nonyloxy)-6-(octylamino)cyclohexane-1,2,3,4-tetraol .....	92
3.30 (1R,2S,3R,4S,5S,6R)-5-(hexylamino)-6-(nonyloxy)cyclohexane-1,2,3,4-tetraol .....	93
3.31 (1R,2S,3R,4S,5S,6R)-5-(butylamino)-6-(nonyloxy)cyclohexane-1,2,3,4-tetraol .....	94
3.32 (1S,2R,3S,4R,5R,6S)-5-(hexyloxy)-6-(octylamino)cyclohexane-1,2,3,4-tetraol .....	95
3.33 (1R,2S,3R,4S,5S,6R)-5-(butylamino)-6-(hexyloxy)cyclohexane-1,2,3,4-tetraol .....	96
3.34 (1R,2S,3S,4R,5S,6R)-2-azido-3,4,5,6-tetrakis(benzyloxy)cyclohexyl methanesulfonate .....	97
3.35 (2S,3R,4R,5S)-2,3,4,5-tetrakis(benzyloxy)-7-azabicyclo[4.1.0]heptanes .....	98
3.36 (2S,3R,4R,5S)-2,3,4,5-tetrakis(benzyloxy)-7-octyl-7-azabicyclo[4.1.0]heptanes.....	99
3.37 (2S,3R,4R,5S)-2,3,4,5-tetrakis(benzyloxy)-7-hexyl-7-azabicyclo[4.1.0]heptane.....	100
3.38 (2S,3R,4R,5S)-2,3,4,5-tetrakis(benzyloxy)-7-butyl-7-azabicyclo[4.1.0]heptanes .....	101
3.39 (2S,3R,4R,5S)-7-octyl-7-azabicyclo[4.1.0]heptane-2,3,4,5-tetraol .....	102
3.40 (2S,3R,4R,5S)-7-hexyl-7-azabicyclo[4.1.0]heptane-2,3,4,5-tetraol .....	103
3.41 (2S,3R,4R,5S)-7-butyl-7-azabicyclo[4.1.0]heptane-2,3,4,5-tetraol.....	104
<b>Chapter 6: Enzymology.....</b>	<b>105</b>
6.1 Production of ABG .....	105
6.2 ABG and GCase Competitive Kinetics .....	106
<b>Chapter 7: NMR Spectra .....</b>	<b>108</b>
<sup>1</sup> H NMR Spectrum (500 MHz, CD <sub>2</sub> OD) of 3.04 .....	108
<sup>1</sup> H NMR Spectrum (500 MHz, D <sub>2</sub> O) of 3.05.....	109

<sup>13</sup> C NMR Spectrum (500 MHz, D <sub>2</sub> O) of 3.05.....	109
<sup>1</sup> H NMR Spectrum (500 MHz, CD <sub>3</sub> OD) of 3.07 .....	110
<sup>13</sup> C NMR Spectrum (500 MHz, CD <sub>3</sub> OD) of 3.07 .....	110
<sup>1</sup> H NMR Spectrum (500 MHz, CDCl <sub>3</sub> ) of 3.11 .....	111
<sup>13</sup> C NMR Spectrum (500 MHz, CDCl <sub>3</sub> ) of 3.11 .....	111
<sup>1</sup> H NMR Spectrum (500 MHz, CDCl <sub>3</sub> ) of 3.12 .....	112
<sup>13</sup> C NMR Spectrum (500 MHz, CDCl <sub>3</sub> ) of 3.12 .....	112
<sup>1</sup> H NMR Spectrum (500 MHz, CDCl <sub>3</sub> ) of 3.13 .....	113
<sup>13</sup> C NMR Spectrum (500 MHz, CDCl <sub>3</sub> ) of 3.13 .....	113
<sup>1</sup> H NMR Spectrum (500 MHz, CDCl <sub>3</sub> ) of 3.14 .....	114
<sup>13</sup> C NMR Spectrum (500 MHz, CDCl <sub>3</sub> ) of 3.14 .....	114
<sup>1</sup> H NMR Spectrum (500 MHz, CDCl <sub>3</sub> ) of 3.16 .....	115
<sup>13</sup> C NMR Spectrum (500 MHz, CDCl <sub>3</sub> ) of 3.16 .....	115
<sup>1</sup> H NMR Spectrum (500 MHz, CDCl <sub>3</sub> ) of 3.17 .....	116
<sup>13</sup> C NMR Spectrum (500 MHz, CDCl <sub>3</sub> ) of 3.17 .....	116
<sup>1</sup> H NMR Spectrum (500 MHz, CD <sub>3</sub> OD) of 3.19 .....	117
<sup>13</sup> C NMR Spectrum (500 MHz, CD <sub>3</sub> OD) of 3.19 .....	117
<sup>1</sup> H NMR Spectrum (500 MHz, CD <sub>3</sub> OD) of 3.20 .....	118
<sup>13</sup> C NMR Spectrum (500 MHz, CD <sub>3</sub> OD) of 3.20 .....	118
<sup>1</sup> H NMR Spectrum (500 MHz, CD <sub>3</sub> OD) of 3.21 .....	119
<sup>13</sup> C NMR Spectrum (500 MHz, CD <sub>3</sub> OD) of 3.21 .....	119
<sup>1</sup> H NMR Spectrum (500 MHz, CDCl <sub>3</sub> ) of 3.22 .....	120
<sup>13</sup> C NMR Spectrum (500 MHz, CDCl <sub>3</sub> ) of 3.22 .....	120
<sup>1</sup> H NMR Spectrum (500 MHz, CDCl <sub>3</sub> ) of 3.23 .....	121
<sup>13</sup> C NMR Spectrum (500 MHz, CDCl <sub>3</sub> ) of 3.23 .....	121
<sup>1</sup> H NMR Spectrum (500 MHz, CDCl <sub>3</sub> ) of 3.24 .....	122
<sup>13</sup> C NMR Spectrum (500 MHz, CDCl <sub>3</sub> ) of 3.24 .....	122
<sup>1</sup> H NMR Spectrum (500 MHz, CDCl <sub>3</sub> ) of 3.25 .....	123
<sup>13</sup> C NMR Spectrum (500 MHz, CDCl <sub>3</sub> ) of 3.25 .....	123
<sup>1</sup> H NMR Spectrum (500 MHz, CDCl <sub>3</sub> ) of 3.26 .....	124
<sup>13</sup> C NMR Spectrum (500 MHz, CDCl <sub>3</sub> ) of 3.26 .....	124
<sup>1</sup> H NMR Spectrum (500 MHz, CDCl <sub>3</sub> ) of 3.27 .....	125

<sup>13</sup> C NMR Spectrum (500 MHz, CDCl <sub>3</sub> ) of 3.27 .....	125
<sup>1</sup> H NMR Spectrum (500 MHz, CDCl <sub>3</sub> ) of 3.28 .....	126
<sup>13</sup> C NMR Spectrum (500 MHz, CDCl <sub>3</sub> ) of 3.28 .....	126
<sup>1</sup> H NMR Spectrum (500 MHz, CD <sub>3</sub> OD) of 3.29 .....	127
<sup>13</sup> C NMR Spectrum (500 MHz, CD <sub>3</sub> OD) of 3.29 .....	127
<sup>13</sup> C NMR Spectrum (500 MHz, CD <sub>3</sub> OD) of 3.30 .....	128
<sup>1</sup> H NMR Spectrum (500 MHz, CD <sub>3</sub> OD) of 3.31 .....	129
<sup>13</sup> C NMR Spectrum (500 MHz, CD <sub>3</sub> OD) of 3.31 .....	129
<sup>1</sup> H NMR Spectrum (500 MHz, CD <sub>3</sub> OD) of 3.32 .....	130
<sup>13</sup> C NMR Spectrum (500 MHz, CD <sub>3</sub> OD) of 3.32 .....	130
<sup>1</sup> H NMR Spectrum (500 MHz, CD <sub>3</sub> OD) of 3.33 .....	131
<sup>13</sup> C NMR Spectrum (500 MHz, CD <sub>3</sub> OD) of 3.33 .....	131
<sup>1</sup> H NMR Spectrum (500 MHz, D <sub>2</sub> O) of 3.35.....	132
<sup>13</sup> C NMR Spectrum (500 MHz, D <sub>2</sub> O) of 3.35.....	132
<sup>1</sup> H NMR Spectrum (500 MHz, CDCl <sub>3</sub> ) of 3.36 .....	133
<sup>13</sup> C NMR Spectrum (500 MHz, CDCl <sub>3</sub> ) of 3.36 .....	133
<sup>1</sup> H NMR Spectrum (500 MHz, CDCl <sub>3</sub> ) of 3.37 .....	134
<sup>13</sup> C NMR Spectrum (500 MHz, CDCl <sub>3</sub> ) of 3.37 .....	134
<sup>1</sup> H NMR Spectrum (500 MHz, CDCl <sub>3</sub> ) of 3.38 .....	135
<sup>13</sup> C NMR Spectrum (500 MHz, CDCl <sub>3</sub> ) of 3.38 .....	135
<sup>1</sup> H NMR Spectrum (500 MHz, CD <sub>3</sub> OD) of 3.39 .....	136
<sup>13</sup> C NMR Spectrum (500 MHz, CD <sub>3</sub> OD) of 3.39 .....	136
<sup>1</sup> H NMR Spectrum (500 MHz, CD <sub>3</sub> OD) of 3.40 .....	137
<sup>13</sup> C NMR Spectrum (500 MHz, CD <sub>3</sub> OD) of 3.40 .....	137
<sup>1</sup> H NMR Spectrum (500 MHz, CD <sub>3</sub> OD) of 3.41 .....	138
<sup>13</sup> C NMR Spectrum (500 MHz, CD <sub>3</sub> OD) of 3.41 .....	138
<b>Chapter 8: Appendix .....</b>	<b>146</b>
8.1 Equations for Fundamental Enzyme Kinetics .....	146
8.1.1 Michaelis-Menten Kinetics .....	146
8.1.2 Enzyme Kinetics with a Reversible Inhibitor.....	148
8.1.3 Enzyme Kinetics with a Mechanism-Based Inactivator .....	151

## List of Tables

Table 2.3.1: $K_i$ values and comparison of N-alkylated competitive inhibitors.....	35
Table 2.3.2: $K_i$ values and comparison of O-alkylated competitive inhibitors.....	38
Table 2.3.3: $K_i$ values and comparison of O- and N-alkylated competitive inhibitors .....	46
Table 4.2.1: $K_i$ and $k_i$ values and comparison of GCCase inactivators.....	64

## List of Figures

Figure 1.1: A general glycosidase-catalyzed hydrolysis reaction of a glucoside.....	1
Figure 1.1.1: Stereochemical result of inverting and retaining glycosidase catalyzed reactions.....	3
Figure 1.4.1: Examples of non-covalent Iminosugar Inhibitors .....	19
Figure 1.4.2: Proposed transition states for $\beta$ -glucosidase and $\alpha$ -glucosidase .....	21
Figure 1.4.3: Examples of non-covalent Inosamine inhibitors.....	22
Figure 2.1: NMR spectra of 3.20 chelated to Pd/C and after precipitation of Pd/C.....	27
Figure 2.2: SDS-PAGE of purified ABG enzyme .....	32
Figure 2.3.1: Nonlinear regression plots of the competitive inhibitor 3.12 with GCCase and ABG .....	37
Figure 2.3.2: Nonlinear regression plots of the competitive inhibitor 3.19 with GCCase and ABG .....	39
Figure 2.3.3: Nonlinear regression plots of the competitive inhibitor 3.20 with GCCase and ABG .....	39
Figure 2.3.4: Nonlinear regression plots of the competitive inhibitor 3.21with GCCase and ABG .....	40
Figure 2.3.5: Nonlinear regression plots of the competitive inhibitor 3.32 with GCCase and ABG .....	42

Figure 2.3.6: Nonlinear regression plots of the competitive inhibitor 3.33 with GCase and ABG .....	42
Figure 2.3.7: Nonlinear regression plots of the competitive inhibitor 3.29 with GCase and ABG .....	43
Figure 2.3.8: Nonlinear regression plots of the competitive inhibitor 3.30 with GCase and ABG .....	43
Figure 2.3.9: Nonlinear regression plots of the competitive inhibitor 3.31 with GCase and ABG .....	44
Figure 4.2.1: Plots of remaining enzyme activity over time and observed rate constants of inactivation versus the concentration of inhibitor 3.41 with Abg.....	58
Figure 4.2.2: Plots of remaining enzyme activity over time and observed rate constants of inactivation versus the concentration of inhibitor 3.40 with Abg.....	59
Figure 4.2.3: Plots of remaining enzyme activity over time and observed rate constants of inactivation versus the concentration of inhibitor 3.39 with Abg.....	59
Figure 4.2.4: Plots of remaining enzyme activity over time and observed rate constants of inactivation versus the concentration of inhibitor 3.41 with GCase.....	61
Figure 4.2.5: Plots of remaining enzyme activity over time and observed rate constants of inactivation versus the concentration of inhibitor 3.40 with GCase.....	62
Figure 4.2.6: Plots of remaining enzyme activity over time and observed rate constants of inactivation versus the concentration of inhibitor 3.39 with GCase.....	63
Figure 4.2.7: Total absorbance of untreated cell lysate controls .....	66
Figure 4.2.8: Residual activity of cell lyates relative to untreated lysate blank for buffers containing 1.2% sodium taurocholate and buffers containing 0.2% sodium taurocholate.....	66
Figure A1: A general plot displaying M-M enzyme kinetics.....	148

## List of Schemes

Scheme 1.1.1.1: Accepted mechanism of inverting $\beta$ -glucosidase.....	4
Scheme 1.1.1.2: Accepted mechanism of retaining $\beta$ -glucosidase .....	6
Scheme 1.2.1: The enzymatic degradation of gangliosides in the lysosome .....	10
Scheme 1.2.2: Therapeutic strategies to reduce GlcCer storage in Gaucher disease .....	14
Scheme 1.2.3: Glucocerebrosidase catalyzed hydrolysis of glucosylceramide .....	16
Scheme 2.1: Synthesis of the Substrate 2,4-dinitrophenyl- $\beta$ -D-Glucopyranoside .....	23
Scheme 2.2: Synthesis of N-alkylated Inhibitors.....	28
Scheme 2.3: Synthesis of O- and N-alkylated Inhibitors.....	31
Scheme 3.1.1: Mechanism of formation of reactive aglycone from affinity labels.....	49
Scheme 3.1.2: Mechanism of mechanism-based inhibitors .....	50
Scheme 4.1: Synthesis of Aziridine Inactivators .....	55
Scheme 4.2: Mechanism of the inhibition of GCase by alkylated conduritol aziridine .....	56
Scheme 4.3: Enzyme kinetics involving an irreversible mechanism-based inhibitor .....	57

## List of Abbreviations

Å	Angstrom
ABG	<i>Agrobacterium sp.</i> β-glucosidase
AcCl	Acetyl Chloride
AcOH	Acetic Acid
AU	Absorbance Unit
BnBr	Benzyl Bromide
BSA	Bovine Serum Albumin
CAZY	Carbohydrate-Active enzymes
CBA	Cytosolic β-Glucosidase
CH <sub>3</sub> CN	Acetonitrile
CNS	Central Nervous System
2,4-DNP-β-D-Glc	2,4-dinitrophenyl β-D-glucopyranoside
DNFB	2,4-dinitrofluorobenzene
DNJ	Deoxynojirimycin
DNP	2,4-dinitrophenyl
DMF	Dimethylformamide
2,2-DMP	2,2-dimethoxypropane

DMSO	Dimethylsulfoxide
EET	Enzyme Enhancement Therapy
ER	Endoplasmic Reticulum
ERAD	Endoplasmic Reticulum Associated Degradation
ERT	Enzyme Replacement Therapy
EtOAc	Ethyl Acetate
EtOH	Ethanol
FG	Fagomine
GCase	Glucocerebrosidase
Glc	Glucose
GlcCer	Glucosylceramide
Glu	Glutamic Acid
HCl	Hydrochloric acid
HIV	Human Immunodeficiency Virus
Hz	Hertz
I	Inhibitor
IFG	Isofagomine

$k_{\text{cat}}/k_{\text{non}}$	Ratio of rate constants for catalyzed and non-catalyzed reactions
$k_{\text{cat}}$	Catalytic rate constant (turnover number)
kDa	Kilodalton
$k_i$	Rate constant of inactivation
$K_i$	Dissociation constant for the enzyme-inhibitor complex
$K_m$	Michaelis constant of a substrate
$K_{\text{obs}}$	Observed pseudo-first order rate constant
LSD	Lysosomal Storage Disease
MeOH	Methanol
Mesyl	Methanesulfonyl
M-M	Michaelis-Menton
NC-IUBMB	Nomenclature Committee of the International Union of Biochemistry and Molecular Biology
NLGCase	Non-Lysosomal Glucocerebrosidase
NMR	Nuclear Magnetic Resonance
PC	Phosphatidylcholine
Pd/C	Palladium on carbon

PET	Positron Emission Tomography
Pyr	Pyridine
SDS	Sodium Dodecyl Sulfate
SRT	Substrate Reduction Therapy
THF	Tetrahydrofuran
TsOH	p-toluenesulfonic acid
UV	Ultraviolet light
Vis	Visible light
$V_{\max}$	Maximum velocity of an enzyme-catalyzed reaction

## **Acknowledgments**

I would like to sincerely thank my supervisor, Dr. Christopher P. Phenix, for his guidance, knowledge and support given to me over the past few years. I have learned so much from him throughout this project and he has made this process a rewarding and enjoyable experience. I couldn't have asked for a better supervisor.

I would like to thank all of my fellow lab members for their friendship and support over the years, especially Dr. Morshed Chowdhury and Dr. Ignace Moya, whose assistance and knowledge have helped me out in so many ways throughout the project. Stacey Tokar, who paved the way and brought me up to speed when I first started. Shardul Bhilopa, for the HeLa cell work. Brady Vigliarolo, and Amanda Luby, who have helped me along the way, and all the members of TBTRI who helped organize activities that made each week fun and enjoyable.

I would also like to thank my committee members, Dr. Spivak and Dr. Jiang. I couldn't have started this project when I did without their support. Dr. Mike Campbell who helped interpret our more challenging results. I thank the Lakehead University Department of Chemistry and all of the faculty and staff that have supported me, Mike Sorokupud for the consistent troubleshooting of the NMR, and Grzegorz Kepka for running the MS.

I owe my thanks to those who have previously worked on Lysosomal Storage Disorder projects with ABG and GCCase, Dr. Brian Rempel and Tara Hill. It helped greatly to follow working methods and use their optimized enzyme conditions.

Finally, I would like to thank my family who have always encouraged and supported me.

## Chapter 1: General Introduction

### 1.1 Glycosidases

Glycosidases (glycoside hydrolases) carry out the hydrolytic cleavage of the carbon – oxygen acetal or glycosidic bond. The glycosidic bond is formed between the carbon of the glycone and oxygen of the aglycone and is cleaved by the enzyme in the presence of water (**Figure 1.1**).

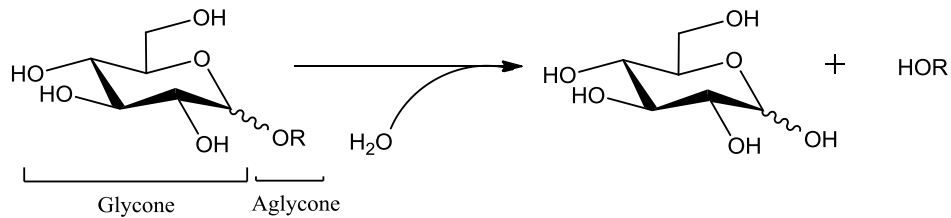


**Figure 1.1:** A general glycosidase-catalyzed hydrolysis reaction of a glucoside.

Glycosidases have been classified in a variety of ways based on the following properties:

- 1) **Cleavage site.** Glycosidases that hydrolyze the glycosidic bond within an oligosaccharide chain are called endo-glycosidases, while those that hydrolyze the residues at terminal ends are called exo-glycosidases.
- 2) **Anomeric specificity to the substrate.** Glycosidases typically catalyze the hydrolysis of either  $\alpha$ - or  $\beta$ - glycosidic linkages and will be unable to, or have minimal capability to, hydrolyze the alternate anomer.
- 3) **Mechanism of hydrolysis.** Glycosidase release the product glycone having a specific  $\alpha$ - or  $\beta$ - stereochemistry at the anomeric carbon through the use of either an inverting or retaining mechanism when hydrolyzing the glycosidic linkage.
- 4) **Reaction catalyzed.** Many enzymes have been categorized by the Nomenclature Committee of the International Union of Biochemistry and Molecular Biology (NC-IUBMB) based on the reaction they catalyze and can be found on the peer reviewed<sup>1</sup> website <http://www.enzyme->

[database.org](http://database.org). Hydrolases are class 3 enzymes given an Enzyme Commission number of EC 3 followed by a number indicating the bond hydrolyzed, the catalytic mechanism, and a further subclass linked to the specific enzyme. For example,  $\beta$ -D-glucocerebrosidase is EC 3.2.1.45, where the 3 indicates the enzyme is a hydrolase, 3.2 specifies a glycosidase, 3.2.1 indicates an O-glycosidase, and finally 3.2.1.45 indicating specifically  $\beta$ -D-glucocerebrosidase.

- 5) **Amino acid sequence.** Glycosidases have been classified based on their amino acid sequence and folding similarities into a large peer reviewed<sup>2</sup> Carbohydrate-Active enZYmes (CAZY) database that can be found at <http://www.cazy.org>. Glycosidases with similar sequences are grouped into one of 132 families, and the families are grouped into 14 different clans based on the folded protein structure.

Glycosidases are important enzymes because of their ability to enhance the reaction rates for the selective hydrolysis of a variety of saccharides necessary for vital cell functions such as energy storage and production, cell wall composition, and signalling molecules.<sup>3</sup> Glycosidases are known to be one of the most efficient enzymes capable of the hydrolysis of molecules like cellulose, with an effective  $10^{17}(k_{\text{cat}}/k_{\text{non}})$  rate enhancement.<sup>4</sup> To put this into perspective, the half-life for the spontaneous hydrolysis of cellulose is 4.7 million years,<sup>4a</sup> while the glycosidase-catalyzed half-life can be as low as 0.693ms.<sup>4b</sup>

### 1.1.1 Glycosidase Mechanisms

Glycosides can exist in two possible diastereomeric configurations depending on the orientation of the bond at the anomeric carbon. Drawn in Haworth projections, if the group attached to the anomeric carbon is on the same side of the ring as the carbon atom that determines the configuration (D- or L-), then it is the  $\beta$ -anomer, and if they are on opposite sides, then it is the  $\alpha$ -anomer.

Glycosidases catalyze the hydrolysis of a specific glycosidic linkage using a mechanism that results in the retention or inversion of the stereochemistry at the anomeric center (**Figure 1.1.1**).

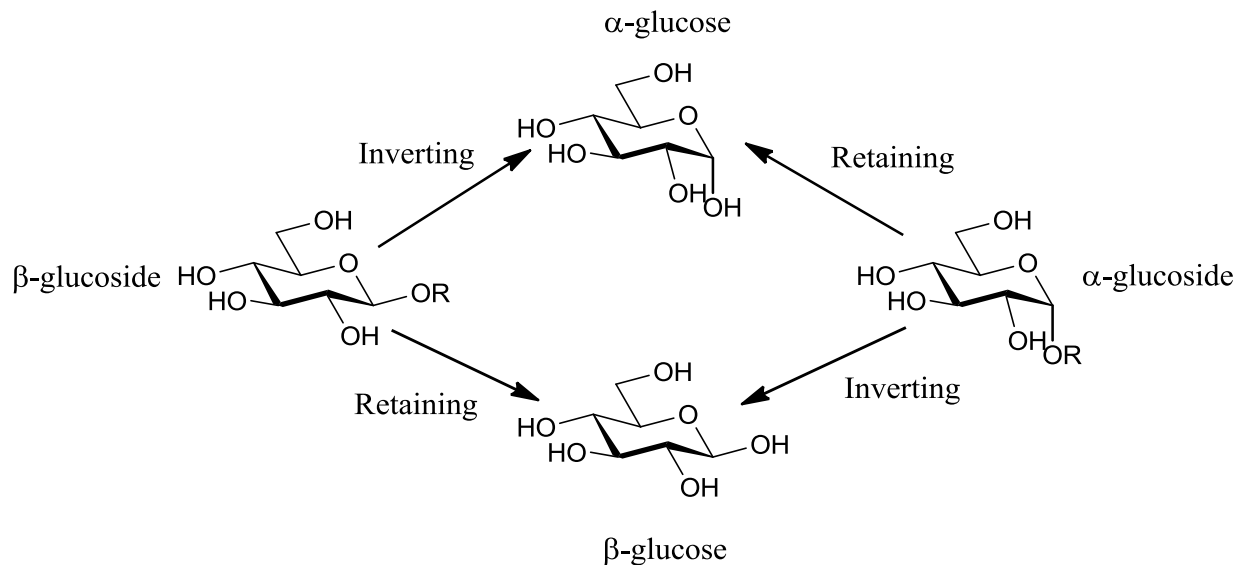


**Figure 1.1.1:** Stereochemical result of inverting and retaining glycosidase catalyzed reactions

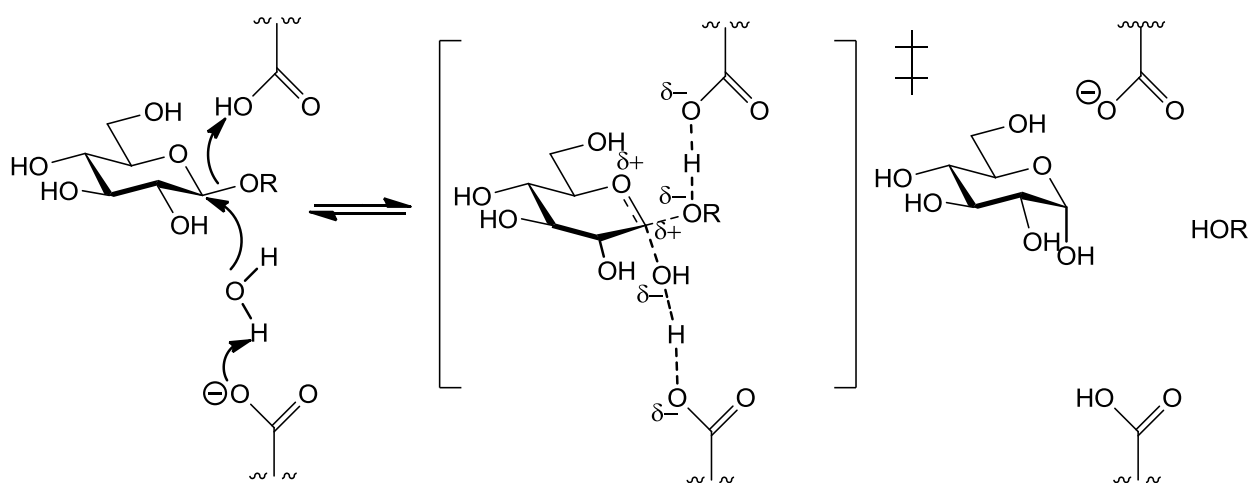
There are many different glycosidases that use a variety of mechanisms to catalyze their hydrolytic reactions including substrate assisted catalysis, proton transferring networks, non-carboxylate residues, and exogenous bases and nucleophiles.<sup>5</sup> However, for the purpose of this thesis, we will discuss only the most common and thoroughly studied carboxylic glycosidases that rely on carboxylic acid functional groups for catalysis.

### 1.1.1.1 Inverting glycosidases

During hydrolysis, an inverting glycosidase catalyzes the inversion of the anomeric carbon in the reactant to the alternate anomer in the product. For example, a  $\beta$ -inverting glucosidase will hydrolyze a  $\beta$ -glucoside producing  $\alpha$ -glucose as the glycone product. These glycosidases rely on a pair of carboxylic acid functional groups (Glu or Asp) located on average 10.5 Å apart which allows for simultaneous binding of both the substrate and water in the active site.<sup>3, 4b</sup> In the unbound state, one of the

carboxylic acid residues within the active site is deprotonated acting as a general base while the other remains protonated and acts as a general acid. The reaction occurs through a single displacement mechanism where the general base removes a proton from water to enhance its nucleophilicity, promoting the oxygen to attack the anomeric carbon of the substrate, while the general acid protonates the leaving aglycone oxygen allowing the products to dissociate.<sup>5</sup> The reaction results in the formation of an oxocarbenium ion-like transition state which is stabilized through flattening of the sugar into a half-chair or B boat conformation to favor hydrogen bonding between the substrate and nucleophile and through electrostatic interactions.<sup>4b</sup> The mechanism of a general inverting  $\beta$ -glucosidase is shown in

**Scheme 1.1.1.1.**



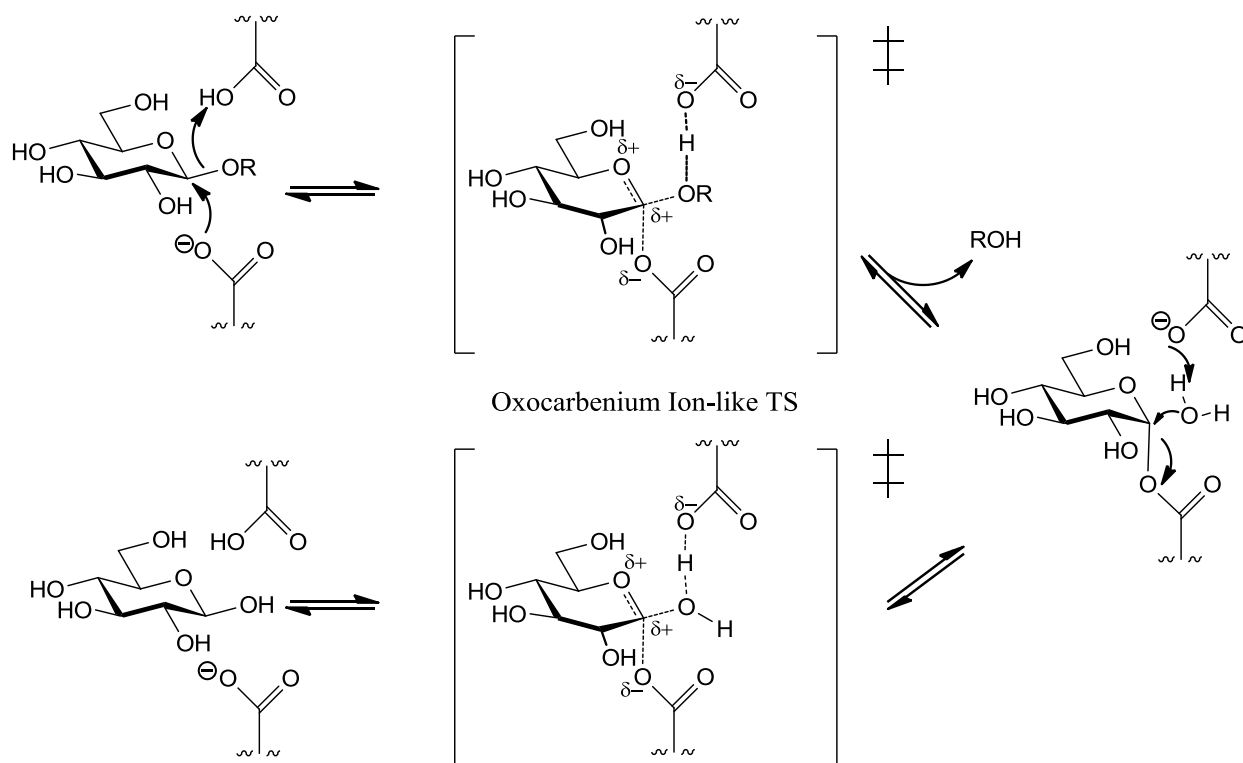
**Scheme 1.1.1.1:** Accepted mechanism of inverting  $\beta$ -glucosidase

### 1.1.1.2 Retaining glycosidases

The majority of retaining glycosidases use a double displacement mechanism involving two inversion steps that result in the net retention of the anomeric configuration in the reactant and product. Proposed by Koshland in 1953,<sup>6</sup> the first step in catalysis involves glycosylation of the enzyme forming a covalent glycosyl-enzyme intermediate followed by a deglycosylation step. Retaining

glycosidases utilize a pair of carboxylic acid functional groups (Glu or Asp) that are 5.5 Å apart, spaced much closer together than the carboxylic acid functional groups found 10 Å apart in inverting glycosidases. Having the pair of carboxylic acid functional groups 5.5 Å apart prevents simultaneous binding of water and substrate in the enzyme's active site, thus preventing direct hydrolysis of the substrate and permitting the two step double displacement reaction.<sup>3, 4b</sup> In the first step of catalysis, one of the carboxylic acids, in the basic form, acts as a catalytic nucleophile attacking the anomeric carbon and displacing the aglycone group from the sugar ring. The second carboxylic acid simultaneously protonates the leaving oxygen thus promoting formation of the covalent glycosyl-enzyme intermediate and the liberated aglycone product.<sup>4b</sup> The second step of the mechanism occurs through hydrolysis of the glycosyl-enzyme intermediate assisted by the carboxylate residue acting as a general base. This step produces free enzyme and the glycone having the retained stereochemistry at the anomeric carbon.<sup>4b</sup> In both catalytic steps there is an oxocarbenium ion-like transition state formed and stabilized through hydrogen bonding and electrostatic interaction with various active site residues.<sup>4b</sup>

The mechanism of a general retaining glycosidase is shown in **Scheme 1.1.1.2**.



**Scheme 1.1.1.2:** Accepted mechanism of retaining  $\beta$ -glucosidase

In 1967 an alternate mechanism was proposed by Phillips<sup>7</sup> which involved formation of an ion-pair intermediate where the carbonium ion would be shared with the ring oxygen causing the ring to take up the half-chair conformation. This translates to an oxocarbenium-ion transition state in the half-chair conformation. The formation of a covalent intermediate in the mechanism of retaining glycosidases was later confirmed through the use of  $\alpha$ -deuterium isotope effects and active site irreversible inhibition. Studies involving  $\alpha$ -deuterium isotope effects showed the hydrolysis of glucosyl-enzyme intermediates (deglycosylation step) gave  $k_H/k_D = 1.2-1.25$ .<sup>8</sup> A  $k_H/k_D > 1$  indicates a decreasing coordination number from the intermediate to the transition state. In the retaining glycosidase mechanism, a  $k_H/k_D > 1$  is only possible when the substrate is covalently attached because the anomeric carbon changes from  $sp^3$  to  $sp^2$  going from the transition state to the product. If there was an ion-pair

intermediate as theorized by Phillips, then coordination would increase from  $sp^2$  to  $sp^3$  and a  $k_H/k_D < 1$  would result. Further evidence of a covalent intermediate in the double displacement mechanism comes from X-ray crystallography and mass spectroscopy studies with active site irreversible inhibitors such as 2-deoxy-2-fluoro-D-glycosyl fluorides<sup>9</sup> revealing the formation of a covalent inhibitor-enzyme intermediate. The inclusion of the electronegative fluorine at the C2 position of glucose destabilizes the oxocarbenium ion-like transition states resulting in trapping and observation of the covalent intermediate.<sup>10</sup>

### 1.1.2 Glycosidase Inhibitors

Glycosidases are involved in a wide variety of pathways within the cell so inhibiting activity of specific glycosidases can reveal information about what pathways are modified in disease states and how glycosidases can be regulated to restore normal function. Glycosidase inhibitors have shown therapeutic potential for the treatment of viral infection, diabetes, obesity, cancer, and genetic disorders.<sup>11</sup> Viral infections such as influenza, hepatitis and HIV may be treated by disrupting cell-virus recognition through inhibiting the activation of signalling oligosaccharides on the cell surface.<sup>11b</sup> Diabetes and obesity can be treated by inhibiting intestinal glycosidases to lower blood glucose levels<sup>11b</sup> or inhibiting hepatic glucose production.<sup>12</sup> Elevated levels of glycosidases in the cells and tumor microenvironment are seen in malignant cancers and could be inhibited to prevent metastasis.<sup>13</sup> Clinical trials are currently ongoing for genetic disorders such as lysosomal storage diseases where there are deficiencies in glycosidases that may be treated with competitive glycosidase inhibitors acting as pharmacological chaperones.<sup>12, 14</sup> In addition, glycosidase inhibitors are very important tools for medical and biotechnological studies due to their ability to modify cellular functions.

Glycosidase inhibitors can be classified by their interaction with the enzyme as covalent or non-covalent inhibitors. Covalent inhibitors will form an irreversible covalent bond with the enzyme, usually

to one of the residues in the active site which inactivates the enzyme. Covalent inhibitors can bind to a non-active site pocket on the enzyme but need to induce a conformational change of the active site to inactivate the enzyme. Non-covalent inhibitors bind reversibly to the enzyme acting as competitive, non-competitive and uncompetitive inhibitors.

## 1.2 Lysosomal Storage Diseases

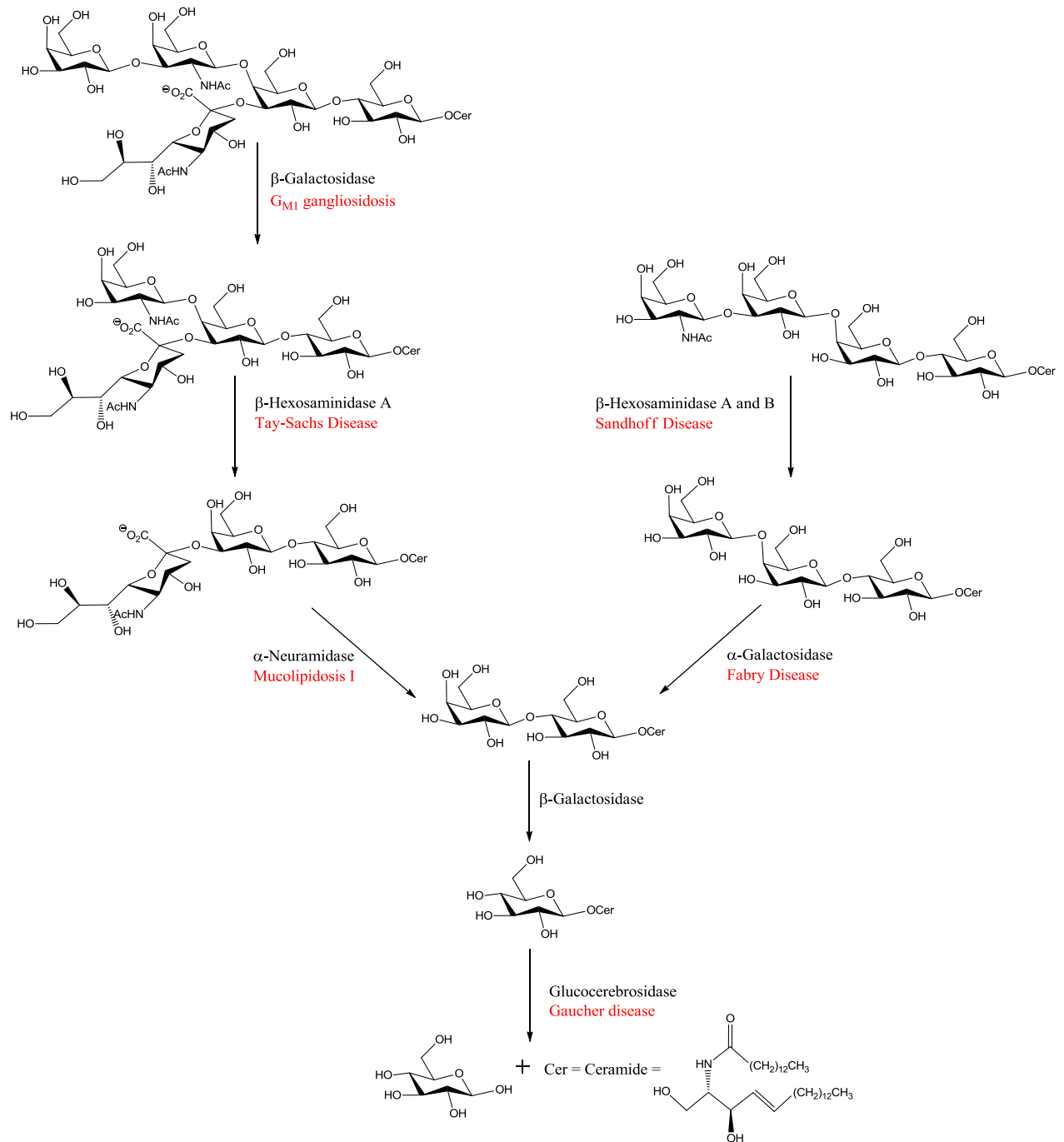
Lysosomal storage diseases (LSDs) are a group of genetic disorders in which there is a deficiency in the proteins involved in the lysosomal catabolic pathways. Lysosomes are organelles within cells that break down and recycle cellular waste materials through the action of over 50 hydrolytic enzymes from various enzyme classes. Deficiency in the lysosomal proteins results in accumulation of partially processed substrates within the lysosome leading to complex and variable disease symptoms. Some of the most well studied LSDs include Tay Sachs, Fabry, Pompe and Gaucher diseases.<sup>14a, 14c, 15</sup> Of the known LSDs, all are caused by autosomal recessive genes, except for the X-linked recessive genes involved in Hunter's syndrome and Fabry's disease, and most involve nervous system function.<sup>16</sup> There are 46 LSDs that can be classified into six categories based on their functional defect:<sup>16</sup>

- 1) **Lysosomal hydrolase.** The gene encoding one of the 50 lysosomal hydrolases is mutated resulting in the expression of a crippled enzyme that is structurally unstable or unable to properly catalyze substrate degradation within the lysosome.
- 2) **Post-translational processing.** Multiple sulfatase deficiency (MSD) is the only LSD in this category. Post-translational modification of a cysteine residue into an aldehyde is required for all sulfatases to function but modification of the cysteine residue in the enzyme does not occur in MSD resulting in the excess storage of sulfate containing lipids in the lysosome.
- 3) **Trafficking of lysosomal enzymes.** This category includes multiple types of Mucopolidosis LSDs. N-acetylglucosamine-1-phosphate transferase, one of the many enzymes responsible for

attaching signalling molecules to lysosomal enzymes, is defective so the lysosomal enzymes are not recognized for transported into the lysosome.

- 4) **Lysosomal enzyme protection.** Galactosialidosis is the only LSD in this category. Its mechanism is poorly understood but a mutation of the protective protein, Cathepsin A, prevents the formation of a stabilizing complex with  $\beta$ -galactosidase and  $\alpha$ -neuramidase resulting in their deficiencies.
- 5) **Soluble non-enzymatic proteins.** LSDs in this category result from deficiencies in various soluble proteins such as the lipid transfer proteins in  $G_{M2}$  gangliosidosis activator protein deficiency. These proteins interact with other proteins to form complexes, modify activity, or activate transcription.
- 6) **Transmembrane non-enzyme proteins.** Transport proteins responsible for the selective transport of materials across the cell and lysosomal membranes are deficient. For example, Nieman-Pick C can be caused by a defective cholesterol transporter or defective lysosomal-cholesterol binding protein.

Of the 46 lysosomal disorders, 29 of them are due to defects in a lysosomal hydrolase. Many of these hydrolases are part of long catabolic pathways that become interrupted resulting in the excessive storage of partially processed substrates. The catabolic pathway of gangliosides within the lysosomes can be seen in **Scheme 1.2.1**.



**Scheme 1.2.1:** The enzymatic degradation of gangliosides in the lysosome. Enzymes are shown in black and the diseases resulting from their deficiency are shown in red. Adapted from Butters et al.<sup>17</sup>

Within the lysosomal hydrolase class of LSD's, the specific mutation affects the nature and severity of the disease symptoms. However, even with commonly found mutations, the pathology and

progression cannot be reliably predicted due to the many downstream pathways affected by substrate accumulation.<sup>18</sup> This is exemplified by patients with the same genotype and genetic background displaying a range of different phenotypes for a given LSD.<sup>18</sup> Most LSDs display infantile, juvenile and adult forms named for the stage of life most complications can be detected and diagnosed. The infantile forms are the most severe with virtually no residual enzyme activity resulting in early death due to neurological involvement while the juvenile and adult forms have low to moderate residual activity, slowly develop and are less severe.<sup>18-19</sup>

The specific mutations found in the gene encoding the hydrolase that causes the LSDs can dramatically affect both protein stability and catalytic activity. Enzymes are synthesized by ribosomes in the endoplasmic reticulum (ER) in an unfolded state. The protein then begins to form a proper 3-dimensional structure, typically with the aid of various helper molecules that promote the formation of the folded conformation.<sup>19</sup> Proteins that do not fold properly can aggregate and lead to cell toxicity. Therefore, misfolded proteins are recognized by a quality control mechanism that labels unfolded proteins with ubiquitin directing them into the endoplasmic reticulum associated degradation (ERAD) pathway.<sup>19</sup> The consistent destruction of the misfolded lysosomal enzyme in the ERAD pathway ultimately leads to insufficient levels of enzyme reaching the lysosome. Critically, experiments have shown that only 10-20% residual enzyme activity is sufficient to prevent substrate accumulation in both Gaucher and Tay-Sachs diseases.<sup>17</sup>

Since most mutations in the amino acid sequence lead to the expression of an enzyme that maintains catalytic activity, various therapeutic strategies have been developed to improve delivery of the functional enzyme to the lysosomes including enzyme replacement therapy (ERT) and enzyme enhancement therapies (EET) by using pharmacological chaperones. Alternatively, substrate reduction

therapy (SRT) blocks the metabolic pathways that generate the substrates in order to decrease the rate of substrate accumulation within the lysosomes.

### **1.2.1 Enzyme Replacement Therapy**

Enzyme replacement therapy attempts to supplement the residual enzyme activity of the defective enzyme by exogenous administration of a recombinant and modified enzyme. Recombinant enzymes must be modified to display glycan chains on the surface of the protein that target endocytotic receptors found on specific cell types affected by the specific LSDs.<sup>14a</sup> Different cell targets require distinct oligosaccharides including important terminal residues such as mannose, mannose-6-phosphate, and asialoglycoprotein that target the mannose receptor, mannose-6-phosphate receptor and asialoglycoprotein receptor respectively.<sup>14a</sup> Once bound to the receptor, the receptor-enzyme complex is internalized into the cell through endocytosis thus delivering functional enzyme to the lysosomes of the diseased cells. Despite having enormous success with the treatment of several LSDs such as Gaucher, Fabry, Pompe, MPS I, MPS II, and MPS VI diseases<sup>14c</sup>, there are several limitations with ERT such as the inability to reduce secondary symptoms from substrate storage such as inflammation and apoptosis, the inability to penetrate the blood-brain barrier to treat neurological symptoms, the potential to develop an immune response to the recombinant enzyme and the expensive costs of therapy (\$90,000-\$720,000 annually per patient<sup>14c</sup>).<sup>14a</sup>

### **1.2.2 Substrate Reduction Therapy**

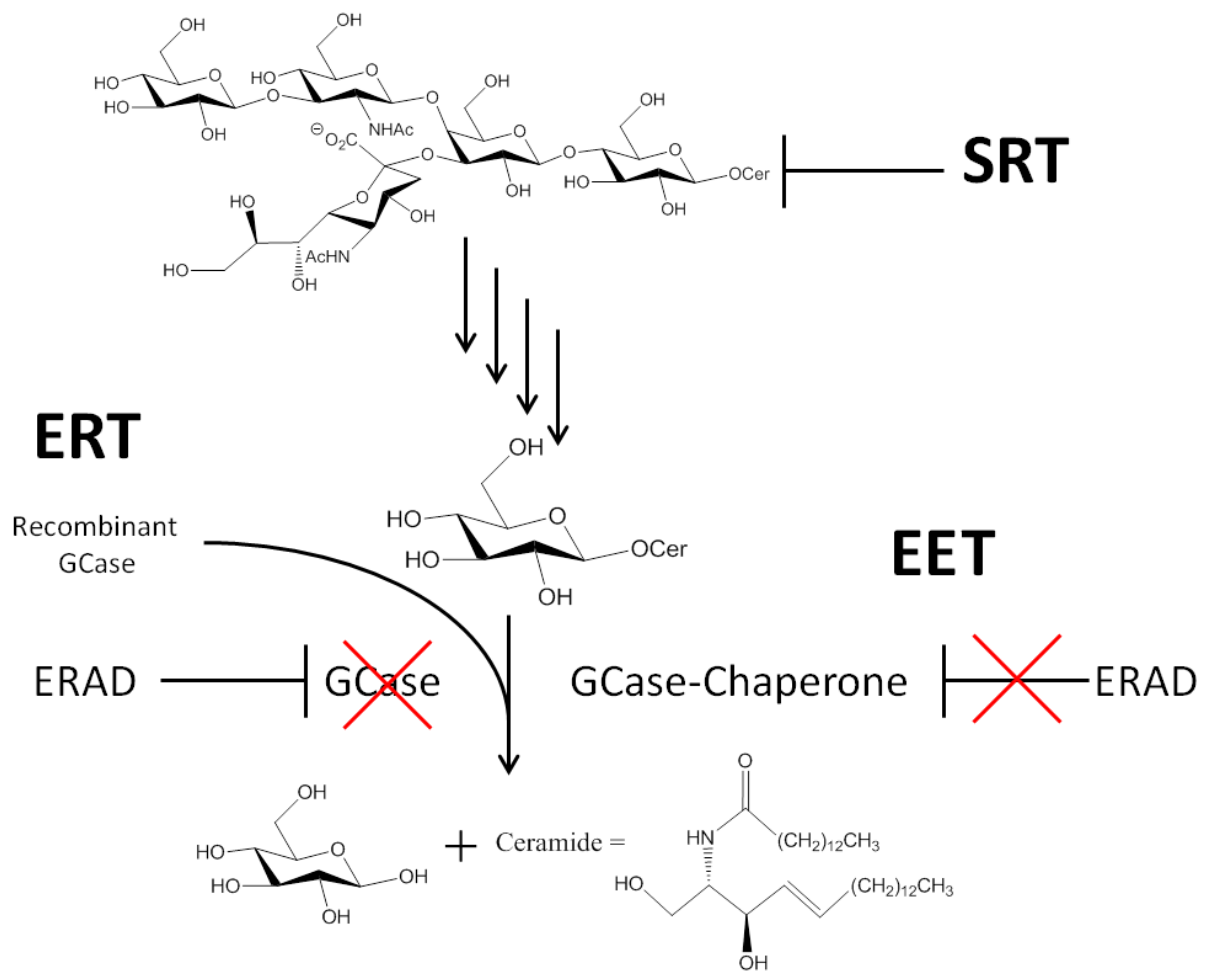
Substrate reduction therapy is often used concurrently with ERT to treat LSDs. ERT functions to remove accumulated substrate by delivering enzyme to the lysosomes while SRT prevents substrate accumulation by blocking the upstream metabolic pathways that produce the substrate as a normal part of metabolism. SRT requires the administration of inhibitor molecules that will partially inhibit enzymes involved in the synthesis of the target substrate.<sup>17</sup> Currently, SRT has been applied to the inhibition of

enzymes involved in glycosphingolipid synthesis and has shown potential to improve symptoms of LSDs caused by deficiencies in the glycosphingolipid catabolic pathway.<sup>14a, 17</sup> Gaucher disease, which is caused by a defect in the lysosomal  $\beta$ -glucosidase glucocerebrosidase (GCCase), is the first disease used for evaluating SRTs. There are now a number of inhibitors targeting ceramide-specific glucosyltransferase used in clinical trials such as N-butyl-deoxynojirimycin.<sup>17</sup> There can be wide ranging problems with SRT for the treatment of LSDs because the metabolic pathways inhibited normally perform vital functions for the cells. The side effects can become especially significant when applying the treatment to young children during development.<sup>18</sup> However, these small molecule inhibitors are capable of passing the blood-brain barrier and can therefore improve the outcome of patients with neurological involvement which are expressed in the severe LSD cases at young ages. Currently the only clinically approved and commercially available compound for SRT is Zavesca<sup>®</sup> (N-butyl-deoxynojirimycin) for the treatment of Gaucher and Niemann-Pick diseases but many compounds are currently in clinical trials.<sup>20</sup>

### **1.2.3 Enzyme Enhancement Therapy**

Enzyme enhancement therapy (EET) involves the use of pharmacological chaperones that are able to enhance the residual enzyme activity by stabilizing the properly folded mutant enzymes and preventing degradation by ERAD. As mentioned above, many LSDs result from a genetic mutation that results in the expression of a catalytically active mutant protein that is degraded prior to trafficking into the lysosome. In order to bypass the ERAD quality control mechanism, a defective enzyme would need to enter a properly folded state long enough to be transported out of the ER and trafficked into the lysosome. A potential solution is to use a competitive inhibitor that binds to the active site of the enzyme stabilizing the folded conformation. Once the catalytically active mutant enzyme enters the lysosome, excessively stored substrate outcompetes the inhibitor and partial restoration of the pathway can result. Although the idea of using competitive inhibitors to increase enzymatic activity is counterintuitive, experiments have clearly demonstrated that this strategy is effective at increasing

lysosomal hydrolase activity.<sup>19</sup> In fact, EET as a new therapy for Gaucher disease has already been shown to be an effective treatment for individuals who have mutations that retain enzymatic activity.<sup>21</sup> Individuals with mutations that abolish catalytic activity do not show any improvement with EET chaperones<sup>21</sup> clearly indicating that the improvements observed with EETs are due to increased enzyme transport and reduced ERAD. The three therapeutic strategies for the treatment of Gaucher disease are summarized in **Scheme 1.2.1** below.



**Scheme 1.2.2:** The three therapeutic strategies, SRT, ERT and EET, employed to reduce GlcCer storage in the treatment of Gaucher disease.

### 1.2.4 Gaucher Disease

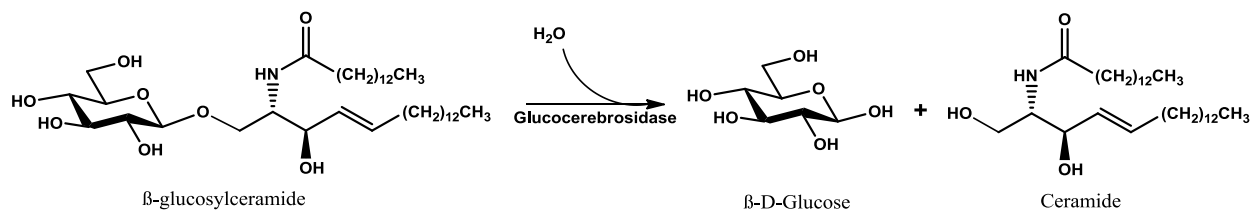
Phillip Gaucher first identified a patient with Gaucher disease in 1882 based on the enlarged spleen of a 34 year old woman.<sup>22</sup> Gaucher disease is the most common lysosomal storage disorder occurring with a frequency of one in 40,000-50,000 live births<sup>23</sup> compared to the one in 7,700<sup>24</sup> occurrence of all lysosomal storage disorders combined. Certain ethnic groups can have variable prevalence of these diseases like the Ashkenazi Jews who have a one in 800 frequency of Gaucher disease.<sup>21</sup> Gaucher disease results from more than 300 known mutations in the GBA gene coding for  $\beta$ -glucocerebrosidase (GCase).<sup>22</sup> The resulting mutant enzyme is degraded through ERAD resulting in the accumulation of the substrate glucosylceramide (GlcCer) within the lysosomes leading to the disease state. The severity of the disease depends not only on the residual enzyme activity in the lysosomes, but also the extent of macrophage involvement. Macrophages may be activated either by the excess storage of GlcCer due to sphingolipid's ability to trigger inflammation and apoptosis, or activated by cellular pathways detecting the abnormal folding of protein within the ER which can also initiate inflammation and apoptosis.<sup>23</sup> There is some evidence supporting the influence of protein misfolding being the primary cause of the disease symptoms when there is CNS involvement due to extensive neuronal death without requiring accumulation of GlcCer.<sup>23</sup>

Patients with Gaucher disease are diagnosed at an average age of 9.5 years<sup>24</sup> and can present as one of three different pathologies. The most prevalent form of Gaucher disease is Type 1 which is a non-neuropathic form affecting 90% of Gaucher patients.<sup>14a</sup> This form characterized by the presence of hepatosplenomegaly and bone disease with frequent occurrence of haematological disorders and growth retardation.<sup>23</sup> Type 2 Gaucher disease is the most severe form of the disease with a median age at death of 9 months.<sup>23</sup> The disease symptoms can be expressed within the first few days of life and present with hepatosplenomegaly and severe neurodegeneration. Type 3 Gaucher disease is an

intermediate form of the disease and can present with variable severities of hepatosplenomegaly, bone disease and neurodegeneration.<sup>23</sup>

### 1.2.5 Glucocerebrosidase

GCCase (EC 3.2.1.45) is a retaining  $\beta$ -glucosidase enzyme of glycosidase hydrolase family 30<sup>2</sup> responsible for the cleavage of  $\beta$ -glucosylceramide into the glycone,  $\beta$ -D-glucose, which is readily used by the cell, and the aglycone, ceramide, which is further catabolised into sphingosine and fatty acids by other enzymes in the glycosphingolipid degradation pathway (**Scheme 1.2.1**).<sup>25</sup>



**Scheme 1.2.3:** Glucocerebrosidase catalyzed hydrolysis of glucosylceramide

Since GCCase is a retaining  $\beta$ -glucosidase, it utilizes the double displacement mechanism (**Scheme 1.1.1.2**) with Glu<sup>340</sup> as the catalytic nucleophile and Glu<sup>235</sup> as the general acid/base.<sup>26</sup> In order to access the GlcCer within the lysosome, GCCase requires Saposin C which is hypothesized to act as a GlcCer “solubilizer” or as “liftase” proteins.<sup>27</sup> In the solubilizer model, saposin C would extract GlcCer from the phospholipid bilayer forming a soluble lipid-protein complex and allow interaction with the aqueous soluble GCCase.<sup>27</sup> In the liftase model, both saposin C and GCCase would bind to the lipid bilayer with saposin C functioning to facilitate access to GlcCer within the membrane.<sup>27</sup> In addition to saposin C, negatively charged lipids such as 1,2-diacyl-sn-3-phosphoinositol and bis(monoacylglycero)phosphate as well as low pH are required for full GCCase activity.<sup>27</sup>

While the primary location of GlcCer catabolism is within the lysosome, a second integral membrane GCCase capable of GlcCer hydrolysis has been identified.<sup>25</sup> This non-lysosomal GCCase

(NLGCase) exhibits no homology with GCase and has different substrate and inhibitor specificities.<sup>25</sup> NLGCase is encoded on a unique GBA2 gene allowing it to remain functional in patients with Gaucher disease mutations.<sup>25</sup> NLGCase catabolism of GlcCer generates ceramide that is rapidly converted into sphingomyelin by transfer of phosphorylcholine to ceramide from phosphatidylcholine (PC).<sup>25</sup> In patients with Gaucher disease, it has been shown that PC synthesis has been increased<sup>25</sup> indicating an up-regulation in the conversion of ceramide to sphingomyelin and therefore increase in GlcCer catabolism by NLGCase. The presence of this second GCase may explain why only certain organs containing cells with abundant lysosomes like macrophages are primarily affected while others remain normal in Gaucher patients.

Broad specificity cytosolic  $\beta$ -glucosidase (CBA), is a third enzyme present in cells that is capable of GlcCer hydrolysis.<sup>28</sup> As the name suggests, CBA is capable of hydrolyzing a wide variety of both natural and artificial  $\beta$ -D-glucoside,  $\beta$ -D-galactoside,  $\beta$ -D-fucoside,  $\beta$ -D-xyloside, and  $\alpha$ -L-arabinoside compounds.<sup>29</sup> CBA is encoded on the GBA3 gene and is thought to be responsible for some of the variability seen in Gaucher disease, but there is also strong evidence contradicting this idea.<sup>28-29, 29c</sup>

Cerezyme™ (imiglucerase), the second generation recombinant GCase used for the treatment of Gaucher disease, is produced by genetically engineered Chinese hamster ovary cells (CHOC) and differs from the human GCase at position 495 where an arginine residue has been replaced by a histidine. The enzymes generated by the CHOC have complex oligosaccharide chains at three of the four glycosylation sites on the enzyme and are expressed as a glycoprotein terminating with sialyl or galactosyl groups.<sup>30</sup> In order for Cerezyme to be properly recognized by the mannose receptors on macrophages, the primary cell type involved in Gaucher disease, the glycan chains must terminate with mannose residues. To produce terminal mannose residues on the glycan chains, the enzyme is treated with neuraminidase,  $\beta$ -galactosidase, and  $\beta$ -N acetylglucosaminidase. A third generation enzyme, Velaglucerase, has been

recently produced in fibrosarcoma cells and contains highly mannosylated chains that terminate in mannose, thus avoiding the costly enzymatic glycan modification steps required for Cerezyme. Dispute over whether Velaglucerase has greater uptake than Cerezyme due to the extent of mannose expression on the enzyme surface cannot be proven due to the current inability to track and monitor the extent of enzyme uptake within affected cells or diseased organs. This highlights the need for improved methods to monitor the biodistribution of exogenously administered enzyme in order to evaluate new forms of the enzyme, improve the efficiency of recombinant enzyme therapeutics and develop the most effective treatment options.

### **1.3 Research Objectives**

There are two main aims of this thesis. The first is the synthesis and enzymatic evaluation of novel aminocyclitols as potential chemical chaperones for the treatment of Gaucher disease. Various aminocyclitol derivatives have been synthesized in order to determine the influence of alkyl chain length and chain position on affinity towards recombinant GCCase. Various combinations of chain length and position can allow for the generation of more specific and efficient pharmacological chaperones to treat the various forms of Gaucher disease. The second aim is the synthesis and enzymatic evaluation of alkylated aziridine derived aminocyclitols that are hypothesized to act as mechanism-based inhibitors of glycosidases. By alkylating the aziridine with a hydrophobic moiety we aim to generate a specific and effective inactivator of GCCase useful for cell studies, a potential activity based probe for analyzing GCCase activity in complex mixtures, and a fluorescent or radioactive labelling agent potentially useful for tracking the injected enzyme in vivo using non-invasive procedures such as optical or PET imaging.

## Part A: Aminocyclitol Competitive Inhibitors of Glucocerebrosidase

### 1.4 Introduction

#### 1.4.1 Non-covalent Glycosidase Inhibitors

Non-covalent glycosidase inhibitors are among the most studied glycosidase inhibitors. The majority of these compounds have been discovered in nature<sup>11a</sup> or designed to resemble the transition state structure of the hydrolysis reaction.<sup>11c</sup> Estimated from the rate enhancement of glycosidases of  $10^{17}(k_{\text{cat}}/k_{\text{non}})$ , the dissociation constant of the transition state must be less than  $10^{-22} \text{ M}^{11c}$  indicating the theoretical possibility of analogue inhibitors with  $K_i$  in the same magnitude.<sup>11b</sup> There are a number of different types of natural compounds that mimic the transition state structure such as piperidines, pyrrolidines, indolizidines, pyrrolizidines, and nortropanes.<sup>11a</sup> Some of the most thoroughly studied inhibitors include the iminosugars<sup>11-12, 31</sup> and aminocyclitols.<sup>31a, 32</sup> Both the iminosugars and aminocyclitols are heterocyclic polyhydroxylated compounds containing a nitrogen atom that is protonated and positively charged at physiological pH. Some examples of iminosugars are deoxynojirimycin (DNJ), fagomine (FG), and isofagomine (IFG) (**Figure 1.4.1**).

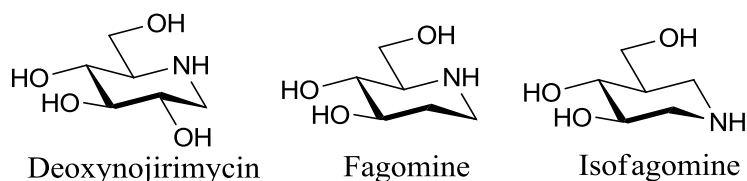


**Figure 1.4.1:** Examples of potent non-covalent iminosugar inhibitors

DNJ was first synthesized in 1968 and was later isolated from Mulberry tree roots and from multiple strains of *Bacillus* and *Streptomyces*.<sup>11a</sup> FG is a naturally occurring compound isolated from the seeds of Japanese buckwheat and Moreton Bay chestnut.<sup>11a</sup> IFG was rationally designed as a glycosidase inhibitor and synthesized in 1994.<sup>33</sup> DNJ has comparable  $K_i$  values to IFG while IFG generally exhibits a greater ability to inhibit the activity of glycosidases than FG. Both DNJ and IFG are in a chair

conformation and are positively charged under physiological conditions but differ in both the positioning of the nitrogen atom and the lack of 2-hydroxyl group found in IFG.<sup>34</sup> It has been shown that the removal of the hydroxyl group in IFG does not substantially influence its affinity to  $\alpha$ - and  $\beta$ -glycosidases.<sup>34</sup> Deoxynojirimycin was shown to have  $K_i$  values of 47 $\mu$ M, and 25 $\mu$ M while isofagomine has  $K_i$  values of 0.11 $\mu$ M and 86 $\mu$ M with  $\beta$ -glucosidase (sweet almonds) and  $\alpha$ -glucosidase (yeast) respectively.<sup>34</sup> This suggests that the positively charged nitrogen of the glucosidase inhibitors should be at the anomeric position to specifically target  $\beta$ -glucosidases and in the position adjacent to the anomeric carbon to target  $\alpha$ -glucosidases. An explanation for the observed differences in binding affinity for DNJ and IFG towards  $\alpha$  and  $\beta$  glycosidases was hypothesized by Withers<sup>4b</sup> to involve *syn* interactions between the oxygens of the nucleophilic carboxylate with the anomeric carbon and 2-hydroxyl group of the substrate in  $\beta$ -glycosidases. In contrast, there is *syn* interaction between the oxygens of the nucleophilic carboxylate with the anomeric carbon and endocyclic oxygen in  $\alpha$ -glycosidases (**Figure 1.4.2 a) and b)**). This theory is supported by the observation that isofagomine, with a nitrogen at the anomeric position of the glucose substrate, results in greater inhibition of  $\beta$ -glycosidases while deoxynojirimycin, with the nitrogen at the adjacent position, has stronger inhibition of  $\alpha$ -glycosidases (**Figure 1.4.2 c) and d)**). These observations demonstrate that inhibitor specificity to the desired glycosidase may be tailored by adding a positively charged atom in the position favored by the target glycosidase.

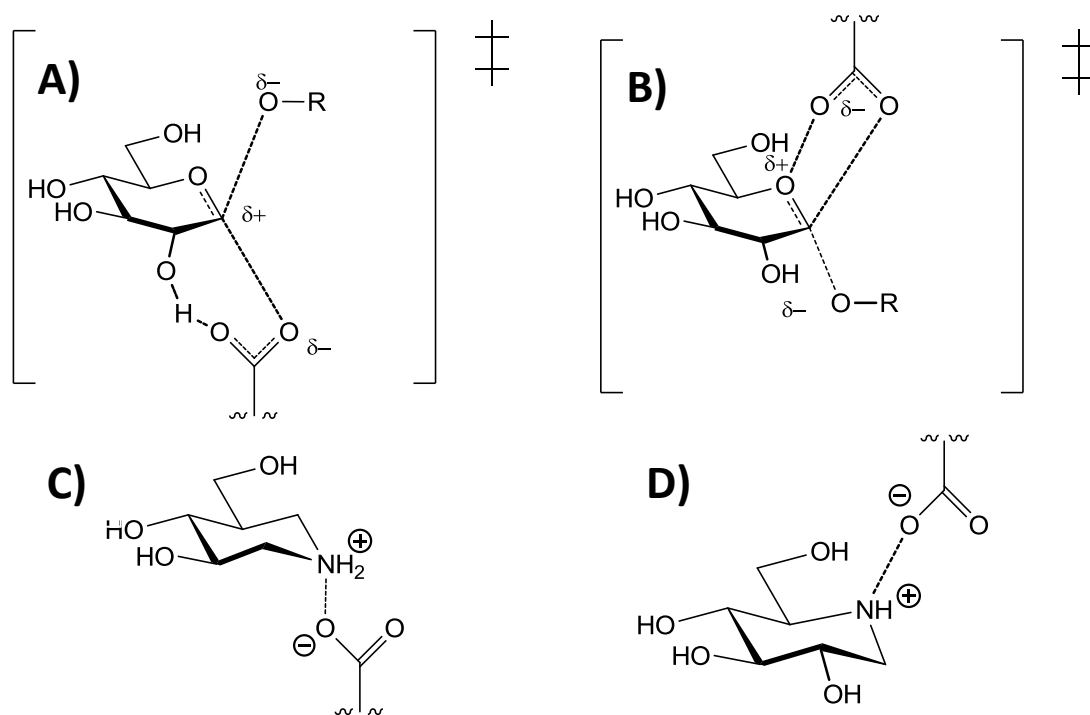


**Figure 1.4.2:** Proposed transition states for A)  $\beta$ -glucosidase, B)  $\alpha$ -glucosidase. Corresponding inhibitors C) Isofagomine, D) deoxynojirimycin. Adapted from Zechel and Withers.<sup>4b</sup>

Aminocyclitols have recently been studied as glycosidase inhibitors because of their antibiotic properties.<sup>35</sup> It was discovered in the 1970s that saccharide compounds containing a valienamine component were capable of inhibiting  $\alpha$ -glucosidase activity in the intestines.<sup>36</sup> Effort was then put forth to develop inhibitors containing the valienamine and valioline components as potential therapeutic agents for diabetes by limiting monosaccharide uptake in the intestines through inhibition of intestinal  $\alpha$ -glycosidases (**Figure 1.4.3**).<sup>11c, 36</sup> This later expanded into the development of novel aminocyclitols designed to inhibit a variety of different glycosidase targets. Of particular interest were a number of inosamine derivatives that displayed promise as inhibitors of glucocerebrosidase (GCase), the  $\beta$ -glucosidase involved in Gaucher disease.<sup>32a</sup> These compounds were derivatives of a myo-inositol with one of the hydroxyl groups replaced with an alkylated nitrogen showing micromolar  $K_i$  values towards the recombinant glucocerebrosidase, imiglucerase (**Figure 1.4.3**).<sup>32a</sup> Initial results show that inosamine

derivatives can function as potent inhibitors of GCase, but derivatives are needed to understand the structure-function relationships in order to optimize  $K_i$  values while improving aqueous solubility, membrane permeability, glucosidase selectivity and chemical stability.

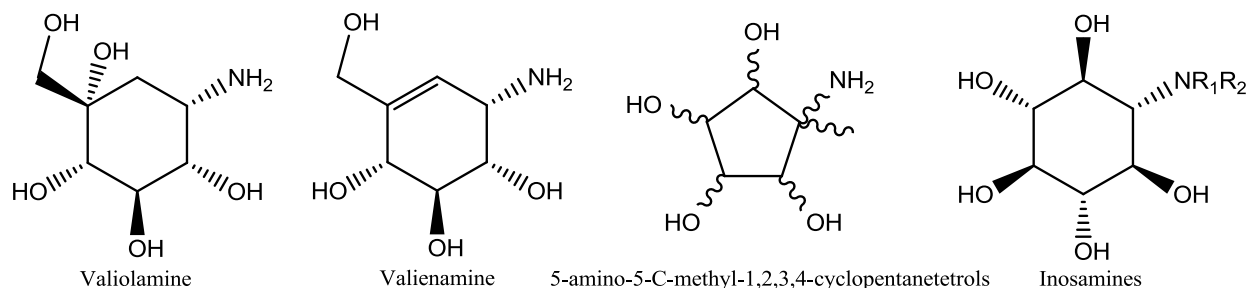


**Figure 1.4.3:** Examples of non-covalent inosamine glucosidase inhibitors<sup>32a, 36-37</sup>

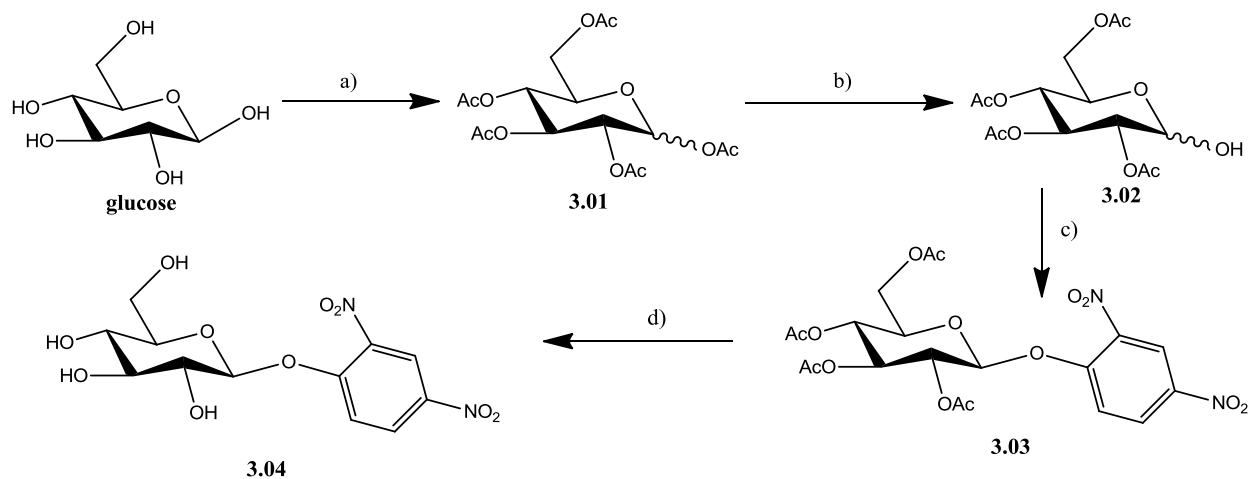
## Chapter 2: Results and Discussion

### 2.1 Synthesis

#### 2.1.1 Synthesis of Substrate 2,4-dinitrophenyl- $\beta$ -D-glucopyranoside (2,4-DNP- $\beta$ -D-glc)

Several colorimetric substrates have been synthesized and used for kinetic studies on GCase. Of them, 2,4-dinitrophenyl- $\beta$ -D-glucopyranoside is the most commonly used because it is readily hydrolyzed by  $\beta$ -glucosidases, it releases 2,4-dinitrophenolate that strongly absorbs at 400nm under acidic pH enabling continuous assays and is conveniently synthesized. Because this substrate is not commercially available, 2,4-DNP- $\beta$ -D-Glc was synthesized as shown in **Scheme 2.1**.

### Scheme 2.1: Synthesis of the Substrate 2,4-dinitrophenyl- $\beta$ -D-Glucopyranoside



Reagents and conditions: **a)**  $\text{Ac}_2\text{O}$ , pyr,  $0^\circ\text{C}$ -RT, 17Hrs, 95%, **b)** hydrazine acetate, DMF,  $55^\circ\text{C}$ , 2Hrs, 91%, **c)** 2,4-dinitrofluorobenzene, DABCO, DMF, RT, Dark, 51-61%, **d)**  $\text{AcCl}$ , MeOH,  $4^\circ\text{C}$ , 48Hrs, 37%.

Compound **3.01** was synthesized by treating D-Glucose with acetic anhydride in pyridine, resulting in a mixture of the  $\alpha$ - and  $\beta$ - anomer (92:8 ratio).<sup>38</sup> The selective removal of acetate from the anomeric group was achieved by hydrazine acetate in DMF to produce compound **3.02** which rapidly interconverts between the  $\alpha$  and  $\beta$  forms.<sup>39</sup> DABCO, a sterically hindered base, was utilized in the nucleophilic aromatic substitution of 2,4-dinitrofluorobenzene resulting in the selective formation of the  $\beta$  anomer (9:1 ratio) of **3.03** in 51-61% yield.<sup>40</sup> The stereoselectivity of this reaction has been attributed to steric hindrance of 2,4-dinitrophenol which favors the equatorial position and the kinetic anomeric effect or the  $\beta$ -effect where the nucleophilicity of the alkoxide is enhanced by electron-electron repulsion from both lone pairs of the ring oxygen when in the equatorial position.<sup>41</sup> Purification of the  $\beta$  from the  $\alpha$  anomer was easily accomplished by recrystallization in ethanol. Global deprotection of the acetyl groups proceeded in  $\text{HCl}$ /methanol followed by purification on silica gel and recrystallization in methanol-diethyl ether to give compound **3.04** in 37% yield.

### 2.1.2 Synthesis of N-alkylated Inhibitors

The design of lead compounds to be used as competitive inhibitors of GCCase would require a molecule structurally similar to GlcCer, a feature which may add high affinity and specificity to GCCase. GlcCer contains a polyhydroxylated  $\beta$ -D-glucose scaffold with a long branching lipophilic ceramide moiety at the anomeric position (**Scheme 1.2.3**). Inositol is a polyhydroxylated cyclohexane ring and can be considered a glucose mimic because of the equatorial positions of all hydroxyl groups. To mimic the hydrophobic ceramide varying lengths of carbon chains could be installed onto the cyclohexane ring thus introducing the potential for hydrophobic interactions inside the ceramide binding site of GCCase. Additionally, a permanently positive charge added to the inhibitor may mimic the oxocarbenium-ion like transition state typical of  $\beta$ -retaining glucosidases like GCCase as well as introduce potential ionic interactions with the active site glutamate. Collectively, inositol derivatives containing five hydroxyls in equatorial positions at C2-C6 and a positively charged amine at C1 modified with lipophilic chains of varying lengths could be used to evaluate the structure-activity relationships of the alkylated aminocyclitols with GCCase.

Compound **3.07** was synthesized following literature procedures by heating 2,2-dimethoxypropane in the presence of toluene sulphonic acid.<sup>42</sup> Selective formation of the thermodynamically favored trans-isopropylidene was achieved at high temperature followed by cooling the reaction to room temperature allowing time for hydrolysis of the less stable *cis*-isopropylidene kinetic product in ethanol and diethyl ether over 2 hours. Neutralization with triethylamine immediately initiates precipitation of **3.05** which is subsequently purified by recrystallization from ethanol to give **3.05** in 62% yield. Benzylation of **3.05** in DMF was achieved by deprotonating the remaining hydroxyl groups of inositol with NaH followed by nucleophilic substitution by benzyl bromide.<sup>43</sup> Aqueous workup and purification on silica gel provided **3.06** in 80% yield. Removal of isopropylidene was accomplished in refluxing AcOH and water followed by purification on silica gel to give diol **3.07** as a white powder in

66% yield. Regioselective protection of the equatorial hydroxyl group of diol **3.07** was achieved by nucleophilic enhancement of the equatorial oxygen.<sup>44</sup> The procedure begins by forming the stannylene complex by refluxing the compound in the presence of dibutyltin oxide in toluene using a Dean-Stark apparatus to remove the generated water.<sup>45</sup> Association of two stannylene complexes results in axial hydroxyl groups interacting with two tin atoms while equatorial groups interact with a single tin atom. This causes the equatorial oxygens to hold a greater negative charge allowing for selective nucleophilic substitution in the equatorial position. Once the stannylene was formed, the toluene was removed and replaced with acetonitrile, a solvent which coordinates with tin in the stannylene intermediate to further enhance the nucleophilicity of the oxygen atoms.<sup>44</sup> Finally, fluoride ion was added to the reaction as a catalyst to give **3.08** in 80% yield.<sup>44</sup> Danishefsky,<sup>46</sup> and later clarified by Nagashima,<sup>47</sup> hypothesized that the fluoride anion attacks the tin atom to form a pentacoordinated complex that can dissociate resulting in a highly reactive alkoxide atom *in situ*.<sup>48</sup> The introduction of a nitrogen containing group at carbon 2 as well as conversion of the inositol from the myo to the scyllo configuration was achieved by mesylation of the free hydroxyl group followed by azidolysis with sodium azide in DMF. The S<sub>N</sub>2 mechanism provided the scyllo-azide **3.09** at 69% yield over both steps. Reduction of the azide with lithium aluminum hydride in THF provided the primary amine **3.09** in 98% yield. Previous reports describe the reductive amination of the inosamine with an aldehyde in the presence of sodium cyanoborohydride and acetic acid.<sup>49</sup> However, this method suffered from slow reaction times and a large quantity of dialkylated side product while leaving unreacted starting material. An improved stepwise method was found which involved generating a large quantity of the imine by using excess aldehyde in methanol followed by rapid reduction of both imine and aldehyde by using the stronger reducing agent NaBH<sub>4</sub>.<sup>50</sup> The stepwise reductive amination method prevents dialkylation and provided compound **3.10** at 70% yield compared to the concerted method at 25% yield. The presence of the N-alkylated product was confirmed by the characteristic quartet of triplets (J = 11, 7Hz) at ~δ 2.8 ppm in

the  $^1\text{H}$  NMR spectrum (**appendix page 110**) corresponding to the two hydrogens of the first carbon on the alkyl chain. Global deprotection of the benzylated inosamine **3.11** using hydrogenolysis with Pd/C and  $\text{H}_2$  proved to be exceptionally difficult as observed with similar compounds.<sup>51</sup> Initial attempts following a published procedure<sup>52</sup> failed to deprotect the benzyl ethers in our hands. THF is known to form clathrate cages to trap hydrogen gas and promote hydrogenolysis reactions.<sup>53</sup> Although the use of THF produced partially debenzylated products after several days under atmospheric pressure, the reaction stalled most likely due to poisoning of the Pd/C catalyst. Despite the low yields, we were able to isolate small amounts of **3.12** for NMR using flash column chromatography. Interestingly, the NMR spectrum appeared to confirm the structure of **3.12**, however, broad peaks without distinct coupling patterns were obtained regardless of concentration of products and solvent choice. We hypothesized that Pd may be coordinated to the inosamine ring thus affecting the NMR spectrum through line broadening effects. To further investigate this hypothesis, we dissolved the isolated inosamine **3.12** in water followed by the addition of  $\text{NH}_4\text{OH}$ , conditions known to form an insoluble  $(\text{NH}_3)_2\text{PdCl}_2$  complex. Addition of the  $\text{NH}_4\text{OH}$  to compound **3.12** resulted in the formation of a dark precipitate indicating the presence of contaminating Pd/C. A decrease in the overall mass by 64% resulted, corresponding to the loss of a single Pd/C per two molecules of **3.12**. After Pd/C removal the NMR spectrum sharpened considerably as shown in **Figure 2.1**. Although this procedure produced **3.12** in only 25% yield, sufficient quantities of the aminocyclitol were obtained in order to conduct inhibitor studies. Interestingly, the NMR spectra of several previously published aminocyclitols appear to suggest Pd contamination in some of their samples thus questioning the validity of the biological data obtained.<sup>32c, 32d, 54</sup>

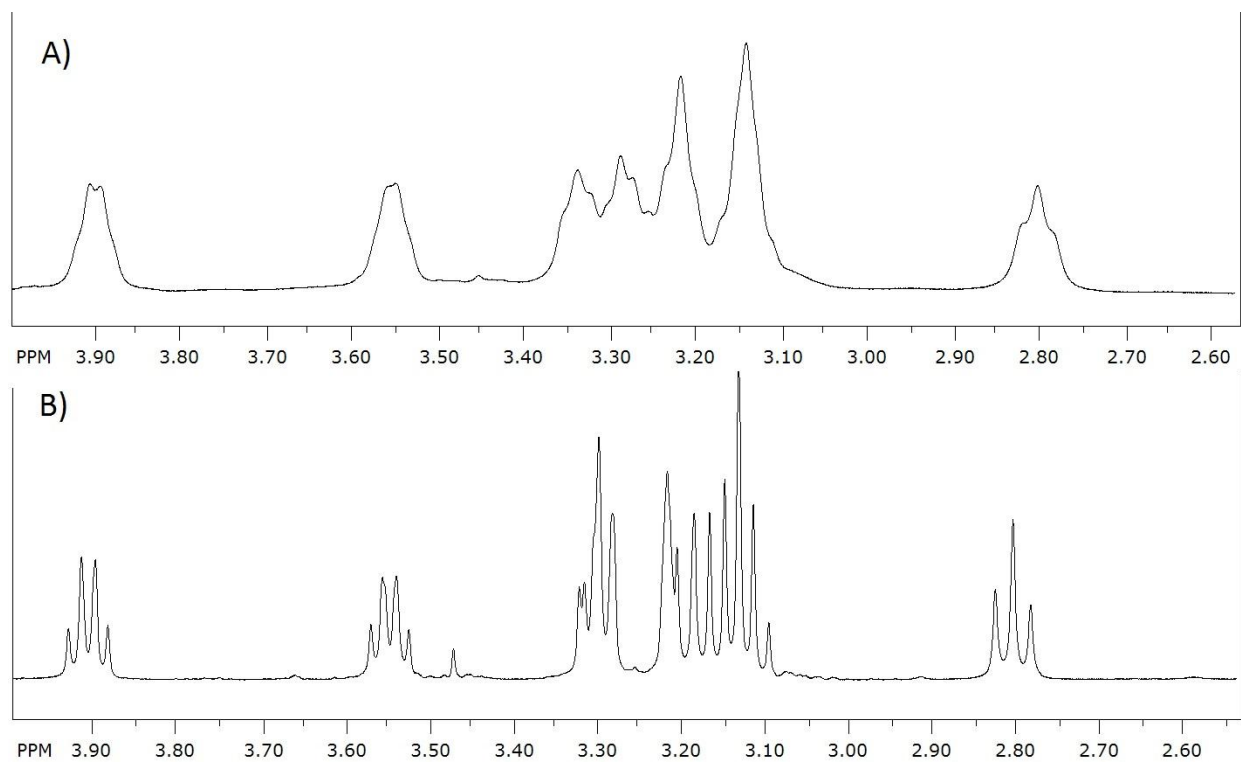
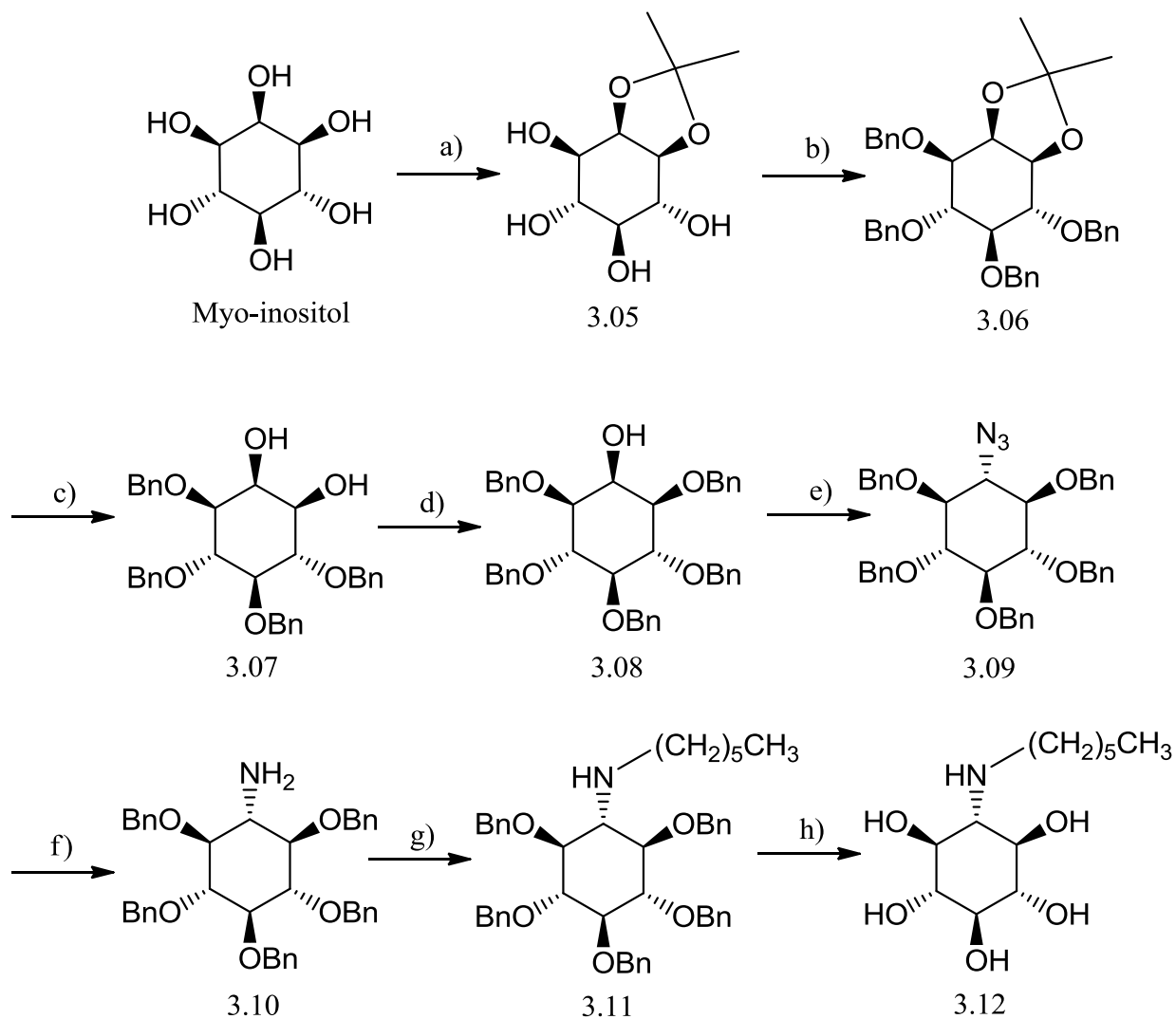


**Figure 2.1:** NMR spectra of **3.20** **A)** Compound hypothesized to be chelated to Pd/C. **B)** Compound after precipitation of Pd/C.

**Scheme 2.2: Synthesis of N-alkylated Inhibitors**



Reagents and Conditions: **(a)** 2,2-DMP, TsOH, DMSO, EtOH, 90°C; then add Et<sub>2</sub>O, Et<sub>3</sub>N, rt, 62% **(b)** NaH, BnBr, DMF, 0°C – rt **(c)** HOAc, H<sub>2</sub>O, reflux, 53% **(d)** dibutyltin oxide, BnBr, CH<sub>3</sub>CN, tetrabutylammonium bromide, 80% **(e)** 1) Mesyl Chloride, pyr, rt. 2) NaN<sub>3</sub>, DMF, 85°C 69% **(f)** LiAlH<sub>4</sub>, Et<sub>2</sub>O, 0°C – rt. 100% **(g)** n-C<sub>6</sub>H<sub>12</sub>O, NaBH<sub>3</sub>CN, MeOH 25% **(h)** Pd/C, MeOH, HCl, H<sub>2</sub> (50PSI).

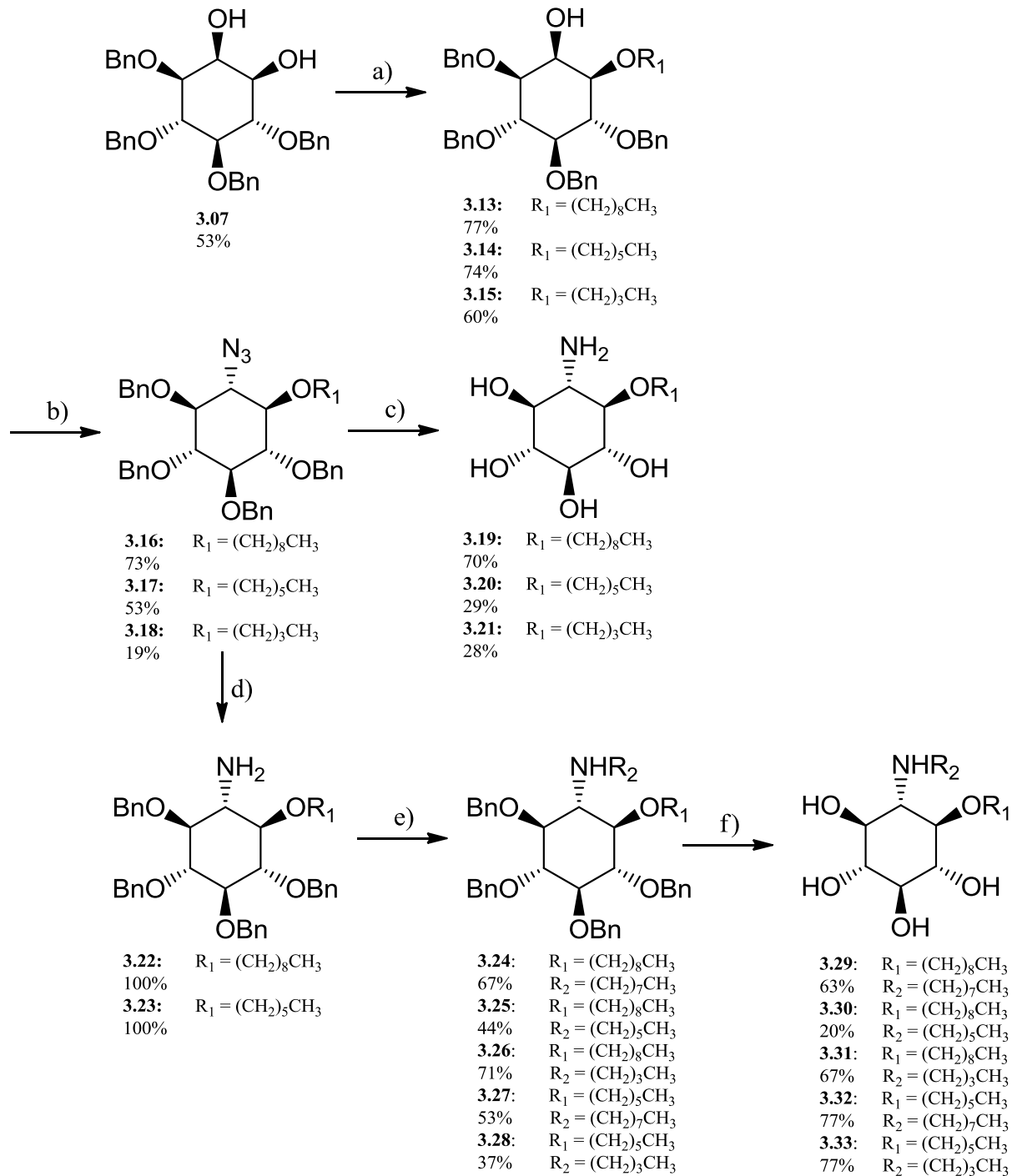
### 2.1.3 Synthesis of O-alkylated Inhibitors and O- and N-alkylated Inhibitors

Synthesis of the O- and N-alkylated inhibitors started from the racemic tetrabenzyl inositol **3.07** shown in **Scheme 2.3**. Selective alkylation of the equatorial hydroxyl group was performed using the dibutyltin oxide method described above. Alkylation of the equatorial oxygen was achieved with the corresponding 1-bromo alkane in DMF utilizing CsF as a fluoride catalyst provided the butyl, hexyl, and octyl derivatives, **3.18**, **3.17**, and **3.16**, in 60%, 74%, and 77% yields respectively. The presence of the O-alkylated derivative was confirmed by two characteristic doublet of triplets ( $J = 7, 6\text{Hz}$ ) that can appear as a quartet at  $\sim\delta 3.6$  and  $\sim\delta 3.7$  and correspond to diastereotopic hydrogens from the first carbon of the alkyl chain. Conversion of the free secondary alcohol to inverted azide was facilitated by mesylation followed by azidolysis. After the azidolysis reaction, reduction with  $\text{LiAlH}_4$  afforded the corresponding protected primary amine. Reduction of the azide and hydrogenolysis of the benzyl ethers was achieved by Pd/C, HCl, and MeOH with  $\text{H}_{2(g)}$  at 50 PSI to provide the primary amines **3.19**, **3.20**, and **3.21** in 70%, 29%, and 28% yield respectively. As observed for compound **3.12**, chelation of the free aminocyclitols to Pd/C appeared to occur for the hexyl and butyl chain compounds **3.20** and **3.21** using NMR and the  $\text{NH}_4\text{OH}$  precipitation method. Interestingly, nonyl inosamine **3.19** did not appear to have sufficient affinity for Pd as the shorter chain derivatives which was reflected in the much higher recoverable yield and distinct peaks in the NMR spectrum (**appendix page 116**).

To generate the O- and N-alkylated inhibitors we first reduced the azides using lithium aluminum hydride in THF to provide the primary amines **3.22** and **3.23** in quantitative yield. Alkylation of the amine was achieved by using the two step reductive amination discussed above for compounds **3.24-3.28**. The presence of the N-alkylated product was again confirmed by the presence of a characteristic quartet of triplets ( $J = 11, 7\text{Hz}$ ) at  $\sim\delta 2.8\text{ppm}$  corresponding to the two hydrogens of the first carbon on the alkyl chain. Hydrogenolysis of the benzyl ethers was achieved by Pd/C, HCl, and MeOH with  $\text{H}_{2(g)}$  at 50 PSI to provide the O- and N-alkylated compounds **3.29**, **3.30**, **3.31**, **3.32**, and **3.33**

in 63%, 20%, 67%, 77% and 77% yield respectively. As observed for the nonyl inosamine derivative **3.19**, no visible precipitation of Pd/C was observed for the dialkylated compounds after the addition of  $\text{NH}_4\text{OH}$ , demonstrating that these compounds did not form a stable complex with Pd. In addition, clear coupling patterns were observed in NMR spectra clearly indicating the lack of Pd contamination.

**Scheme 2.3: Synthesis of O- and N-alkylated Inhibitors**



Reagents and Conditions: **(a)** 1) Dibutyltin oxide, toluene, reflux 2) CsF, n-C<sub>8</sub>H<sub>17</sub>Br or n-C<sub>6</sub>H<sub>13</sub>Br, DMF **(b)**

**1)** Mesyl Chloride, pyr, rt. **2)** NaN<sub>3</sub>, DMF, 85°C **(c)** Pd/C, MeOH, HCl, H<sub>2</sub> (50PSI) **(d)** LiAlH<sub>4</sub>, Et<sub>2</sub>O, 0°C – rt.

**(e)** n-C<sub>8</sub>H<sub>16</sub>O or n-C<sub>6</sub>H<sub>12</sub>O or n-C<sub>4</sub>H<sub>8</sub>O, NaBH<sub>4</sub>, MeOH **(f)** Pd/C, MeOH, HCl, H<sub>2</sub> (50PSI)

## 2.2 Expression and Purification of a Model $\beta$ -glucosidase ABG

*Agrobacterium sp.*  $\beta$ -Glucosidase (ABG) is a well-studied, inexpensive and stable  $\beta$ -glucosidase often used as an initial control enzyme for evaluating novel glycosidase inhibitors. The enzyme is readily produced from *Escherichia coli*, is accepting of unnatural colorimetric substrates and has been subjected to a variety of  $\beta$ -glucosidase inhibitor studies.<sup>10, 55</sup> Importantly, both ABG and GCase are retaining enzymes and employ the double displacement mechanism relying on a pair of Glu residues in the enzyme active site.<sup>55a</sup> The ABG gene was kindly provided by Dr. Stephen Withers in a pET28b expression plasmid that is engineered to produce a hexahistidine-tagged enzyme in *Escherichia coli*. Expression and purification of ABG using Ni-NTA affinity column chromatography yielded pure enzyme as shown in

**Figure 2.2.**

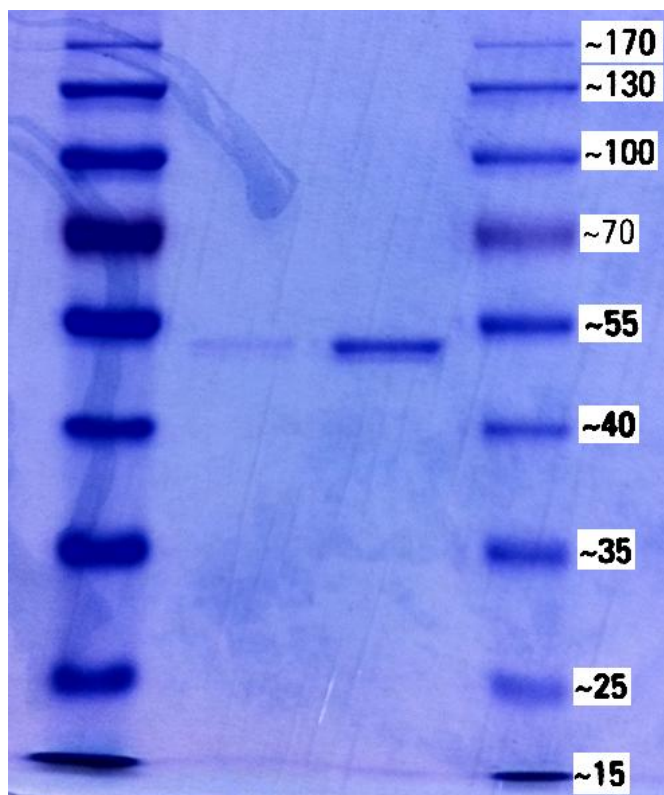


**Figure 2.2:** SDS-PAGE of purified ABG solution. Lanes 1 and 4) PageRuler prestained protein ladder. Lane 2) 5  $\mu$ L ABG solution. Lane 3) 10  $\mu$ L ABG solution

### 2.3 Enzyme Inhibition Studies with ABG and GCase

All synthesized potential chaperone compounds were evaluated as competitive inhibitors of ABG and GCase. Although there is no crystal structure for ABG, it is known from substrate specificity and inhibition studies that ABG does not possess a well-defined or large hydrophobic binding pocket adjacent to the active site. Therefore, inhibitors with hydrophobic groups should have lower  $K_i$  values for GCase over ABG. As a consequence, comparing inhibitor activities with ABG and GCase allows for insight into the reactivity and specificity of the inhibitors with the other  $\beta$ -glucosidases that would be present in a living system.

The concentrations of the synthetic substrate 2,4-DNP- $\beta$ -D-Glc were chosen to be within a range ( $5 \times K_M$  to  $K_M/3$ ). Michaelis-Menten curves were generated for each enzyme to verify that the  $K_M$  is comparable to literature values where the  $K_M$  of 2,4-DNP- $\beta$ -D-Glc for ABG is 31  $\mu$ M,<sup>55a</sup> and GCase is 1.6 mM.<sup>56</sup> In all cases, initial rates were monitored at 400 nm and were well within the linear region of each time activity curve. Each inhibitor was tested at six concentrations that were determined by using a crude  $IC_{50}$  value to estimate the  $K_i$  value. The data was fit to the competitive inhibition equation using the GraphPad Prism software utilizing **Equation 2.1** where  $V$  = initial velocity,  $K_M$  is the Michaelis constant of the substrate,  $V_{max}$  is the maximum reaction velocity,  $[I]$  is inhibitor concentration,  $[S]$  is substrate concentration and  $K_i$  is the dissociation constant for the enzyme-inhibitor complex.

**Equation 2.1:**

$$V = \frac{V_{max}[S]}{K_m \left(1 + \frac{[I]}{K_i}\right) + [S]}$$

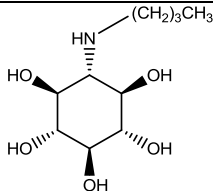
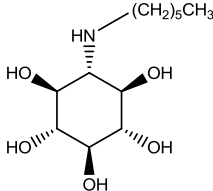
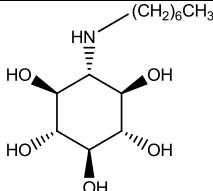
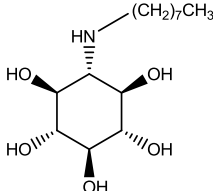
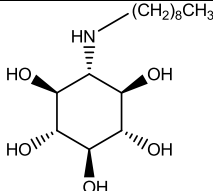
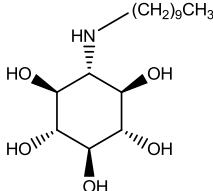
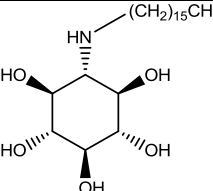
This equation remains valid under steady state conditions and when  $[S]$  and  $[I]$  are much greater than  $[E]$ . The  $[S]$  and  $[I]$  must be much greater than  $[E]$  in order to ensure that the total concentrations of  $[S]$  and  $[I]$  are consistent while monitoring initial enzymatic rates in the presence of inhibitor. If the concentrations of  $[S]$  and  $[I]$  are approaching to or less than  $[E]$ , the case when assays are performed on

low nM level competitive inhibitors, the concentration of [I] is significantly lowered when bound to the enzyme.<sup>57</sup> For all of our inhibition assays, [S] and [I] are  $> 10 \times [E]$  thus fulfilling the mathematical requirements to solve for  $K_i$ . Representation and analysis of competitive inhibition data was historically done through the use of Lineweaver-Burke transformations due to the limited availability of nonlinear regression algorithms and the visual appeal of the Lineweaver-Burke linear regression model. However, determining  $K_i$  values requires transformation of the data from non-linear into linear representation which distorts experimental errors at low concentrations of inhibitor and substrate.<sup>58</sup> This model has been proven obsolete due to violating assumptions of linear regression which requires uncertainty values to be known resulting in inaccurate calculations of slopes and intercepts.<sup>58-59</sup> Therefore, non-linear regression analysis with the Graphpad Prism software was used to calculate  $K_i$  values and associated error for all inhibitors tested in this thesis and the corresponding graphs are shown for each assay.

### **2.3.1 Kinetic Analysis of the Inhibition of ABG and GCase by the N-alkylated Inhibitor 3.12**

Compound **3.12** was the only inhibitor synthesized over the course of this work that was alkylated solely at the nitrogen of the inosamine ring. Previous reports indicate that a series of N-alkylated scyllo-inosamine inhibitors of various alkyl chain lengths do indeed bind to GCase with increasing affinity corresponding to chain length increases from 4 to 16 carbons.<sup>32b, 32c</sup> We sought to synthesize an N-alkylated inhibitor to compare our compound against existing inhibitors and to validate our enzyme preparations and kinetic methods. Compound **3.12** was synthesized and tested against GCase using competitive inhibition and yielded a  $K_i$  value that fit well within the expected range from the series of inhibitors that can be seen in **Table 2.3.1**.

**Table 2.3.1:**  $K_i$  values and comparison of N-alkylated competitive inhibitors

Inhibitor Structure	$K_i$ ( $\mu\text{M}$ )	Relative Binding Affinity
	39.4	1
 <p><b>3.12</b></p>	$17.8 \pm 1.42$	2.21
	15.5	2.54
	10.4	3.79
	1.9	20.7
	0.3	131
	0.4	98.5

\*Data for **3.12** came from this work, all other data came from Egido-Gabas et al.<sup>32b</sup>

The  $K_i$  value obtained for **3.12** follows the trend published by Egido-Gabas<sup>32b</sup> indicating our enzyme kinetic assays used to evaluate our inhibitors were valid. This was especially critical considering Dr. Lorne Clark from Children's Hospital in Vancouver provided us with Cerezyme from left-over patient vials. Therefore, we wanted to confirm that the enzyme preparation was fully active and properly stored. The non-linear regression plot for **3.12** with ABG and GCCase can be seen in **Figure 2.3.1**.

When analyzing the data obtained from previously reported N-alkylated inosamines, several important trends emerge. To begin, only modest improvements were observed upon increasing chain length from the pentyl to the octyl chains. This indicates that the alkyl chain must be at least 8 carbons long to significantly occupy the hydrophobic pocket of GCCase. A second interesting point was that the 16 carbon derivative showed lower binding affinity or an increased  $K_i$  when compared to the 10 carbon derivative.<sup>32b</sup> This was an unexpected result since the length of the ceramide hydrophobic chain is 16 carbons. To help understand the kinetic components of binding affinity, the inhibition constant can be expressed as the ratio between the rate of inhibitor dissociation and the rate of inhibitor association (**Equation 2.2**). Therefore, compounds having very low  $K_i$  values must rapidly bind to the protein and only very slowly dissociate away from the binding site.

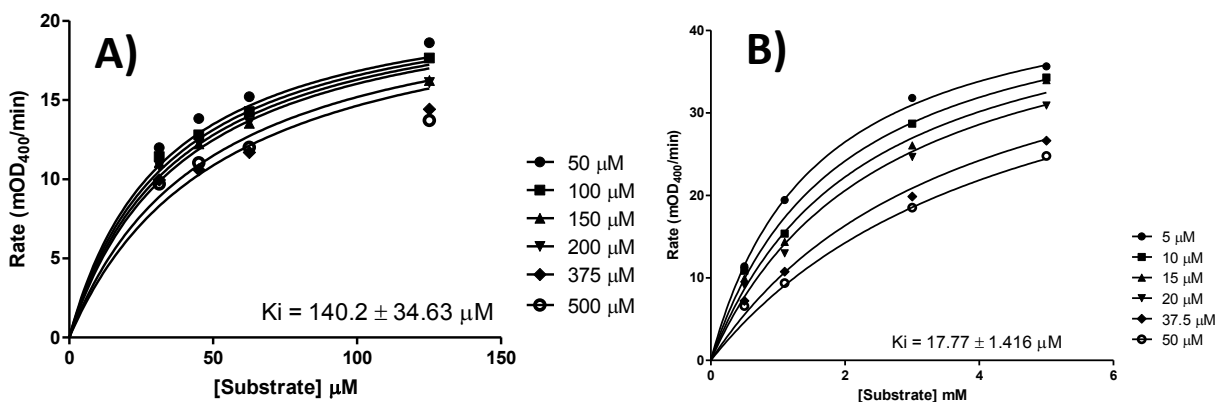
**Equation 2.2:**

$$K_i = \frac{k_{-i}}{k_i}$$

The increased  $K_i$  from the 16 carbon inhibitor with respect to the 10 carbon inhibitor would imply that although the dissociation of the inhibitor ( $k_{-i}$ ) may be slower through stronger binding, the rate at which the 16 carbon inhibitor binds ( $k_i$ ) was decreased resulting in the increased  $K_i$ . However, it is currently unknown how GCCase catalyzes the hydrolysis of the GlcCer in the natural environment with the help of saposin C. It is likely that the lipid chain is partially buried in the membrane bilayer or saposin C during hydrolysis by GCCase. Alternatively, the 16 carbon inosamine derivative may have low solubility under the assay conditions used. As a consequence, aggregation of the inhibitor and non-

specific inhibition of GCCase may occur as occasionally observed in poorly soluble compounds.<sup>60</sup> The inhibition of another enzyme was not performed over the course of Delgado's work and therefore aggregation of the alkylated inosamine and non-specific inhibition cannot be ruled out.

To ensure that our compound **3.12** inhibited other  $\beta$ -glucosidases and did not possess a reactive contaminant or form inhibitor aggregates, we used ABG as a control enzyme. As expected, **3.12** was a good inhibitor of ABG but not to the same extent as GCCase. In addition, the presence of the N-alkyl chain did not improve binding affinity when compared to the known inhibitor gluconolactone (with a  $K_i$  = 1.4  $\mu$ M determined in our lab consistent with previously published results).<sup>55b</sup> This data clearly demonstrates that the inhibitor preparation contained no reactive contaminants, did not form inhibitor aggregates and the assay conditions used were suitable for both GCCase and ABG.

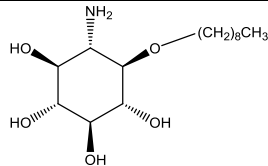
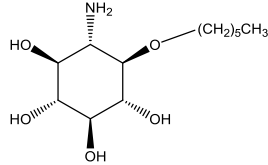
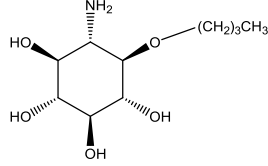


**Figure 2.3.1:** Nonlinear regression plots of the competitive inhibitor **3.12** using the substrate 2,4-DNP- $\beta$ -D-Glc. A) Inhibition of ABG. B) Inhibition of GCCase.

### 2.3.2 Kinetic Analysis of the Inhibition of ABG and GCCase by O-alkylated Inhibitors **3.19**, **3.20** and **3.21**

When we were confident that ABG and GCCase were producing data consistent with previous studies and our enzymatic assays were reliable, we next investigated the influence of alkyl chain length on the O-alkylated inosamine derivatives inhibitors **3.19**, **3.20** and **3.21**.

**Table 2.3.2**  $K_i$  values and comparison of O-alkylated competitive inhibitors

Inhibitor Structure	ID	GCCase $K_i$ ( $\mu\text{M}$ )	Relative Affinity with GCCase	ABG $K_i$ ( $\mu\text{M}$ )	Relative Affinity with ABG
	<b>3.19</b>	$7.40 \pm 1.13$ $\mu\text{M}$	11.3	$93.8 \pm 9.10$ $\mu\text{M}$	9.08
	<b>3.20</b>	$77.7 \pm 14.0$ $\mu\text{M}$	1.07	$849 \pm 131$ $\mu\text{M}$	1.00
	<b>3.21</b>	$83.3 \pm 12.9$ $\mu\text{M}$	1.00	$852 \pm 122$ $\mu\text{M}$	1.00

From the  $K_i$  values of the O-alkylated inosamines we observe that increasing the alkyl chain length corresponded to a higher affinity or a lower  $K_i$  value for GCCase, similar to what was reported for the N-alkylated inhibitors. The O-nonyl derivative **3.19** shows a  $K_i$  value in the low  $\mu\text{M}$  range, a value consistent with the octyl and nonyl N-alkylated derivatives.

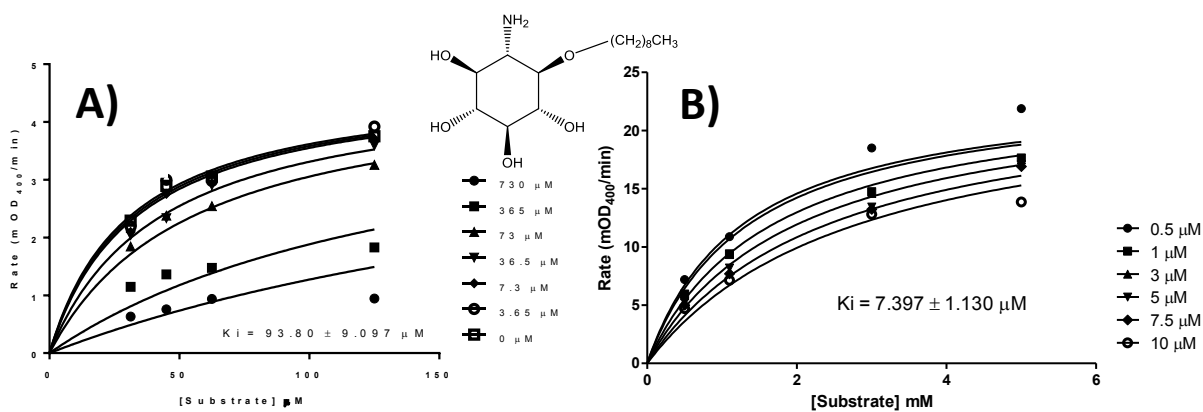


**Figure 2.3.2:** Nonlinear regression plots of the competitive inhibitor **3.19** using the substrate 2,4-DNP-β-D-Glc A)Inhibition of ABG. B) Inhibition of GCCase.

This indicates that the position of the alkyl chain in relation to the positively charged amine may not dramatically affect molecular recognition, suggesting that N,O-dialkylated inosamines may be very potent inhibitors. As expected from the N-alkyl inhibitors, the hexyl and butyl inosamines **3.20** and **3.21** had similar affinity toward GCCase with  $K_i$  values near  $80\mu\text{M}$ .

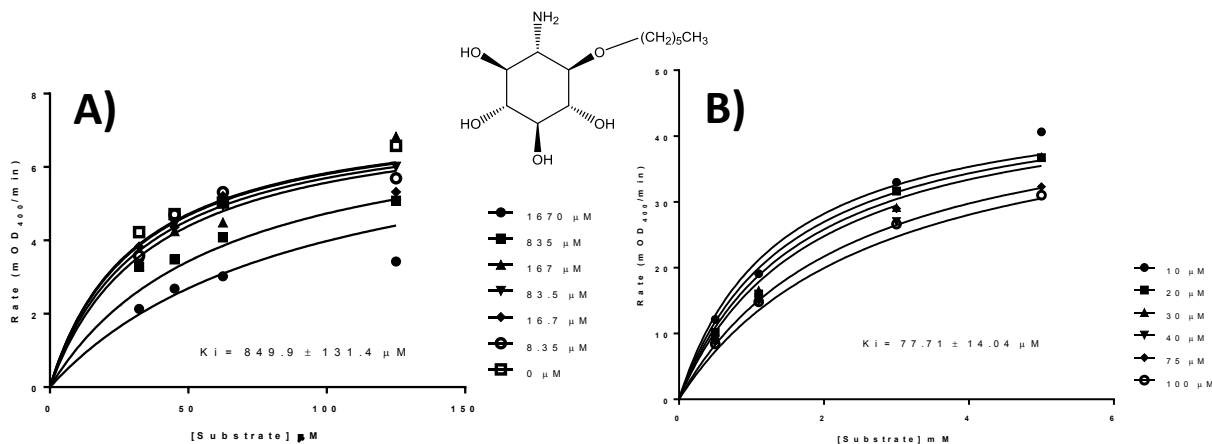


**Figure 2.3.3:** Nonlinear regression plots of the competitive inhibitor **3.20** using the substrate 2,4-DNP-β-D-Glc A)Inhibition of ABG. B) Inhibition of GCCase.

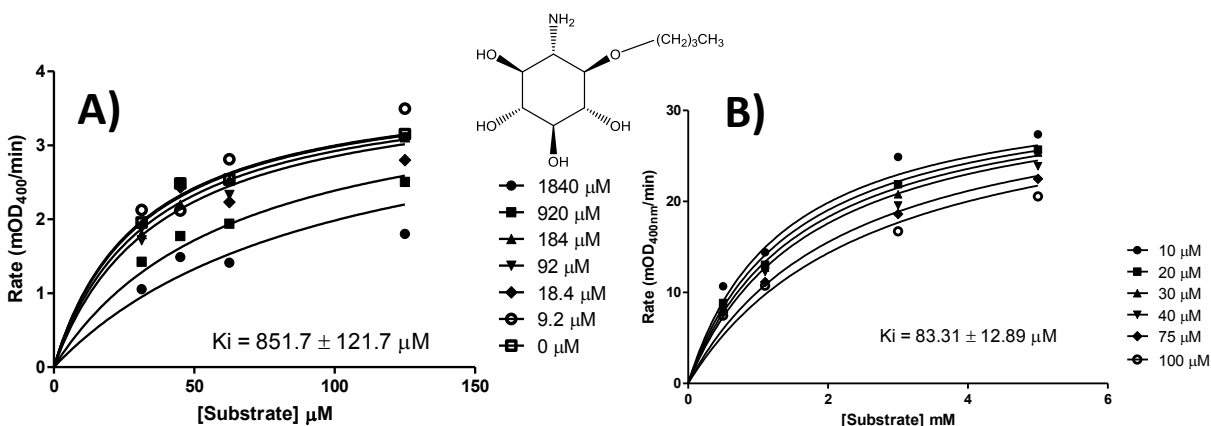


**Figure 2.3.4:** Nonlinear regression plots of the competitive inhibitor **3.21** using the substrate 2,4-DNP-β-D-Glc. A) Inhibition of ABG. B) Inhibition of GCCase.

When testing the inosamines with ABG, inhibitor **3.19** was measured to have  $K_i$  value of 93.80 μM. In contrast, the hexyl and butyl derivatives **3.20** and **3.21** were poor inhibitors with  $K_i$  values in the mM range. We observed nearly an identical increase in the relative  $K_i$  values of the inhibitors when increasing chain length from the butyl/hexyl to nonyl alkyl chains for both ABG and GCCase.

It is interesting to note that for both GCCase and ABG there was statistically no difference between the  $K_i$  values obtained for the hexyl and butyl derivatives. This may indicate that the O-alkyl chain of four and six carbons in length were not sufficiently long enough to occupy the hydrophobic areas within both GCCase and ABG and therefore associate and dissociate from the enzyme at roughly the same rate. However, the nonyl chain showed a large decrease in  $K_i$  for both ABG and GCCase indicating a very tight association. There are a number of difficulties in making structure-activity relationships based solely on  $K_i$  due to many possible interactions affecting  $K_i$  that cannot be accounted for without additional complex experiments. For example, these inositol compounds have the potential to form micelles. Longer alkyl chain derivatives could form micelles at lower concentrations thus resulting in less accessible inhibitor and higher observed  $K_i$  values. For our analysis we have to assume these additional interactions are negligible.

The  $K_i$  of the nonyl derivative **3.19** was similar in magnitude compared to the N-alkylated derivative. Importantly, the N-alkylated inosamines displayed a large change in the  $K_i$  values between the octyl and nonyl derivatives which was similar to the difference between the O-alkylated hexyl and nonyl derivatives. This dramatic change in  $K_i$  supports our hypothesis of the presence of a hydrophobic pocket at a location corresponding to carbons 9 and 10 of the alkyl chains within GCCase. Critically, these experiments indicate that derivatives having both N- and O-alkylated chains may indeed produce chaperones with very low  $K_i$  values, therefore warranting the synthesis and evaluation of dialkylated inosamines.

### **2.3.3 Kinetic Analysis of the Inhibition of ABG and GCCase by O- and N-alkylated Inhibitors 3.29-3.33**

The O- and N- doubly alkylated inhibitors were expected to have the highest affinity to GCCase due to the structural similarity to the glucocerebrosides and based on our results with the mono-alkylated inhibitors above. However, one significant difference is that the lipid moiety of glucosylceramide branches at 2 carbons away from the glucose ring in contrast to the inosamines in which both alkyl chains are directly attached to the inositol ring. To evaluate our hypothesis that dialkylated inositols will make potent inhibitors of GCCase, compounds **3.29-3.33** were tested as inhibitors of both ABG and GCCase.

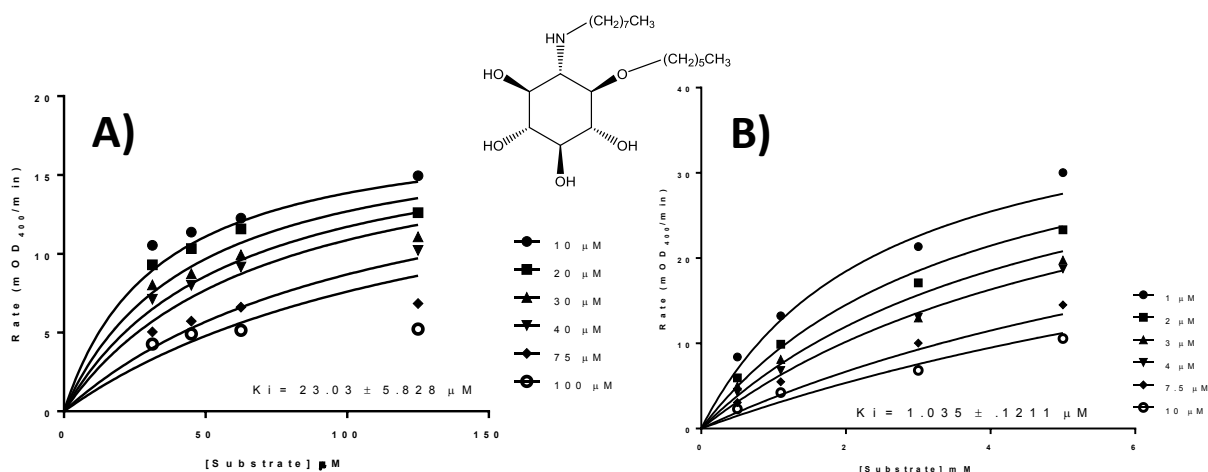


**Figure 2.3.5:** Nonlinear regression plots of the competitive inhibitor **3.32** using the substrate 2,4-DNP- $\beta$ -D-Glc A) Inhibition of ABG. B) Inhibition of GCCase.

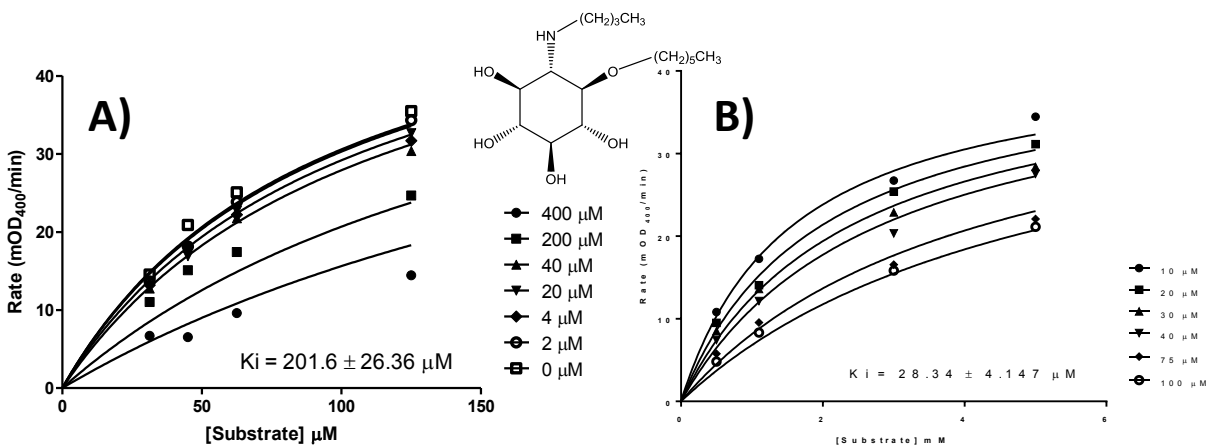


**Figure 2.3.6:** Nonlinear regression plots of the competitive inhibitor **3.33** using the substrate 2,4-DNP- $\beta$ -D-Glc A) Inhibition of ABG. B) Inhibition of GCCase.

We will start by looking at the  $K_i$  values for the various N-alkylated, O-nonyl derivatives for GCCase as shown in **Table 2.3.3**; all of which were very potent inhibitors of GCCase. The N-alkyl, O-nonyl derivatives **3.29-3.31** differ by increasing the N-chain length from butyl to hexyl to octyl. Interestingly, there was no significant difference in  $K_i$  values between the octyl and hexyl chains on the N which was clearly observed in the N-alkylated compounds from Egido-Gabasi.<sup>32b</sup> In contrast, the butyl inhibitor **3.31** showed a more significant 19-fold increase in  $K_i$  from the hexyl derivative **3.30** than the 2.5-fold increase that was observed in the N-alkylated compounds.<sup>32b</sup>

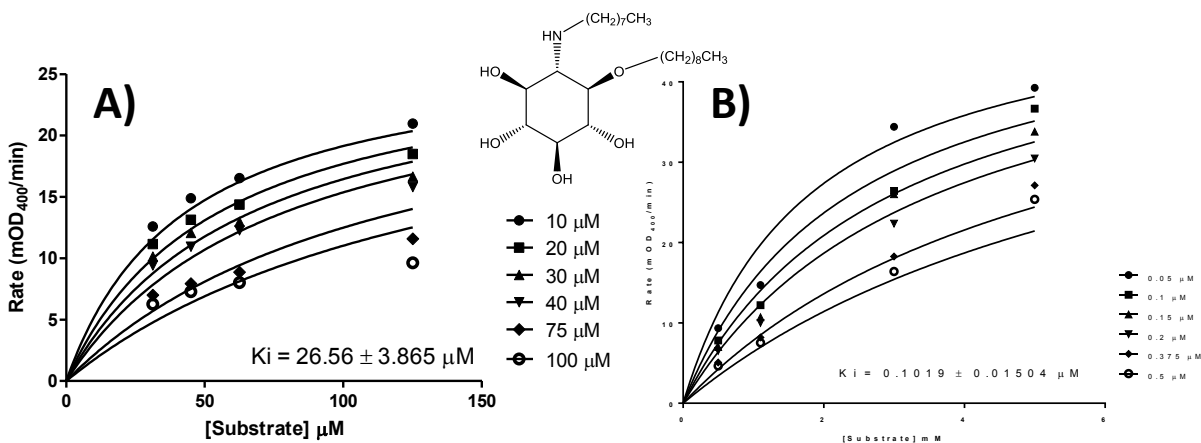


**Figure 2.3.7:** Nonlinear regression plots of the competitive inhibitor **3.29** using the substrate 2,4-DNP-β-D-Glc. A) Inhibition of ABG. B) Inhibition of GCCase.

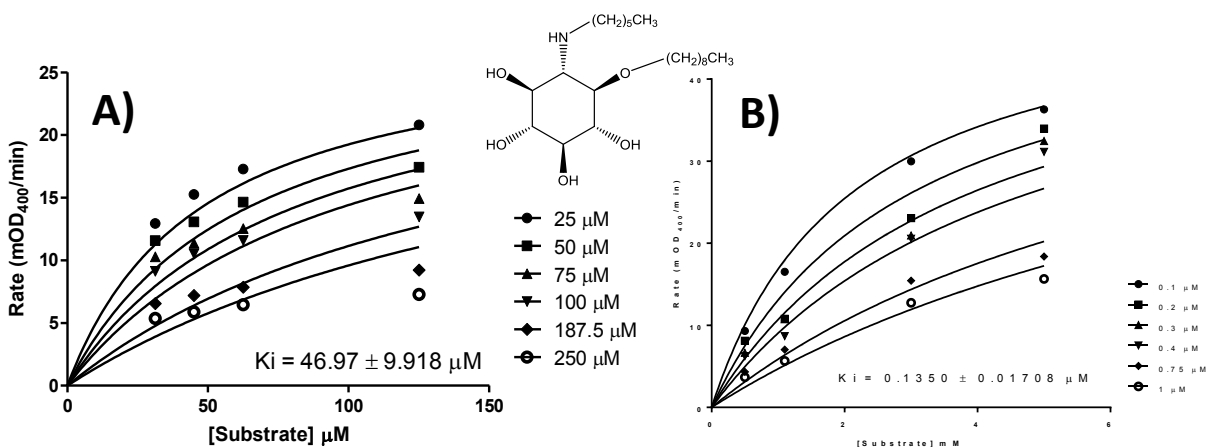


**Figure 2.3.8:** Nonlinear regression plots of the competitive inhibitor **3.30** using the substrate 2,4-DNP-β-D-Glc. A) Inhibition of ABG. B) Inhibition of GCCase.

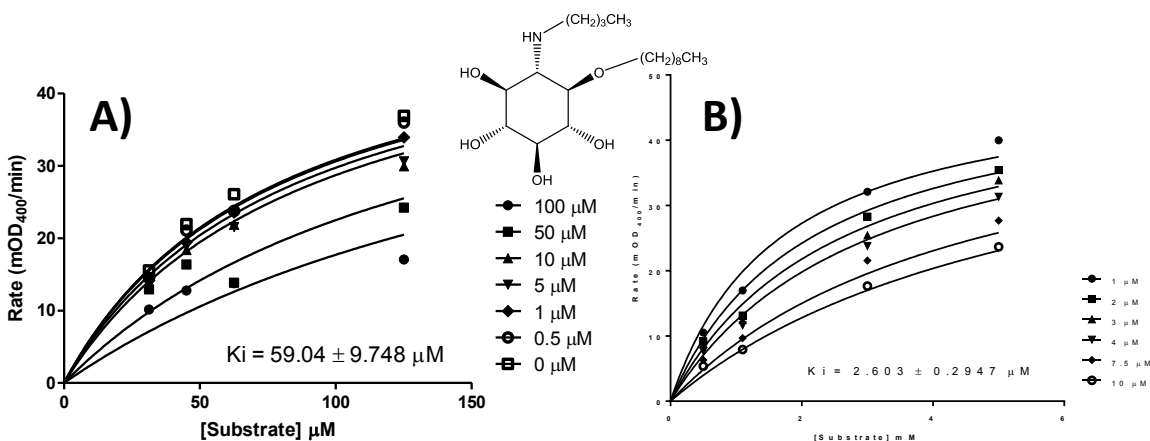


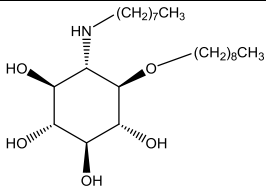
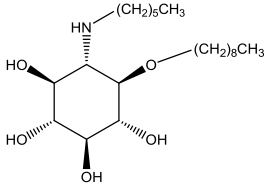
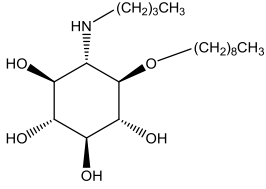
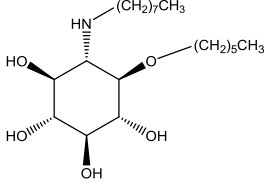
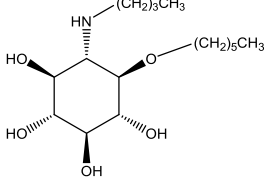
**Figure 2.3.9:** Nonlinear regression plots of the competitive inhibitor **3.31** using the substrate 2,4-DNP-β-D-Glc A) Inhibition of ABG. B) Inhibition of GCCase.

The N-octyl, O-hexyl derivative **3.32** was found to be a 2.5-fold better inhibitor than the N-butyl, O-nonyl inhibitor **3.31**. Interestingly, the N-butyl, O-hexyl inhibitor **3.32** was significantly less effective than the other dialkylated inhibitors and only slightly better than the N-butyl compound from Egido-Gabas<sup>32b</sup> demonstrating the need for alkyl chain lengths to be at least 8 carbons long to significantly occupy the hydrophobic pocket of GCCase. Generally, increasing the O-alkyl chain length from six to nine carbons gives a 10-fold decrease in  $K_i$  value which corresponds to the same 10-fold decrease in  $K_i$  value observed in the singly O-alkylated inhibitors. However, increasing the N-alkyl chain length from four to eight carbons gives a 25-fold decrease in  $K_i$  value which does not compare to the 3.8-fold decrease in  $K_i$  value observed in the singly N-alkylated inhibitors. From this data, there is a dependent relationship between the length of the N-alkyl chain and the O-alkyl chain while the influence of the O-alkyl chain remains independent of the N-alkyl chain. This suggests that binding of the O-alkyl chain may indirectly influence the binding site for the N-alkyl chain thereby modifying its binding affinity. The design of future dialkylated inosamine inhibitors should take advantage of this relationship by further increasing the N-alkyl chain length in order to see the greatest change in  $K_i$  values.

When testing the inhibitors with ABG, the inosamines **3.29-3.32** show  $K_i$  values in a range of 23-59 μM while inhibitor **3.33** has a significantly higher  $K_i$  value of 201.6 μM. The N-alkyl, O-nonyl

inosamines **3.29-3.31** show no significant difference in  $K_i$  values between the butyl and hexyl derivatives, but a 2-fold difference from the octyl derivative. Surprisingly, the N-octyl, O-hexyl inosamine **3.32** was found to have a lower  $K_i$  value than N-octyl, O-nonyl inhibitor **3.29**. The lower  $K_i$  value of **3.32** can be explained by the lack of a well-defined hydrophobic binding pocket in ABG to accommodate the O-alkyl groups while there are N-alkyl groups also present and thereby decreasing binding affinity through steric hindrance. Therefore, the general trend for the N-octyl, O-alkyl inhibitors is a reversal of the trend shown by the singly O-alkylated inhibitors, where the O-alkyl chain lengths above 6 carbons increase  $K_i$  values.

**Table 2.3.3:**  $K_i$  values and comparison of O- and N-alkylated competitive inhibitors

Inhibitor Structure	ID	GCase $K_i$ ( $\mu\text{M}$ )	ABG $K_i$ ( $\mu\text{M}$ )
	<b>3.29</b>	$0.102 \pm 0.0150$	$26.6 \pm 3.87$
	<b>3.30</b>	$0.135 \pm 0.0171$	$47.0 \pm 9.92$
	<b>3.31</b>	$2.60 \pm 0.29$	$59.0 \pm 9.75$
	<b>3.32</b>	$1.04 \pm 0.121$	$23.0 \pm 5.83$
	<b>3.33</b>	$28.3 \pm 4.15$	$201 \pm 26.4$

### 2.3.4 Conclusions and Future Work

In summary, one N-alkylated compound, **3.12**, three O-alkylated compounds, **3.19**, **3.20**, and **3.21**, and five N- and O- doubly alkylated compounds, **3.29-3.33**, were synthesized as novel aminocyclitol inhibitors. All aminocyclitols were evaluated for their ability to competitively inhibit GCase and ABG through measurement of their  $K_i$  values. Trends between the alkyl chain length and binding

affinity were found showing that increasing alkyl chain length lowers  $K_i$  in each case. The most effective inhibitors synthesized, **3.29** and **3.30**, gave exceptionally low  $K_i$  values of 101.9 and 135.0 nM respectively suggesting that these structures are excellent lead compounds for the design of more advanced chemical chaperones. In addition, these compounds are potent inhibitors to warrant chaperoning studies using cell lines that express mutant GCCase.<sup>21, 32b, 54</sup>

### 2.3.5 Special Note

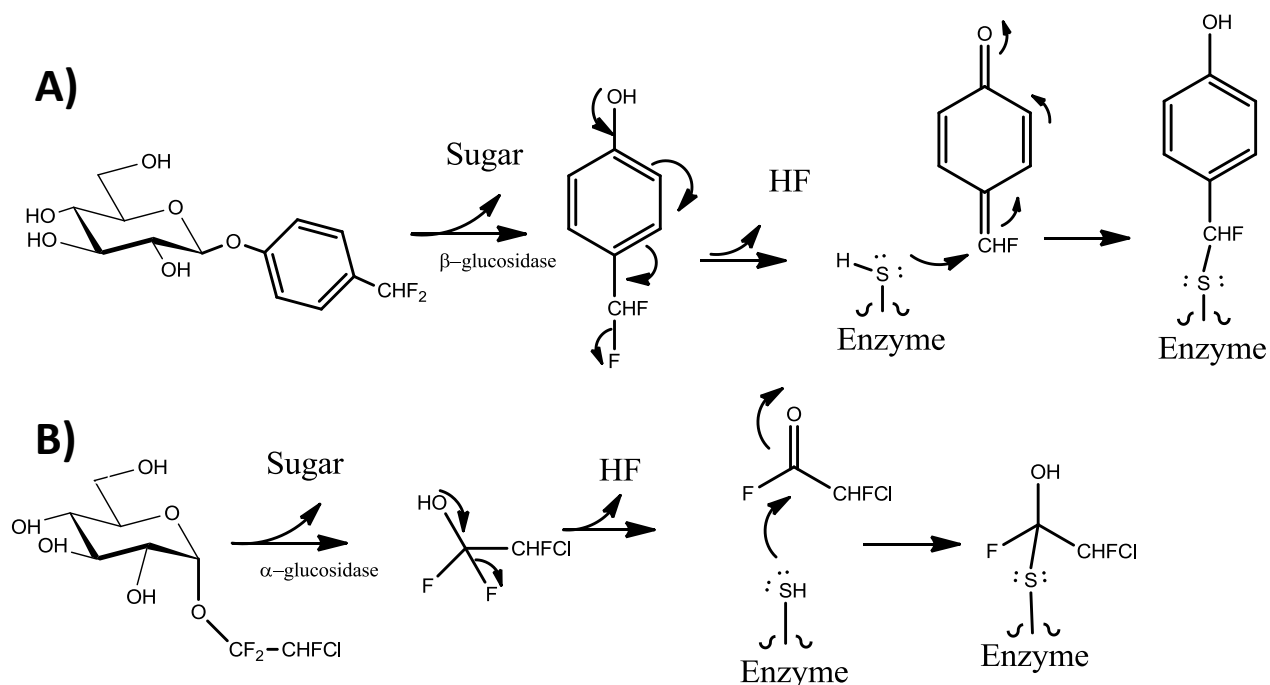
During the second year of this project, similar dialkylated aminocyclitol compounds were synthesized and evaluated as chemical chaperones for GCCase published by Ana Trapero et al.<sup>32d</sup> In this study, the authors reported aminocyclitols bearing two nonyl chains both in the myo- and scyllo-configuration confirming that the dialkylated inosamines are indeed potent inhibitors of GCCase and were effective at raising lysosomal levels of mutant enzyme. Interestingly the myo-derivative had a remarkable  $K_i$  of 1nM despite having an axial substituent on the cyclohexane ring which is not found in the substrate GlcCer. This suggests GCCase preferentially binds to inosamines in the myo-configuration and these structures, in contrast to the expected scyllo-configured isomers, may be best suited as pharmacological chaperones of GCCase.

## Part B: Mechanism-based Aziridine Glucocerebroside Inhibitors

### 3.1 Introduction

#### 3.1.1 Covalent Glycosidase Inhibitors

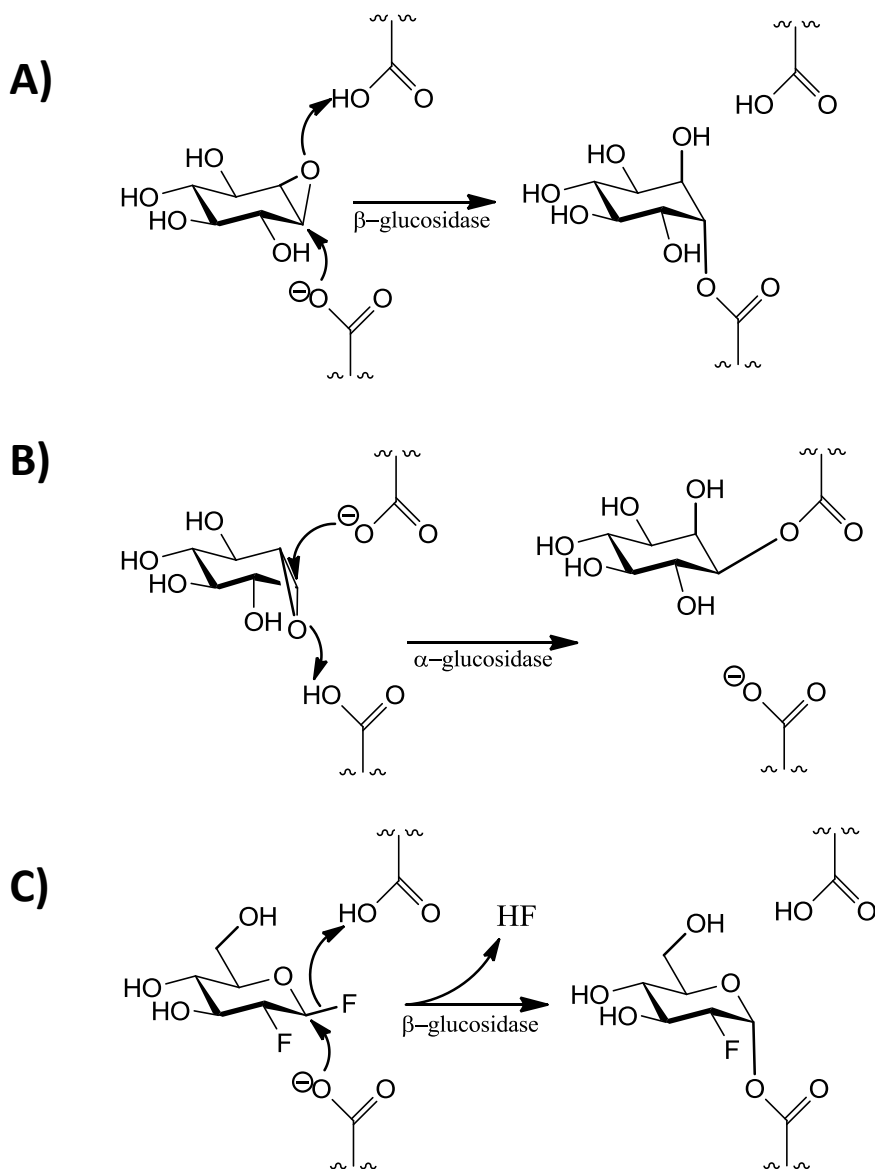
Covalent or suicide inhibitors are molecules that irreversibly inhibit enzyme activity by forming a covalent bond with the amino acid residues required for catalysis thereby causing enzyme inactivation. Covalent inhibitors have been used extensively to further our understanding of glycosidase enzymology and biochemistry, to identify active site residues, elucidate catalytic mechanisms and to study the effect of selectively inactivating the enzyme in a living system. Covalent inhibitors can be further categorized into affinity labels or mechanism-based inhibitors.<sup>61</sup> Affinity labels are substrate analog inhibitors that contain a highly reactive aglycone. Nucleophilic attack of the electrophilic portion of the affinity label usually occurs within the active site at one of the enzyme's catalytic residues. This leads to the release of a highly reactive aglycone that covalently bonds to amino acid residues in the nearby region inactivating the enzyme.<sup>61</sup> The aglycone released from affinity labels can be inherently chemically reactive or can be induced with secondary effects like with photo-reactive labels. Two examples of affinity labels can be seen with 4-difluoromethylphenoxy- $\beta$ -D-glucose and 2-chloro-1,1,2-trifluoroethoxy- $\alpha$ -D-glucose (**Scheme 3.1.1**).



**Scheme 3.1.1:** Mechanism of formation of reactive aglycone from affinity labels **A)** Aglycone 4-(fluoromethylene)cyclohexa-2,5-dienone from 4-difluoromethylphenoxy-β-D-glucose, **B)** Aglycone 2-chloro-2-fluoroacetyl fluoride from 2-chloro-1,1,2-trifluoroethoxy-α-D-glucose. Adapted from Rempel and Withers.<sup>61</sup>

Mechanism-based inhibitors are stable to spontaneous decomposition but will react with active site residues to form a covalent bond after partial processing by the enzyme's normal catalytic mechanism.<sup>61</sup> Nucleophilic attack of an electrophilic portion of the mechanism-based inhibitor occurs within the active site thus inactivating the enzyme. Mechanism-based inhibitors have proven to be valuable tools for identifying the active site residues and elucidating the catalytic mechanism of glycosidases by radioactive labelling the inhibitors and sequencing the radioactive peptides.<sup>61</sup> Examples of well-studied mechanism-based β-glucosidase inhibitors and their inactivation mechanisms can be seen with conduritol-β-epoxide and 2-deoxy-2-fluoro-β-D-glucosyl fluoride (**Scheme 3.1.2**). For many covalent inhibitors of glycosidases, the formation of the glycosyl-enzyme intermediate is an irreversible

process. For example, the spontaneous hydrolysis reactivation half-life of 2-deoxy-2-fluoro- $\beta$ -D-glucosyl-enzyme intermediate covalently bound to human GCase is  $1300\text{min}^{-1}$ .<sup>62</sup> However, catalytic activity of the inactivated enzymes can be restored through hydrolysis of the covalently bound glycosyl-enzyme species or through transglycosylation onto a suitable acceptor substrate.<sup>61</sup>



**Scheme 3.1.2:** Mechanism of mechanism-based inhibitors **A)** conduritol- $\beta$ -epoxide with  $\beta$ -glucosidase, **B)** conduritol- $\beta$ -epoxide with  $\alpha$ -glucosidase, **C)** 2-deoxy-2-fluoro- $\beta$ -D-glucosyl fluoride with  $\beta$ -glucosidase.

Adapted from Rempel and Withers<sup>61</sup>

In addition to identifying active site residues and catalytic mechanisms, covalent inhibitors can also be used to label enzymes to monitor intracellular trafficking or the biodistribution of enzymes injected into living animals or humans. Knowledge of the biodistribution of recombinant enzymes in enzyme replacement therapy (ERT) is vital to determine its ability to target specific tissues and the tissue half-lives in order to improve the design of the enzyme and provide the most effective treatment.<sup>63</sup> Standard biodistribution monitoring procedures typically involve covalent inhibitors called activity based-probes that contain a labelling molecule such as a fluorophore or affinity tag.<sup>64</sup> The probes are introduced to cell lysates, cell systems, or animal models and subsequently analyzed by fluorescence or mass spectroscopy to determine the extent of enzyme uptake within the target cells.<sup>64</sup>

The major drawback of using fluorescent activity based probes involves limitations in the detection techniques due to the shallow depth that the probes can be analyzed within tissues. Therefore, tissues from multiple organs and locations must be biopsied in to determine biodistribution in humans. A potential solution is to use nuclear-based techniques such as PET which enable whole body imaging thereby providing substantially more information on the biodistribution of the enzymes *in vivo* in a single experiment. However, introducing a positron emitting label during protein synthesis is impossible due to the short half-life of commonly used isotopes such as <sup>18</sup>F (109.8min) and surface attachment of radiolabelled prosthetic groups, antibodies or peptides may alter the biodistribution and biological activities of the enzymes *in vivo*.<sup>63</sup> An alternative method is to radioactively label an enzyme with an <sup>18</sup>F labelled mechanism-based inhibitor and use PET to determine the biodistribution. Indeed, this strategy was successfully demonstrated with the recombinant enzyme Cerezyme®.<sup>63</sup> The work involved synthesis of an <sup>18</sup>F labelled mechanism-based inhibitor, 2,4-dinitrophenyl-2-deoxy-2-[<sup>18</sup>F]-fluoro-β-D-glucopyranoside, that covalently labelled the active site of the recombinant GCCase. Since no significant conformational changes can be detected in the 2-fluoroglucosyl-enzyme intermediate by X-ray crystallography,<sup>4b</sup> the normal biodistribution of the enzyme can be followed *in vivo*. However, the

labelling agent used in this report failed to produce sufficient levels of  $^{18}\text{F}$  labelled Cerezyme required for human imaging due to slow labelling rates of the enzyme. This required extended incubation times incompatible with the short half-life of the  $^{18}\text{F}$  isotope. In addition, a highly efficient and specific inhibitor may enable the *in vivo* molecular imaging of GCCase activity to assess Cerezyme therapy or act as a potential diagnostic for Gaucher disease.

## Chapter 4: Results and Discussion

### 4.1 Synthesis

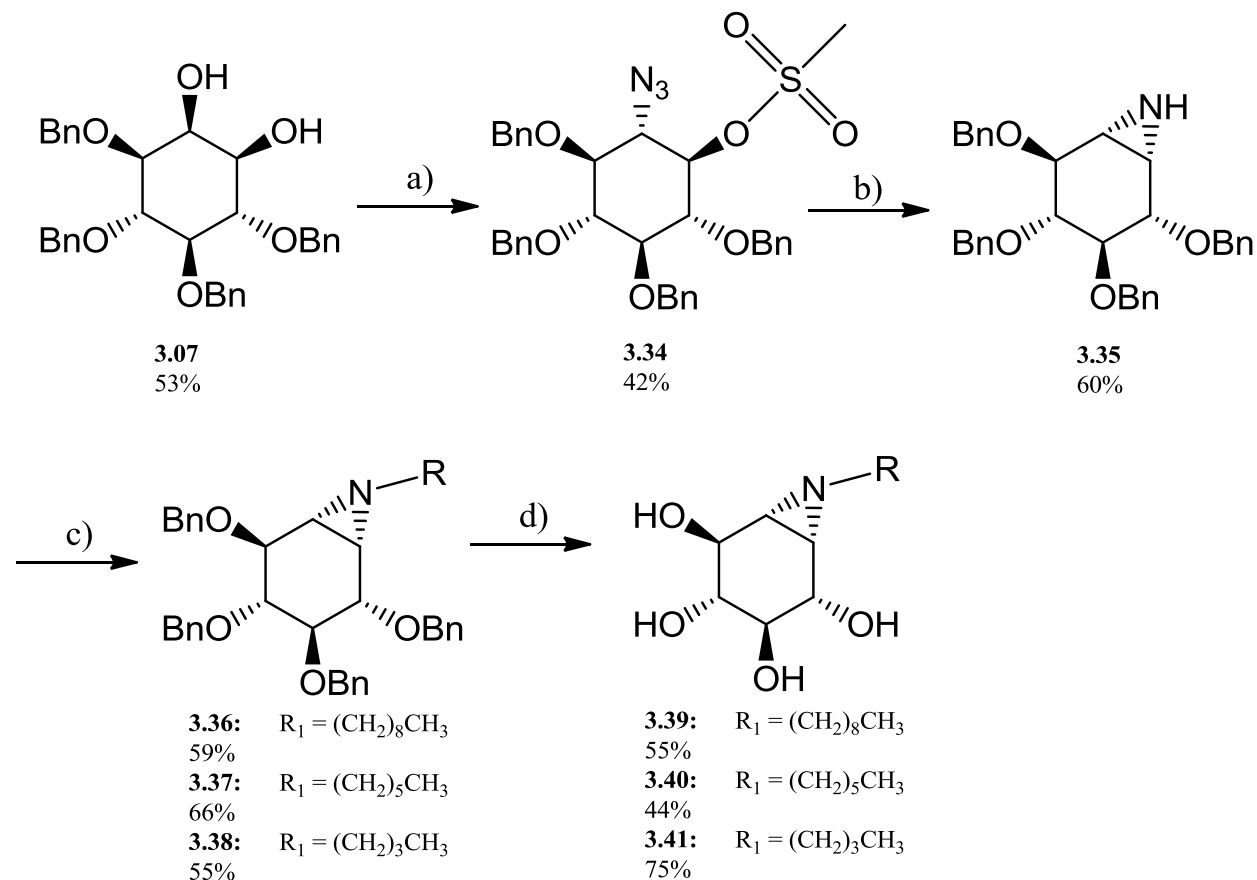
#### 4.1.1 Synthesis of Aziridine Inhibitors

Based on the success of the aminocyclitols as inhibitors of GCCase, we sought to adapt this chemistry to synthesize alkylated conduritol aziridines that we hypothesized to be efficient mechanism-based inhibitors of  $\beta$ -glucosidases. Synthesis of the aziridine inhibitor began from racemic tetrabenzyl inositol **3.07** and is shown in (**Scheme 4.1**). Both the equatorial and axial oxygens of the tetrabenzyl **3.07** were activated through mesylation using methanesulfonyl chloride in pyridine. Regioselective azidolysis of the axial mesyl group at C2 proceeded smoothly, most likely due to steric hindrance provided by the equatorial benzyl groups to facilitate preferential attack of the free equatorial site by the  $\text{S}_{\text{N}}2$  reaction to give the desired azido mesylate **3.34** in 42%.<sup>65</sup> Intramolecular cyclization occurs presumably in a similar method to those described<sup>66</sup> where reduction of the azide by lithium aluminum hydride evolves  $\text{N}_{2(\text{g})}$  leaving the negatively charged nitrogen to attack the adjacent carbon to form the aziridine **3.35** in 60% yield. Formation of the aziridine structure was evident by NMR spectroscopy which displayed the unique doublet at  $\delta 2.33$  ( $J = 6\text{Hz}$ ) and doublet of doublets at  $\delta 2.55$  ( $J = 6, 3\text{Hz}$ ) corresponding to H1 and H6, typical of bicyclic [4.1.0] aziridine compounds.<sup>67</sup> Attempts at alkylation of the aziridine following the reductive amination procedure for primary amines in the presence of sodium cyanoborohydride and acetic acid failed.<sup>49</sup> An alternative method of alkylation was pursued by refluxing the iodoalkane in a DCM-50% NaOH mixture with a phase transfer catalyst tetrabutylammonium

chloride but suffered from poor yields while leaving unreacted starting material.<sup>68</sup> Alkylation of the aziridine was achieved by using potassium carbonate and the corresponding 1-iodoalkane in DMF to provide the octyl, hexyl and butyl derivatives in 59%, 66%, and 55% yields respectively. Reactions involving the derivatization of the aziridine nitrogen are limited due to the reactivity of the highly strained aziridine ring.<sup>69</sup> Consequently, global deprotection of the benzyl ethers failed using similar conditions described for the above compounds. Initial attempts using Pd/C, HCl, and MeOH with H<sub>2(g)</sub> at 50 PSI resulted in the complete loss of starting materials resulting in unidentified amines. Aziridines have been shown to have increased sensitivity to nucleophilic attack under acidic conditions,<sup>70</sup> however the hydrogenolysis reaction performed in the absence of HCl did not improve the outcome. It has also been previously shown that hydrogenation of aziridines with Pd/C in ethanol can cause ring opening and rearrangement<sup>71</sup> so a similar competing reaction may have occurred. NMR and mass spectroscopy of the products of hydrogenolysis with Pd/C did not correspond to the ring opening by nucleophilic attack of water or methanol, or any elimination product. Adjusting the pressure, pH, solvents, length of reaction and combinations of conditions afforded no improvements. Therefore an alternate route for hydrogenolysis through Birch reduction was attempted. Access to NH<sub>3(g)</sub> was limited due to high costs, however commercially available alkali metals impregnated on silica gel (M-SG) had been shown to perform Birch reduction-like reactions under mild conditions.<sup>72</sup> The simple procedure requires stirring the compound in the presence of the non-pyrophoric stage I Na<sub>2</sub>K-SG which should have the reactivity equivalent to neat alkali metals<sup>73</sup> in anhydrous THF at room temperature, however, no reaction was observed for the protected aziridines. Modifications to the procedure including increased quantities of Na<sub>2</sub>K-SG and increased temperature failed promote the reduction. Finally, a cost effective method for the production of NH<sub>3(l)</sub> necessary for Birch reduction was developed where concentrated NH<sub>4</sub>OH was gently heated to release NH<sub>3(g)</sub>. The NH<sub>3(g)</sub> gas was then passed through several water condensers and drying tubes containing CaSO<sub>4</sub> before being collected into the reaction vessel using a dry ice condenser.

There was potential for destruction of the compound due to base-catalyzed eliminative ring opening that can occur with aziridines in the presence of superbases<sup>69</sup> so minimizing the reaction time was desired. Birch reduction of a tribenzylated iminosugar showed near instantaneous removal of the benzyl ethers as the reaction was quenched immediately after addition of the compound to the reductive solution.<sup>74</sup> Initial attempts with protected aziridine **3.41** displayed no observable deprotection when immediately stopping the reaction after addition. Reaction times of 5, 10 and 15 minutes did not improve the reaction yield, however quantitative recovery of the starting material suggested stability of the protected aziridines under these harsh conditions. A four hour reaction was attempted resulting in the complete consumption of starting material and a yield of 55%, 44% and 75% for the octyl, hexyl and butyl compounds **3.39**, **3.40**, **3.41** respectively following column chromatography.

#### Scheme 4.1: Synthesis of Aziridine Inactivators



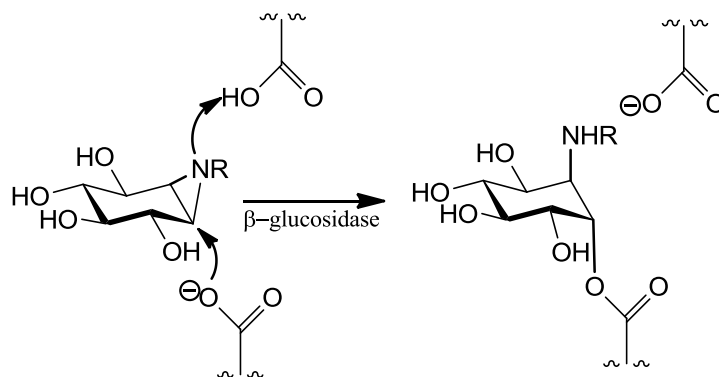
Reagents and Conditions: **(a)** 1) Mesyl Chloride, pyr, rt. 2)  $NaN_3$ , DMF, 85°C. **(b)**  $LiAlH_4$ , ether, 0 – rt. **(c)**

$K_2CO_3$ ,  $C_8H_{17}I$  or  $C_6H_{13}I$  or  $C_4H_9I$ , DMF, 50°C. **(d)**  $Na_{(s)}$ ,  $NH_{3(l)}$ , THF, -78°C.

#### 4.2 Kinetic Analysis of the Irreversible Inhibition of ABG and GCase by Aziridine Inhibitors 3.39-3.41

There are a number of known covalent and mechanism based irreversible inhibitors of GCase including activated fluorosugars,<sup>75</sup> conduritol aziridine, gluconolactone, cyclophellitol and conduritol epoxide.<sup>31a</sup> The epoxides and aziridines are mechanism based inhibitors that are protonated or become protonated in the active site to increase reactivity towards nucleophilic attack by a catalytic nucleophile leading to covalent binding within the active site of the enzyme.<sup>67</sup> To introduce specificity towards

GCCase, we decided to synthesize aziridines alkylated with lipid chains which we hypothesized would lead to efficient, specific, and cell membrane permeable GCCase inhibitors (**Scheme 4.2**).



**Scheme 4.2:** Hypothesized mechanism of the inhibition of GCCase by alkylated condurititol aziridine. R = butyl, hexyl, or octyl.

To determine the rate of enzyme inactivation, a range of eight concentrations of the inhibitor predicted to surround the  $K_i$  value were incubated with either GCCase or ABG and the reaction mixtures were assayed for residual enzyme activity at different time intervals. Small aliquots of the inactivation solution were withdrawn and diluted 20-fold in 96 well plates containing  $2 \times K_M$  of the substrate 2,4-DNP- $\beta$ -D-Glc. Dilution of the reaction mixture effectively halts further inactivation by diluting the inhibitor and active site competition by excess substrate. The velocity data was fit to the one phase decay equation using the GraphPad Prism software utilizing **Equation 4.1**.

**Equation 4.1:** 
$$Y = (Y_0 - \text{Plateau})e^{(-K_{obs} * X)} + \text{Plateau}$$

Using **Equation 2.3** gives the observed rate constant of inactivation ( $K_{obs}$ ).  $K_{obs}$  values can be plotted against inactivator concentration and fit to one of two equations, **Equation 4.2** or **Equation 4.3**.

**Equation 4.2** 
$$k_{obs} = \frac{k_i [I]}{K_i + [I]}$$

**Equation 4.3**

$$k_{obs} = \frac{k_i[I]}{K_i}$$

**Scheme 4.3:** General scheme for enzyme kinetics involving an irreversible mechanism-based inhibitor.



In **Scheme 4.3**  $k_i$  is the rate constant for inactivation, and  $K_i$  is the dissociation constant for the Enzyme-Inhibitor complex ( $k_{-1}/k_1$ ). Inactivation data follows **Equation 4.2** when saturation of the enzyme occurs at high inhibitor concentrations and allows for separation of  $k_i$  and  $K_i$  values. The data will have an observable curve when the equation can be used effectively. In cases where saturation cannot be observed due to rapid inactivation of the enzyme at high concentrations of inhibitor, the data will appear linear and **Equation 4.3** must be used which gives the second order rate constant as the ratio of  $k_i$  to  $K_i$ . All of the inhibitors followed **Equation 4.2** with ABG and followed **Equation 4.3** with GCase. The kinetic analysis of the aziridine inhibitors can be seen in **Figures 4.2.1-4.2.6**.

Previous work using conduritol aziridine found that it was an efficient mechanism-based inhibitor of  $\beta$ -glucosidase from *Agrobacterium faecalis* (previously *Alcaligenes faecalis*) (pABG5,  $K_i = 3.0$  mM and  $k_i = 0.077 \text{ min}^{-1}$ ),  $\alpha$ -glucosidase from yeast ( $K_i = 9.5$  mM and  $k_i$  of  $0.39 \text{ min}^{-1}$ ),<sup>67</sup> and  $\beta$ -D-glucosidase from almonds ( $IC_{50} = 0.22 \text{ } \mu\text{g/mL}$ ).<sup>76</sup> However, conduritol aziridines have never been tested on GCase or ABG.

#### 4.2.1 Inactivation rates of ABG with Inhibitors 3.39, 3.40 and 3.41

The kinetic plot for the butyl derivative **3.41** with ABG clearly demonstrates that the butyl aziridine is an efficient inactivator of this enzyme with  $K_i = 3795 \text{ } \mu\text{M}$  and  $k_i = 0.05250 \text{ min}^{-1}$ . As shown in **Figure 4.2.1**, full inactivation of ABG required high concentrations of inhibitor approaching the solubility limits of the aziridine and long incubation times. This results in an incomplete plot of  $k_{obs}$  versus

concentration of inhibitor and less accurate values for  $K_i$  and  $k_i$ . In comparison to the O-butyl inosamine **3.21**, and assuming that  $k_1$  and  $k_{-1}$  are much larger than  $k_i$ , the butyl aziridine has less binding affinity towards ABG having a 4.5 fold increase in the  $K_i$  value.

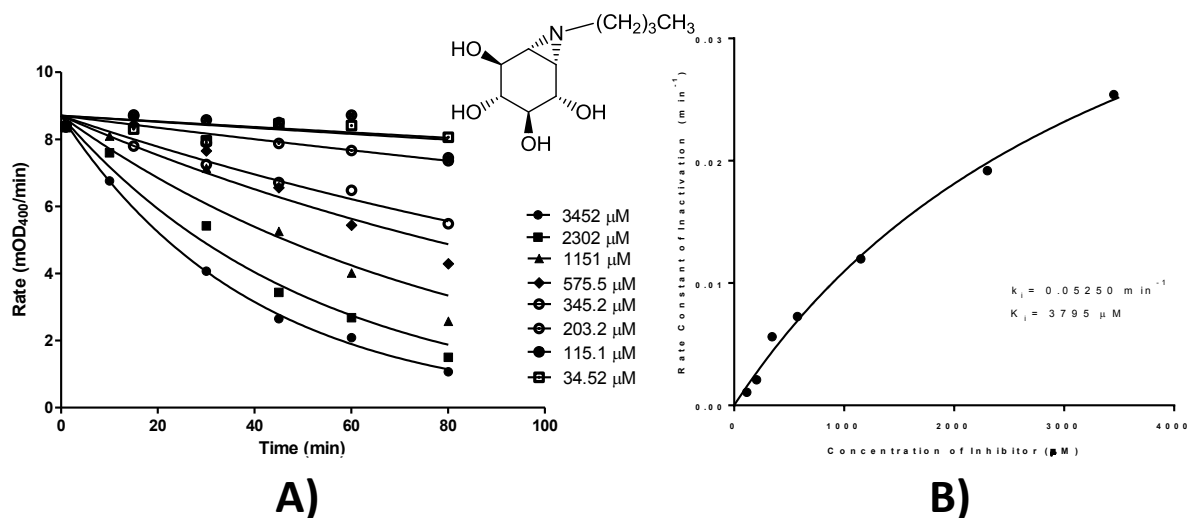


**Figure 4.2.1:** Inactivation of Abg with **3.41**. a) Plot of remaining enzyme activity over time at the indicated inhibitor concentrations fitted to a one phase decay equation. b) Plot of the observed rate constants of inactivation versus the concentration of inhibitor.

The next compound we assessed was the hexyl derivative **3.40**. As shown in **Figure 4.2.2**, this compound had a much lower  $K_i$  value of 572.2  $\mu\text{M}$  corresponding to a 6.6 fold decrease in  $K_i$  in comparison to the butyl derivative which had a  $K_i$  value of 3795  $\mu\text{M}$ . The significant improvement in the  $K_i$  value by extending the chain from butyl to hexyl shows that the alkyl chain of the hexyl aziridine was sufficiently long enough to occupy the hydrophobic pocket of ABG, differing from the O-alkylated inhibitors that required alkyl chains longer than six carbons. In comparison to the N-hexyl inosamine **3.12** and O-hexyl inosamine **3.20**, the hexyl aziridine has an intermediate binding affinity towards ABG giving a 4 fold increase in  $K_i$  value from **3.12**, and a 1.5 fold decrease in the  $K_i$  value from **3.20**.

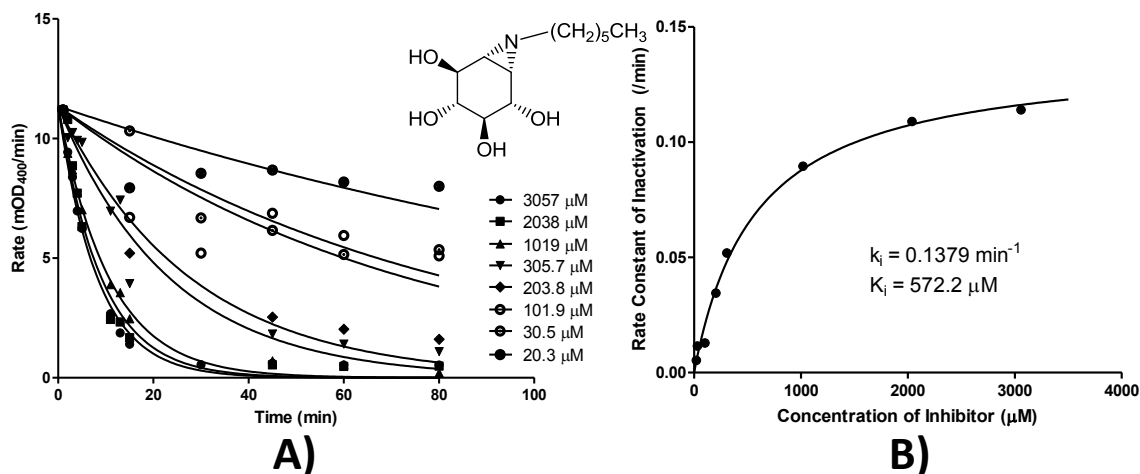


**Figure 4.2.2:** Inactivation of Abg with **3.40**. a) Plot of remaining enzyme activity over time at the indicated inhibitor concentrations fitted to a one phase decay equation. b) Plot of the observed rate constants of inactivation versus the concentration of inhibitor.

When alkyl chain length is increased to eight carbons, as in inhibitor **3.39**, we see a 2 fold decrease in  $K_i$  compared to the hexyl derivative **3.40** with a  $K_i$  of  $282.5\mu\text{M}$ ; a less substantial decrease in  $K_i$  than observed between the butyl and hexyl aziridine derivatives **3.40** and **3.41** (**Figure 4.2.3**). This relative change in  $K_i$  value is much less than was found with the O-hexyl and O-nonyl inosamines **3.19** and **3.20**. In comparison with the O-nonyl inosamine **3.19**, the octyl aziridine has less binding affinity towards ABG with a 3 fold increase in the  $K_i$  value.

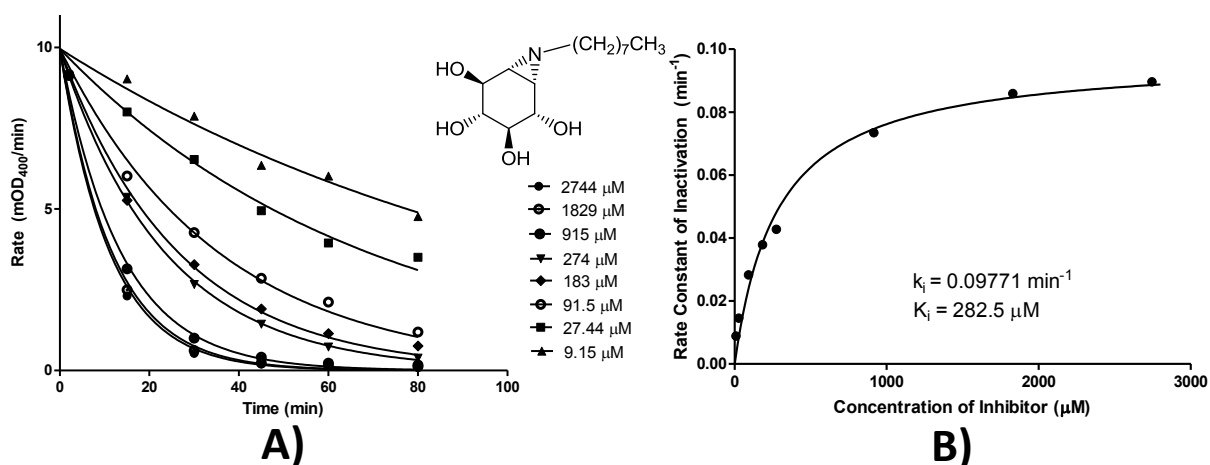


**Figure 4.2.3:** Inactivation of Abg with **3.39**. a) Plot of remaining enzyme activity over time at the indicated inhibitor concentrations fitted to a one phase decay equation. b) Plot of the observed rate constants of inactivation versus the concentration of inhibitor.

In summary, the  $K_i$  values of the aziridine inhibitors with ABG followed the general trend of decreasing  $K_i$  values or improving binding affinity as alkyl chain length increases. However, the measured  $K_i$  values of the aziridines were much higher or had lower affinity to ABG when compared to the reversible inosamine inhibitors of identical chain length. This observation may be due in part to the  $pK_a$  of the nitrogen of the alkylated aziridines at the pH used for the ABG assay which was 6.8. Although we did not determine the  $pK_a$  of our alkylated aziridines, previous reports indicate that the conjugate acid of the unalkylated aziridine has a  $pK_a$  of 7.98.<sup>69</sup> Since the  $pK_a$  of the secondary amine dimethylamine is 10.68 and the tertiary trimethylamine is 9.80, the  $pK_a$  of the alkylated aziridine may be approximately 7.1. Therefore, in the ABG assay buffer (pH 6.8) a significant percentage of the inhibitor would be present as the neutral amine. This could potentially explain the lower affinity of the aziridines towards ABG in comparison to the alkylated inosamine described in Part A. The inactivation rate ( $k_i$ ) of each aziridine with ABG remained roughly the same magnitude of  $0.1 \text{ min}^{-1}$  for all inhibitors. This value is comparable to the measured inactivation rate constant of conduritol inositol determined to be a  $k_i$  value of  $0.077 \text{ min}^{-1}$  with pABG5.<sup>67</sup>

#### 4.2.2 Inactivation Rates of GCCase with Inhibitors 3.39, 3.40 and 3.41

With each of the alkylated aziridines synthesized in this work, rapid inactivation of GCCase prevented us from determining the individual  $K_i$  and  $k_i$  values. This is because at saturating concentrations of inhibitor, the enzyme is almost instantaneously inactivated. For example, the least reactive butyl derivative completely inactivated GCCase at  $100 \mu\text{M}$  in  $\sim 10$  minutes. As a result, we could only determine the second order rate constant  $k_i/K_i$ , a parameter still useful to rank the efficiency of the various inactivators of GCCase.

The butyl aziridine **3.41** is a highly efficient inactivator of GCCase with an impressive  $k_i/K_i = 3.837 \text{ mM}^{-1}\text{min}^{-1}$ . As shown in **Figure 4.2.4**, full inactivation of GCCase could be achieved using relatively low

concentration of 100  $\mu\text{M}$  inhibitor in  $\sim 10$  minutes. To allow for comparisons to the competitive inhibitors, we can approximate the  $k_i$  value to the value obtained for ABG ( $\sim 0.1 \text{min}^{-1}$ ) which gives an approximate  $K_i$  value for **3.41** of 26  $\mu\text{M}$ . This approximate  $K_i$  value would be moderately better than the  $K_i$  values obtained with the N-butyl and O-butyl inhibitors indicating improved binding affinity with the butyl aziridine inhibitor.

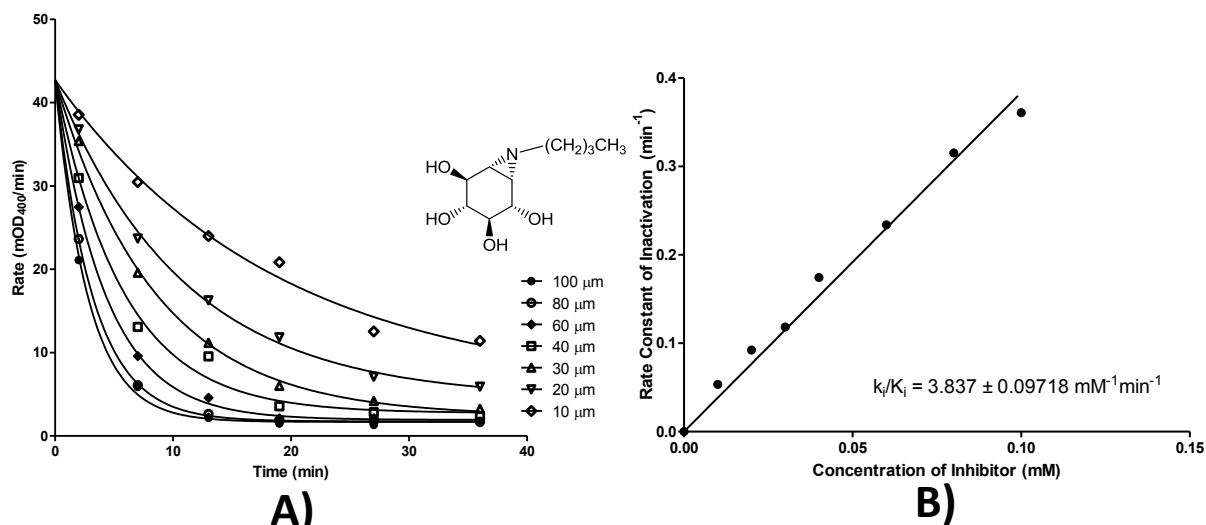


**Figure 4.2.4:** Inactivation of GCCase with **3.41**. a) Plot of remaining enzyme activity over time at the indicated inhibitor concentrations fitted to a one phase decay equation. b) Plot of the observed rate constants of inactivation versus the concentration of inhibitor.

The hexyl aziridine **3.40** is an exceptionally potent inhibitor of GCCase with a  $k_i/K_i = 645.4 \text{ mM}^{-1} \text{min}^{-1}$ . As shown in **Figure 4.2.5**, full inactivation of GCCase could be achieved using the low concentration of 1.6  $\mu\text{M}$  in less than 5 minutes. If we approximate the  $k_i$  value to the value obtained for ABG ( $\sim 0.1 \text{min}^{-1}$ ), we obtain a  $K_i$  value for **3.40** of 154 nM. This approximate  $K_i$  value would be far better than the  $K_i$  values obtained with the N-hexyl and O-hexyl inhibitors indicating significantly improved binding affinity with the hexyl aziridine inhibitor.

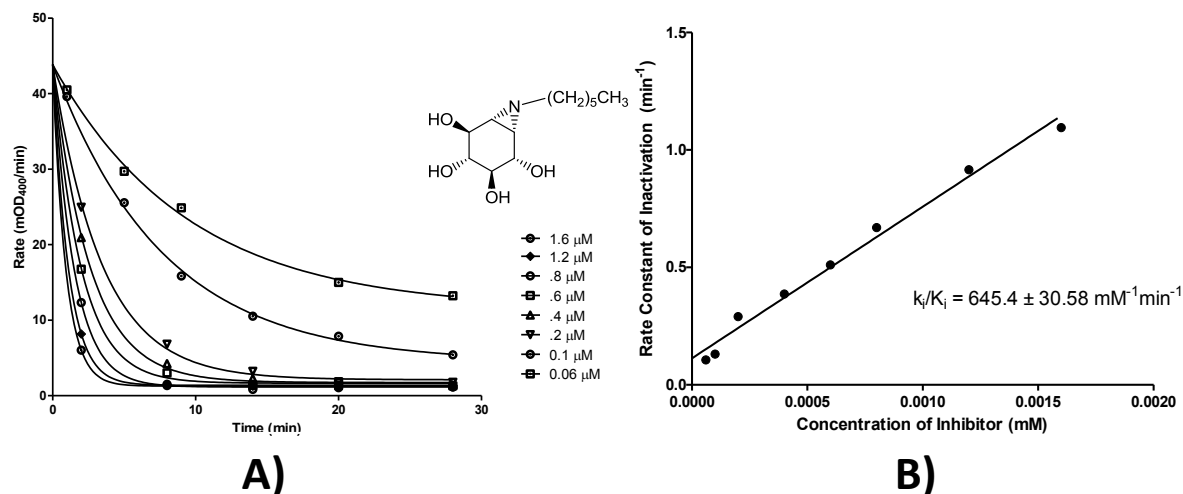


**Figure 4.2.5:** Inactivation of GCCase with **3.40**. a) Plot of remaining enzyme activity over time at the indicated inhibitor concentrations fitted to a one phase decay equation. b) Plot of the observed rate constants of inactivation versus the concentration of inhibitor.

The octyl aziridine is the most potent aziridine inhibitor tested with GCCase, providing a 37.5 fold better  $k_i/K_i$  of  $3674 \text{ mM}^{-1}\text{min}^{-1}$  (**Figure 4.2.6**). For comparison purposes, the well-studied mechanism-based inactivator of GCCase 2-deoxy-2-fluoro- $\beta$ -D-glucosyl fluoride has a  $k_i/K_i$  of  $0.0227\text{mM}^{-1}\text{min}^{-1}$ <sup>62</sup> while the Dioctyl (2-deoxy-2-fluoro- $\beta$ -D-glucopyranosyl) phosphate is the best reported inactivator of GCCase with a  $k_i/K_i$  of  $98\text{mM}^{-1}\text{min}^{-1}$ .<sup>56</sup> The octyl derivative **3.39** is capable of near complete inactivation of GCCase within 40 minutes at equimolar concentrations and complete inactivation in 20 minutes at 1.5 x concentration. In comparison, the same amount of Dioctyl (2-deoxy-2-fluoro- $\beta$ -D-glucopyranosyl) phosphate would require 1600 minutes and 800 minutes for the same levels of inactivation in GCCase. If we approximate the  $k_i$  value to the value obtained for ABG ( $\sim 0.1\text{min}^{-1}$ ), we obtain an approximate  $K_i$  value for **3.39** of 27 nM. This approximate  $K_i$  value would be significantly better than the  $K_i$  values obtained with the N-nonyl and O-nonyl inhibitors.

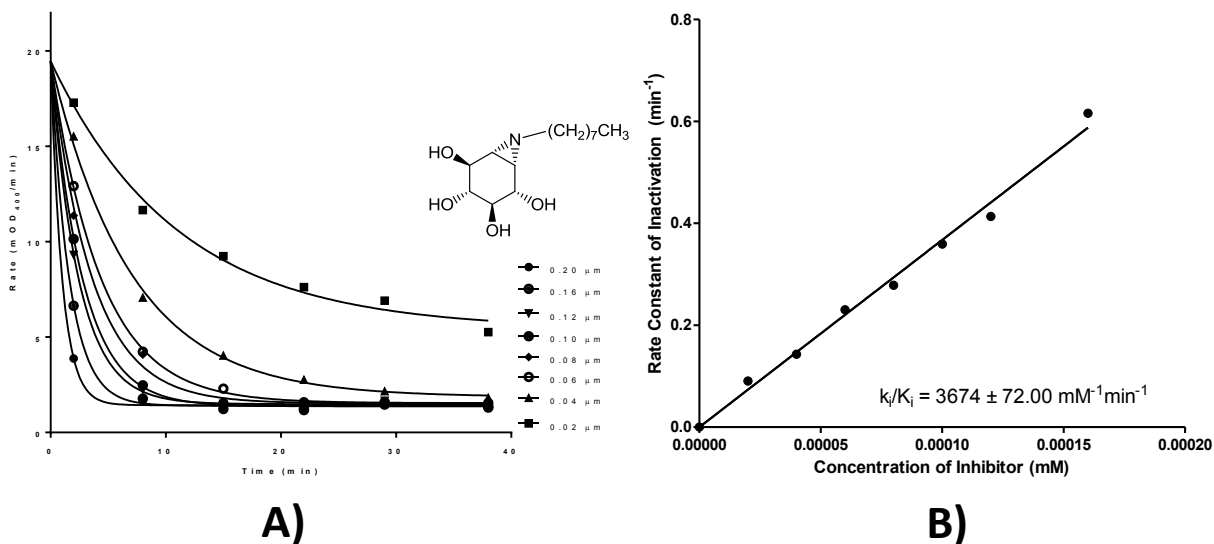


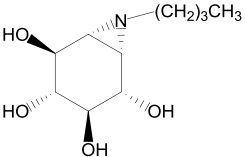
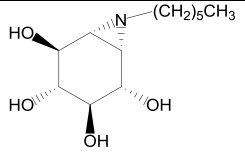
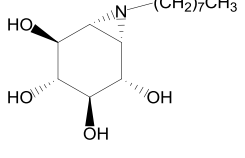
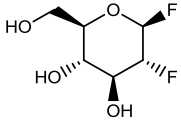
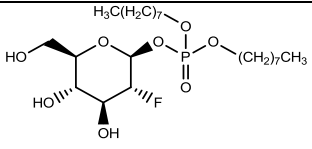
**Figure 4.2.6:** Inactivation of GCCase with **3.39**. a) Plot of remaining enzyme activity over time at the indicated inhibitor concentrations fitted to a one phase decay equation. b) Plot of the observed rate constants of inactivation versus the concentration of inhibitor.

To test for a highly reactive impurity in the inhibitor preparations, experiments were performed using concentration of the enzyme approaching the concentration of inactivator.<sup>56</sup> Based on the NMR spectra of compounds **3.39-3.41**, we can safely assume that the aziridine purity was  $\geq 95\%$ . Therefore, if inhibitor preparations were to contain a reactive but trace contaminant that was inactivating the enzyme, this compound would be at very dilute concentrations (i.e. a maximum value of 5% relative to the aziridine inhibitor). If the concentration of enzyme is greater than the trace impurity and complete inactivation of the enzyme is still observed in short reaction times, then the contaminant cannot be responsible for the inactivation. All aziridines synthesized in this thesis were incubated at stoichiometric levels of enzyme leading to the expected level of inactivation indicating that the aziridines were indeed responsible for the observed inhibition.

In summary, the aziridine derivatives were potent inhibitors of GCCase following the general trend of improved inactivation rates as alkyl chain length increases (summarized in **Table 4.2.1**). This

change in  $k_i/K_i$  values was much more pronounced than what was observed for the reversible competitive inhibitors and enzyme inactivation can be attributed solely to the aziridine inhibitors.

**Table 4.2.1:**  $K_i$  and  $k_i$  values and comparison of GCCase inactivators

Inhibitor Structure	ID	ABG $k_i/K_i$ ( $\text{mM}^{-1}\text{min}^{-1}$ )	Relative Change ABG	GCCase $k_i/K_i$ ( $\text{mM}^{-1}\text{min}^{-1}$ )	Relative Change GCCase
	<b>3.41</b>	.0138	1	$3.84 \pm 0.0972$	1
	<b>3.40</b>	0.241	17.42	$645 \pm 30.6$	168
	<b>3.39</b>	0.346	25.01	$3670 \pm 72.0$	958
	2-deoxy-2-fluoro- $\beta$ -D-glucosyl fluoride	12.6	911	0.0227	0.00592
	Diocetyl (2-deoxy-2-fluoro- $\beta$ -D-glucopyranosyl) phosphate	17	1229.2	98	26

#### 4.2.3 Turnover of the Inhibitor-Enzyme Covalent Intermediate

$\beta$ -Glycosidases inactivated by mechanism based inhibitors can reactivate by spontaneous hydrolysis of the covalent enzyme-inhibitor complex or by transglycosylation of the inhibitor onto an

acceptor sugar.<sup>4b</sup> It is important to know the reactivation rates for our inhibitors in order to ensure they remain covalently bound sufficiently long enough to function as persistent inhibitors for cell studies, as activity based probes for analyzing GCCase activity in complex mixtures, and as labelling agents for PET imaging. Reactivation of GCCase was measured by completely inactivating GCCase in a minimal concentration of the aziridine followed by removal of the free inhibitor using a desalting column. The inactivated enzyme was then incubated in assay buffer with high levels of 2,4-DNP-Glc and continuously monitored over 12 hours. Only spontaneous hydrolysis of the 2,4-DNP-Glc was observed over the entire 12 hour time period indicating that the aziridine-GCCase covalent intermediate is very stable and no free enzyme is regenerated. These results are expected because no reactivation was observed in pABG5 inactivated with conduritol aziridine.<sup>67</sup> For comparison purposes, the fluorosugar 2-deoxy-2-fluoro- $\beta$ -D-glucosyl fluoride, which forms a 2-fluoroglucosyl-GCCase intermediate, reactivates with a 1300 minute half-life indicating that the aziridine compounds have enormous potential as irreversible inhibitors and labeling agents for both cell and in vivo studies.<sup>75</sup>

#### **4.2.4 Kinetic Analysis of the Inactivation of GCCase in Cell Lysates by Aziridine Inhibitors 3.39-3.41**

To test the efficacy of the aziridine inhibitors in a cellular environment and to determine if the inhibitors are cell membrane permeable, a cell based assay was performed. HeLa cervical cancer cells were seeded into 16 well plates and grown to 80% confluency in media containing DMEM supplemented with 10% serum. The aziridine inhibitors were then incubated with the cells overnight at concentrations of 10 nM, 100 nM and 1  $\mu$ M. The following day, the cells were washed, lysed and the supernatant stored at -80°C until needed. In addition to GCCase, cells can contain four isoforms of GCCase called GBA1, GBA2 and GBA3, as well as NLGCCase, and a broad-specificity  $\beta$ -glucosidase.<sup>77</sup> Due to the presence of these competing  $\beta$ -glucosidases in cell lysate preparations, conditions were carefully chosen biased towards GCCase activity. This included the addition of the anionic detergent sodium taurocholate as well

as the use of the GCase fluorescent substrate 4-methylumbelliferyl  $\beta$ -D-glucose (4-MuGlc). Previous studies indicate that sodium taurocholate, in addition to enhancing GCase activity, can simultaneously inhibit  $\beta$ -glucosidase activity dependent on its concentration.<sup>78</sup> For example, 40-60% of  $\beta$ -glucosidase activity is inhibited when 0.2% sodium taurocholate is used, while increasing the detergent to 1.2% inhibits 95-97% of  $\beta$ -glucosidase activity in partially purified  $\beta$ -glucosidase from human liver.<sup>78</sup>

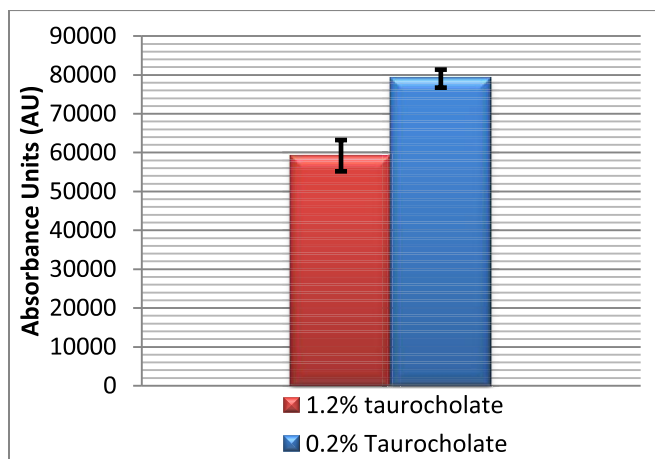


**Figure 4.2.7:** Total absorbance of untreated cell lysate controls. Error bars are the standard deviation based on three experiments.

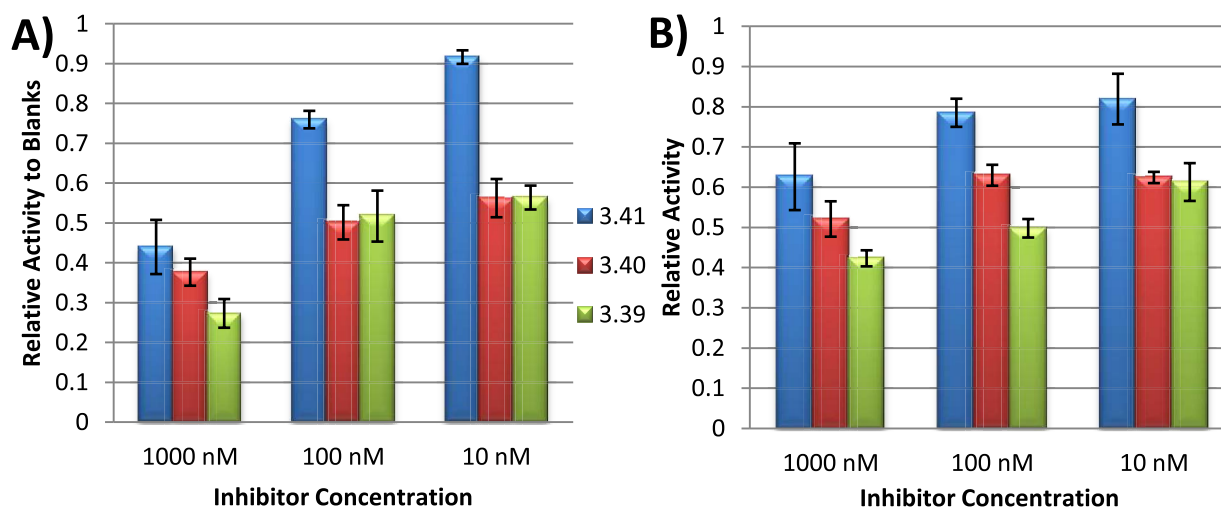


**Figure 4.2.8:** Residual activity of cell lysates relative to untreated lysate blank for **A)** buffers containing 1.2% sodium taurocholate. **B)** buffers containing 0.2% sodium taurocholate. Each bar represents the

lysate absorbance relative to untreated controls and the error bars are the standard deviations based on three experiments.

We therefore decided to try two separate experiments using 0.2% and 1.2% sodium taurocholate in the assay buffer. As shown in **Figure 4.2.8** the sodium taurocholate did indeed affect the total  $\beta$ -glucosidase activity in cell lysates. The total  $\beta$ -glucosidase activities in the untreated lysates were 59212 AU and 79043 AU for 1.2% and 0.2% sodium taurocholate respectively (**Figure 4.2.7**). The change in absorbance results from the increase in GCase activity and decrease in  $\beta$ -glucosidase activity indicating non-specific glucosidase activity was decreased more than GCase activity was stimulated.

For the butyl derivative **3.41** in 1.2% sodium taurocholate, a slight inhibition of  $\beta$ -glucosidase activity at 10 nM was observed leaving 91% residual  $\beta$ -glucosidase activity. Increasing the concentration to 100 nM showed greater inhibition of the  $\beta$ -glucosidases but still left 76% of the remaining activity. However, when the inhibitor concentration was increased to 1  $\mu$ M, a much stronger inhibition resulted with 44% residual  $\beta$ -glucosidase activity. As expected from the kinetic data, the butyl derivative was the least effective inhibitor. The hexyl derivative **3.40** inhibited ~50% of the  $\beta$ -glucosidase activity at 10 nM and 100 nM concentration. When concentration of **3.40** was increased to 1  $\mu$ M, the hexyl aziridine effectively inhibited  $\beta$ -glucosidase activity with 37% remaining activity. The nonyl derivative **3.39** was expected to be the most potent inhibitor based on our kinetics studies but showed no significant difference from the hexyl derivative **3.40** at 10 nM and 100 nM inhibitor concentrations. However, we observed the highest inhibition of the  $\beta$ -glucosidases by inhibitor **3.39** at 1  $\mu$ M concentration where only 27% residual  $\beta$ -glucosidase activity remained after treatment. At 1  $\mu$ M inhibitor concentration, the residual  $\beta$ -glucosidase activity corresponded to the kinetic data for inhibitors **3.41**, **3.40** and **3.39** showing 44%, 38%, and 26% residual enzyme activity respectively. At lower concentrations the efficacy of the hexyl

and octyl derivatives **3.40** and **3.39** are similar while the butyl derivative **3.41** is clearly a less effective  $\beta$ -glucosidase inhibitor.

It is difficult to determine the degree of selectivity that the aziridines inhibit GCCase over the other glycosidases in the cell lysates using these assays conditions. In addition, the presence of multiple  $\beta$ -glucosidases whose expression and catalytic activity is unknown in HeLa cells can dramatically affect the resulting cell studies. It is also unclear if the cell permeability of each compound significantly differs thereby influencing the intracellular concentration of the inhibitor and affecting inactivation rates. However, we can conclude that cells treated with the aziridine inhibitors produce cell lysates with significantly lower GCCase activity, clearly demonstrating that the aziridine inhibitors are efficient and cell permeable inactivators of GCCase. These compounds have enormous potential as mechanism-based inactivators of GCCase for cell studies, GCCase labeling agents or lead compounds for advanced molecular imaging probes to assess GCCase activity *in vivo*.

#### **4.3 Conclusions and Future Work**

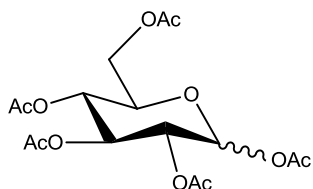
Further experimentation is required to determine the selectivity of the aziridine inhibitors towards GCCase over  $\beta$ -glucosidases in human cells. This can be easily accomplished by designing fluorescent aziridines to label the various glucosidases separated by SDS-PAGE. Additionally, cell studies at low temperatures will be necessary to determine if the inhibitors enter the cells through spontaneous cell permeability or active transport. Modifications to the inhibitors such as increased alkyl chain lengths or additional functional groups could then be made to increase the efficiency, specificity, and cell membrane permeability of the inhibitors. Finally, labelling the aziridines with  $^{18}\text{F}$  can allow tracking of Cerezyme to explore biodistribution of the enzyme and assess ERT using PET.

## Chapter 5: Experimental

### 5.1 General Considerations:

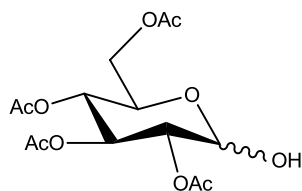
All buffers and reagents were obtained from Fisher Scientific or Sigma-Aldrich without further purification. Synthetic reactions were monitored by TLC using precoated silica gel plates (Silicycle 60F<sub>254</sub>, 0.25mm thickness). Compounds were detected by ultraviolet light ( $\lambda = 254\text{nm}$ ) followed by visualization with ammonium molybdate (10% w/v in 2M H<sub>2</sub>SO<sub>4</sub>), permanganate (1% w/v in water), or ninhydrin (1.5% w/v solution in butanol), each with heating. Flash chromatography was performed using Silicycle silica gel (230-400 mesh). NMR spectra were obtained using a Varian Unity Inova 500 MHz spectrometer dissolving samples in the appropriate deuterated solvents (CDCl<sub>3</sub>, CD<sub>3</sub>OD or D<sub>2</sub>O). Chemical shifts were reported in ppm downfield from tetramethylsilane. Low resolution ESI mass spectrometry was performed on a Dionex UHPLC Bruker amaZon X Ion Trap Mass Spectrometer.

#### 3.01 1,2,3,4,6-Penta-O-acetyl- $\beta$ -D-glucopyranose



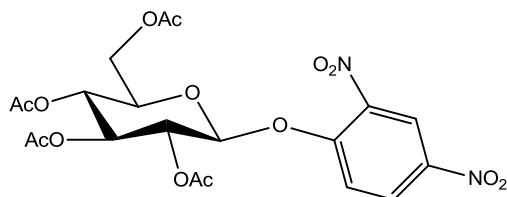
A solution of D-glucose (3.00 g, 16.7mmol) in anhydrous pyridine (30mL) was cooled to 0°C in an ice bath under argon. Acetic anhydride (12.3ml, 130mmol) was added dropwise and stirred at room temperature for 17 hours. The solution was then concentrated under reduced pressure, co-evaporating with toluene and the residue was purified by flash chromatography on silica gel (2:1, Hexanes:EtOAc) to yield 3.01 (92:8,  $\alpha$ : $\beta$ ) as a white powder (6.22g, 15.85mmol, 95% over two steps). Spectra were consistent with known data.<sup>38</sup>

### 3.02 2,3,4,6-Tetra-O-acetyl-β-D-glucopyranose



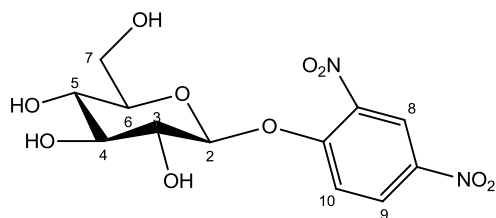
Hydrazine acetate (1.634g, 17.75mmol) was added to a solution of **3.01** (6.22g, 15.85mmol) in DMF (100mL) and allowed to stir for 2 hours under argon. EtOAc (200mL) was then added followed by saturated NaHCO<sub>3</sub> to precipitate excess hydrazine acetate and the solids removed by filtering through celite. The organics were then washed with water (2 x 100ml), brine (1 x 100mL), dried with MgSO<sub>4</sub> and concentrated under reduced pressure to give a slightly yellow syrup (5.52g, 15.85mmol ~100%). The compound was sufficiently pure for use in the synthesis of **3.03**. Spectra was consistent with known data.<sup>39</sup>

### 3.03 1-(2,4-dinitrophenoxy)-2,3,4,6-Tetra-O-acetyl-β-D-glucopyranose



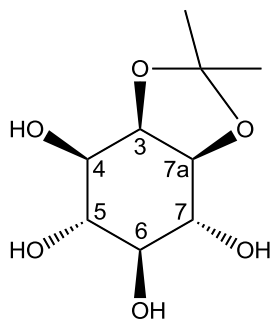
DABCO (1.991g, 17.75mmol) and 2,4-dinitrofluorobenzene (2.232mL, 17.75mmol) were added to a solution of **3.02** (5.52g, 15.85mmol) in anhydrous DMF (175mL) and allowed to stir overnight under argon and in the dark. The solution was concentrated under reduced pressure by co-evaporating with toluene. The organics were dissolved in DCM (200mL) and washed with saturated NaHCO<sub>3</sub> (1 x 200mL), water (2 x 200mL) brine (1 x 200mL), dried over MgSO<sub>4</sub>, then concentrated under reduced pressure. The product was recrystallized from ethanol to yield a white powder (4.17g, 8.11mmol, 51.1%). Spectra was consistent with known data.<sup>40</sup>

### 3.04 2,4-dinitrophenyl- $\beta$ -D-glucopyranoside



A solution of **3.03** (4.17g, 8.12mmol) in anhydrous methanol (200mL) is cooled to 0°C in an ice bath. AcCl (4.91mL, 69.1mmol) was added dropwise to the solution and allowed to stir for 48 hours at 4°C under argon. Solvents were removed under reduced pressure and the residue was partially purified by flash chromatography on silica gel (17:2:1 EtOAc:MeOH:AcOH). The product was then recrystallized from MeOH-Ether-Hexanes to yield a cream colored powder (1.04g, 2.99mmol, 36.8%). <sup>1</sup>H NMR (500 MHz, CD<sub>3</sub>OD)  $\delta$  3.49-3.93 (m, 6H, **H3**, **H4**, **H5**, **H6**, **H7a**, **H7b**), 5.38-5.40 (d, J = 7.5Hz, 1H, **H2**), 7.57-7.58 (d, J = 10Hz, 1H, **H10**), 8.49-8.51 (d, J = 10Hz, 1H, **H10**), 8.86 (s, 1H, **H8**). Spectra was consistent with known data.<sup>40</sup>

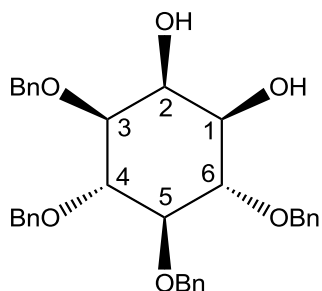
### 3.05 (3aR,4R,5S,6S,7R,7aS)-2,2-dimethylhexahydrobenzo[d][1,3]dioxole-4,5,6,7-tetraol



To a solution of myo-inositol (20.0g, 111 mmol) in DMSO (65mL), 2,2-dimethoxypropane (34mL, 274.2mmol) and p-toluenesulfonic acid (0.200g, 1.05mmol) were added. The mixture was heated at 90°C until a clear solution was formed (~30 minutes) and then cooled down to room temperature. Ethanol (80mL) and diethyl ether (400mL) were added and allowed to stir for 2 hours. Then, triethylamine (4mL) was added and allowed to stir for 4 hours. The reaction was allowed to sit

overnight resulting in a white precipitate. The solids were isolated by vacuum filtration, washed with a 1:5 solution of methanol-diethyl ether (100mL), and allowed to dry by suction. The residue was dissolved in hot ethanol and solids removed by vacuum filtration. The filtrate was then purified by recrystallization from ethanol and solids washed with cold diethyl ether to give a white powder (15.09g, 68.52mmol, 62%).  $^1\text{H}$  NMR (500 MHz,  $\text{D}_2\text{O}$ )  $\delta$  1.37 (s, 3H,  $\text{CH}_3$ ), 1.51 (s, 3H,  $\text{CH}_3$ ), 3.22-3.25 (t,  $J = 10\text{Hz}$ , 1H, **H4**), 3.54-3.58 (dd,  $J = 10, 8\text{Hz}$ , 1H, **H7**) 3.58-3.62 (t,  $J = 10\text{Hz}$ , 1H, **H6**), 3.81-3.84 (dd,  $J = 10, 4\text{Hz}$ , 1H, **H5**), 4.03-4.05 (dd,  $J = 8, 5\text{Hz}$ , 1H, **H7a**), 4.45-4.47 (t,  $J = 5\text{Hz}$ , 1H, **H3**).  $^{13}\text{C}$  NMR (500 MHz,  $\text{D}_2\text{O}$ )  $\delta$  25.04 ( $\text{CH}_3$ ), 27.22 ( $\text{CH}_3$ ), 69.32 (**C7**), 72.12 (**C4**), 72.48 (**C5**), 74.56 (**C6**), 75.99 (**C3**), 78.45 (**C7a**), 110.34 ( $\text{CH}(\text{CH}_3)_2$ ).

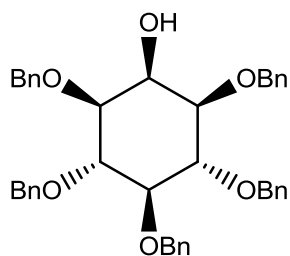
### 3.07 (1R,2R,3S,4R,5R,6S)-3,4,5,6-tetrakis(benzyloxy)cyclohexane-1,2-diol



A solution of **3.05** (10g, 45.41mmol) in dry DMF (300mL) was cooled to  $0^\circ\text{C}$  in an ice bath under argon. NaH (60% in oil, 6.54g, 227.1mmol) was slowly added to the open flask to allow venting of hydrogen gas. After stirring for 15 minutes, benzyl bromide (32.58mL, 272.5mmol) was added dropwise and the mixture was allowed to stir for 2 days at room temperature under argon. The reaction was quenched by the slow addition of water (50mL) and allowed to stir for 30 minutes allowing hydrogen gas to escape. The solution was concentrated under reduced pressure by co-evaporating with toluene for the azeotropic removal of DMF. The residue was dissolved in diethyl ether (100mL), washed with water (3 x 100mL), brine (1 x 100mL), dried over  $\text{Na}_2\text{SO}_4$ , and concentrated under reduced pressure. The residue was purified by flash chromatography on silica gel (4:1:1% Hexanes to EtOAc to TEA) to give the

clear colorless oil **3.06**. Then, the residue was added to a solution of water (75mL) and glacial acetic acid (300mL) and allowed to reflux for 3 hours. Solvents were removed under reduced pressure and the residue was purified by flash chromatography on silica gel (2:1, Hexanes:EtOAc) to yield **3.07** as a white powder (12.97g, 23.99mmol, 53% over two steps).  $^1\text{H}$  NMR (500 MHz,  $\text{CD}_3\text{OD}$ )  $\delta$  3.43-3.46 (t,  $J = 9.5\text{Hz}$ , 1H, **H1**), 3.46-3.49 (dd,  $J = 9.5, 3\text{Hz}$ , 1H, **H5**), 3.52-3.54 (dd,  $J = 9.5, 3\text{Hz}$ , 1H, **H4**), 3.80-3.84 (t,  $J = 9.5\text{Hz}$ , 1H, **H3**), 3.93-3.97 (t,  $J = 9.5\text{Hz}$ , 1H, **H6**), 4.17-4.18 (t,  $J = 3\text{Hz}$ , 1H, **H2**), 4.62-4.93 (m, 8H, CH-**CH**<sub>2</sub>-O), 7.23-7.42 (m, 20H, **phenyl**).  $^{13}\text{C}$  NMR (500 MHz,  $\text{CD}_3\text{OD}$ )  $\delta$  69.67 (C1), 71.68 (**C**CH<sub>2</sub>-O), 71.98(**C**CH<sub>2</sub>-O), 75.03(**C**CH<sub>2</sub>-O), 75.21(**C**CH<sub>2</sub>-O), 80.12 (**C5**), 81.30 (**C4**), 81.77 (**C3**), 83.13 (**C6**), 127.06 (**CH**, phenyl), 127.07 (**CH**, phenyl), 127.10 (**CH**, phenyl), 127.26 (**CH**, phenyl), 127.35 (**CH**, phenyl), 127.59 (**CH**, phenyl), 127.62 (**CH**, phenyl), 127.65 (**CH**, phenyl), 127.68 (**CH**, phenyl), 127.70 (**CH**, phenyl), 127.75 (**CH**, phenyl), 127.79 (**CH**, phenyl), 127.81 (**CH**, phenyl), 127.85 (**CH**, phenyl), 127.94 (**CH**, phenyl), 138.48 (**C**-CH<sub>2</sub>-O, phenyl), 138.84 (**C**-CH<sub>2</sub>-O, phenyl), 138.88 (**C**-CH<sub>2</sub>-O, phenyl), 139.02 (**C**-CH<sub>2</sub>-O, phenyl).

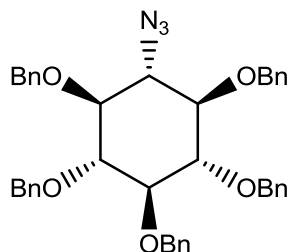
### **3.08 (1r,2R,3S,4r,5R,6S)-2,3,4,5,6-pentakis(benzyloxy)cyclohexanol**



Tetrabutyl ammonium bromide (3.80g, 11.8mmol), dibutyltin oxide (2.90g, 11.6mmol) and benzyl bromide (2.00mL, 16.7mmol) are added to a solution of **3.07** (6.00g, 11.1mmol) in acetonitrile and allowed to reflux overnight with stirring. The solution was concentrated under reduced pressure. The residue was dissolved in diethyl ether (100mL), washed with water (3 x 100mL), brine (1 x 100mL), dried over  $\text{Na}_2\text{SO}_4$ , and concentrated under reduced pressure then dissolved in diethyl ether (150mL), washed with water (1 x 100mL), dried over  $\text{Na}_2\text{SO}_4$ , and again concentrated under reduced pressure. The

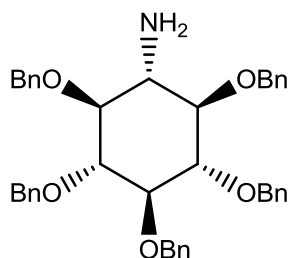
residue was purified by recrystallization from hot methanol and solids washed with cold methanol to give white crystals (5.49g, 8.71mmol, 78%).

### 3.09 (1R,2S,3r,4R,5S,6s)-6-azido-1,2,3,4,5-pentabenzoyloxycyclohexane



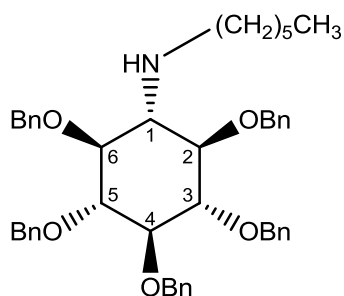
A solution of **3.08** (1.19g, 1.89mmol) in pyridine (10mL) was cooled to 0°C in an ice bath. Methanesulfonyl chloride (1.46mL, 18.9 mmol) was added dropwise and allowed to stir at room temperature overnight and under argon. The solution was then concentrated under reduced pressure, co-evaporating with toluene. The residue was dissolved in diethyl ether (100mL) and washed with water (1 x 100mL), 1M HCl (1 x 100mL), saturated NaHCO<sub>3</sub> (1 x 100mL), brine (1 x 100mL), dried over Na<sub>2</sub>SO<sub>4</sub>, then concentrated under reduced pressure to yield an orange solid. The thoroughly dried mixture was dissolved in DMF (25mL). NaN<sub>3</sub> (1.17g, 17.9mmol) was added and the solution heated to 80°C, stirring under argon for 2 days. The reaction was then concentrated under reduced pressure, co-evaporating with toluene. The residue was redissolved in EtOAc (50mL), washed with water (1 x 50mL), brine (1 x 50mL) and dried over Na<sub>2</sub>SO<sub>4</sub>, then concentrated under reduced pressure. The residue was purified by flash chromatography on silica gel (11:1 Hexanes:EtOAc) to yield **3.17** as a clear oil (860mg, 1.31mmol, 69%). Spectra was consistent with known data.

### 3.10 (1s,2R,3S,4r,5R,6S)-2,3,4,5,6-pentakis(benzyloxy)cyclohexanamine



A solution of **3.09** (860mg, 1.31mmol) in THF (30mL) was cooled to 0°C in an ice bath. LiAlH<sub>4</sub> (100mg, 2.76mmol) was then slowly added and allowed to stir for 2 hours at 0°C and under argon. EtOAc (20mL) was added to the solution to quench the reaction and allowed to stir for an additional 30 minutes. The organics were washed with water (1 x 50mL), brine (1 x 50mL), dried over Na<sub>2</sub>SO<sub>4</sub>, and concentrated under reduced pressure to yield a white solid (810mg, 1.28mmol, 98%). Spectra was consistent with known data.

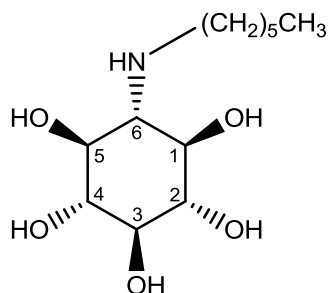
### 3.11 (1s,2R,3S,4r,5R,6S)-2,3,4,5,6-pentakis(benzyloxy)-N-hexylcyclohexanamine



Hexanal (45μL, 0.37mmol) was added to a mixture of **3.23** (200mg, 0.318mmol) in 30mL of dry methanol. NaBH<sub>3</sub>CN (40mg, 0.64mmol) and AcOH (50μL, 0.87mmol) were then added stirring at room temperature for four days under argon. To quench the reaction 5mL of water was added and allowed to stir for 15 minutes turning the clear solution to a cloudy white mixture. Diethyl ether (3 x 25mL) was added to the aqueous solution to extract the organics. The organic portion was dried with brine (1 x 25mL) and Na<sub>2</sub>SO<sub>4</sub>, then concentrated under reduced pressure. The resulting residue was purified by

flash chromatography on silica gel (1:1:3.5% Hexanes: EtOAc:AcOH) to give **3.11** as cream colored solid (56mg, 0.079mmol, 25%).  $^1\text{H}$  NMR (500 MHz,  $\text{CDCl}_3$ )  $\delta$  0.82-0.89 (m, 3H,  $\underline{\text{CH}_3}$ ), 1.16-1.38 (m, 8H,  $\underline{\text{CH}_2}$ ), 2.17 (broad s, 1H,  $\underline{\text{NH}}$ ), 2.59-2.63 (t,  $J = 10\text{Hz}$ , 1H,  $\underline{\text{H1}}$ ), 2.71-2.81 (m, 2H,  $\underline{\text{NH-CH}_2}$ ), 3.40-3.63 (m, 5H,  $\underline{\text{H2}}$ ,  $\underline{\text{H3}}$ ,  $\underline{\text{H4}}$ ,  $\underline{\text{H5}}$ ,  $\underline{\text{H6}}$ ), 4.72-4.97 (m, 10H,  $\underline{\text{O-CH}_2}$ ), 7.23-7.35 (m, 25H,  $\underline{\text{phenyl}}$ ).  $^{13}\text{C}$  NMR (500 MHz,  $\text{CDCl}_3$ )  $\delta$  14.21 ( $\underline{\text{C}}_3$ ), 21.05 ( $\underline{\text{C}}_2$ ), 22.74 ( $\underline{\text{C}}_2$ ), 27.30 ( $\underline{\text{C}}_2$ ), 30.30 ( $\underline{\text{C}}_2$ ), 31.92 ( $\underline{\text{C}}_2$ ), 60.41 ( $\underline{\text{C1}}$ ), 75.55 ( $\underline{\text{C3}}$ ), 75.79 ( $\underline{\text{C5}}$ ), 79.76 ( $\underline{\text{C4}}$ ), 84.45 ( $\underline{\text{C6}}$ ), 84.69 ( $\underline{\text{C2}}$ ), 127.42 ( $\underline{\text{C}}_H$ , phenyl), 127.56 ( $\underline{\text{C}}_H$ , phenyl), 127.61 ( $\underline{\text{C}}_H$ , phenyl), 127.67 ( $\underline{\text{C}}_H$ , phenyl), 127.75 ( $\underline{\text{C}}_H$ , phenyl), 127.79 ( $\underline{\text{C}}_H$ , phenyl), 127.83 ( $\underline{\text{C}}_H$ , phenyl), 127.85 ( $\underline{\text{C}}_H$ , phenyl), 128.02 ( $\underline{\text{C}}_H$ , phenyl), 128.26 ( $\underline{\text{C}}_H$ , phenyl), 128.39 ( $\underline{\text{C}}_H$ , phenyl), 128.45 ( $\underline{\text{C}}_H$ , phenyl), 128.52 ( $\underline{\text{C}}_H$ , phenyl), 138.25 ( $\underline{\text{C-CH}_2\text{-O}}$ , phenyl), 138.41 ( $\underline{\text{C-CH}_2\text{-O}}$ , phenyl), 138.53 ( $\underline{\text{C-CH}_2\text{-O}}$ , phenyl), 138.61 ( $\underline{\text{C-CH}_2\text{-O}}$ , phenyl), 138.92 ( $\underline{\text{C-CH}_2\text{-O}}$ , phenyl).

### 3.12 (1R,2S,3r,4R,5S,6s)-6-(hexylamino)cyclohexane-1,2,3,4,5-pentaol

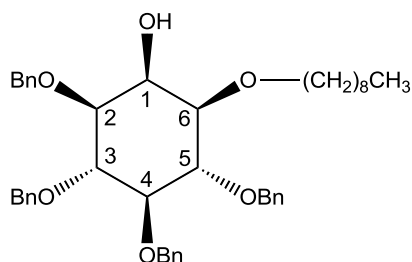


Concentrated HCl (5 drops) was added to a solution of **3.11** (56mg, 0.079mmol) in THF (5mL).

The system was flushed with argon followed by the addition of 10% Pd/C (50mg, 0.038mmol). The vessel was then repeatedly filled and evacuated with hydrogen and the mixture was hydrogenated at atmospheric pressure at 70°C for 16 hours with stirring. The catalyst was removed by vacuum filtration through a plug of Celite and was washed with methanol (20mL). The filtrate was concentrated under reduced pressure to provide a yellow oil. The oil was purified by flash chromatography on silica gel (4:1:1% Hexanes: EtOAc:TEA). Fractions containing the product were concentrated then lyophilized to yield the HCl salt of **3.12** as a white powder (6.0mg, 0.020mmol, 25%).  $^1\text{H}$  NMR (500 MHz,  $\text{D}_2\text{O}$ )  $\delta$  0.80-

0.88 (m, 3H, CH<sub>3</sub>), 1.21-1.40 (m, 6H, CH<sub>3</sub>), 1.60-1.68 (m, 2H, N-CH<sub>2</sub>-CH<sub>2</sub>), 1.85-1.91 (m, 4H, OH), 2.94-3.07 (m, 3H, N-CH<sub>2</sub>, H1), 3.26-3.40 (m, 3H, H3, H4, H5), 3.52-3.61 (m, 2H, H2, H6) <sup>13</sup>C NMR (500 MHz, CDCl<sub>3</sub>) δ 13.14 (CH<sub>3</sub>), 21.68 (CH<sub>2</sub>), 25.39 (CH<sub>2</sub>), 26.24 (CH<sub>2</sub>), 30.38 (CH<sub>2</sub>), 45.10 (N-CH<sub>2</sub>), 60.87 (H1), 69.00 (H2, H6), 72.94 (H4), 74.43 (H3, H5). LRMS (ESI) m/z: 263.1 [M + H]<sup>+</sup> Calculated for C<sub>12</sub>H<sub>26</sub>NO<sub>5</sub><sup>+</sup>: 264.1805

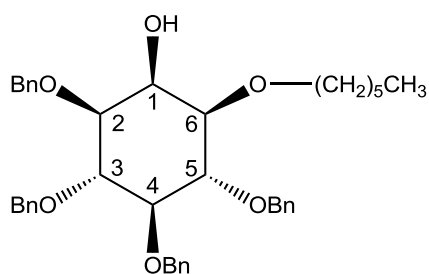
### 3.13 (1S,2S,3R,4R,5S,6R)-2,3,4,5-tetrakis(benzyloxy)-6-(nonyloxy)cyclohexanol



Dibutyltin oxide (0.760g, 3.047mmol) was added to a solution of **3.07** (1.500g, 2.77mmol) in toluene (25mL). The mixture was refluxed overnight using a Dean-Stark apparatus to remove water as the reaction proceeds. The reaction was concentrated under reduced pressure to leave a dark yellow oil that foams aggressively before hardening into a thick syrup. The syrup was dissolved in DMF (25mL) followed by the addition of Cesium fluoride (0.841g, 5.54mmol) and 1-bromononane (0.582mL, 3.047mmol) and the mixture allowed to stir under argon for 2 days at room temperature. The insoluble components were removed by vacuum filtration through celite and which was washed with EtOAc. The solution was concentrated under reduced pressure by co-evaporating with toluene. The residue was dissolved in diethyl ether (50mL), washed with water (50mL), brine (50mL), dried over Na<sub>2</sub>SO<sub>4</sub>, and concentrated under reduced pressure. The residue was purified by flash chromatography on silica gel (6:1, Hexanes:EtOAc) to yield BA83 as a brown oil (1.47g, 2.204mmol, 79.5%). <sup>1</sup>H NMR (500 MHz, CDCl<sub>3</sub>) δ 0.94-0.98 (t, J = 7Hz, 3H, CH<sub>3</sub>), 1.31-1.51 (m, 12H, CH<sub>2</sub>), 1.67-1.73 (pentet, J = 7Hz, 2H, O-CH<sub>2</sub>-CH<sub>2</sub>), 2.56 (s, 1H, OH), 3.29-3.32 (dd, J = 9.5, 3.5Hz, 1H, H4), 3.48-3.51 (dd, J = 9.5, 3.5Hz, 1H, H3), 3.51-3.55 (t, J = 9.5Hz, 1H, H6), 3.61-3.66 (dt, J = 9, 7Hz, 1H, O-CH<sub>2</sub>), 3.70-3.74 (dt, J = 9, 7Hz, 1H, O-CH<sub>2</sub>), 3.97-4.01 (t, J =

9.5Hz, 1H, **H2**), 4.06-4.10 (t, J = 9.5Hz, 1H, **H5**), 4.34-4.35 (t, J = 2.5Hz, 1H, **H1**), 4.82-4.99 (m, 8H, CH-**CH2**-O), 7.28-7.45 (m, 20H, **phenyl**). <sup>13</sup>C NMR (500 MHz, CDCl<sub>3</sub>) δ 14.21 (**CH**<sub>3</sub>), 22.75 (**CH**<sub>2</sub>), 26.26 (**CH**<sub>2</sub>), 29.36 (**CH**<sub>2</sub>), 29.59 (**CH**<sub>2</sub>), 29.62 (**CH**<sub>2</sub>), 30.24 (**CH**<sub>2</sub>), 31.95 (**CH**<sub>2</sub>), 67.35 (**C1**), 71.17 (**CH**<sub>2</sub>-O-C2), 72.81 (**C3**), 75.96 (**CH**<sub>2</sub>-O-C2), 76.02 (**CH**<sub>2</sub>-O-C2), 76.06 (**CH**<sub>2</sub>-O-C2), 80.04 (**C6**), 80.65 (**C2**), 81.21 (**C5**), 81.29 (**C4**), 83.19 (**CH**<sub>2</sub>-**CH**<sub>2</sub>-O), 127.60 (**CH**, phenyl), 127.61 (**CH**, phenyl), 127.65 (**CH**, phenyl), 127.90 (**CH**, phenyl), 127.92 (**CH**, phenyl), 128.04 (**CH**, phenyl), 128.12 (**CH**, phenyl), 128.39 (**CH**, phenyl), 128.42 (**CH**, phenyl), 128.43 (**CH**, phenyl), 128.53 (**CH**, phenyl), 138.10 (**C**-CH<sub>2</sub>-O, phenyl), 138.81 (**C**-CH<sub>2</sub>-O, phenyl), 138.81 (**C**-CH<sub>2</sub>-O, phenyl), 138.91 (**C**-CH<sub>2</sub>-O, phenyl).

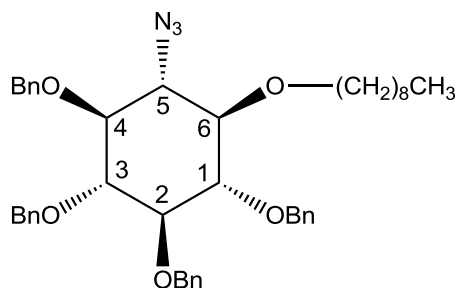
### 3.14 (1S,2S,3R,4R,5S,6R)-2,3,4,5-tetrakis(benzyloxy)-6-(hexyloxy)cyclohexanol



Dibutyltin oxide (380mg, 1.53mmol) was added to a solution of **3.07** (750mg, 1.39mmol) in toluene (15mL). The mixture was refluxed overnight using a Dean-Stark apparatus to remove water as the reaction proceeds. The reaction was concentrated under reduced pressure to leave a dark yellow oil that foams aggressively before hardening into a thick syrup. The syrup was dissolved in DMF (10mL) followed by the addition of Cesium fluoride (421mg, 2.77mmol) and 1-bromohexane (0.214mL, 1.53mmol) and the mixture allowed to stir under argon for 2 days at room temperature. The insoluble components were removed by vacuum filtration through celite and which was washed with EtOAc. The solution was concentrated under reduced pressure by co-evaporating with toluene. The residue was dissolved in diethyl ether (50mL), washed with water (50mL), brine (50mL), dried over Na<sub>2</sub>SO<sub>4</sub>, and concentrated under reduced pressure. The residue was purified by flash chromatography on silica gel

(5:1, Hexanes:EtOAc) to yield **3.14** as a brown oil (650mg, 1.02mmol, 73.9%).  $^1\text{H}$  NMR (500 MHz,  $\text{CDCl}_3$ )  $\delta$  0.86-0.89 (t,  $J = 7\text{Hz}$ , 3H, **CH<sub>3</sub>**), 1.24-1.37 (m, 6H, **CH<sub>2</sub>**), 1.59-1.64 (quintet, 7Hz, 2H, O-CH<sub>2</sub>-**CH<sub>2</sub>**), 2.47 (s, 1H, **OH**), 3.22-3.24 (dd,  $J = 9, 3\text{Hz}$ , 1H, **H6**) 3.41-3.43 (dd,  $J = 9, 3\text{Hz}$ , 1H, **H2**), 3.43-3.47 (t,  $J = 9\text{Hz}$ , 1H, **H3**), 3.54-3.58 (dt,  $J = 9, 7\text{Hz}$ , 1H, O-**CH<sub>2</sub>**), 3.62-3.67 (dt,  $J = 9, 7\text{Hz}$ , 1H, O-**CH<sub>2</sub>**), 3.89-3.93 (t,  $J = 9\text{Hz}$ , 1H, **H5**), 3.98-4.02 (t,  $J = 9\text{Hz}$ , 1H, **H4**), 4.26-4.27 (t,  $J = 3\text{Hz}$ , 1H, **H1**), 4.74-4.91 (m, 8H, CH-**CH<sub>2</sub>**-O), 7.24-7.38 (m, 20H, **phenyl**).  $^{13}\text{C}$  NMR (500 MHz,  $\text{CDCl}_3$ )  $\delta$  14.13 (**CH<sub>3</sub>**), 22.65 (**CH<sub>2</sub>**), 25.90 (**CH<sub>2</sub>**), 30.18 (**CH<sub>2</sub>**), 31.75 (**CH<sub>2</sub>**), 67.32 (**C1**), 71.17(**CH<sub>2</sub>**-O-C2), 72.81 (**C3**), 75.96 (CH-**CH<sub>2</sub>**-O), 76.01 (CH-**CH<sub>2</sub>**-O), 76.06 (CH-**CH<sub>2</sub>**-O), 80.00 (**C6**), 80.60 (**C2**), 81.16 (**C5**), 81.26 (**C4**), 83.15 (CH<sub>2</sub>-**CH<sub>2</sub>**-O), 127.60 (**CH**, phenyl), 127.61 (**CH**, phenyl), 127.65 (**CH**, phenyl), 127.91 (**CH**, phenyl), 128.04 (**CH**, phenyl), 128.11 (**CH**, phenyl), 128.38 (**CH**, phenyl), 128.41 (**CH**, phenyl), 128.52 (**CH**, phenyl), 138.05 (**C**-CH<sub>2</sub>-O, phenyl), 138.76 (**C**-CH<sub>2</sub>-O, phenyl), 138.85 (**C**-CH<sub>2</sub>-O, phenyl).

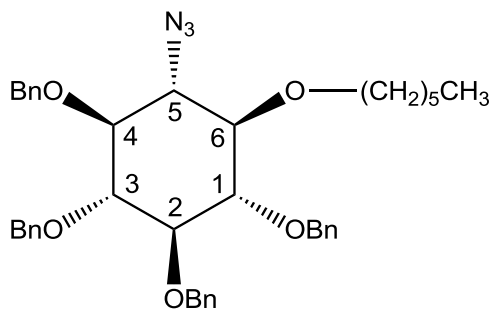
**3.16 (((((1S,2R,3R,4S,5R,6R)-5-azido-6-(nonyloxy)cyclohexane-1,2,3,4-tetraol)tetrakis(oxy))tetrakis(methylene))tetrabenzene**



A solution of BA83 (1.39g, 2.084mmol) in pyridine (5mL) was cooled to 0°C in an ice bath. Methanesulfonyl chloride (0.81 mL, 10.42mmol) was added dropwise and allowed to stir at room temperature overnight and under argon. The solution was then concentrated under reduced pressure, co-evaporating with toluene. The residue was dissolved in diethyl ether (100mL) and washed with water (2 x 100mL), 1M HCl (1 x 100mL), saturated  $\text{NaHCO}_3$  (1 x 100mL), brine (1 x 100mL), dried over  $\text{Na}_2\text{SO}_4$ , then concentrated under reduced pressure to yield a golden yellow syrup (1.40g). The thoroughly dried

mixture was dissolved in DMF (20mL).  $\text{NaN}_3$  (1.29g, 19.80mmol) was added and allowed to stir at room temperature and under argon for 2 days. The reaction was then concentrated under reduced pressure, co-evaporating with toluene. The residue was redissolved in EtOAc (50mL), washed with water (1 x 50mL), brine (1 x 50mL) and dried over  $\text{Na}_2\text{SO}_4$ , then concentrated under reduced pressure. The residue was purified by flash chromatography on silica gel (25:1 Hexanes:EtOAc) to yield BA85 as a clear, faintly yellow oil (0.92g, 1.330mmol, 64%).  $^1\text{H}$  NMR (500 MHz,  $\text{CDCl}_3$ )  $\delta$  0.86-0.89 (t,  $J$  = 7Hz, 3H, **CH<sub>3</sub>**), 1.25-1.35 (m, 12H, **CH<sub>2</sub>**), 1.61-1.65 (sextet,  $J$  = 7Hz, 2H, O-**CH<sub>2</sub>-CH<sub>2</sub>-CH<sub>2</sub>**), 3.12-3.16 (t,  $J$  = 10Hz, 1H, **H<sub>2</sub>**), 3.27-3.30 (t,  $J$  = 10Hz, 1H, **H<sub>3</sub>**), 3.38-3.54 (m, 4H, **H<sub>1</sub>**, **H<sub>4</sub>**, **H<sub>5</sub>**, **H<sub>6</sub>**), 3.74-3.76 (q,  $J$  = 7Hz, 1H, O-**CH<sub>2</sub>-CH<sub>2</sub>**), 3.81-3.83 (q,  $J$  = 7Hz, 1H, O-**CH<sub>2</sub>-CH<sub>2</sub>**), 4.83-4.88 (m, 8H, CH-**CH<sub>2</sub>-O**), 7.24-7.34 (m, 20H, **phenyl**).  $^{13}\text{C}$  NMR (500 MHz,  $\text{CDCl}_3$ )  $\delta$  14.18 (**CH<sub>3</sub>**), 22.72 (**CH<sub>2</sub>**), 26.15 (**CH<sub>2</sub>**), 29.32 (**CH<sub>2</sub>**), 29.59 (**CH<sub>2</sub>**), 30.38 (**CH<sub>2</sub>**), 31.92 (**CH<sub>2</sub>**), 66.93(**C<sub>5</sub>**), 74.27(O-**CH<sub>2</sub>-CH<sub>2</sub>**), 75.99-76.05 (O-**CH<sub>2</sub>-CH**), 81.01(**C<sub>3</sub>**), 81.42 (**C<sub>1</sub>**), 82.52 (**C<sub>2</sub>**), 83.27 (**C<sub>4</sub>**), 83.31 (**C<sub>6</sub>**), 127.78 (**CH**, phenyl), 127.85 (**CH**, phenyl), 127.90 (**CH**, phenyl), 127.97 (**CH**, phenyl), 128.27 (**CH**, phenyl), 128.48 (**CH**, phenyl), 137.86 (**C-CH<sub>2</sub>-O**, phenyl), 138.31 (**C-CH<sub>2</sub>-O**, phenyl).

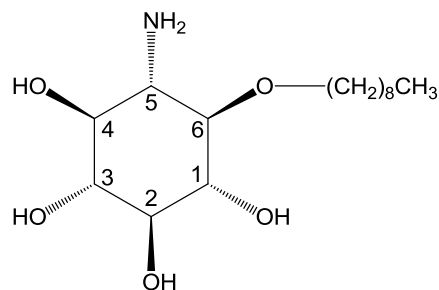
### 3.17 (((((1S,2R,3R,4S,5R,6R)-5-azido-6-(hexyloxy)cyclohexane-1,2,3,4-tetraol)tetrakis(oxy))tetrakis(methylene))tetrabenzene



A solution of **3.14** (650mg, 1.03mmol) in pyridine (10mL) was cooled to 0°C in an ice bath. Methanesulfonyl chloride (0.397mL, 5.13mmol) was added dropwise and allowed to stir at room temperature overnight and under argon. The solution was then concentrated under reduced pressure, co-evaporating with toluene. The residue was dissolved in diethyl ether (100mL) and washed with water

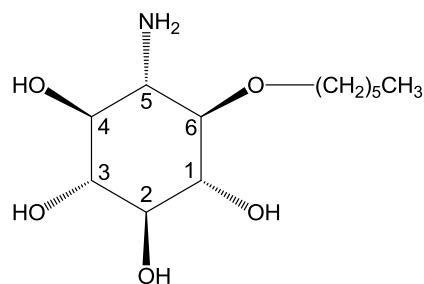
(2 x 100mL), 1M HCl (1 x 100mL), saturated NaHCO<sub>3</sub> (1 x 100mL), brine (1 x 100mL), dried over Na<sub>2</sub>SO<sub>4</sub>, then concentrated under reduced pressure to yield a golden yellow syrup. The thoroughly dried mixture was dissolved in DMF (20mL). NaN<sub>3</sub> (600mg, 9.23mmol) was added and allowed to stir at room temperature and under argon for 2 days. The reaction was then concentrated under reduced pressure, co-evaporating with toluene. The residue was redissolved in EtOAc (50mL), washed with water (1 x 50mL), brine (1 x 50mL) and dried over Na<sub>2</sub>SO<sub>4</sub>, then concentrated under reduced pressure. The residue was purified by flash chromatography on silica gel (25:1 Hexanes:EtOAc) to yield **3.17** as a clear, faintly yellow oil (354mg, 0.5448mmol, 53%). <sup>1</sup>H NMR (500 MHz, CDCl<sub>3</sub>) δ 0.86-0.88 (t, J = 7Hz, 3H, CH<sub>3</sub>), 1.24-1.38 (m, , 6H, CH<sub>2</sub>), 1.58-1.68 (octet, J = 7Hz, 2H, O-CH<sub>2</sub>-CH<sub>2</sub>), 3.12-3.16 (t, J = 9Hz, 1H, H5), 3.27-3.30 (t, J = 9Hz, 1H, H1), 3.37-3.41 (t, J = 9Hz, 1H, H2), 3.44-3.50(m, 2H, H3, H4), 3.51-3.56 (q, J = 9Hz, 1H, H6), 3.73-3.78 (dt, J = 9, 7Hz, 1H, O-CH<sub>2</sub>), 3.81-3.85 (dt, J = 9, 7Hz, 1H, O-CH<sub>2</sub>), 4.81-4.88 (m, 8H, CH-CH<sub>2</sub>-O), 7.19-7.36 (m, 20H, phenyl). <sup>13</sup>C NMR (500 MHz, CDCl<sub>3</sub>) δ 14.14 (CH<sub>3</sub>), 22.70 (CH<sub>2</sub>), 25.86 (CH<sub>2</sub>), 30.39 (CH<sub>2</sub>), 31.81 (CH<sub>2</sub>), 67.03 (C5), 74.28 (O-CH<sub>2</sub>-CH), 75.98 (O-CH<sub>2</sub>-CH), 76.01 (O-CH<sub>2</sub>-CH), 76.01 (O-CH<sub>2</sub>-CH), 76.07 (O-CH<sub>2</sub>-CH), 81.09 (C3), 81.50(C1), 82.60 (C2), 83.34 (C4), 83.38 (C6), 127.77 (CH, phenyl), 127.79 (CH, phenyl), 127.81 (CH, phenyl), 127.87 (CH, phenyl), 127.88 (CH, phenyl), 127.90 (CH, phenyl), 127.91 (CH, phenyl), 127.93 (CH, phenyl), 127.94 (CH, phenyl), 127.99 (CH, phenyl), 128.29 (CH, phenyl), 128.48 (CH, phenyl), 128.49 (CH, phenyl), 128.51 (CH, phenyl), 128.51 (CH, phenyl), 128.52 (CH, phenyl), 128.55 (CH, phenyl), 128.56 (CH, phenyl), 137.96 (C-CH<sub>2</sub>-O, phenyl), 138.39 (C-CH<sub>2</sub>-O, phenyl), 138.40 (C-CH<sub>2</sub>-O, phenyl), 138.42 (C-CH<sub>2</sub>-O, phenyl).

### 3.19 (1R,2S,3R,4S,5S,6R)-5-amino-6-(nonyloxy)cyclohexane-1,2,3,4-tetraol



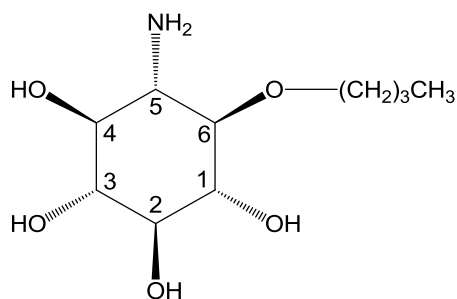
In a high pressure reaction vessel, concentrated HCl (5 drops) was added to a solution of **3.16** (150mg, 0.225mmol) in methanol (10mL). The system was flushed with argon followed by the addition of 10% Pd/C (120mg, 0.113mmol). The vessel was then repeatedly filled and evacuated with hydrogen and the mixture was hydrogenated at 50 psi for 16 hours with stirring. The catalyst was removed by vacuum filtration through a plug of Celite and was washed with methanol (20mL). The filtrate was concentrated under reduced pressure to provide a white powder. The residue was dissolved in water (2mL), basified with concentrated NH<sub>4</sub>OH (1mL) to yield a black precipitate and the solution was purified by reversed phase chromatography (Thermo Scientific, Hypersep C18, 2000mg, 15mL ) using a gradient of water to methanol (0% to 100% MeOH at 20% increments). Fractions containing the product were concentrated then lyophilized to yield the HCl salt of **3.19** as a white powder (54mg, 0.16mmol, 70%). <sup>1</sup>H NMR (500 MHz, CD<sub>3</sub>OD) δ 0.88-0.91 (t, J = 7Hz, 3H, CH<sub>3</sub>), 1.24-1.37 (m, 12H, CH<sub>2</sub>), 1.57-1.65 (octet, J = 7Hz, 2H, O-CH<sub>2</sub>-CH<sub>2</sub>), 2.60-2.64 (t, J = 9Hz, 1H, H5), 2.93-2.97 (t, J = 9Hz, 1H, H6), 3.10-3.20 (m, 3H, H2, H3, H4), 3.30-3.35 (m, 1H, H1), 3.57-3.62 (dt, J = 9, 7Hz, 1H, O-CH<sub>2</sub>), 3.94-3.99 (dt, J = 9, 7Hz, 1H, O-CH<sub>2</sub>). <sup>13</sup>C NMR (500 MHz, CD<sub>3</sub>OD) δ 13.06 (CH<sub>3</sub>), 22.35 (CH<sub>2</sub>), 25.85 (CH<sub>2</sub>), 29.05 (CH<sub>2</sub>), 29.30 (CH<sub>2</sub>), 29.34 (CH<sub>2</sub>), 30.03 (CH<sub>2</sub>), 31.67 (CH<sub>2</sub>), 55.23 (C5), 72.85 (O-CH<sub>2</sub>), 73.72 (C1), 74.57 (C4), 75.27 (C2), 75.67 (C3), 82.52 (C6). LRMS (ESI) m/z: 292.2 [M + H]<sup>+</sup> Calculated for C<sub>14</sub>H<sub>30</sub>NO<sub>5</sub><sup>+</sup>: 292.2118

### 3.20 (1R,2S,3R,4S,5S,6R)-5-amino-6-(hexyloxy)cyclohexane-1,2,3,4-tetraol



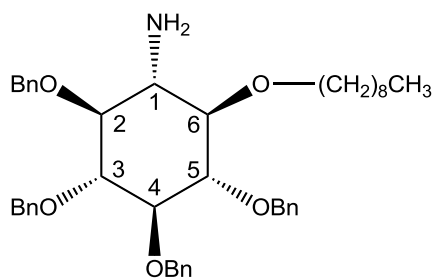
In a high pressure reaction vessel, concentrated HCl (5 drops) was added to a solution of **3.17** (354mg, 0.545mmol) in methanol (15mL). The system was flushed with argon followed by the addition of 10% Pd/C (290mg, 0.272mmol). The vessel was then repeatedly filled and evacuated with hydrogen and the mixture was hydrogenated at 50 psi for 16 hours with stirring. The catalyst was removed by vacuum filtration through a plug of Celite and was washed with methanol (20mL). The filtrate was concentrated under reduced pressure to provide a white powder. The residue was dissolved in water (2mL), basified with concentrated NH<sub>4</sub>OH (1mL) to yield a black precipitate and the solution was purified by reversed phase chromatography (Thermo Scientific, Hypersep C18, 2000mg, 15mL ) using a gradient of water to methanol (0% to 100% MeOH at 20% increments). Fractions containing the product were concentrated then lyophilized to yield the HCl salt of **3.20** as a white powder (47mg, 0.16mmol, 29%). <sup>1</sup>H NMR (500 MHz, CD<sub>3</sub>OD) δ 0.80-0.82 (t, J = 7Hz, 3H, CH<sub>3</sub>), 1.23-1.28 (m, 6H, CH<sub>2</sub>), 1.53-1.57 (pentet, J = 7Hz, 2H, O-CH<sub>2</sub>-CH<sub>2</sub>), 2.78-2.82 (t, J = 10hz, 1H, H5), 3.10-3.32 (m, 5H, H1, H2, H3, H4, H6), 3.53-3.57 (q, J = 7Hz, 1H, O-CH<sub>2</sub>), 3.89-3.93 (q, J = 7Hz, 1H, O-CH<sub>2</sub>). <sup>13</sup>C NMR (500 MHz, CD<sub>3</sub>OD) δ 13.06 (CH<sub>3</sub>), 22.33 (CH<sub>2</sub>), 25.33 (CH<sub>2</sub>), 29.69 (CH<sub>2</sub>), 31.57 (CH<sub>2</sub>), 55.48 (C5), 70.14 (O-CH<sub>2</sub>), 73.02 (C1), 74.18 (C4), 74.86 (C2), 75.73 (C3), 78.07 (C6). LRMS (ESI) m/z: 264.2 [M + H]<sup>+</sup> Calculated for C<sub>12</sub>H<sub>26</sub>NO<sub>5</sub><sup>+</sup>: 236.1492

### 3.21(1R,2S,3R,4S,5S,6R)-5-amino-6-butoxycyclohexane-1,2,3,4-tetraol



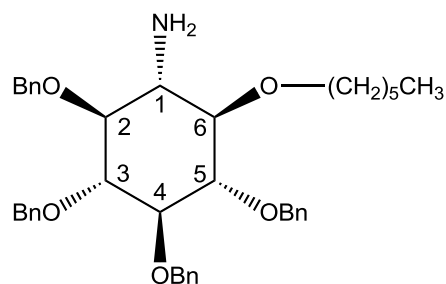
In a high pressure reaction vessel, concentrated HCl (4 drops) was added to a solution of **3.18** (95mg, 0.545mmol) in methanol (10mL). The system was flushed with argon followed by the addition of 10% Pd/C (85mg, 0.080mmol). The vessel was then repeatedly filled and evacuated with hydrogen and the mixture was hydrogenated at 50 psi for 16 hours with stirring. The catalyst was removed by vacuum filtration through a plug of Celite and was washed with methanol (20mL). The filtrate was concentrated under reduced pressure to provide a white powder. The residue was dissolved in water (2mL), basified with concentrated NH<sub>4</sub>OH (1mL) to yield a black precipitate and the solution was purified by reversed phase chromatography (Thermo Scientific, Hypersep C18, 2000mg, 15mL ) using a gradient of water to methanol (0% to 100% MeOH at 20% increments). Fractions containing the product were concentrated then lyophilized to yield the HCl salt of **3.20** as a slightly brown powder (12mg, 0.045mmol, 28%). <sup>1</sup>H NMR (500 MHz, CD<sub>3</sub>OD) δ 0.89-0.92 (t, J = 7Hz, 3H, CH<sub>3</sub>), 1.32-1.38 (Hexet, J = 7Hz, 2H, CH<sub>2</sub>-CH<sub>3</sub>), 1.57-1.64 (Hexet, J = 7Hz, 2H, O-CH<sub>2</sub>-CH<sub>2</sub>), 2.84-2.89 (t, J = 10Hz, 1H, H5), 3.16-3.39 (m, 5H, H1, H2, H3, H4, H6) 3.59-3.64 (q, J = 7Hz, 1H, O-CH<sub>2</sub>), 3.96-4.00 (q, J = 7Hz, 1H, O-CH<sub>2</sub>). <sup>13</sup>C NMR (500 MHz, CD<sub>3</sub>OD) δ 13.00 (C<sub>3</sub>), 18.78 (C<sub>2</sub>), 31.84 (C<sub>2</sub>), 55.49 (C5), 70.13 (O-C<sub>2</sub>), 72.69 (C1), 74.17 (C4), 74.85 (C2), 75.73 (C3), 78.04 (C6). LRMS (ESI) m/z: 236.1 [M + H]<sup>+</sup> Calculated for C<sub>10</sub>H<sub>22</sub>NO<sub>5</sub><sup>+</sup>: 236.1492

### 3.22 (1R,2S,3R,4R,5S,6R)-2,3,4,5-tetrakis(benzyloxy)-6-(nonyloxy)cyclohexanamine



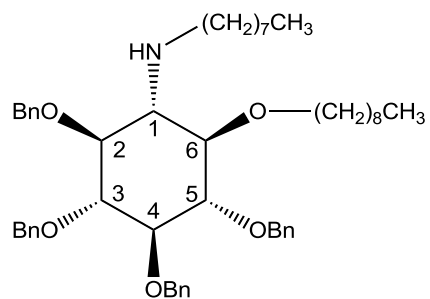
A solution of BA107 (1.43g, 2.07mmol) in THF (30mL) was cooled to 0°C in an ice bath. LiAlH<sub>4</sub> (165mg, 4.34mmol) was then slowly added and allowed to stir for 2.5 hours at 0°C and under argon. EtOAc (20mL) was added to the solution to quench the reaction and allowed to stir for an additional 30 minutes. The organics were washed with water (1 x 50mL), brine (1 x 50mL), dried over Na<sub>2</sub>SO<sub>4</sub>, and concentrated under reduced pressure to yield a white solid (1.38g, 2.07mmol, 100%). <sup>1</sup>H NMR (500 MHz, CDCl<sub>3</sub>) δ 0.90-0.95 (t, J = 7Hz, 3H, **CH<sub>3</sub>**), 1.30-1.41 (m, 12H, **CH<sub>2</sub>**), 1.59-1.69 (octet, J = 7Hz, 2H, O-CH<sub>2</sub>-**CH<sub>2</sub>**-CH<sub>2</sub>), 1.92-1.96 (broad s, 2H, **NH<sub>2</sub>**), 2.92-2.96 (t, J = 10Hz, 1H, **H<sub>1</sub>**), 3.17-3.21 (t, J = 9Hz, 1H, **H<sub>2</sub>**), 3.36-3.40 (t, J = 9Hz, 1H, **H<sub>6</sub>**), 3.56-3.72 (m, 4H, **H<sub>3</sub>, H<sub>4</sub>, H<sub>5</sub>**, O-**CH<sub>2</sub>**-CH<sub>2</sub>), 3.96-4.01 (dq, J = 10, 6Hz, 1H, O-**CH<sub>2</sub>**-CH<sub>2</sub>), 4.74-5.06 (m, 8H, O-**CH<sub>2</sub>**-C, phenyl), 7.30-7.41 (m, 20H, **phenyl**). <sup>13</sup>C NMR (500 MHz, CDCl<sub>3</sub>) δ 14.17 (**CH<sub>3</sub>**), 22.72 (**CH<sub>2</sub>**), 26.22 (**CH<sub>2</sub>**), 29.30 (**CH<sub>2</sub>**), 29.57 (**CH<sub>2</sub>**), 29.60 (**CH<sub>2</sub>**), 30.57 (**CH<sub>2</sub>**), 31.90 (**CH<sub>2</sub>**), 55.46 (**C<sub>1</sub>**), 74.05 (**C<sub>3</sub>**), 75.77 (O-**CH<sub>2</sub>**-C), 75.81 (O-**CH<sub>2</sub>**-C), 75.88 (O-**CH<sub>2</sub>**-C), 76.05 (O-**CH<sub>2</sub>**-C), 82.75 (**C<sub>5</sub>**), 83.16 (**C<sub>4</sub>**), 83.54 (**C<sub>2</sub>**), 84.36 (**C<sub>6</sub>**), 127.68 (**CH**, phenyl), 127.71 (**CH**, phenyl), 127.73 (**CH**, phenyl), 127.86 (**CH**, phenyl), 127.88 (**CH**, phenyl), 127.93 (**CH**, phenyl), 128.46 (**CH**, phenyl), 128.50 (**CH**, phenyl), 128.59 (**CH**, phenyl), 138.44 (**C**-CH<sub>2</sub>-O, phenyl), 138.44 (**C**-CH<sub>2</sub>-O, phenyl), 138.51 (**C**-CH<sub>2</sub>-O, phenyl).

### 3.23 (1R,2S,3R,4R,5S,6R)-2,3,4,5-tetrakis(benzyloxy)-6-(hexyloxy)cyclohexanamine



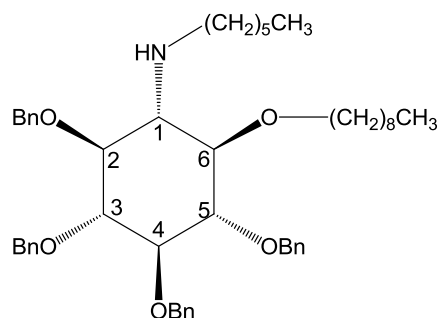
A solution of BA191 (**3.17**) (1.10g, 1.69mmol) in THF (30mL) was cooled to 0°C in an ice bath. LiAlH<sub>4</sub> (135mg, 3.56mmol) was then slowly added and allowed to stir for 2.5 hours at 0°C and under argon. EtOAc (20mL) was added to the solution to quench the reaction and allowed to stir for an additional 30 minutes. The organics were washed with water (1 x 50mL), brine (1 x 50mL), dried over Na<sub>2</sub>SO<sub>4</sub>, and concentrated under reduced pressure to yield a white solid (1.03g, 1.65mmol, 98%). <sup>1</sup>H NMR (500 MHz, CDCl<sub>3</sub>) δ 0.84-0.87 (t, J = 7Hz, 3H, CH<sub>3</sub>), 1.22-1.34 (m, 6H, CH<sub>2</sub>), 1.51-1.64 (octet, J = 7Hz, 2H, O-CH<sub>2</sub>-CH<sub>2</sub>-CH<sub>2</sub>), 1.85 (broad s, 2H, NH<sub>2</sub>), 2.87-2.91 (t, J = 10Hz, 1H, H<sub>1</sub>), 3.12-3.15 (t, J = 9Hz, 1H, H<sub>2</sub>), 3.30-3.34 (t, J = 9Hz, 1H, H<sub>6</sub>), 3.37-3.67 (m, 4H, H<sub>3</sub>, H<sub>4</sub>, H<sub>5</sub>, O-CH<sub>2</sub>-CH<sub>2</sub>), 3.91-3.96 (q, J = 7Hz, 1H, O-CH<sub>2</sub>-CH<sub>2</sub>), 4.61-5.00 (m, 8H, O-CH<sub>2</sub>-C, phenyl), 7.19-7.34 (m, 20H, phenyl). <sup>13</sup>C NMR (500 MHz, CDCl<sub>3</sub>) δ 14.13 (C<sub>3</sub>), 22.68 (C<sub>2</sub>), 25.90 (C<sub>2</sub>), 30.55 (C<sub>2</sub>), 31.78 (C<sub>2</sub>), 55.51 (C1), 74.05 (C3), 75.82-76.05 (O-C<sub>2</sub>-C), 82.82 (C5), 83.21 (C4), 83.58 (C2), 84.39 (C6), 127.68 (C<sub>H</sub>, phenyl), 127.71 (C<sub>H</sub>, phenyl), 127.73 (C<sub>H</sub>, phenyl), 127.85 (C<sub>H</sub>, phenyl), 127.87 (C<sub>H</sub>, phenyl), 127.93 (C<sub>H</sub>, phenyl), 127.94 (C<sub>H</sub>, phenyl), 127.96 (C<sub>H</sub>, phenyl), 127.98 (C<sub>H</sub>, phenyl), 128.42 (C<sub>H</sub>, phenyl), 128.42 (C<sub>H</sub>, phenyl), 128.44 (C<sub>H</sub>, phenyl), 128.46 (C<sub>H</sub>, phenyl), 128.49 (C<sub>H</sub>, phenyl), 128.58 (C<sub>H</sub>, phenyl), 138.43 (C-CH<sub>2</sub>-O, phenyl), 138.44 (C-CH<sub>2</sub>-O, phenyl), 138.51 (C-CH<sub>2</sub>-O, phenyl).

### 3.24 (1R,2S,3R,4R,5S,6R)-2,3,4,5-tetrakis(benzyloxy)-6-(nonyloxy)-N-octylcyclohexanamine



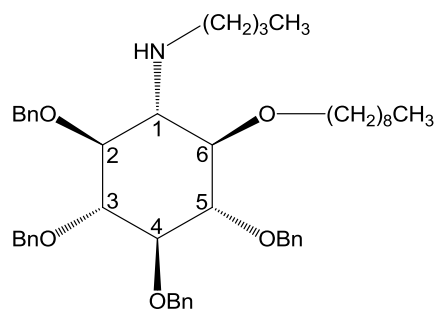
Octanal (42.21 $\mu$ L, 0.270mmol) was added to a solution of **3.22** (120mg, 0.180mmol) in 5mL of dry methanol and was stirred at room temperature overnight and under argon. NaBH<sub>4</sub> (13.6mg, 0.360mmol) was then carefully added and allowed to stir for 30 minutes. To quench the reaction 5mL of a 1M NaOH solution was added and allowed to stir for another 15 minutes. Diethyl ether (25mL) was added to the aqueous solution to extract the organics, and then washed once with water (25mL). The organic portion was dried with brine (25mL) and Na<sub>2</sub>SO<sub>4</sub>, then concentrated under reduced pressure. The resulting residue was purified by flash chromatography on silica gel (10:1 Hexanes: EtOAc) to give **3.24** as cream colored solid (94mg, 0.121mmol, 67%). <sup>1</sup>H NMR (500 MHz, CDCl<sub>3</sub>)  $\delta$  0.83 (t, J = 7Hz, 6H, CH<sub>3</sub>), 1.19-1.36 (m, 24H, CH<sub>2</sub>), 1.38-1.44 (m, 2H, N-CH<sub>2</sub>-CH<sub>2</sub>), 1.53-1.63 (m, 2H, O-CH<sub>2</sub>-CH<sub>2</sub>), 1.78 (broad s, 1H, NH), 2.53-2.57 (t, J = 10Hz, 1H, H1), 2.73-2.83 (qt, J = 11, 7Hz, 2H, N-CH<sub>2</sub>), 3.15-3.18 (dt, J = 10, 8Hz, 1H, H2), 3.34-3.38 (t, J = 10Hz, 1H, H6), 3.50-3.53 (dd, J = 7, 3Hz, 1H, H4), 3.54-3.65 (m, 3H, H3, H5, O-CH<sub>2</sub>), 3.89-3.94 (q, J = 8Hz, 1H, O-CH<sub>2</sub>), 4.72-4.96 (m, 8H, CH-CH<sub>2</sub>-O), 7.24-7.34 (m, 20H, phenyl). <sup>13</sup>C NMR (500 MHz, CDCl<sub>3</sub>)  $\delta$  14.16 (CH<sub>3</sub>), 22.72 (CH<sub>2</sub>), 26.31 (CH<sub>2</sub>), 27.39 (CH<sub>2</sub>), 29.34 (CH<sub>2</sub>), 29.63 (CH<sub>2</sub>), 30.61 (CH<sub>2</sub>), 30.86 (CH<sub>2</sub>), 31.91 (CH<sub>2</sub>), 50.37 (CH<sub>2</sub>-NH), 62.20 (C1), 73.93 (C3), 75.62 (O-CH<sub>2</sub>-Phenyl), 75.82 (O-CH<sub>2</sub>-Phenyl), 75.86 (O-CH<sub>2</sub>-Phenyl), 75.97 (O-CH<sub>2</sub>-Phenyl), 82.41 (C5), 82.80 (C4), 83.24 (C2), 84.40 (C6), 127.68 (CH, phenyl), 127.86 (CH, phenyl), 127.97 (CH, phenyl), 128.45 (CH, phenyl), 128.52 (CH, phenyl), 138.52 (C-CH<sub>2</sub>-O).

### 3.25 (1R,2S,3R,4R,5S,6R)-2,3,4,5-tetrakis(benzyloxy)-N-hexyl-6-(nonyloxy)cyclohexanamine



Hexanal (33 $\mu$ L, 0.27mmol) was added to a solution of B109 (120mg, 0.180mmol) in 5mL of dry methanol and was stirred at room temperature overnight and under argon. NaBH<sub>4</sub> (14mg, 0.37mmol) was then carefully added and allowed to stir for 30 minutes. To quench the reaction 5mL of a 1M NaOH solution was added and allowed to stir for another 15 minutes. Diethyl ether (25mL) was added to the aqueous solution to extract the organics, and then washed once with water (25mL). The organic portion was dried with brine (25mL) and Na<sub>2</sub>SO<sub>4</sub>, and then concentrated under reduced pressure. The resulting residue was purified by flash chromatography on silica gel (10:1 hexanes: EtOAc) to give **3.28** as cream colored solid (59mg, 0.079mmol, 44%). <sup>1</sup>H NMR (500 MHz, CDCl<sub>3</sub>)  $\delta$  0.83-0.92 (dt, J = 7, 3Hz, 6H, CH<sub>3</sub>), 1.20-1.37 (m, 18H, CH<sub>2</sub>), 1.40-1.46 (pentet, J = 7Hz, 2H, NH-CH<sub>2</sub>-CH<sub>2</sub>), 1.54-1.64 (hextet, J = 7Hz, 2H, O-CH<sub>2</sub>-CH<sub>2</sub>), 1.97 (broad s, 1H, NH), 2.53-2.57 (t, J = 10Hz, 1H, H1), 2.74-2.83 (qt, J = 11, 7Hz, 2H, N-CH<sub>2</sub>), 3.15-3.19 (dt, J = 10, 8Hz, 1H, H2), 3.34-3.38 (t, J = 10Hz, 1H, H6), 3.50-3.65 (m, 4H, H3, H4, H5, O-CH<sub>2</sub>-CH<sub>2</sub>), 3.89-3.94 (dq, J = 7, 6Hz, 1H, O-CH<sub>2</sub>), 4.72-4.96 (m, 8H, CH-CH<sub>2</sub>-O), 7.23-7.35 (m, 20H, phenyl). <sup>13</sup>C NMR (500 MHz, CDCl<sub>3</sub>)  $\delta$  14.12 (CH<sub>3</sub>), 14.16 (CH<sub>3</sub>), 22.68 (CH<sub>2</sub>), 26.30 (CH<sub>2</sub>), 27.06 (CH<sub>2</sub>), 29.32 (CH<sub>2</sub>), 29.62 (CH<sub>2</sub>), 30.61 (CH<sub>2</sub>), 30.81 (CH<sub>2</sub>), 31.85 (CH<sub>2</sub>), 31.91 (CH<sub>2</sub>), 50.38 (N-CH<sub>2</sub>), 62.21(C1), 73.94 (C3), 75.62 (O-CH<sub>2</sub>-Phenyl), 75.82 (O-CH<sub>2</sub>-Phenyl), 75.86 (O-CH<sub>2</sub>-Phenyl), 75.98 (O-CH<sub>2</sub>-Phenyl), 82.39 (C5), 82.79 (C4), 83.24 (C2), 84.40 (C6), 127.68 (CH, phenyl), 127.86 (CH, phenyl), 127.98 (CH, phenyl), 128.45 (CH, phenyl), 128.52 (CH, phenyl), 138.35 (C-CH<sub>2</sub>-O), 138.46 (C-CH<sub>2</sub>-O), 138.51 (C-CH<sub>2</sub>-O)

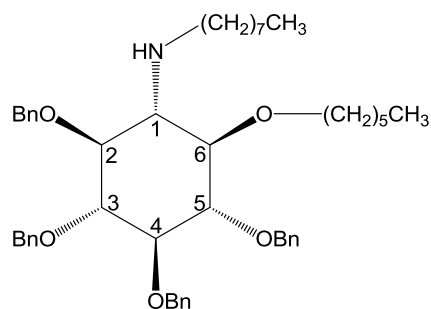
### 3.26 (1R,2S,3R,4R,5S,6R)-2,3,4,5-tetrakis(benzyloxy)-N-butyl-6-(nonyloxy)cyclohexanamine



Butyraldehyde (33 $\mu$ L, 0.37mmol) was added to a solution of B109 (120mg, 0.180mmol) in 5mL of dry methanol and was stirred at room temperature overnight and under argon. NaBH<sub>4</sub> (17mg, 0.45mmol) was then carefully added and allowed to stir for 30 minutes. To quench the reaction 5mL of a 1M NaOH solution was added and allowed to stir for another 15 minutes. Diethyl ether (25mL) was added to the aqueous solution to extract the organics, and then washed once with water (25mL). The organic portion was dried with brine (25mL) and Na<sub>2</sub>SO<sub>4</sub>, and then concentrated under reduced pressure. The resulting residue was purified by flash chromatography on silica gel (10:1 hexanes: EtOAc) to give **3.28** as cream colored solid (92mg, 0.13mmol, 71%). <sup>1</sup>H NMR (500 MHz, CDCl<sub>3</sub>)  $\delta$  0.87-0.90 (dt, J = 7, 2Hz, 6H, CH<sub>3</sub>), 1.25-1.35 (m, 14H, CH<sub>2</sub>), 1.39-1.45 (pentet, J = 7Hz, 2H, N-CH<sub>2</sub>-CH<sub>2</sub>), 1.56-1.63 (hextet, J = 7Hz, 2H, O-CH<sub>2</sub>-CH<sub>2</sub>), 1.99 (broad s, 1H, NH), 2.53-2.57 (t, J = 10Hz, 1H, H1), 2.75-2.85 (qt, J = 11, 7Hz, 2H, N-CH<sub>2</sub>), 3.16-3.19 (dt, J = 10, 8Hz, 1H, H2), 3.35-3.39 (t, J = 10Hz, 1H, H6), 3.51-3.66 (m, 4H, H3, H4, H5, O-CH<sub>2</sub>-CH<sub>2</sub>), 3.90-3.95 (dq, J = 7, 6Hz, 1H, O-CH<sub>2</sub>), 4.73-4.97 (m, 8H, CH-CH<sub>2</sub>-O), 7.25-7.35 (m, 20H, phenyl). <sup>13</sup>C NMR (500 MHz, CDCl<sub>3</sub>)  $\delta$  14.08 (CH<sub>3</sub>), 14.17 (CH<sub>3</sub>), 20.47 (CH<sub>2</sub>), 22.71 (CH<sub>2</sub>), 26.30 (CH<sub>2</sub>), 29.31 (CH<sub>2</sub>), 29.61 (CH<sub>2</sub>), 30.60 (CH<sub>2</sub>), 31.91 (CH<sub>2</sub>), 32.98 (CH<sub>2</sub>), 50.05 (N-CH<sub>2</sub>), 62.22 (C1), 73.94 (C3), 75.65 (O-CH<sub>2</sub>-Phenyl), 75.83 (O-CH<sub>2</sub>-Phenyl), 75.87 (O-CH<sub>2</sub>-Phenyl), 75.98 (O-CH<sub>2</sub>-Phenyl), 82.43 (C5), 82.82 (C4), 83.25 (C2), 84.41 (C6), 127.69 (CH, phenyl), 127.86 (CH, phenyl), 128.00 (CH, phenyl), 128.46 (CH, phenyl), 128.53 (CH, phenyl), 138.47 (C-CH<sub>2</sub>-O), 138.52 (C-CH<sub>2</sub>-O). LRMS (ESI) m/z: 362.3 [M + H]<sup>+</sup>

Calculated for C<sub>19</sub>H<sub>40</sub>NO<sub>5</sub><sup>+</sup>: 362.2901

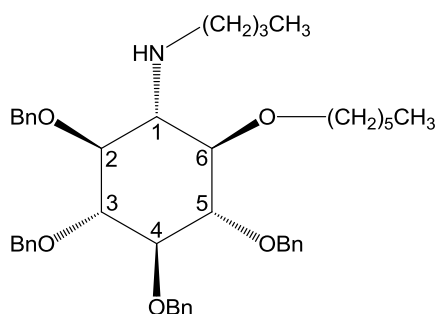
### 3.27 (1R,2S,3R,4R,5S,6R)-2,3,4,5-tetrakis(benzyloxy)-6-(hexyloxy)-N-octylcyclohexanamine



Octanal (100 $\mu$ L, 0.640 mmol) was added to a solution of **3.23** (200mg, 0.321mmol) in 8mL of dry methanol and was stirred at room temperature overnight and under argon. NaBH<sub>4</sub> (30.3mg, 0.801mmol) was then carefully added and allowed to stir for 30 minutes. To quench the reaction 5mL of a 1M NaOH solution was added and allowed to stir for another 15 minutes. Diethyl ether (25mL) was added to the aqueous solution to extract the organics, and then washed once with water (25mL). The organic portion was dried with brine (25mL) and Na<sub>2</sub>SO<sub>4</sub>, and then concentrated under reduced pressure. The resulting residue was purified by flash chromatography on silica gel (6:1 hexanes: EtOAc) to give **3.28** as white solid (125mg, 0.170mmol, 53%). <sup>1</sup>H NMR (500 MHz, CDCl<sub>3</sub>)  $\delta$  0.82-0.89 (m, 6H, CH<sub>3</sub>), 1.14-1.36 (m, 16H, CH<sub>2</sub>), 1.40-1.44 (pentet, J = 7Hz, 2H, NH<sub>2</sub>-CH<sub>2</sub>-CH<sub>2</sub>), 1.52-1.63 (m, 2H, O-CH<sub>2</sub>-CH<sub>2</sub>), 1.72 (broad s, 2H, NH<sub>2</sub>), 2.53-2.57 (t, J = 10Hz, 1H, H1), 2.74-2.83 (qt, J = 11, 7Hz, 2H, NH-CH<sub>2</sub>), 3.15-3.19 (tt, J = 10, 7Hz, 1H, H2), 3.34-3.38 (t, J = 10Hz, 1H, H6), 3.50-3.66 (m, 4H, H3, H4, H5, O-CH<sub>2</sub>-CH<sub>2</sub>), 3.89-3.94 (dq, J = 7, 6Hz, 1H, O-CH<sub>2</sub>), 4.72-4.96 (m, 8H, CH-CH<sub>2</sub>-O), 7.23-7.33 (m, 20H, phenyl). <sup>13</sup>C NMR (500 MHz, CDCl<sub>3</sub>)  $\delta$  14.07 (CH<sub>3</sub>), 14.15 (CH<sub>3</sub>), 22.66 (CH<sub>2</sub>), 22.70 (CH<sub>2</sub>), 22.72 (CH<sub>2</sub>), 25.84 (CH<sub>2</sub>), 25.96 (CH<sub>2</sub>), 27.40 (CH<sub>2</sub>), 29.34 (CH<sub>2</sub>), 29.47 (CH<sub>2</sub>), 29.62 (CH<sub>2</sub>), 30.58 (CH<sub>2</sub>), 30.88 (CH<sub>2</sub>), 31.82 (CH<sub>2</sub>), 31.87 (CH<sub>2</sub>), 31.90 (CH<sub>2</sub>), 32.89 (CH<sub>2</sub>), 50.35 (N-CH<sub>2</sub>), 62.24 (C1), 62.94 (C3), 73.92 (O-CH<sub>2</sub>-CH<sub>2</sub>), 75.59 (O-CH<sub>2</sub>-Phenyl), 75.79 (O-CH<sub>2</sub>-Phenyl), 75.84 (O-CH<sub>2</sub>-Phenyl), 75.95 (O-CH<sub>2</sub>-Phenyl), 82.47 (C5), 82.83 (C4), 83.28 (C2), 84.43 (C6), 127.65 (CH, phenyl), 127.66 (CH, phenyl), 127.78 (CH, phenyl), 127.80 (CH, phenyl), 127.80 (CH, phenyl), 127.81 (CH, phenyl), 127.82 (CH, phenyl), 127.84 (CH, phenyl), 127.86 (CH, phenyl), 127.88 (CH, phenyl), 127.88 (CH,

phenyl), 127.95 (CH, phenyl), 127.97 (CH, phenyl), 128.43 (CH, phenyl), 128.44 (CH, phenyl), 128.45 (CH, phenyl), 128.51 (CH, phenyl), 128.53 (CH, phenyl), 138.43 (C-CH<sub>2</sub>-O), 138.52 (C-CH<sub>2</sub>-O), 138.56 (C-CH<sub>2</sub>-O), 138.59 (C-CH<sub>2</sub>-O).

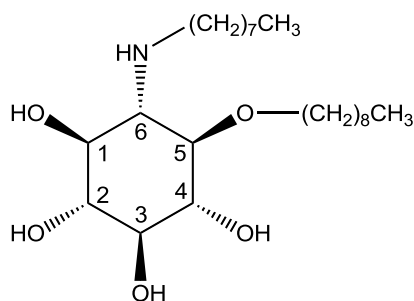
### 3.28 (1R,2S,3R,4R,5S,6R)-2,3,4,5-tetrakis(benzyloxy)-N-butyl-6-(hexyloxy)cyclohexanamine



Butyraldehyde (100 $\mu$ L, 1.13mmol) was added to a solution of **3.23** (200mg, 0.321mmol) in 8mL of dry methanol and was stirred at room temperature overnight and under argon. NaBH<sub>4</sub> (48.5mg, 1.28mmol) was then carefully added and allowed to stir for 30 minutes. To quench the reaction 5mL of a 1M NaOH solution was added and allowed to stir for another 15 minutes. Diethyl ether (25mL) was added to the aqueous solution to extract the organics, and then washed once with water (25mL). The organic portion was dried with brine (25mL) and Na<sub>2</sub>SO<sub>4</sub>, and then concentrated under reduced pressure. The resulting residue was purified by flash chromatography on silica gel (6:1 hexanes: EtOAc) to give **3.28** as cream colored solid (82mg, 0.121mmol, 38%). <sup>1</sup>H NMR (500 MHz, CDCl<sub>3</sub>)  $\delta$  0.85-0.94 (m, 6H, CH<sub>3</sub>), 1.21-1.37 (m, 8H, CH<sub>2</sub>), 1.39-1.45 (pentet, J = 7Hz, 2H, N-CH<sub>2</sub>-CH<sub>2</sub>), 1.54-1.61 (m, 2H, O-CH<sub>2</sub>-CH<sub>2</sub>), 1.78 (broad s, 1H, NH), 2.53-2.57 (t, J = 10Hz, 1H, H1), 2.75-2.84 (m, 2H, N-CH<sub>2</sub>), 3.15-3.17 (t, J = 8Hz, 1H, H2), 3.34-3.37 (t, J = 9Hz, 1H, H6), 3.51-3.66 (m, 4H, H3, H4, H5, O-CH<sub>2</sub>-CH<sub>2</sub>), 3.89-3.94 (q, J = 8Hz, 1H, O-CH<sub>2</sub>), 4.72-4.98 (m, 8H, CH-CH<sub>2</sub>-O), 7.19-7.34 (m, 20H, phenyl). <sup>13</sup>C NMR (500 MHz, CDCl<sub>3</sub>)  $\delta$  14.14 (CH<sub>3</sub>), 20.54 (CH<sub>2</sub>), 22.73 (CH<sub>2</sub>), 26.03 (CH<sub>2</sub>), 30.64 (CH<sub>2</sub>), 31.89 (CH<sub>2</sub>), 33.08 (CH<sub>2</sub>), 50.11 (CH<sub>2</sub>-NH), 62.34 (C1), 74.01 (C3), 75.70 (O-CH<sub>2</sub>-Phenyl), 75.88 (O-CH<sub>2</sub>-Phenyl), 75.93 (O-CH<sub>2</sub>-Phenyl), 76.04 (O-CH<sub>2</sub>-

Phenyl), 82.56 (C5), 82.94 (C4), 83.37 (C2), 84.50 (C6), 127.75 (CH, phenyl), 127.88 (CH, phenyl), 127.93 (CH, phenyl), 128.06 (CH, phenyl), 128.52 (CH, phenyl), 128.60 (CH, phenyl), 138.50 (C-CH<sub>2</sub>-O, phenyl), 138.59 (C-CH<sub>2</sub>-O, phenyl), 138.64 (C-CH<sub>2</sub>-O, phenyl).

### 3.29 (1S,2R,3S,4R,5R,6S)-5-(nonyloxy)-6-(octylamino)cyclohexane-1,2,3,4-tetraol

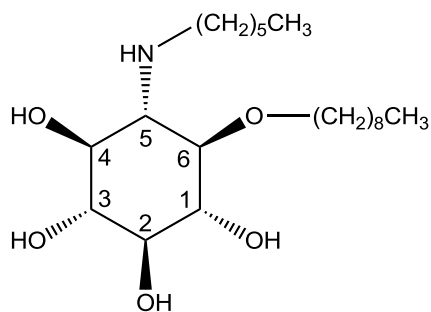


In a high pressure reaction vessel, concentrated HCl (4 drops) was added to a solution of **3.24** (50mg, 0.064mmol) in methanol (4mL). The system was flushed with argon followed by the addition of 10% Pd/C (50mg, 0.038mmol). The vessel was then repeatedly filled and evacuated with hydrogen and the mixture was hydrogenated at 50 psi for 16 hours with stirring. The catalyst was removed by vacuum filtration through a plug of Celite and was washed with methanol (20mL). The filtrate was concentrated under reduced pressure to provide dark orange crystals. The crystals were dissolved in water (2mL), basified with concentrated NH<sub>4</sub>OH (1mL) to yield a black precipitate and the solution was purified by reversed phase chromatography (Thermo Scientific, Hypersep C18, 2000mg, 15mL ) using a gradient of water to methanol (0% to 100% MeOH at 20% increments). Fractions containing the product were concentrated then lyophilized to yield the HCl salt of **3.29** as a pure white powder (16.82mg, 35.6 mmol, 56%). <sup>1</sup>H NMR (500 MHz, CD<sub>3</sub>OD) δ 0.91-0.90 (d, J = 5Hz, 6H, CH<sub>3</sub>), 1.31 (m, 22H, CH<sub>2</sub>-CH<sub>3</sub>), 1.63 (m, 1H, N-CH<sub>2</sub>-CH<sub>2</sub>-CH<sub>2</sub>), 1.75 (m, 1H, O-CH<sub>2</sub>-CH<sub>2</sub>-CH<sub>2</sub>), 3.01-3.03 (m, 1H, N-CH<sub>2</sub>), 3.12 (m, 1H, H6), δ3.21-3.28 (m, 3H, H2, H3, H5), δ3.42-3.44 (m, 1H, N-CH<sub>2</sub>), δ3.52-3.54 (m, 2H, H1, H4), 3.66 (m, 1H, O-CH<sub>2</sub>), 4.16 (m, 1H, O-CH<sub>2</sub>). <sup>13</sup>C NMR (500 MHz, CD<sub>3</sub>OD) δ 13.11(CH<sub>3</sub>), 22.37 (CH<sub>2</sub>), 22.39 (CH<sub>2</sub>), 25.94 (CH<sub>2</sub>), 26.00 (CH<sub>2</sub>), 26.39 (CH<sub>2</sub>), 28.93 (CH<sub>2</sub>), 29.14 (CH<sub>2</sub>), 29.45 (CH<sub>2</sub>), 29.47 (CH<sub>2</sub>), 30.16 (CH<sub>2</sub>), 31.60 (CH<sub>2</sub>), 31.74 (CH<sub>2</sub>),

45.85 (N-CH<sub>2</sub>), 60.80 (C6), 68.79 (C1), 72.74 (C4), 74.03 (C3), 74.91 (C2), 76.24 (O-CH<sub>2</sub>), 76.82 (C5). LRMS

(ESI) m/z: 423.35 [M + Li]<sup>+</sup> Calculated for C<sub>23</sub>H<sub>46</sub>LiNO<sub>5</sub>: 423.3536.

### 3.30 (1R,2S,3R,4S,5S,6R)-5-(hexylamino)-6-(nonyloxy)cyclohexane-1,2,3,4-tetraol

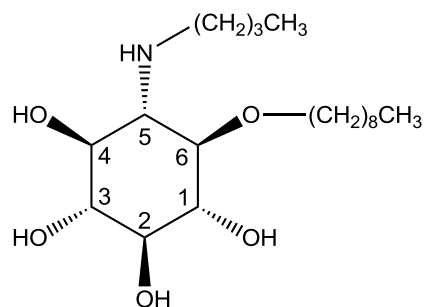


In a high pressure reaction vessel, concentrated HCl (7 drops) was added to a solution of **3.25** (36mg, 0.048mmol) in methanol (7mL). The system was flushed with argon followed by the addition of 10% Pd/C (25mg, 0.023mmol). The vessel was then repeatedly filled and evacuated with hydrogen and the mixture was hydrogenated at 50 psi for 16 hours with stirring. The catalyst was removed by vacuum filtration through a plug of Celite and was washed with methanol (20mL). The filtrate was concentrated under reduced pressure to provide dark orange crystals. The crystals were dissolved in water (2mL), basified with concentrated NH<sub>4</sub>OH (1mL) to yield a black precipitate and the solution was purified by reversed phase chromatography (Thermo Scientific, Hypersep C18, 2000mg, 15mL ) using a gradient of water to methanol (0% to 100% MeOH at 20% increments). Fractions containing the product were concentrated then lyophilized to yield the HCl salt of **3.30** as a white powder (4mg, 0.009mmol, 20%). <sup>1</sup>H NMR (500 MHz, CD<sub>3</sub>OD) δ 0.76-0.88 (m, 6H, CH<sub>3</sub>), 1.15-1.39 (m, 20H, CH<sub>2</sub>), 1.47-1.54 (sextet, J = 7Hz, 2H, NH-CH<sub>2</sub>-CH<sub>2</sub>), 2.52-2.56 (t, J = 10Hz, 1H, H5), 2.79-2.90 (qt, J = 11, 7Hz, 2H, NH-CH<sub>2</sub>), 3.04-3.29 (m, 5H, H1, H2, H3, H4, H6), 3.48-3.52 (dt, J = 7, 2Hz, 1H, O-CH<sub>2</sub>), 3.92-3.97 (dt, J = 7, 6Hz, 1H, O-CH<sub>2</sub>). <sup>13</sup>C NMR (500 MHz, CD<sub>3</sub>OD) δ 13.03 (CH<sub>3</sub>), 24.28 (CH<sub>2</sub>), 25.86 (CH<sub>2</sub>), 26.00 (CH<sub>2</sub>), 26.59 (CH<sub>2</sub>), 26.74 (CH<sub>2</sub>), 29.06 (CH<sub>2</sub>), 29.30 (CH<sub>2</sub>), 29.37 (CH<sub>2</sub>), 30.10 (CH<sub>2</sub>), 30.14 (CH<sub>2</sub>), 31.69 (CH<sub>2</sub>), 46.36 (N-CH<sub>2</sub>), 61.57 (C5), 72.52

(**C4**), 74.35 (**C1**), 75.02 (**C2**), 75.29 (**C3**), 75.80 (O-**C2**), 75.91 (**C6**). LRMS (ESI) m/z: 390.3 [M - H]<sup>+</sup>

Calculated for C<sub>21</sub>H<sub>44</sub>NO<sub>5</sub><sup>+</sup>: 390.3214.

### 3.31 (1R,2S,3R,4S,5S,6R)-5-(butylamino)-6-(nonyloxy)cyclohexane-1,2,3,4-tetraol

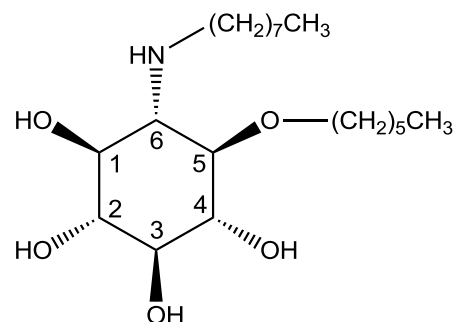


In a high pressure reaction vessel, concentrated HCl (8 drops) was added to a solution of **3.26** (92mg, 0.13mmol) in methanol (8mL). The system was flushed with argon followed by the addition of 10% Pd/C (68mg, 0.064mmol). The vessel was then repeatedly filled and evacuated with hydrogen and the mixture was hydrogenated at 50 psi for 16 hours with stirring. The catalyst was removed by vacuum filtration through a plug of Celite and was washed with methanol (20mL). The filtrate was concentrated under reduced pressure to provide dark orange crystals. The crystals were dissolved in water (2mL), basified with concentrated NH<sub>4</sub>OH (1mL) to yield a black precipitate and the solution was purified by reversed phase chromatography (Thermo Scientific, Hypersep C18, 2000mg, 15mL ) using a gradient of water to methanol (0% to 100% MeOH at 20% increments). Fractions containing the product were concentrated then lyophilized to yield the HCl salt of **3.31** as a pure white powder (34mg, 0.085mmol, 67%). <sup>1</sup>H NMR (500 MHz, CD<sub>3</sub>OD) δ 0.83-0.87 (t, J = 7Hz, 3H, **CH<sub>3</sub>**), 0.94-0.97 (t, J = 7Hz, 3H, **CH<sub>3</sub>**), 1.21-1.35 (m, 12H, **CH<sub>2</sub>**), 1.37-1.44 (sextet, J = 7Hz, 2H, N-CH<sub>2</sub>-CH<sub>2</sub>-**CH<sub>2</sub>**), 1.56-1.61 (quintet, J = 7Hz, 2H, O-CH<sub>2</sub>-**CH<sub>2</sub>**), 1.64-1.70 (quintet, J = 7Hz, 2H, N-CH<sub>2</sub>-**CH<sub>2</sub>**), 2.95-3.00 (t, J = 10 Hz, 1H, **H5**), 3.03-3.08 (dt, J = 12, 8Hz, 1H, NH-**CH<sub>2</sub>**), 3.12-3.22 (m, 3H, **H1**, **H4**, NH-**CH<sub>2</sub>**), 3.36-3.45 (m, 3H, **H2**, **H3**, **H6**), 3.56-3.60 (dt, J = 7, 6Hz, 1H, O-**CH<sub>2</sub>**), 4.07-4.12 (dt, J = 7, 6Hz, 1H, O-**CH<sub>2</sub>**). <sup>13</sup>C NMR (500 MHz, CD<sub>3</sub>OD) 12.56 (**C<sub>3</sub>**), 13.06 (**C<sub>3</sub>**), 19.51 (**C<sub>2</sub>**), 22.34 (**C<sub>2</sub>**), 25.83 (**C<sub>2</sub>**), 27.95 (**C<sub>2</sub>**), 29.05 (**C<sub>2</sub>**), 29.35 (**C<sub>2</sub>**), 29.36 (**C<sub>2</sub>**), 30.03 (**C<sub>2</sub>**), 31.68

(CH<sub>2</sub>), 45.12 (N-CH<sub>2</sub>), 60.68 (C5), 68.64 (C4), 72.67 (C1), 74.04 (C2), 74.86 (C3), 76.17 (O-CH<sub>2</sub>), 76.66 (C6).

LRMS (ESI) m/z: 362.3 [M - H]<sup>+</sup> Calculated for C<sub>19</sub>H<sub>40</sub>NO<sub>5</sub><sup>+</sup>: 362.2901

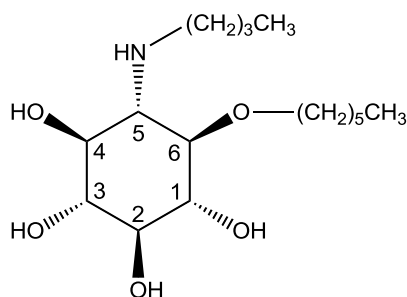
### 3.32 (1S,2R,3S,4R,5R,6S)-5-(hexyloxy)-6-(octylamino)cyclohexane-1,2,3,4-tetraol



In a high pressure reaction vessel, concentrated HCl (5 drops) was added to a solution of **3.27** (125mg, 0.170mmol) in methanol (5mL). The system was flushed with argon followed by the addition of 10% Pd/C (106mg, 1.00mmol). The vessel was then repeatedly filled and evacuated with hydrogen and the mixture was hydrogenated at 50 psi for 16 hours with stirring. The catalyst was removed by vacuum filtration through a plug of Celite and was washed with methanol (20mL). The filtrate was concentrated under reduced pressure to provide dark orange crystals. The crystals were dissolved in water (2mL), basified with concentrated NH<sub>4</sub>OH (1mL) to yield a black precipitate and the solution was purified by reversed phase chromatography (Thermo Scientific, Hypersep C18, 2000mg, 15mL) using a gradient of water to methanol (0% to 100% MeOH at 20% increments). Fractions containing the product were concentrated then lyophilized to yield the HCl salt of **3.29** as a pure white powder (54mg, 0.13mmol, 77%). <sup>1</sup>H NMR (500 MHz, CD<sub>3</sub>OD) δ 0.84-0.90 (m, 6H, CH<sub>3</sub>), 1.24-1.40 (m, 16H CH<sub>2</sub>), 1.56-1.60 (quintet, J = 7Hz, 2H, O-CH<sub>2</sub>-CH<sub>2</sub>), 1.65-1.70 (quintet, J = 7Hz, 2H, N-CH<sub>2</sub>-CH<sub>2</sub>), 2.95-2.99 (t, J = 10Hz, 1H, H6), 3.01-3.44 (m, 7H, H1, H2, H3, H4, H5, N-CH<sub>2</sub>), 3.55-3.60 (dt, J = 7, 6Hz, 1H, O-CH<sub>2</sub>), 4.08-4.12 (dt, J = 7, 6Hz, 1H, O-CH<sub>2</sub>). <sup>13</sup>C NMR (500 MHz, CD<sub>3</sub>OD) δ 13.14 (CH<sub>3</sub>), 13.17 (CH<sub>3</sub>), 22.38 (CH<sub>2</sub>), 22.43 (CH<sub>2</sub>), 25.60 (CH<sub>2</sub>), 25.62 (CH<sub>2</sub>), 26.01 (CH<sub>2</sub>), 26.40 (CH<sub>2</sub>), 28.93 (CH<sub>2</sub>), 29.09 (CH<sub>2</sub>), 29.22 (CH<sub>2</sub>), 30.16 (CH<sub>2</sub>), 31.60 (CH<sub>2</sub>),

31.65 (CH<sub>2</sub>), 31.70 (CH<sub>2</sub>), 32.30 (CH<sub>2</sub>), 46.29 (N-CH<sub>2</sub>), 60.93 (C6), 61.68 (C6), 68.93 (C1), 72.78 (C4), 73.98 (C3), 74.91 (C2), 76.27 (O-CH<sub>2</sub>), 76.94 (C6). LRMS (ESI) m/z: 376.3 [M - H]<sup>+</sup> Calculated for C<sub>20</sub>H<sub>42</sub>NO<sub>5</sub><sup>+</sup>: 376.3057.

### 3.33 (1R,2S,3R,4S,5S,6R)-5-(butylamino)-6-(hexyloxy)cyclohexane-1,2,3,4-tetraol

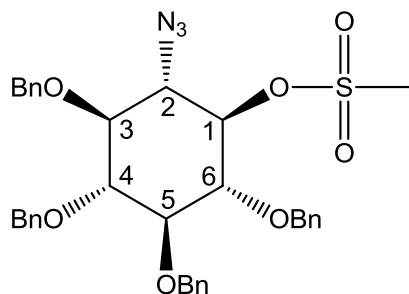


In a high pressure reaction vessel, concentrated HCl (5 drops) was added to a solution of **3.28** (82mg, 0.12mmol) in methanol (5mL). The system was flushed with argon followed by the addition of 10% Pd/C (76mg, 0.071mmol). The vessel was then repeatedly filled and evacuated with hydrogen and the mixture was hydrogenated at 50 psi for 16 hours with stirring. The catalyst was removed by vacuum filtration through a plug of Celite and was washed with methanol (20mL). The filtrate was concentrated under reduced pressure to provide dark orange crystals. The crystals were dissolved in water (2mL), basified with concentrated NH<sub>4</sub>OH (1mL) to yield a black precipitate and the solution was purified by reversed phase chromatography (Thermo Scientific, Hypersep C18, 2000mg, 15mL ) using a gradient of water to methanol (0% to 100% MeOH at 20% increments). Fractions containing the product were concentrated then lyophilized to yield the HCl salt of **3.29** as a pure white powder (33mg, 0.093mmol, 77%). <sup>1</sup>H NMR (500 MHz, CD<sub>3</sub>OD) δ 0.84-0.89 (t, J = 7Hz, 3H, CH<sub>3</sub>), 0.93-0.96 (t, J = 7Hz, 3H, CH<sub>3</sub>), 1.23-1.34 (m, 6H, CH<sub>2</sub>), 1.36-1.43 (sextet, J = 7Hz, 2H, N-CH<sub>2</sub>-CH<sub>2</sub>-CH<sub>2</sub>), 1.55-1.60 (quintet, J = 7Hz, 2H, O-CH<sub>2</sub>-CH<sub>2</sub>), 1.64-1.70 (quintet, J = 7Hz, 2H, N-CH<sub>2</sub>-CH<sub>2</sub>), 2.95-2.99 (t, J = 10Hz, 1H, H5), 3.04-3.46 (m, 7H, H1, H2, H3, H4, H6, N-

$\underline{\text{C}}\underline{\text{H}}_2$ ), 3.56-3.61 (q, J = 7Hz, O- $\underline{\text{C}}\underline{\text{H}}_2$ ), 4.06-4.11 (q, J = 7Hz, O- $\underline{\text{C}}\underline{\text{H}}_2$ ).  $^{13}\text{C}$  NMR (500 MHz,  $\text{CD}_3\text{OD}$ ) 12.99 (N- $(\text{CH}_2)_3$ - $\underline{\text{C}}\underline{\text{H}}_3$ ), 13.27 (O- $(\text{CH}_2)_5$ - $\underline{\text{C}}\underline{\text{H}}_3$ ), 19.85 ( $\underline{\text{C}}\underline{\text{H}}_2$ ), 22.47 ( $\underline{\text{C}}\underline{\text{H}}_2$ ), 25.67 ( $\underline{\text{C}}\underline{\text{H}}_2$ ), 28.19 ( $\underline{\text{C}}\underline{\text{H}}_2$ ), 30.21 ( $\underline{\text{C}}\underline{\text{H}}_2$ ), 31.72 ( $\underline{\text{C}}\underline{\text{H}}_2$ ), 46.41 (N- $\underline{\text{C}}\underline{\text{H}}_2$ ), 61.08 (**C5**), 69.05 (**C4**), 72.89 (**C1**), 74.06 (**C2**), 74.91 (**C3**), 76.27 (O- $\underline{\text{C}}\underline{\text{H}}_2$ ), 77.01 (**C6**).

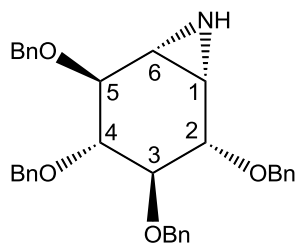
LRMS (ESI) m/z: 320.2 [M - H]<sup>+</sup> Calculated for  $\text{C}_{16}\text{H}_{34}\text{NO}_5^+$ : 320.2431.

### 3.34 (1R,2S,3S,4R,5S,6R)-2-azido-3,4,5,6-tetrakis(benzyloxy)cyclohexyl methanesulfonate



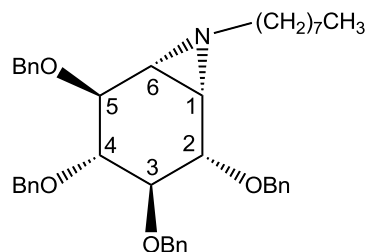
A solution of **3.07** (2.00g, 3.70mmol) in pyridine (8mL) was cooled to 0°C in an ice bath. Methanesulfonyl chloride (1.43 mL 18.49mmol) was added dropwise and allowed to stir at room temperature overnight and under argon. The solution was then concentrated under reduced pressure, co-evaporating with toluene. The residue was dissolved in EtOAc (100mL) and washed with water (100mL), then 1M HCl (100ml) and saturated  $\text{NaHCO}_3$  (100mL). The organics were dried with brine (100mL) and  $\text{Na}_2\text{SO}_4$ , then concentrated under reduced pressure to yield a golden yellow syrup. The thoroughly dry mixture was dissolved in DMF (20mL).  $\text{NaN}_3$  (241mg, 3.71mmol) was added and allowed to stir at room temperature and under argon for 2 days. The reaction was then concentrated under reduced pressure, co-evaporating with toluene. The residue was dissolved in EtOAc (100mL), washed with water (100mL) brine (100mL) and dried over  $\text{Na}_2\text{SO}_4$ , then concentrated under reduced pressure. The residue was purified by flash chromatography on silica gel (12:1 Hexanes: EtOAc) to yield **3.34** as an orange oil (1.01g, 1.57mmol, 42% over both steps). Spectra was consistent with known data.<sup>65</sup>

### 3.35 (2S,3R,4R,5S)-2,3,4,5-tetrakis(benzyloxy)-7-azabicyclo[4.1.0]heptanes



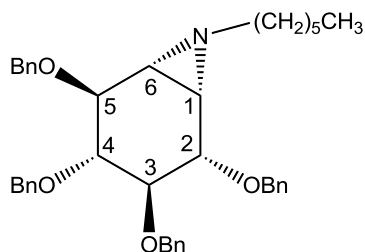
A solution of **3.34** (2.00g, 3.107mmol) in diethyl ether (30mL) was cooled to 0°C in an ice bath. LiAlH<sub>4</sub> (270mg, 7.115mmol) was then slowly added and allowed to stir at room temperature overnight under argon. EtOAc (20mL) was added to the solution and allowed to stir for 30 minutes to quench the reaction. The organics were washed with water (2 x 50mL), brine (50mL), dried over Na<sub>2</sub>SO<sub>4</sub> and concentrated under reduced pressure. The residue was purified by flash chromatography on silica gel (3:1 hexanes: EtOAc) to yield **3.35** as a white solid (970mg, 1.859mmol, 60%). <sup>1</sup>H NMR (500 MHz, CDCl<sub>3</sub>) δ2.32-2.34 (d, J = 6Hz, 1H, **H1**), 2.48-2.50 (dd, J = 6, 3Hz, 1H, **H6**), 3.42-3.45 (dd, J = 10, 8Hz, 1H, **H2**), 3.61-3.65 (t, J = 8Hz, 1H, **H5**), 3.83-3.85 (d, J = 8Hz, 1H, **H3**), 3.86-3.87, (d, J = 3Hz, 1H, **H4**), 4.68-4.85 (m, 8H, **CH<sub>2</sub>-O**), 7.23-7.40 (m, 20H, **phenyl**). <sup>13</sup>C NMR (500 MHz, CD<sub>3</sub>OD) δ33.23 (**C1**), 34.37 (**C6**), 72.84 (**CH<sub>2</sub>-O**), 72.90 (**CH<sub>2</sub>-O**), 75.36 (**CH<sub>2</sub>-O**), 75.85 (**CH<sub>2</sub>-O**), 79.66 (**C2**), 79.84 (**C5**), 81.31 (**C3**), 84.28 (**C4**), 127.49 (**CH**, Phenyl), 127.54 (**CH**, phenyl), 127.59 (**CH**, phenyl), 127.64 (**CH**, phenyl), 127.75 (**CH**, phenyl), 127.80 (**CH**, phenyl), 127.87 (**CH**, phenyl), 127.87 (**CH**, Phenyl), 127.91 (**CH**, Phenyl), 128.04 (**CH**, Phenyl), 128.13 (**CH**, Phenyl), 128.21 (**CH**, phenyl), 128.31 (**CH**, phenyl), 128.34 (**CH**, phenyl), 128.40 (**CH**, phenyl), 128.50 (**CH**, phenyl), 138.17 (**C-CH<sub>2</sub>-O**, phenyl), 138.84 (**C-CH<sub>2</sub>-O**, phenyl), 138.89 (**C-CH<sub>2</sub>-O**, phenyl), 138.91 (**C-CH<sub>2</sub>-O**, phenyl).

### 3.36 (2S,3R,4R,5S)-2,3,4,5-tetrakis(benzyloxy)-7-octyl-7-azabicyclo[4.1.0]heptanes



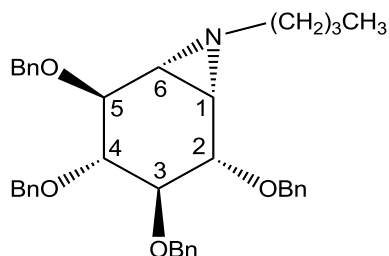
Potassium Carbonate (132mg, 0.959mmol) and 1-iodooctane (0.692ml, 0.383mmol) were added to a solution of **3.35** (250mg, 0.479mol) in dry DMF (15mL) and allowed to stir at 50°C overnight under argon. The solution was then evaporated to dryness under reduced pressure. The residue was dissolved in EtOAc (50mL), washed with water (50mL), brine (50mL), dried over Na<sub>2</sub>SO<sub>4</sub>, and concentrated under reduced pressure. The resulting residue was purified by flash chromatography on silica gel (8:1 hexanes: EtOAc) to give **3.36** as a yellow oil (180mg, 0.284mmol, 59.3%). <sup>1</sup>H NMR (500 MHz, CDCl<sub>3</sub>) δ 0.84-0.92 (t, J = 7Hz, 3H, CH<sub>3</sub>), 1.27-1.38 (m, 10H, CH<sub>2</sub>), 1.48-1.56 (quintet, J = 6Hz, 2H, N-CH<sub>2</sub>-CH<sub>2</sub>), 1.60-1.62 (d, J = 6Hz, 1H, H1), 1.82-1.84 (dd, J = 6, 3Hz, 1H, H6), 2.00-2.05 (dt, J = 11, 7Hz, 1H, N-CH<sub>2</sub>), 2.37-2.42 (dt, J = 11, 7Hz, 1H, N-CH<sub>2</sub>), 3.35-3.39 (dd, 10, 8Hz, 1H, H5), 3.57-3.61 (dd, 10, 8Hz, 1H, H2), 3.77-3.79 (dd, J = 8, 3Hz, 1H, H3), 3.80-3.81 (d, J = 8Hz, 1H, H4), 4.69-4.85 (m, 8H, CH<sub>2</sub>-O), 7.21-7.40 (m, 20H, phenyl). <sup>13</sup>C NMR (500 MHz, CDCl<sub>3</sub>) δ 14.20 (CH<sub>3</sub>), 22.74 (CH<sub>2</sub>), 27.48 (CH<sub>2</sub>), 29.35 (CH<sub>2</sub>), 29.67 (CH<sub>2</sub>), 29.68 (CH<sub>2</sub>), 31.95 (CH<sub>2</sub>), 41.77 (C1), 42.67 (C6), 61.17 (CH<sub>2</sub>-N), 72.59 (CH<sub>2</sub>-O), 72.90 (CH<sub>2</sub>-O), 75.45 (CH<sub>2</sub>-O), 75.91 (CH<sub>2</sub>-O), 80.08 (C2), 80.50 (C5), 81.31 (C3), 84.46 (C4), 127.44 (CH-C, phenyl), 127.49 (CH-C, phenyl), 127.58 (CH-C, phenyl), 127.81 (CH-C, phenyl), 127.85 (CH-C, phenyl), 127.96 (CH-C, phenyl), 128.15 (CH-C, phenyl), 128.37 (CH-C, phenyl), 128.50 (CH-C, phenyl), 138.25 (C-CH<sub>2</sub>-O, phenyl), 139.00 (C-CH<sub>2</sub>-O, phenyl), 139.04 (C-CH<sub>2</sub>-O, phenyl), 139.08 (C-CH<sub>2</sub>-O, phenyl).

### 3.37 (2S,3R,4R,5S)-2,3,4,5-tetrakis(benzyloxy)-7-hexyl-7-azabicyclo[4.1.0]heptane



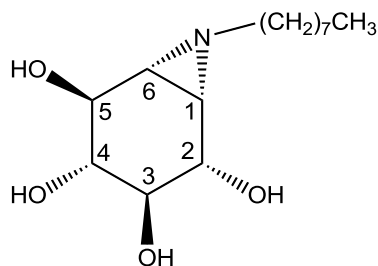
Potassium Carbonate (132mg, 0.959mmol) and 1-iodohexane (0.565ml, 0.383mmol) were added to a solution of **3.35** (250mg, 0.479mmol) in dry DMF (15mL) and allowed to stir at 50°C overnight under argon. The solution was then evaporated to dryness under reduced pressure. The residue was dissolved in EtOAc (50mL), washed with water (50mL), brine (50mL), dried over Na<sub>2</sub>SO<sub>4</sub>, and concentrated under reduced pressure. The resulting residue was purified by flash chromatography on silica gel (8:1 hexanes: EtOAc) to give **3.37** as a white solid (190mg, 0.314mmol, 65.5%). <sup>1</sup>H NMR (500 MHz, CDCl<sub>3</sub>) δ 0.86-0.93(t, J = 7Hz, 3H, CH<sub>3</sub>), 1.24-1.38 (m, 6H, CH<sub>2</sub>), 1.49-1.54 (quintet, J = 6Hz, 2H, N-CH<sub>2</sub>-CH<sub>2</sub>), 1.61-1.62 (d, J = 6Hz, 1H, H1), 1.83-1.85 (dd, J = 6, 3Hz, 1H, H6), 2.01-2.06 (dt, J = 11, 7Hz, 1H, N-CH<sub>2</sub>), 2.37-2.42 (dt, J = 11, 7Hz, 1H, N-CH<sub>2</sub>), 3.36-3.40 (dd, 10, 8Hz, 1H, H5), 3.58-3.62 (dd, 10, 8Hz, 1H, H2), 3.77-3.80 (dd, J = 8, 3Hz, 1H, H3), 3.80-3.82 (d, J = 8Hz, 1H, H4), 4.69-4.85 (m, 8H, CH<sub>2</sub>-O), 7.23-7.40 (m, 20H, phenyl). <sup>13</sup>C NMR (500 MHz, CDCl<sub>3</sub>) δ 14.21 (CH<sub>3</sub>), 22.72 (CH<sub>2</sub>), 27.18 (CH<sub>2</sub>), 29.68 (CH<sub>2</sub>), 31.95 (CH<sub>2</sub>), 41.79 (C1), 42.71 (C6), 61.19 (CH<sub>2</sub>-N), 72.63 (CH<sub>2</sub>-O), 72.93 (CH<sub>2</sub>-O), 75.49 (CH<sub>2</sub>-O), 75.93 (CH<sub>2</sub>-O), 80.11 (C2), 80.53 (C5), 81.35 (C3), 84.50 (C4), 127.48 (CH-C, phenyl), 127.52 (CH-C, phenyl), 127.61 (CH-C, phenyl), 127.84 (CH-C, phenyl), 127.88 (CH-C, phenyl), 128.00 (CH-C, phenyl), 128.17 (CH-C, phenyl), 128.33 (CH-C, phenyl), 128.35 (CH-C, phenyl), 128.40 (CH-C, phenyl), 128.53 (CH-C, phenyl), 138.28(C-CH<sub>2</sub>-O, phenyl), 139.03(C-CH<sub>2</sub>-O, phenyl), 139.07(C-CH<sub>2</sub>-O, phenyl), 139.11(C-CH<sub>2</sub>-O, phenyl).

### 3.38 (2S,3R,4R,5S)-2,3,4,5-tetrakis(benzyloxy)-7-butyl-7-azabicyclo[4.1.0]heptanes



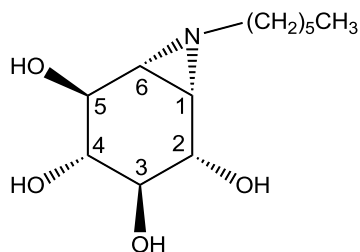
Potassium carbonate (132mg, 0.959mmol) and 1-iodobutane (0.438ml, 0.383mmol) were added to a solution of **3.35** (250mg, 0.479mmol) in dry DMF (15mL) and allowed to stir at 50°C overnight under argon. The solution was then evaporated to dryness under reduced pressure. The residue was dissolved in EtOAc (50mL), washed with water (50mL), brine (50mL), dried over Na<sub>2</sub>SO<sub>4</sub>, and concentrated under reduced pressure. The resulting residue was purified by flash chromatography on silica gel (8:1 hexanes: EtOAc) to give **3.38** as a yellow oil (151mg, 0.261mmol, 54.5%). <sup>1</sup>H NMR (500 MHz, CD<sub>3</sub>OD) δ 0.87-0.93 (t, J = 7.2, 3H, CH<sub>3</sub>), 1.33-1.38 (qd, J = 7, 2.6Hz, 2H, CH<sub>2</sub>-CH<sub>3</sub>), 1.46-1.51 (m, 2H, N-CH<sub>2</sub>-CH<sub>2</sub>) 1.60-1.61(d, J = 6Hz, 1H, H1), 1.82-1.84 (dd, J = 6, 3Hz, 1H, H6) 2.00-2.06 (dt, J = 11, 7Hz, 1H, N-CH<sub>2</sub>), 2.36-2.41 (dt, J = 11, 7Hz, 1H, N-CH<sub>2</sub>), 3.35-3.39 (dd, J = 10, 8Hz, 1H, H5), 3.57-3.61 (dd, J = 10, 8Hz, 1H, H2), 3.76-3.79 (dd, J = 8, 3Hz, 1H, H3), 3.79-3.81 (d, J = 8Hz, 1H, H4), 4.68-4.84 (m, 8H, O-CH<sub>2</sub>), 7.22-7.39(m, 20H, phenyl). <sup>13</sup>C NMR (500 MHz, CD<sub>3</sub>OD) δ 14.20 (CH<sub>3</sub>), 20.59 (CH<sub>2</sub>-CH<sub>3</sub>), 31.82 (N-CH<sub>2</sub>-CH<sub>2</sub>), 41.75 (C1), 42.71 (C6), 60.81 (CH<sub>2</sub>-N), 72.63 (CH<sub>2</sub>-O), 72.92 (CH<sub>2</sub>-O), 75.47 (CH<sub>2</sub>-O), 75.93 (CH<sub>2</sub>-O), 80.12 (C2), 80.52 (C5), 81.30 (C3), 84.50 (C4), 127.47 (CH-C, phenyl), 127.52 (CH-C, phenyl), 127.61 (CH-C, phenyl), 127.84 (CH-C, phenyl), 127.87 (CH-C, phenyl), 127.89 (CH-C, phenyl), 128.02 (CH-C, phenyl), 128.17 (CH-C, phenyl), 128.32 (CH-C, phenyl), 128.34 (CH-C, phenyl), 128.40 (CH-C, phenyl), 128.53 (CH-C, phenyl), 138.27 (C-CH<sub>2</sub>-O, phenyl), 139.02 (C-CH<sub>2</sub>-O, phenyl), 139.07 (C-CH<sub>2</sub>-O, phenyl), 139.10 (C-CH<sub>2</sub>-O, phenyl).

### 3.39 (2S,3R,4R,5S)-7-octyl-7-azabicyclo[4.1.0]heptane-2,3,4,5-tetraol



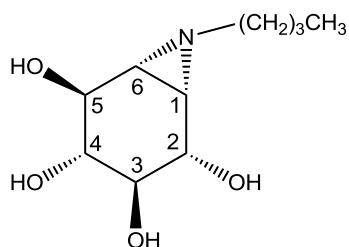
Concentrated  $\text{NH}_4\text{OH}$  (75mL) was heated to  $60^\circ\text{C}$  to release  $\text{NH}_3(\text{g})$  that passes through a cold water condenser and two drying tubes filled with  $\text{CaSO}_4$  that are cooled in an ice bath.  $\text{NH}_3(\text{l})$  (20mL) was condensed by a dry ice condenser into a three neck flask partially submerged in an acetone dry ice slurry kept at  $-78^\circ\text{C}$ . A small chunk of  $\text{Na}(\text{s})$  (~100-200mg, 4.35-8.70mmol) was added to the stirring  $\text{NH}_3(\text{l})$  producing a persistent deep blue color. **3.36** (253mg, 0.399 mmol) dissolved in THF (3mL) and cooled to  $-78^\circ\text{C}$  in the dry ice bath was added to the stirring solution via cannula and allowed to stir for 4 hours. Water (15mL) was added to the solution to quench the reaction and allowed to return to room temperature to slowly evaporate  $\text{NH}_3(\text{l})$ . The solution was concentrated under reduced pressure to remove  $\text{NH}_4\text{OH}$  then redissolved in water (50mL). The organics were extracted with diethyl ether (50mL) and the aqueous was concentrated to dryness under reduced pressure. The resulting residue was purified by flash chromatography on silica gel (gradient 7:1  $\text{CHCl}_3$ :MeOH to 100% MeOH) to give **3.39** as a white powder (60mg, 0.219 mmol, 55%).  $^1\text{H}$  NMR (500 MHz,  $\text{CD}_3\text{OD}$ )  $\delta$  0.91-0.93 (t,  $J = 7\text{Hz}$ , 3H, **CH<sub>3</sub>**), 1.28-1.40 (m, 10H, **CH<sub>2</sub>**), 1.57-1.62 (quintet,  $J = 7\text{Hz}$ , 2H, N-**CH<sub>2</sub>-CH<sub>2</sub>**), 1.64-1.66 (d,  $J = 6\text{Hz}$ , 1H, **H<sub>1</sub>**), 1.94-1.96 (t,  $J = 5\text{Hz}$ , 1H, **H<sub>6</sub>**), 2.14-2.19 (dt,  $J = 11, 7\text{Hz}$ , 1H, N-**CH<sub>2</sub>**), 2.38-2.42(dt,  $J = 11, 7\text{Hz}$ , 1H, N-**CH<sub>2</sub>**), 3.05-3.09 (t,  $J = 9\text{Hz}$ , 1H, **H<sub>3</sub>**), 3.23-3.27(t,  $J = 9\text{Hz}$ , 1H, **H<sub>4</sub>**), 3.64-3.66 (d,  $J = 8\text{Hz}$ , 1H, **H<sub>2</sub>**), 3.70-3.73 (dd,  $J = 8, 3\text{Hz}$ , 1H, **H<sub>5</sub>**).  $^{13}\text{C}$  NMR (500 MHz,  $\text{CD}_3\text{OD}$ )  $\delta$  13.05 (**CH<sub>3</sub>**), 22.34 (**CH<sub>2</sub>**), 27.02(**CH<sub>2</sub>**), 29.01(**CH<sub>2</sub>**), 29.16(**CH<sub>2</sub>**), 29.33(**CH<sub>2</sub>**), 31.64(**CH<sub>2</sub>**), 44.03 (**C<sub>1</sub>**), 44.45 (**C<sub>6</sub>**), 60.69 (N-**CH<sub>2</sub>**), 71.73 (**C<sub>3</sub>**), 72.04 (**C<sub>4</sub>**), 72.68 (**C<sub>5</sub>**), 76.45 (**C<sub>2</sub>**). LRMS (ESI)  $m/z$ : 272.2 [ $\text{M} - \text{H}$ ] $^-$  Calculated for  $\text{C}_{14}\text{H}_{26}\text{NO}_4$ : 272.1867

### 3.40 (2S,3R,4R,5S)-7-hexyl-7-azabicyclo[4.1.0]heptane-2,3,4,5-tetraol



Concentrated  $\text{NH}_4\text{OH}$  (75mL) was heated to  $60^\circ\text{C}$  to release  $\text{NH}_3(\text{g})$  that passes through a cold water condenser and two drying tubes filled with  $\text{CaSO}_4$  that are cooled in an ice bath.  $\text{NH}_3(\text{l})$  (20mL) was condensed by a dry ice condenser into a three neck flask partially submerged in an acetone dry ice slurry kept at  $-78^\circ\text{C}$ . A small chunk of  $\text{Na}(\text{s})$  (~100-200mg, 4.35-8.70mmol) was added to the stirring  $\text{NH}_3(\text{l})$  producing a persistent deep blue color. **3.37** (281mg, 0.464 mmol) dissolved in THF (3mL) and cooled to  $-78^\circ\text{C}$  in the dry ice bath was added to the stirring solution via cannula and allowed to stir for 4 hours. Water (15mL) was added to the solution to quench the reaction and allowed to return to room temperature to slowly evaporate  $\text{NH}_3(\text{l})$ . The solution was concentrated under reduced pressure to remove  $\text{NH}_4\text{OH}$  then redissolved in water (50mL). The organics were extracted with diethyl ether (50mL) and the aqueous was concentrated to dryness under reduced pressure. The resulting residue was purified by flash chromatography on silica gel (gradient 7:1  $\text{CHCl}_3$ :MeOH to 100% MeOH) to give **3.40** as a white powder (50mg, 0.204 mmol, 44%).  $^1\text{H}$  NMR (500 MHz,  $\text{CD}_3\text{OD}$ )  $\delta$ 0.91-0.94 (t,  $J = 7\text{Hz}$ , 3H, **CH<sub>3</sub>**), 1.31-1.41 (m, 6H, **CH<sub>2</sub>**), 1.57-1.63 (quintet,  $J = 7\text{Hz}$ , 2H, N-**CH<sub>2</sub>**), 1.65-1.67 (d,  $J = 7\text{Hz}$ , 1H, **H<sub>1</sub>**), 1.94-1.96 (t,  $J = 5\text{Hz}$ , 1H, **H<sub>6</sub>**), 2.14-2.20 (dt,  $J = 11, 7\text{Hz}$ , 1H, N-**CH<sub>2</sub>**), 2.37-2.42(dt,  $J = 11, 7\text{Hz}$ , 1H, N-**CH<sub>2</sub>**), 3.06-3.10 (t,  $J = 10\text{Hz}$ , 1H, **H<sub>3</sub>**), 3.23-3.27(t,  $J = 10\text{Hz}$ , 1H, **H<sub>4</sub>**), 3.64-3.66 (d,  $J = 8\text{Hz}$ , 1H, **H<sub>2</sub>**), 3.71-3.73 (dd,  $J = 8, 3\text{Hz}$ , 1H, **H<sub>5</sub>**).  $^{13}\text{C}$  NMR (500 MHz,  $\text{CD}_3\text{OD}$ )  $\delta$ 13.02 (**CH<sub>3</sub>**), 22.27 (**CH<sub>2</sub>**), 26.70 (**CH<sub>2</sub>**), 29.13 (**CH<sub>2</sub>**), 31.61 (**CH<sub>2</sub>**), 44.04 (**C<sub>1</sub>**), 44.45 (**C<sub>6</sub>**), 60.69 (**CH<sub>2</sub>-N**), 71.72 (**C<sub>3</sub>**), 72.04 (**C<sub>4</sub>**), 72.68 (**C<sub>5</sub>**), 76.43 (**C<sub>2</sub>**). **LRMS (ESI) m/z:** 244.1 [ $\text{M} - \text{H}$ ]<sup>-</sup> **Calculated for  $\text{C}_{12}\text{H}_{22}\text{NO}_4$ :** 244.1554

### 3.41 (2S,3R,4R,5S)-7-butyl-7-azabicyclo[4.1.0]heptane-2,3,4,5-tetraol



Concentrated  $\text{NH}_4\text{OH}$  (75mL) was heated to  $60^\circ\text{C}$  to release  $\text{NH}_3(\text{g})$  that passes through a cold water condenser and two drying tubes filled with  $\text{CaSO}_4$  that are cooled in an ice bath.  $\text{NH}_3(\text{l})$  (20mL) was condensed by a dry ice condenser into a three neck flask partially submerged in an acetone dry ice slurry kept at  $-78^\circ\text{C}$ . A small chunk of  $\text{Na}(\text{s})$  (~100-200mg, 4.35-8.70mmol) was added to the stirring  $\text{NH}_3(\text{l})$  producing a persistent deep blue color. **3.38** (130mg, 0.215mmol) dissolved in THF (3mL) and cooled to  $-78^\circ\text{C}$  in the dry ice bath was added to the stirring solution via cannula and allowed to stir for 4 hours. Water (15mL) was added to the solution to quench the reaction and allowed to return to room temperature to slowly evaporate  $\text{NH}_3(\text{l})$ . The solution was concentrated under reduced pressure to remove  $\text{NH}_4\text{OH}$  then redissolved in water (50mL). The organics were extracted with diethyl ether (50mL) and the aqueous was concentrated to dryness under reduced pressure. The resulting residue was purified by flash chromatography on silica gel (gradient 7:1  $\text{CHCl}_3$ :MeOH to 100% MeOH) to give **3.41** as a white powder (35mg, 0.1611mmol, 75%).  $^1\text{H}$  NMR (500 MHz,  $\text{CD}_3\text{OD}$ )  $\delta$ 0.94-0.97 (t,  $J = 7$  Hz, 3H, **CH**<sub>3</sub>), 1.37-1.44 (q,  $J = 7$  Hz, 2H, **CH**<sub>2</sub>-**CH**<sub>3</sub>), 1.55-1.61(t,  $J = 7$ Hz, 2H, N-**CH**<sub>2</sub>-**CH**<sub>2</sub>), 1.65-1.66(d,  $J = 6$ Hz, 1H, **H**<sub>1</sub>), 1.95-1.96(m, 1H, **H**<sub>6</sub>), 2.15-2.20 (dt,  $J = 10, 7$ Hz, 1H, N-**CH**<sub>2</sub>), 2.37-2.43 (dt,  $J = 10, 7$ Hz, 1H, N-**CH**<sub>2</sub>), 3.06-3.09(t,  $J = 9$ Hz, 1H, **H**<sub>3</sub>), 3.23-3.27(t,  $J = 9$ Hz, 1H, **H**<sub>4</sub>), 3.64-3.66 (d,  $J = 8$ Hz, 1H, **H**<sub>2</sub>), 3.70-3.73 (d,  $J = 8$ Hz, 1H, **H**<sub>5</sub>).  $^{13}\text{C}$  NMR (500 MHz,  $\text{CD}_3\text{OD}$ )  $\delta$ 13.04 (**C**<sub>3</sub>), 20.12 (**C**<sub>2</sub>), 31.36 (**C**<sub>2</sub>), 44.05 (**C**<sub>1</sub>), 44.43 (**C**<sub>6</sub>), 60.38(**C**<sub>2</sub>-N), 71.73 (**C**<sub>3</sub>), 72.04 (**C**<sub>4</sub>), 72.67 (**C**<sub>5</sub>), 76.44 (**C**<sub>2</sub>). LRMS (ESI)  $m/z$ : 216.1 [ $\text{M} - \text{H}$ ]<sup>-</sup> Calculated for  $\text{C}_{10}\text{H}_{18}\text{NO}_4^-$ : 216.1241

## Chapter 6: Enzymology

### 6.1 Production of ABG

Electro-competent BL21 cells were placed into small vials containing 50 $\mu$ L of LB medium and 50 $\mu$ L of a 10% glycerol:90% water solution. 1 $\mu$ L of pET-24 ABG-wt vector plasmid solution was added then the contents transferred into an electroporator cuvette. The electroporator pulsed at 1200mV for 5.6ms to open the cell membranes followed immediately by 100 $\mu$ L of LB medium. The contents of the cuvette were transferred into a tube containing 5mL of LB media and allowed to grow at 37°C for 1 hr with shaking before 5 $\mu$ L of kanamycin solution (30g/mL) was added. The cells were then plated on a LB media containing kanamycin (30 $\mu$ g/mL) and grown overnight at 37° with shaking. A single colony was selected and inoculated in 10mL of LB media and grown at 37° overnight with shaking then frozen at -85°C.

Frozen cells (1 mL) were selected and grown overnight in a flask containing 25mL of LB medium and 30 $\mu$ g/mL kanamycin to provide concentrated cell mixture. The concentrated cell mixture was added to 450mL of LB medium containing 30 $\mu$ g/mL kanamycin until an  $OD_{600nm} \sim 0.2$  was obtained. The cells were allowed to grow until an optimal concentration for protein expression of  $OD_{600nm} \sim 0.6$  was obtained.

Isopropyl  $\beta$ -D-1-thiogalactopyranoside (450 $\mu$ L, 0.5M) was added to the flask and the cells were grown overnight at room temperature with shaking. The cells were then isolated by centrifugation (10000 x g) and supernatant removed by decanting. Cells were transferred into tubes and resuspended in binding buffer ( 30mM HEPES, 500mM NaCl, pH 8.0) with lysozyme (10mg/mL) followed by sonication (3s pulse, 6s delay, 3min x 3 with 3 min cooling between). The mixture was then centrifuged (10000 x g) to isolate solid cellular components and the supernatant containing ABG. The ABG in the supernatant was purified by loading onto a nickel affinity column, washed (30mM imidazole, 500mM NaCl, pH 7.4), and then eluted (300mM imidazole, 500mM NaCl, pH 7.4). The fractions containing ABG were detected from hydrolysis of the dilute substrate 2,4-DNP- $\beta$ -D-Glc by observing the yellow 2,4-dinitrophenolate product.

The fractions were concentrated using a 10KDa molecular weight cut-off centrifuge tube. The

concentrated solution was then transferred into small vials and concentration determined by UV Vis spectroscopy using the extinction coefficient ( $E_{280\text{nM}} = 2.20\text{cm}^2\text{mg}^{-1}$ ) as a 3.58mg/mL solution.

## 6.2 ABG and GCase Competitive Kinetics

The human  $\beta$ -glucocerebrosidase analogue imiglucerase was obtained from used patient vials of Cerezyme<sup>®</sup> that were donated after use. Full vials contained a solution of 424 units of imiglucerase, 340mg mannitol, 104mg trisodium citrate, 36mg disodium hydrogen citrate, and 1.06mg polysorbate 80 in 10mL water. The buffer used in all kinetics involving GCase was 50mM acetate, 0.2% v/v triton X-100, 0.3% w/v sodium taurocholate and pH 5.5. *Agrobacterium sp.*  $\beta$ -Glucosidase was produced by transforming *Escherichia coli* cells with the ABG plasmid and inducing production of the enzyme as described above. The buffer used in all kinetics involving ABG was 50mM phosphate and pH 6.8. The running buffer used in the cell lysate assays were 0.1% BSA, 0.15% v/v triton x-100, 0.1M phosphate, and either 0.125% sodium taurocholate and pH 5.9, or 1.2% sodium taurocholate and pH 5.5. The stop buffer used in the lysate assays was 0.1M NaOH and 0.1M glycine.

The continuous assays were all performed on the Biotek Synergy 4 hybrid multi-mode reader using 2,4-dinitrophenyl- $\beta$ -D-glucopyranoside (**3.04**) as the substrate. Determined by Bradford assay, the concentration of GCase used for the competitive inhibitors was 4.14nM and for the aziridine inactivators was 41.4nM. Calculated from the ABG extinction coefficient of  $2.20\text{cm}^2/\text{mg}$ , the concentration used for the competitive inhibitors was 5nM and for the aziridine inactivators was 50nM. The reactions were measured by the release of 2,4-dinitrophenolate at 400nM. The initial rates of the reactions were determined from the resulting slope of the absorbance vs. time graphs. For the competitive inhibitors the initial rates were fit to the non-linear regression model of **Equation 2.1** using GraphPad Prism to calculate  $K_i$  values.

**Equation 2.1:**

$$V = \frac{V_{max}[S]}{K_m \left(1 + \frac{[I]}{K_i}\right) + [S]}$$

The aziridine inactivators had their initial rates fit to the one phase decay equation using the GraphPad Prism software utilizing **equation 2.3** to give  $K_{obs}$  which was then fit to **Equation 2.4** with ABG and **Equation 2.5** with GCase.

**Equation 2.3:**

$$Y = (Y_0 - Plateau)e^{(-K*X)} + Plateau$$

**Equation 2.4**

$$k_{obs} = \frac{k_i[I]}{K_i + [I]}$$

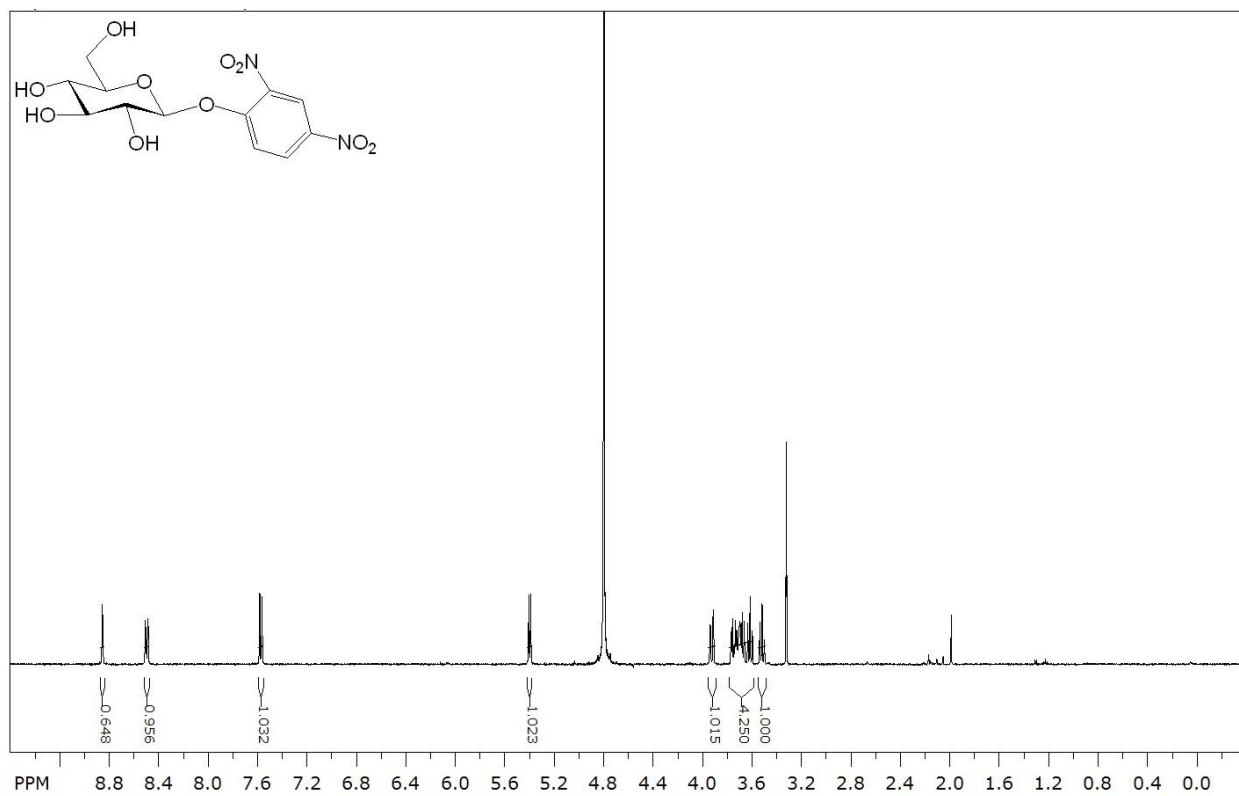
**Equation 2.5**

$$k_{obs} = \frac{k_i[I]}{K_i}$$

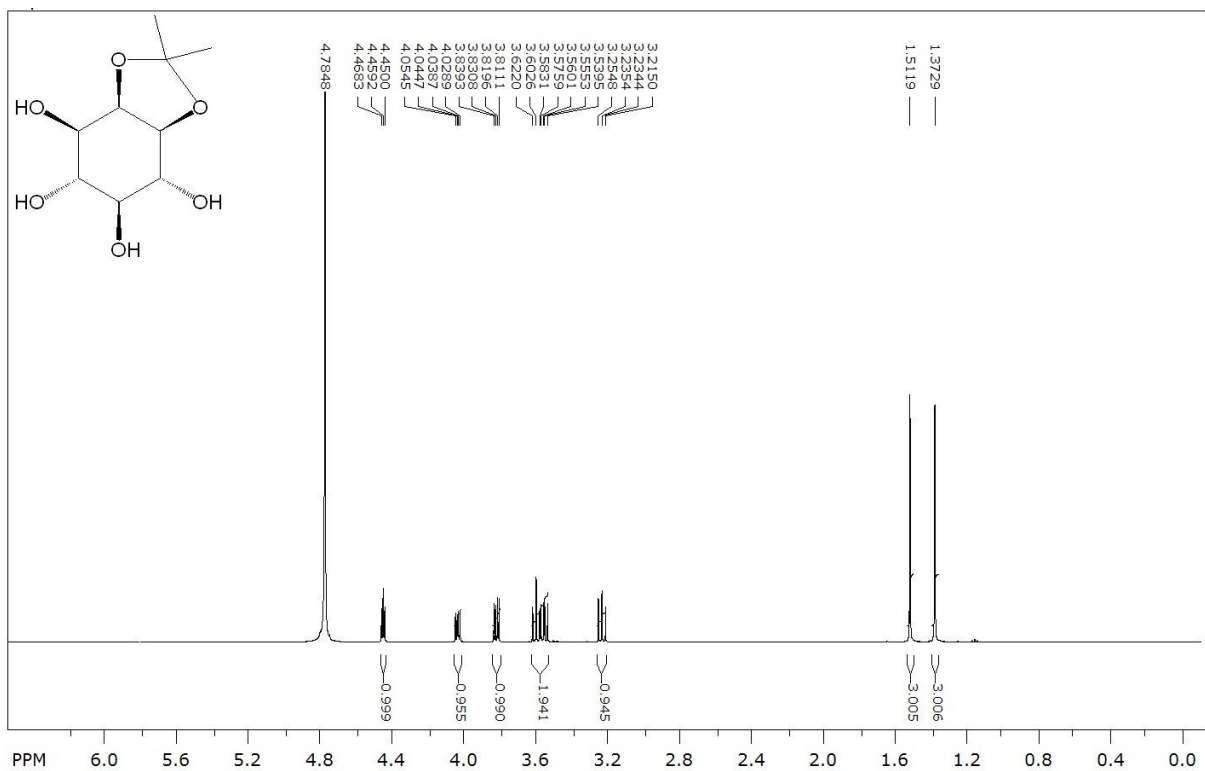
The stopped assays of the cell lysates were all performed on the Biotek Synergy 4 hybrid multi-mode reader and used the substrate 4-methylumbelliferyl  $\beta$ -D-glucopyranoside. HeLa cells were seeded into wells and grown up to 80% confluency in media containing DMEM with 10% serum. The aziridine inhibitors were then incubated with the cells in concentrations of 10nM, 100nM and 1mM overnight. The cells were then washed and lysed. The cell lysate was centrifuged and the supernatant was isolated and frozen at -80°C. A Bradford assay was performed on the lysates to determine the concentration of protein. In triplicate, 10 $\mu$ L of the Lysates in 190 $\mu$ L of buffer were incubated at 37°C before initiation by addition of 4-MuGlc with stirring. After 10 minutes, 50 $\mu$ L of the reaction mixture was removed and added to 200 $\mu$ L of the stop buffer. Then 200 $\mu$ L of the stopped solution was measured for the fluorescence of 4-methylumbelliferone which was excited at 365nm to emit at 448nm. The background emission from spontaneous hydrolysis of 4-MuGlc was removed and the emissions were represented as a relative value to the cell lysate blanks which were not incubated in the presence of any inhibitors.

## Chapter 7: NMR Spectra

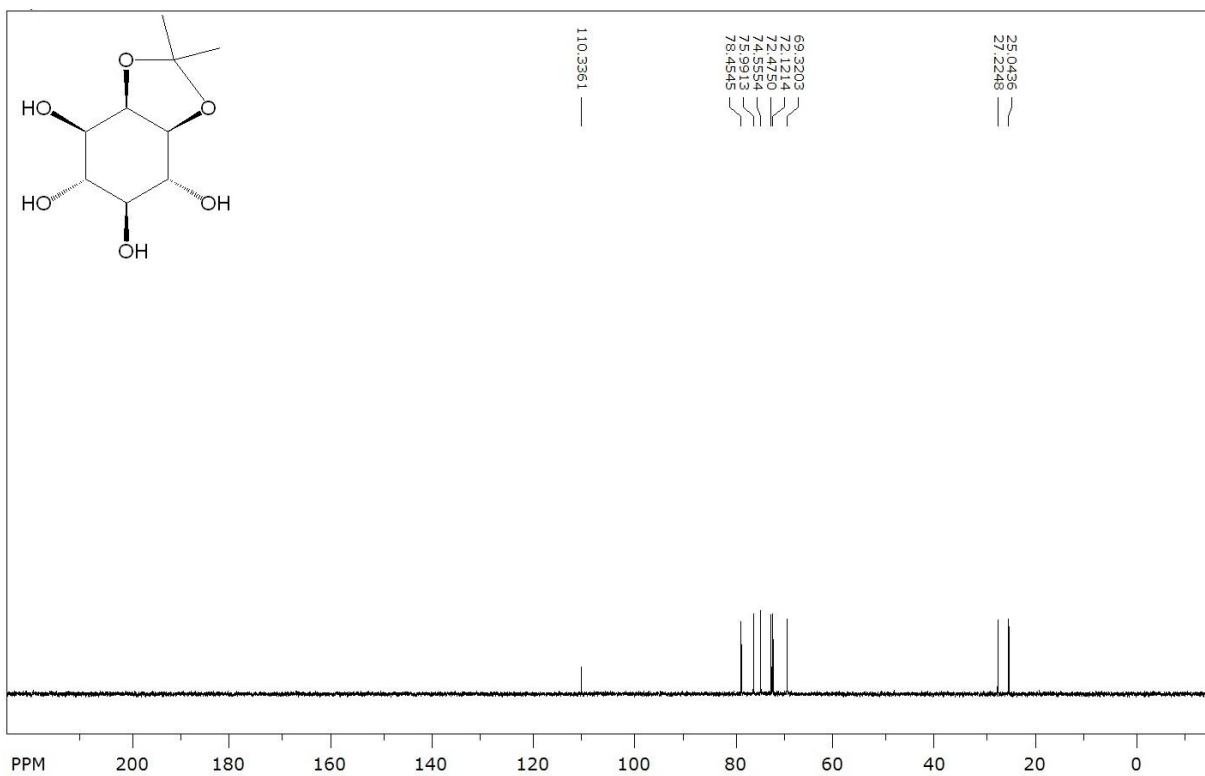
### $^1\text{H}$ NMR Spectrum (500 MHz, $\text{CD}_2\text{OD}$ ) of 3.04



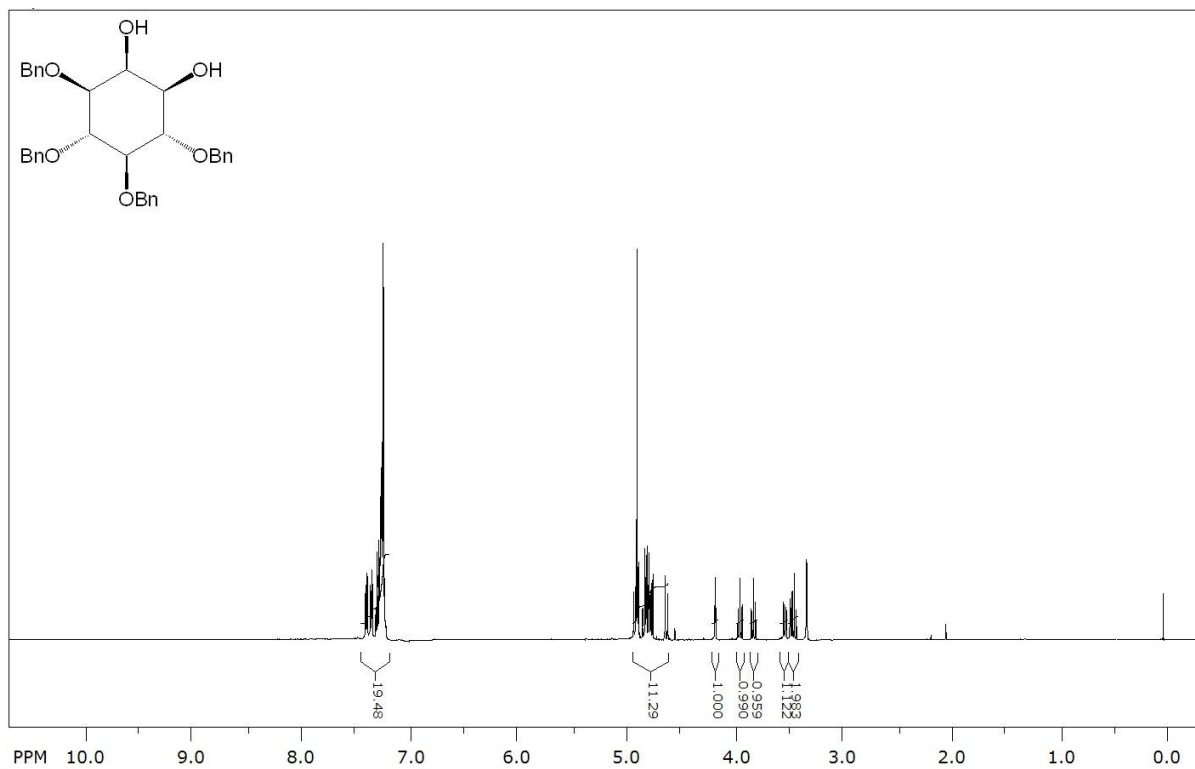
### <sup>1</sup>H NMR Spectrum (500 MHz, D<sub>2</sub>O) of 3.05



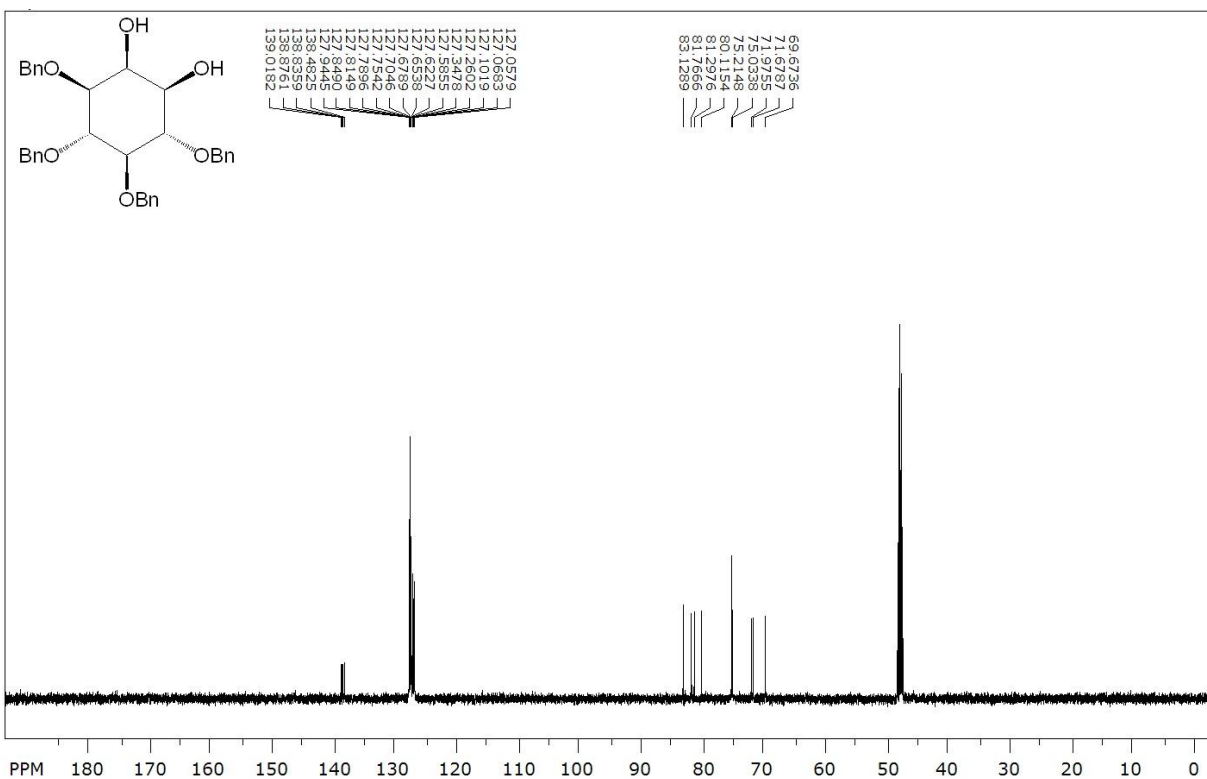
### <sup>13</sup>C NMR Spectrum (500 MHz, D<sub>2</sub>O) of 3.05



### <sup>1</sup>H NMR Spectrum (500 MHz, CD<sub>3</sub>OD) of 3.07

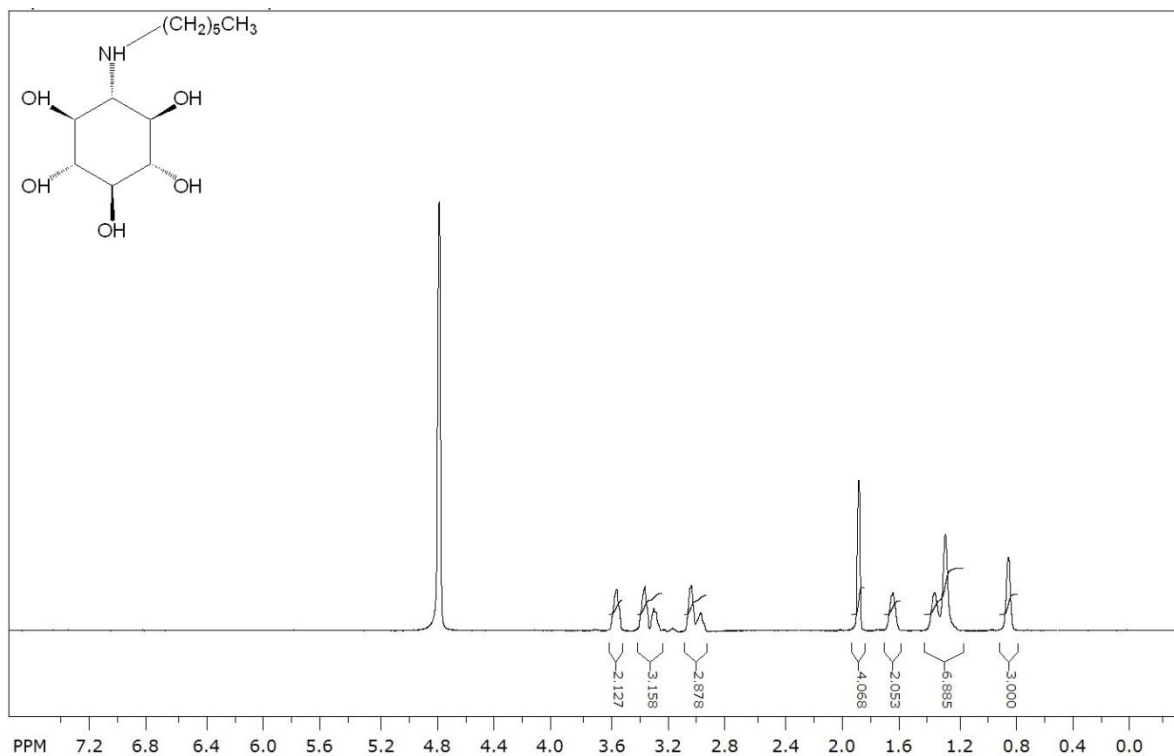


### <sup>13</sup>C NMR Spectrum (500 MHz, CD<sub>3</sub>OD) of 3.07

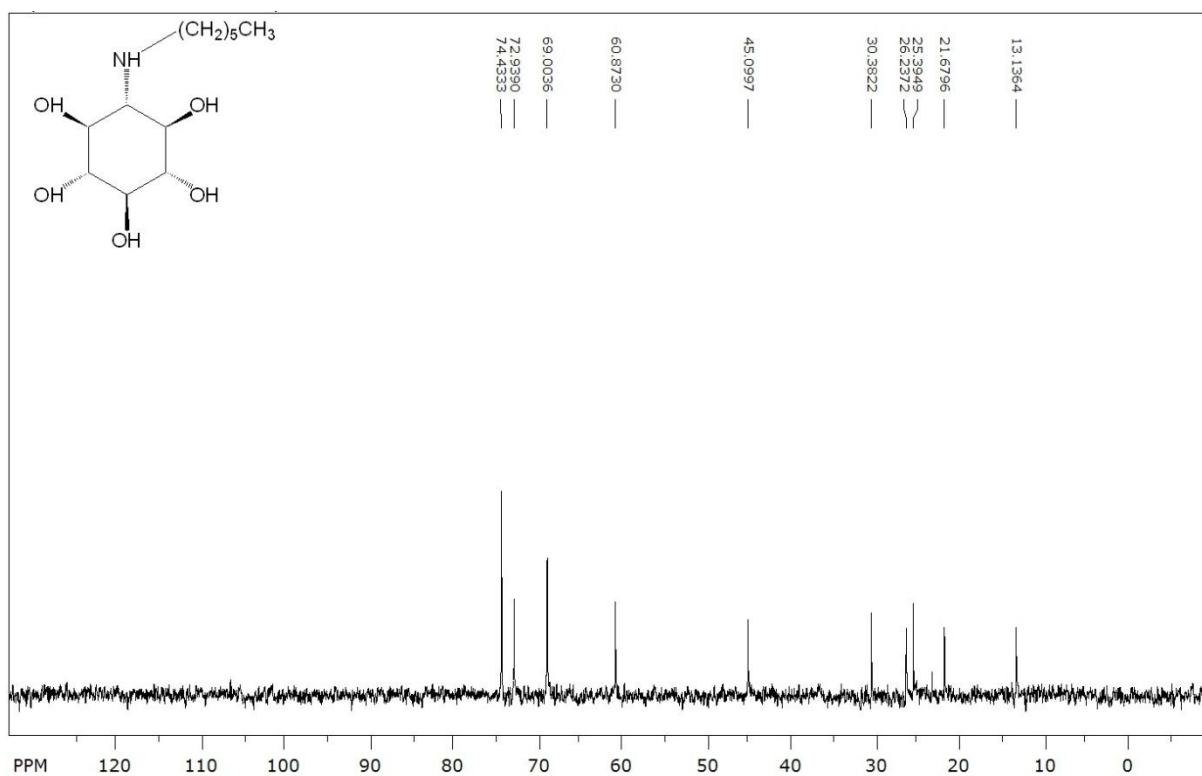




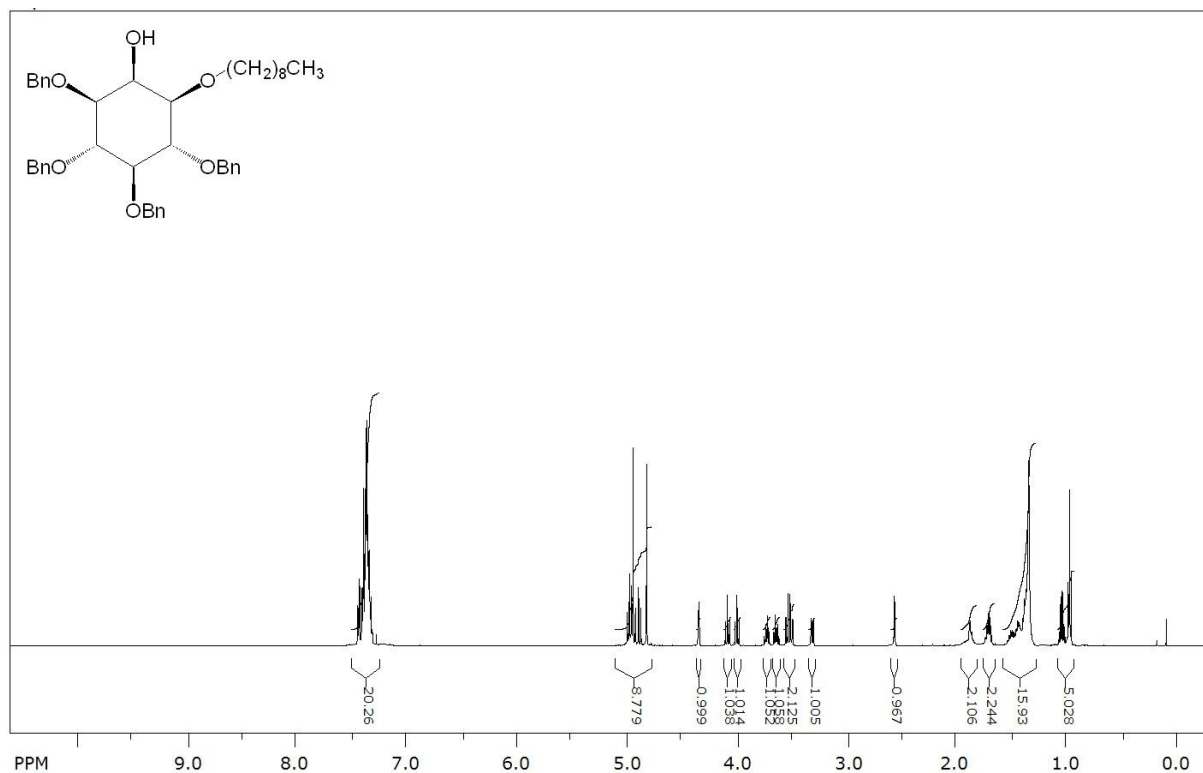
### <sup>1</sup>H NMR Spectrum (500 MHz, CDCl<sub>3</sub>) of 3.12



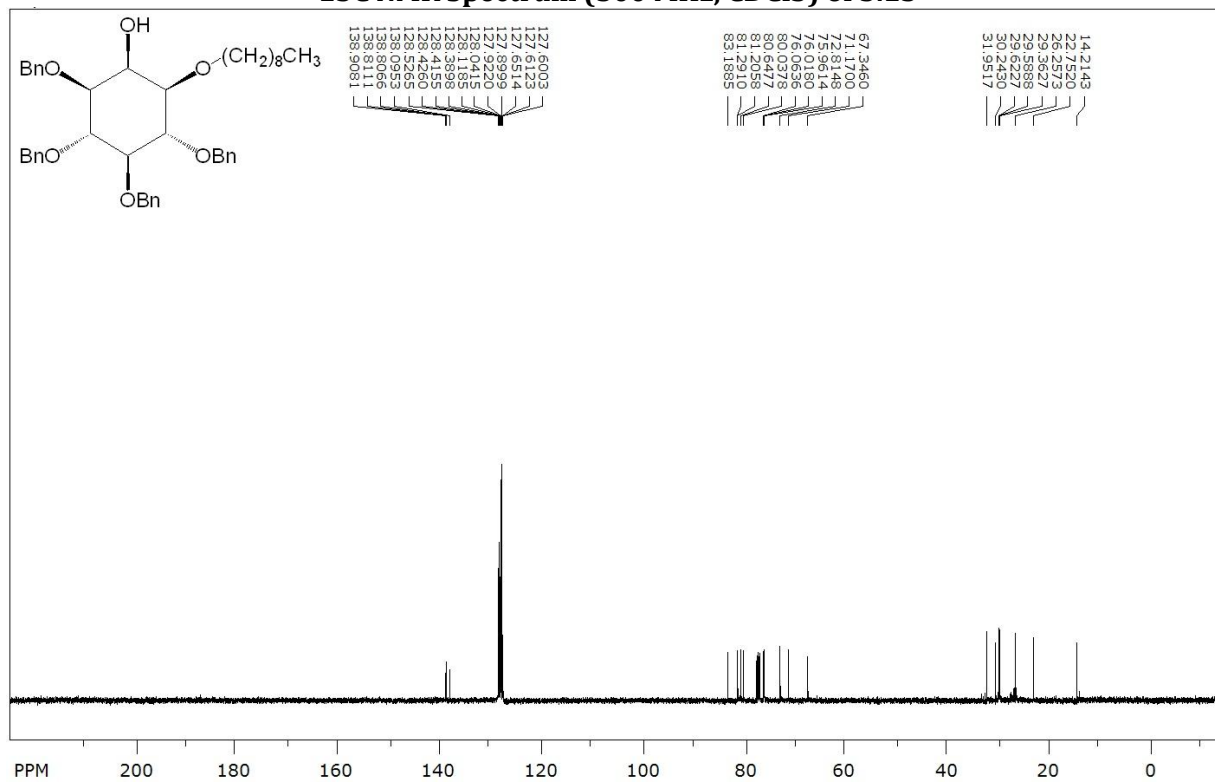
### <sup>13</sup>C NMR Spectrum (500 MHz, CDCl<sub>3</sub>) of 3.12



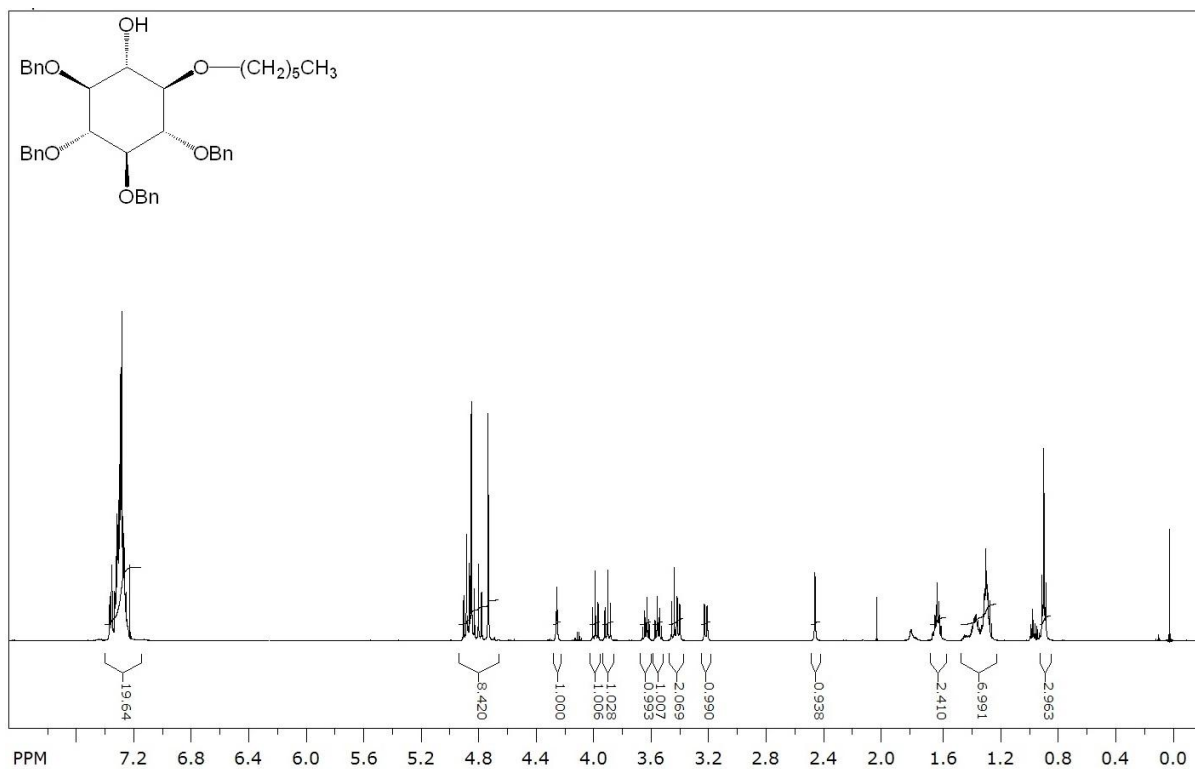
### <sup>1</sup>H NMR Spectrum (500 MHz, CDCl<sub>3</sub>) of 3.13



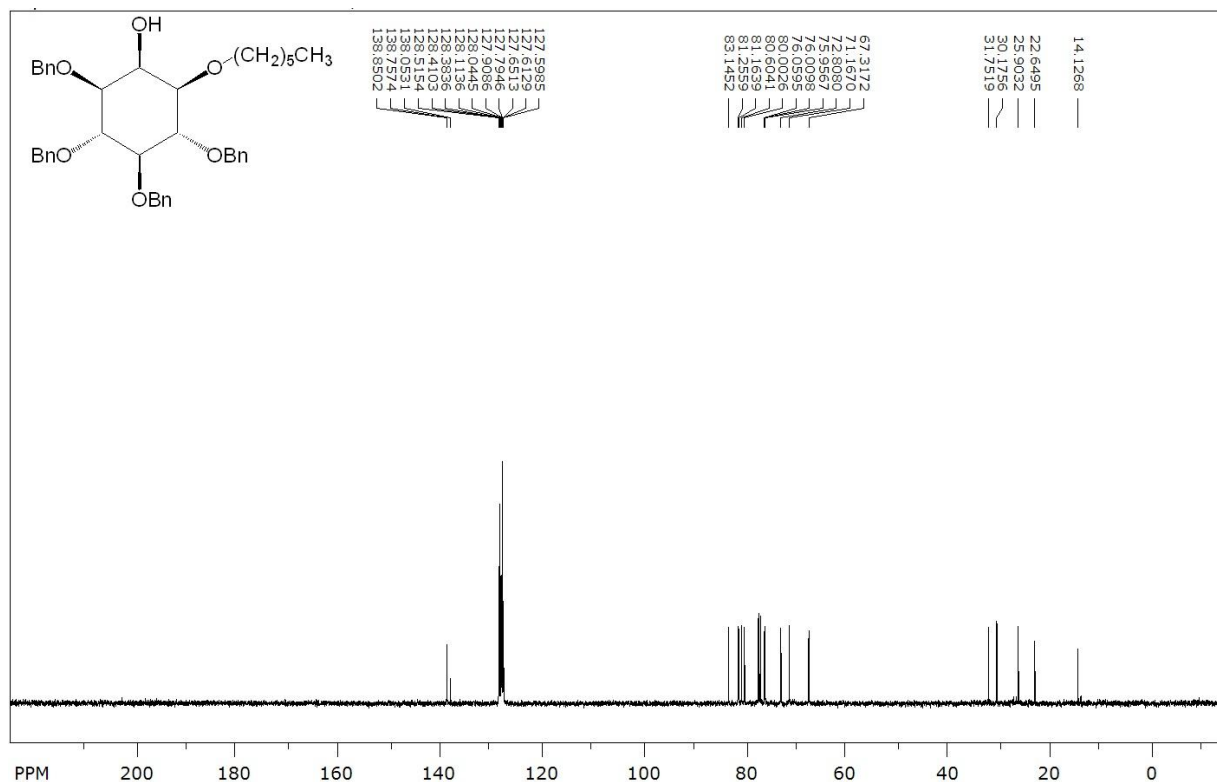
### <sup>13</sup>C NMR Spectrum (500 MHz, CDCl<sub>3</sub>) of 3.13



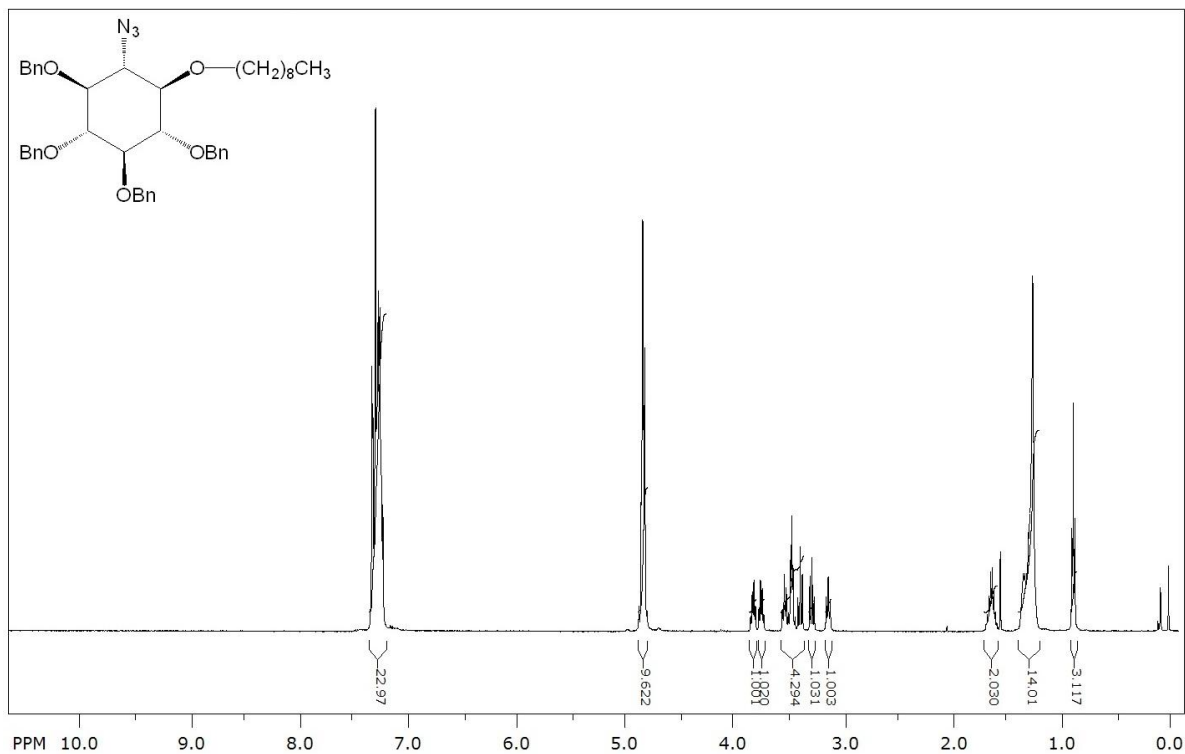
**<sup>1</sup>H NMR Spectrum (500 MHz, CDCl<sub>3</sub>) of 3.14**



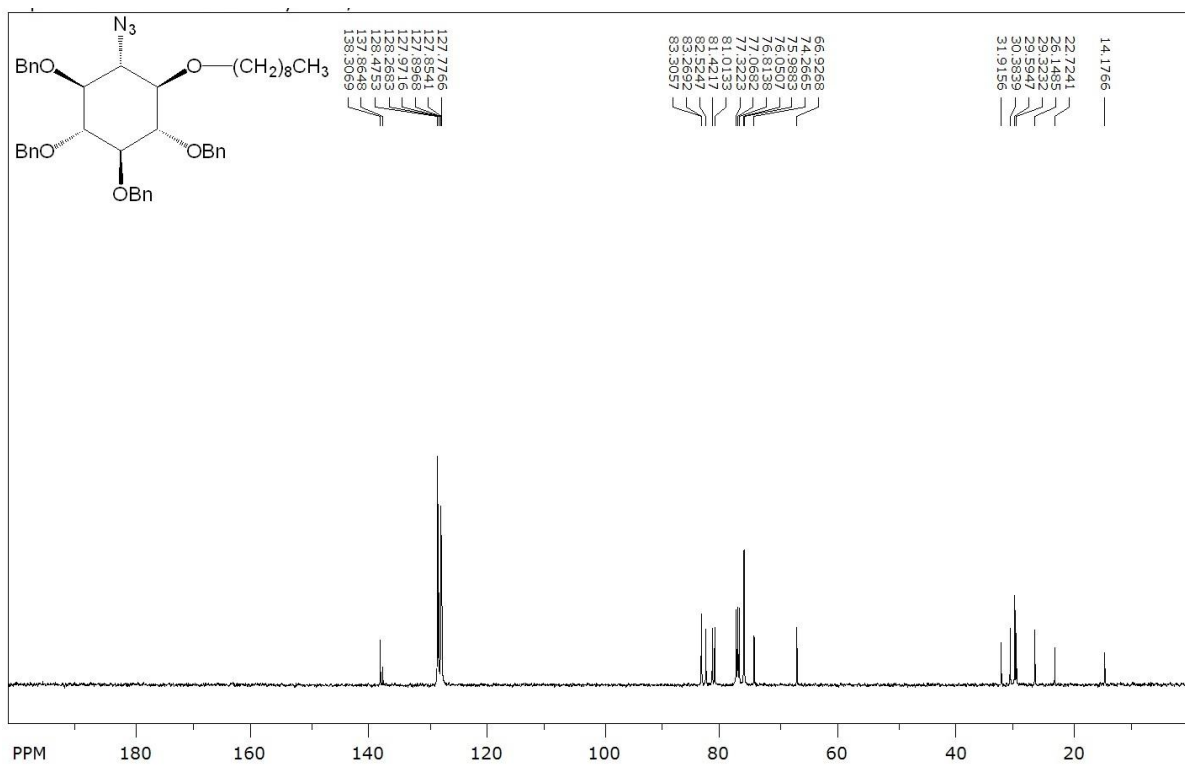
**<sup>13</sup>C NMR Spectrum (500 MHz, CDCl<sub>3</sub>) of 3.14**



**<sup>1</sup>H NMR Spectrum (500 MHz, CDCl<sub>3</sub>) of 3.16**

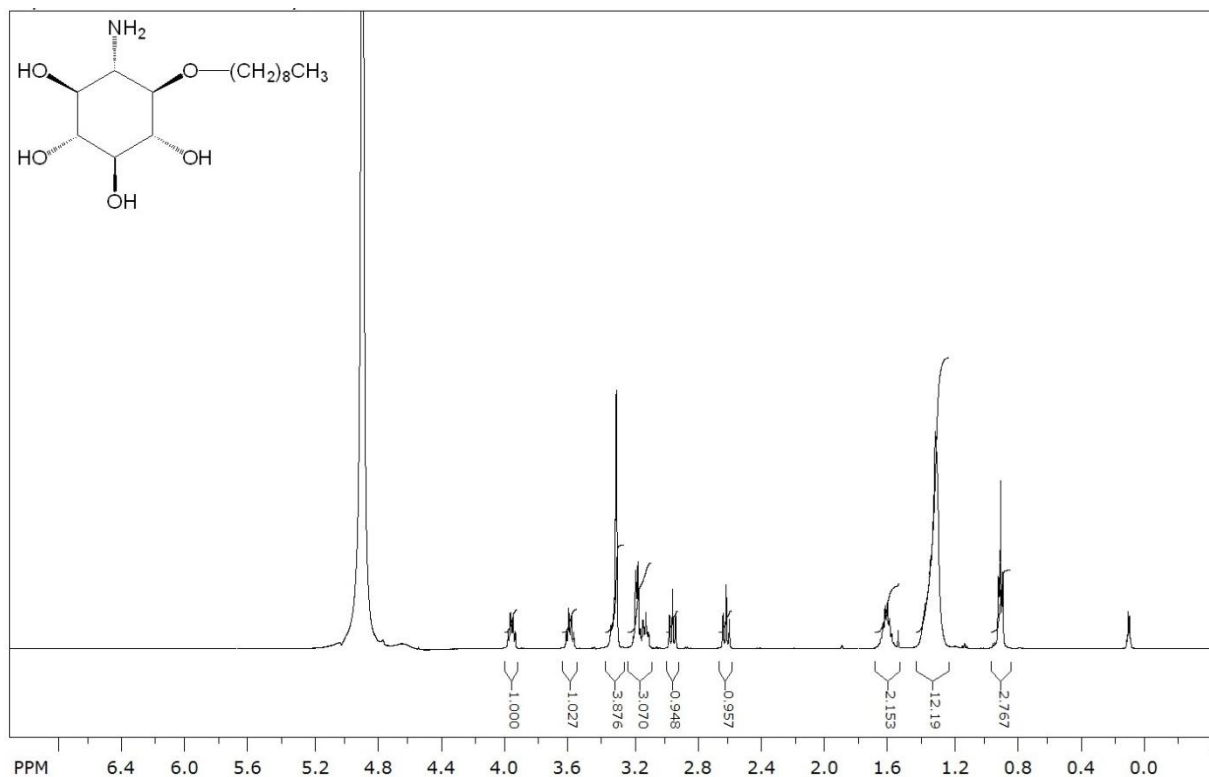


**<sup>13</sup>C NMR Spectrum (500 MHz, CDCl<sub>3</sub>) of 3.16**

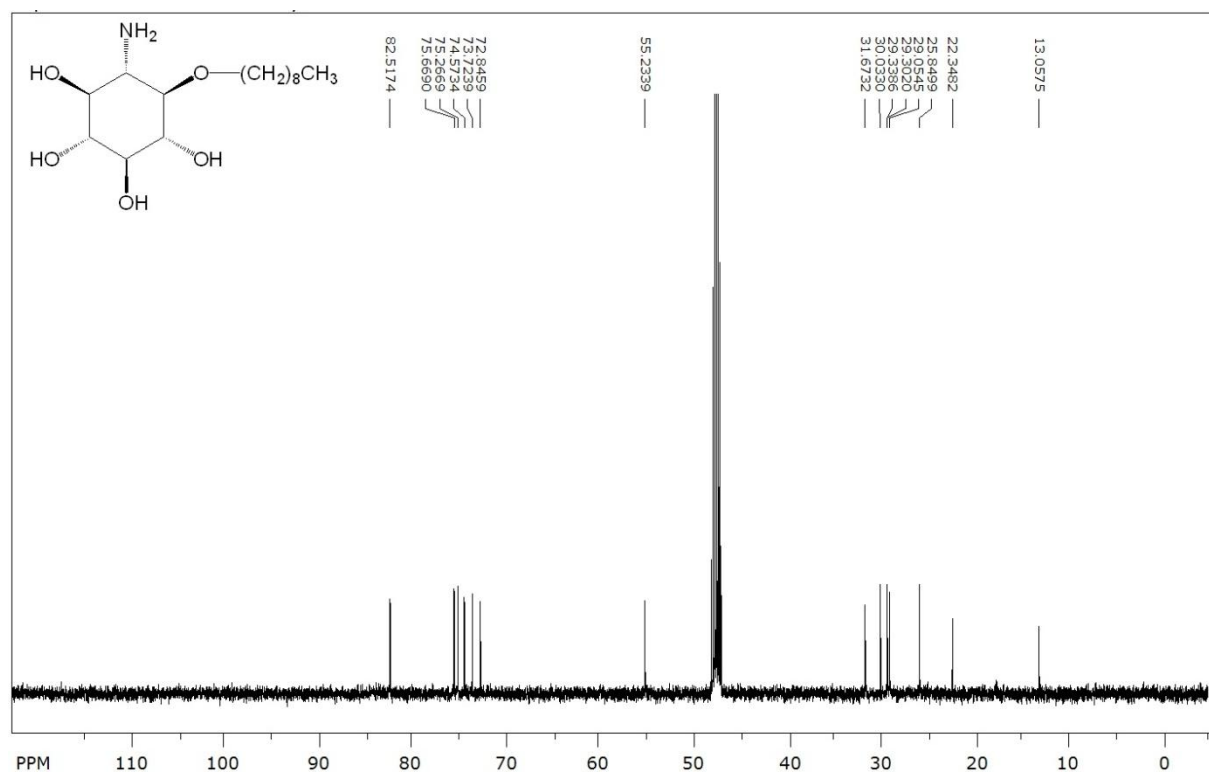




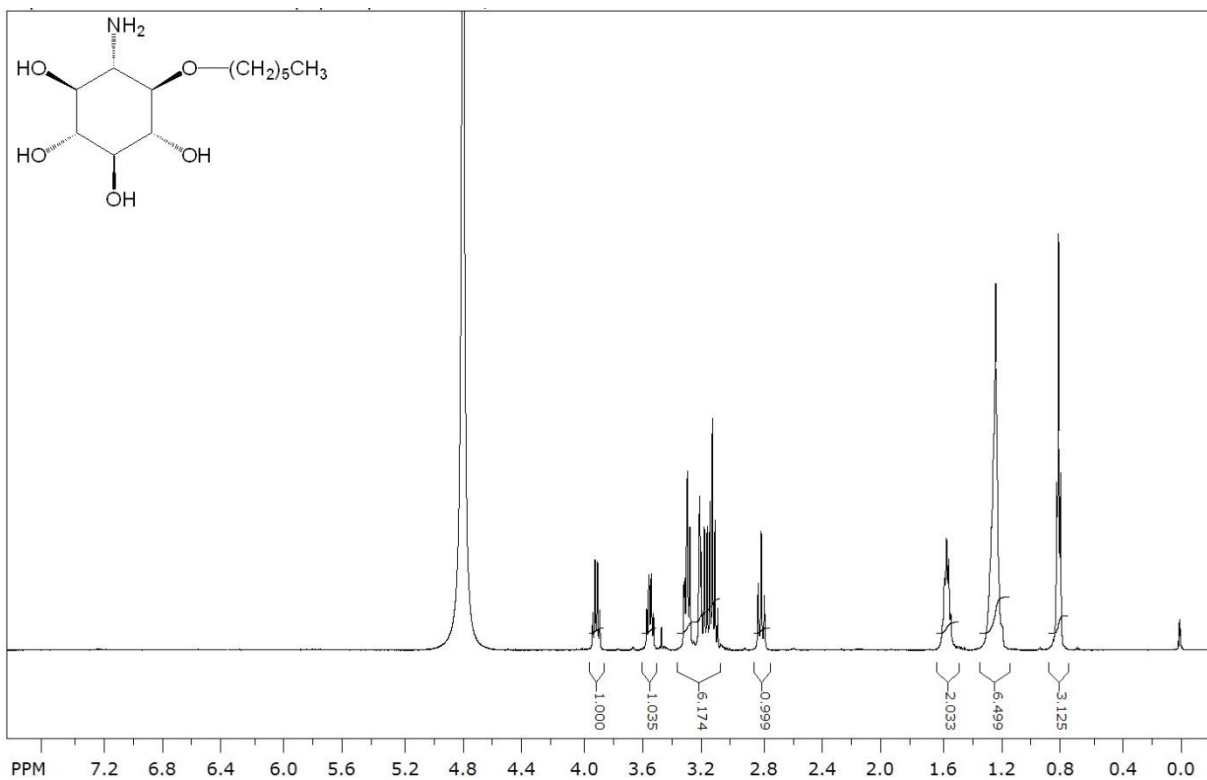
### <sup>1</sup>H NMR Spectrum (500 MHz, CD<sub>3</sub>OD) of 3.19



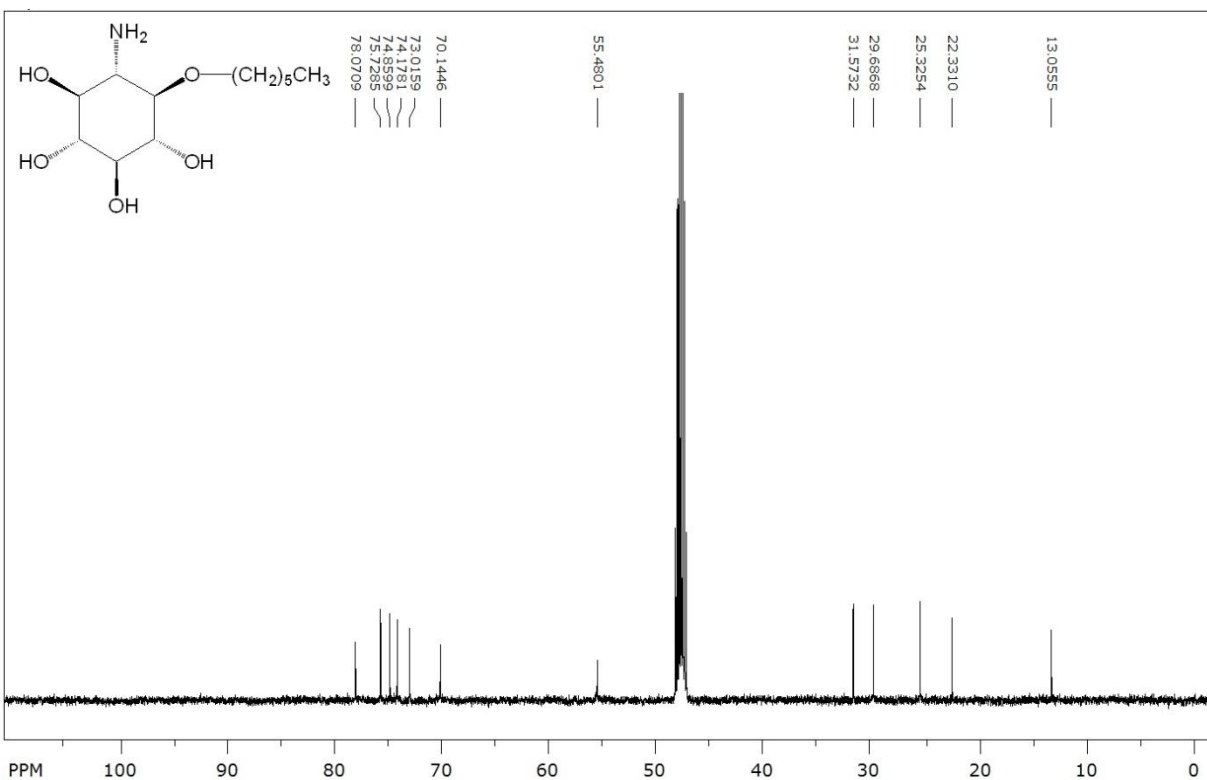
### <sup>13</sup>C NMR Spectrum (500 MHz, CD<sub>3</sub>OD) of 3.19



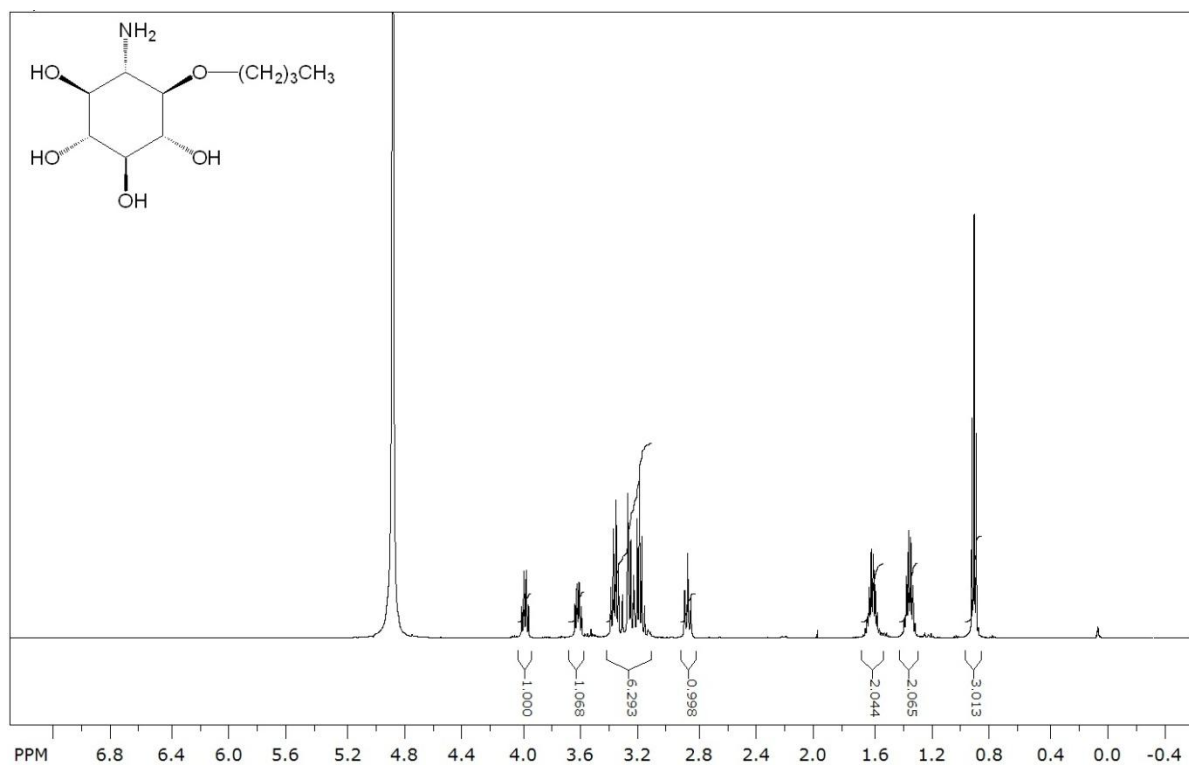
### <sup>1</sup>H NMR Spectrum (500 MHz, CD<sub>3</sub>OD) of 3.20



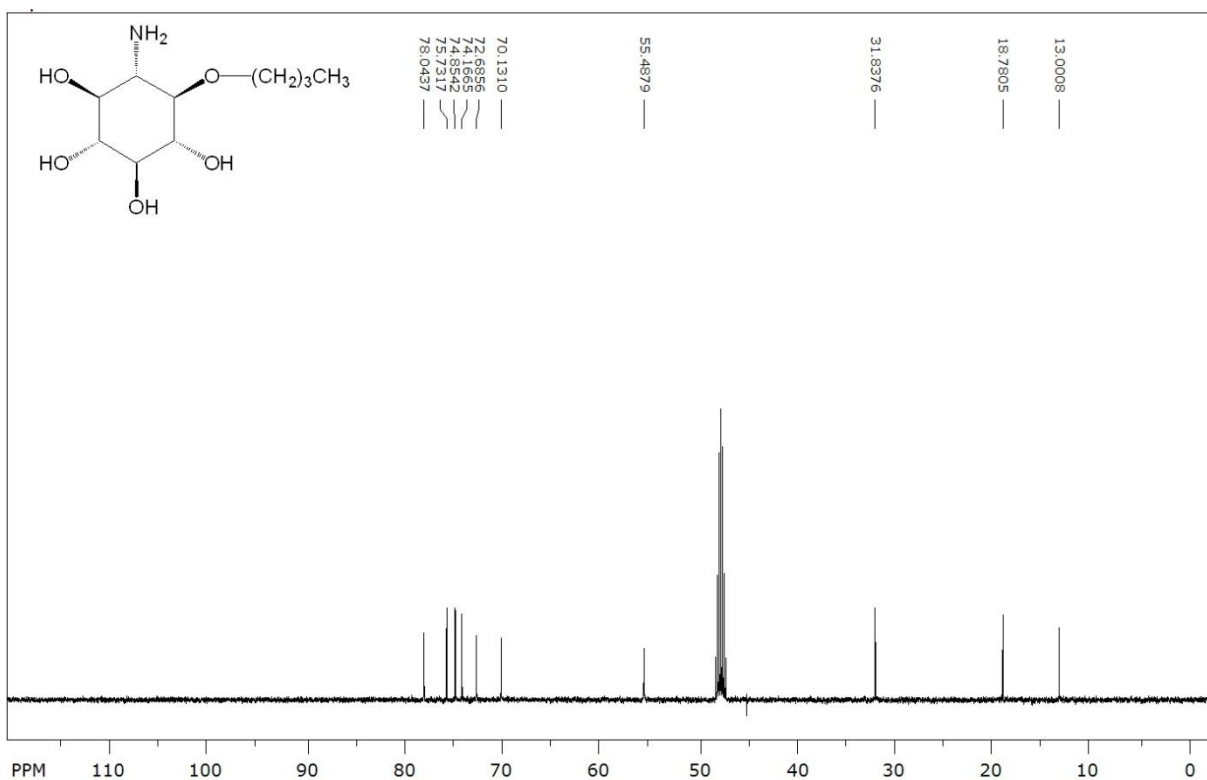
### <sup>13</sup>C NMR Spectrum (500 MHz, CD<sub>3</sub>OD) of 3.20



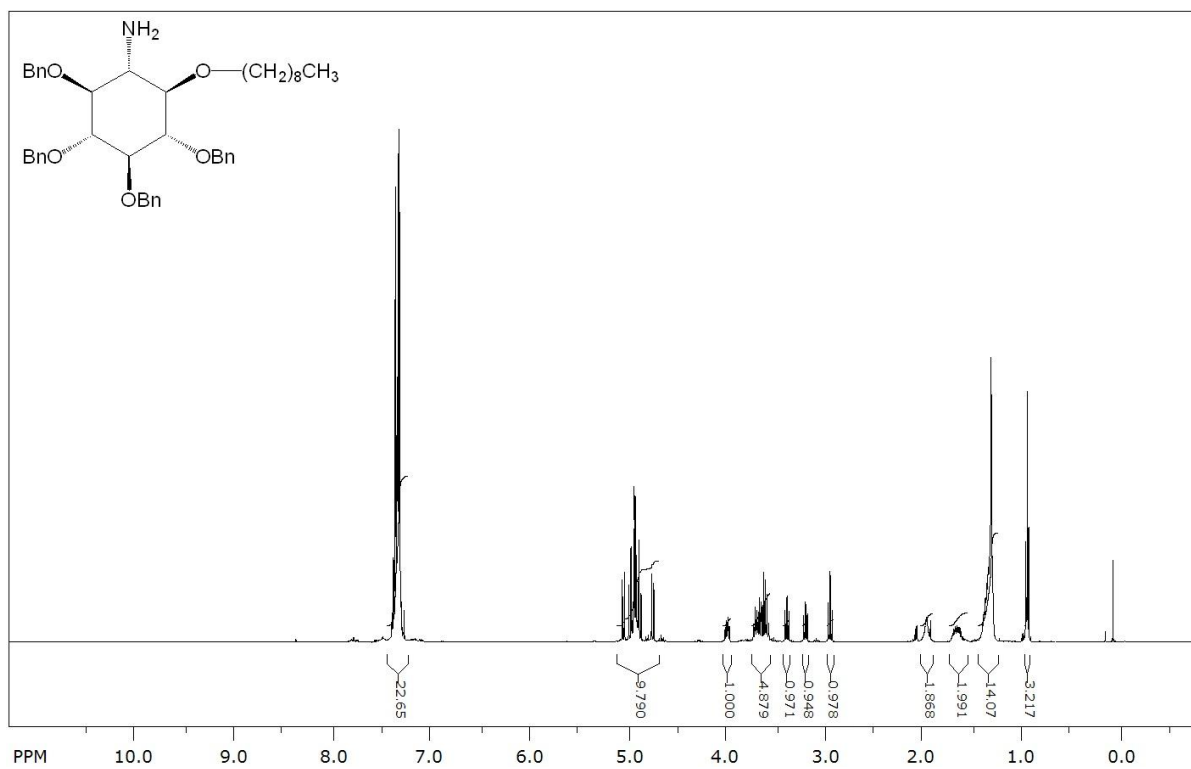
### <sup>1</sup>H NMR Spectrum (500 MHz, CD<sub>3</sub>OD) of 3.21



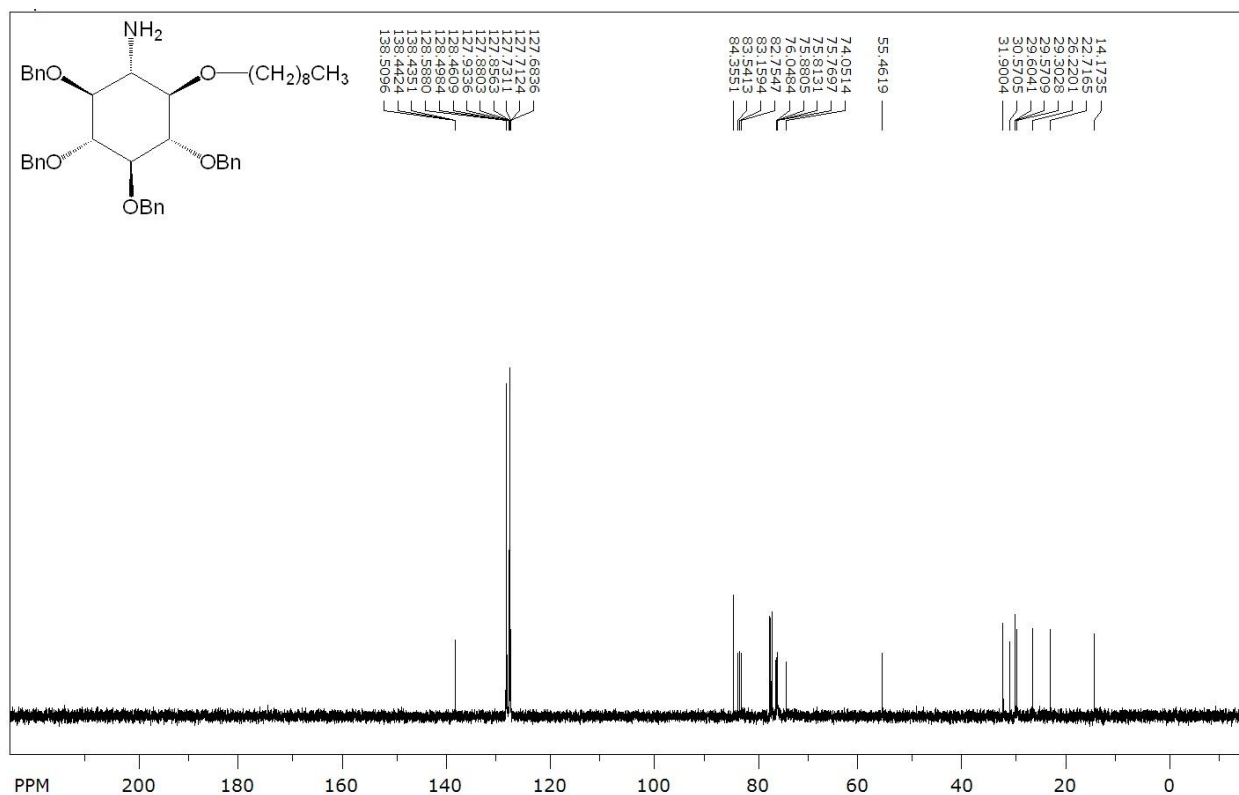
### <sup>13</sup>C NMR Spectrum (500 MHz, CD<sub>3</sub>OD) of 3.21



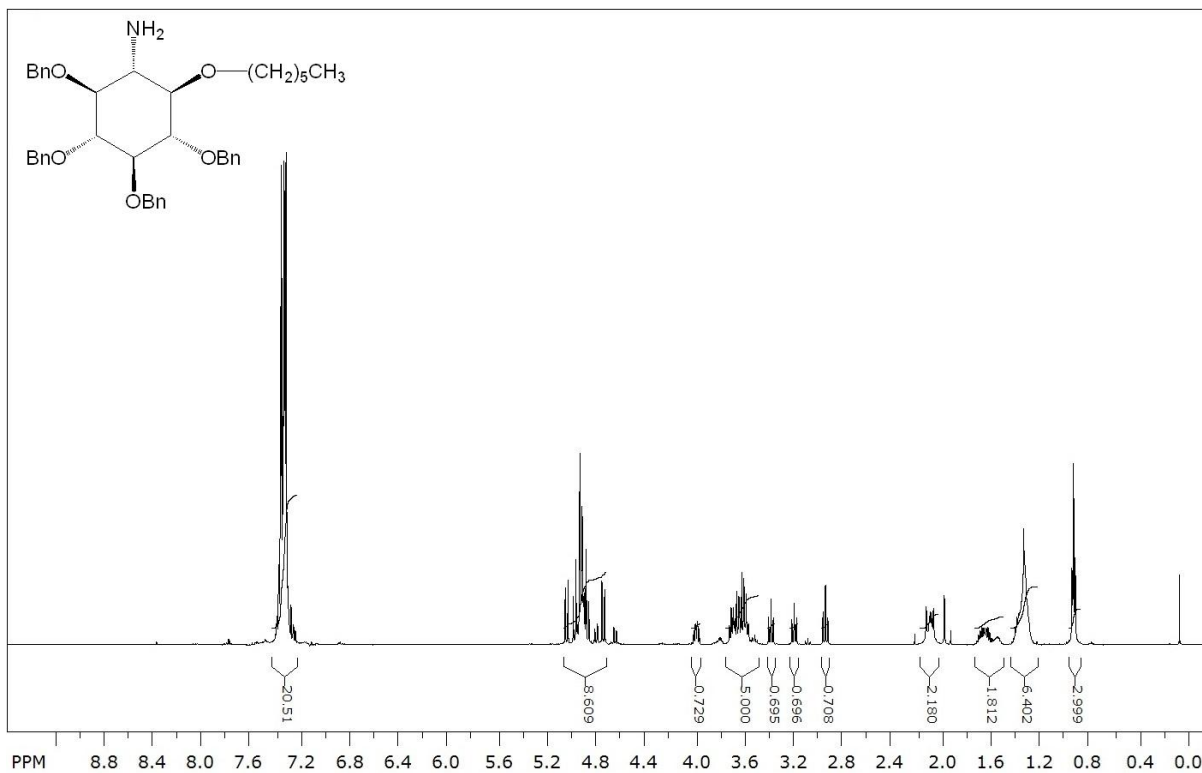
**<sup>1</sup>H NMR Spectrum (500 MHz, CDCl<sub>3</sub>) of 3.22**



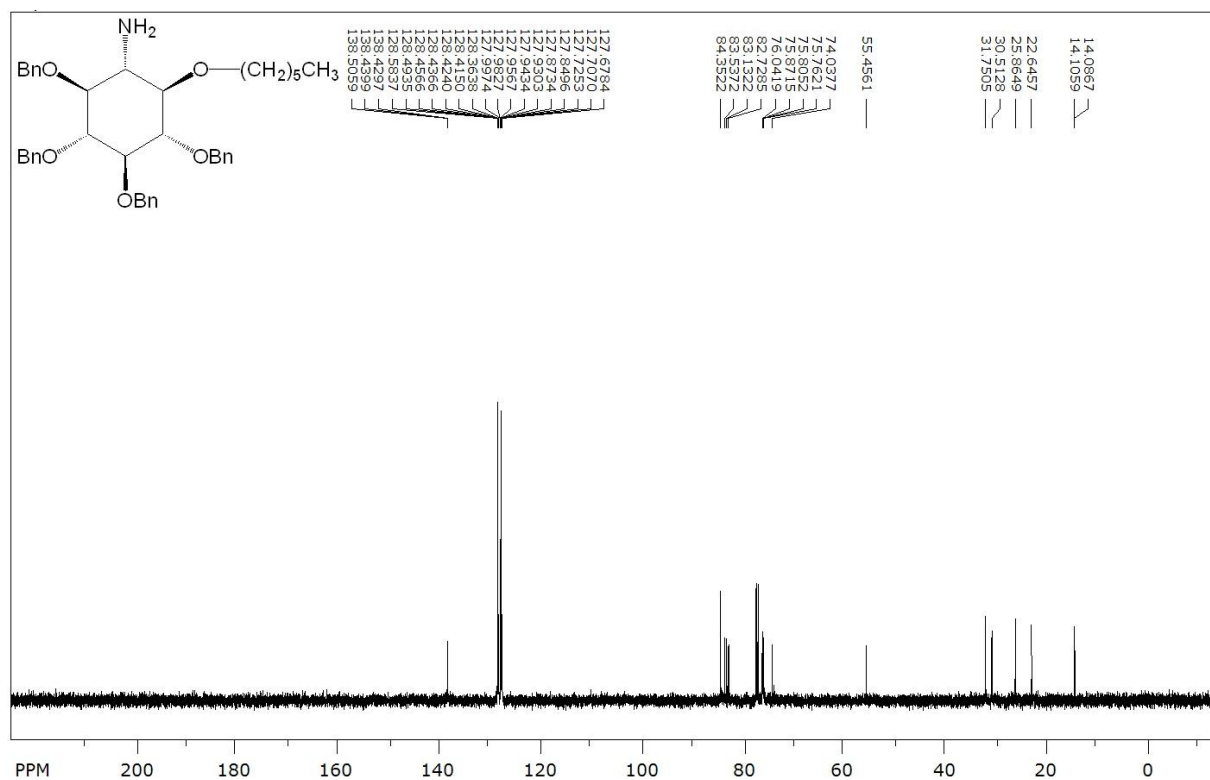
**<sup>13</sup>C NMR Spectrum (500 MHz, CDCl<sub>3</sub>) of 3.22**



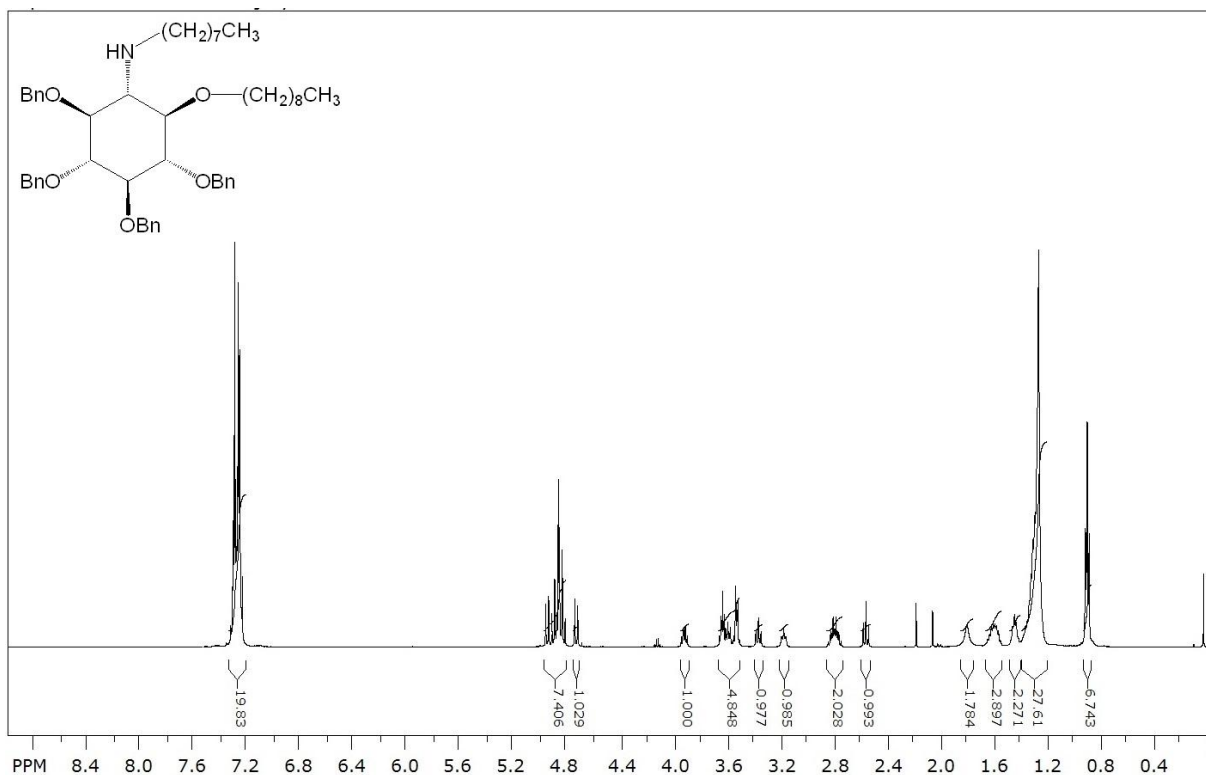
**<sup>1</sup>H NMR Spectrum (500 MHz, CDCl<sub>3</sub>) of 3.23**



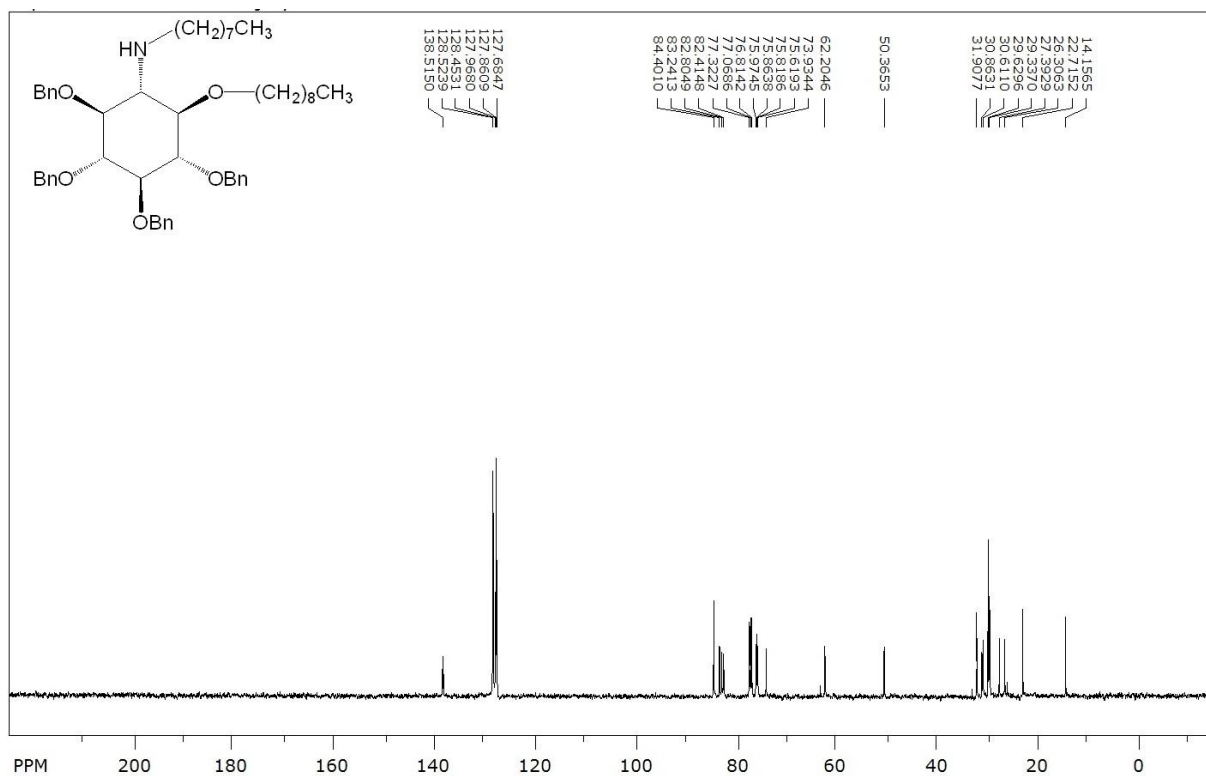
**<sup>13</sup>C NMR Spectrum (500 MHz, CDCl<sub>3</sub>) of 3.23**



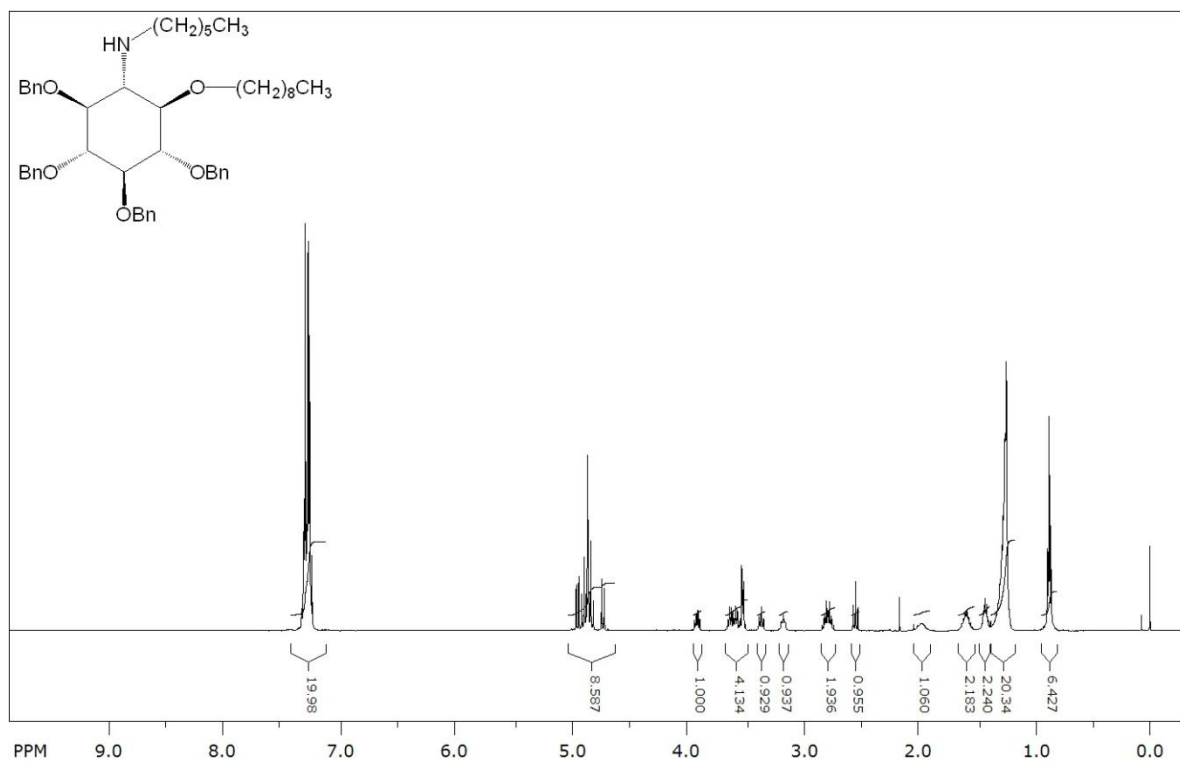
### <sup>1</sup>H NMR Spectrum (500 MHz, CDCl<sub>3</sub>) of 3.24



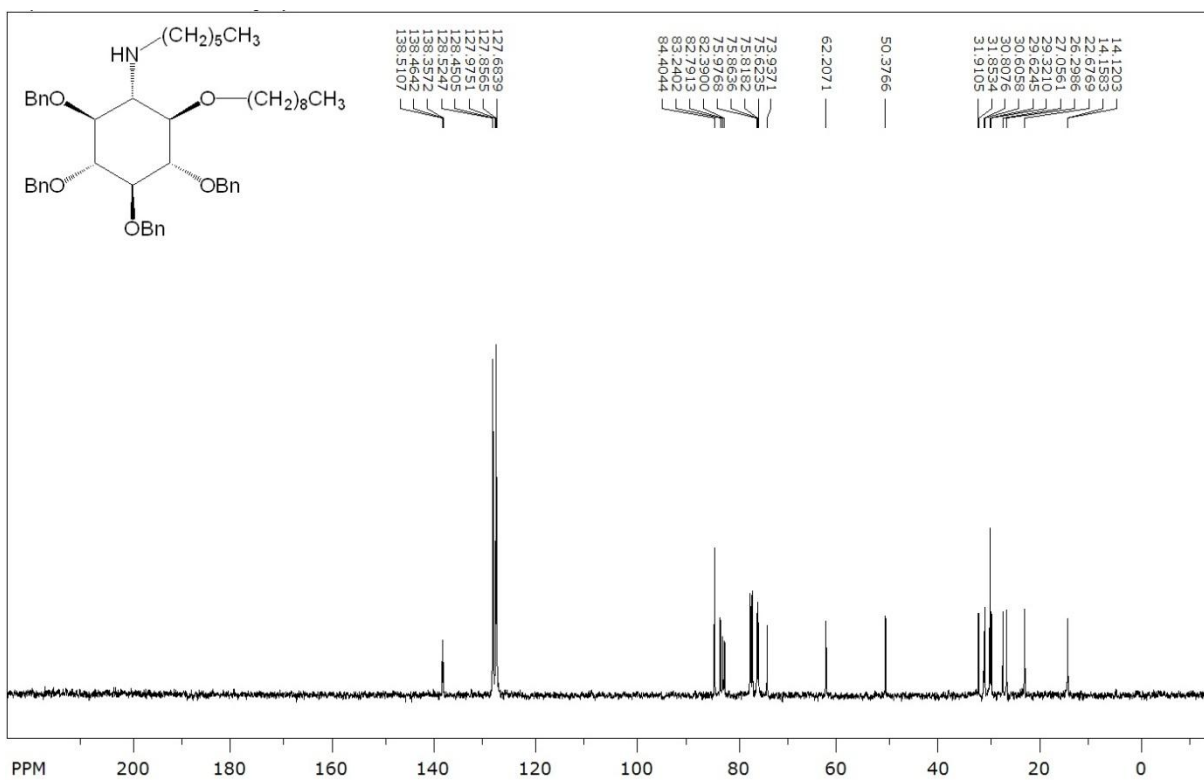
### <sup>13</sup>C NMR Spectrum (500 MHz, CDCl<sub>3</sub>) of 3.24



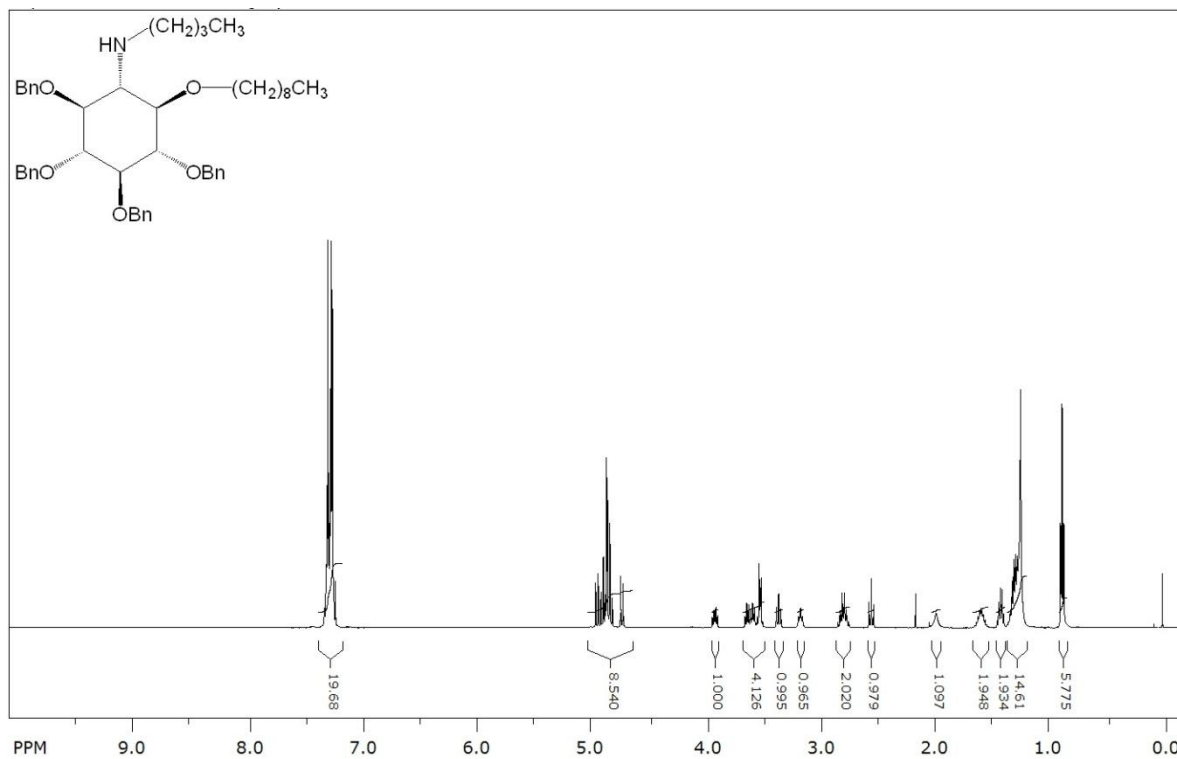
**<sup>1</sup>H NMR Spectrum (500 MHz, CDCl<sub>3</sub>) of 3.25**



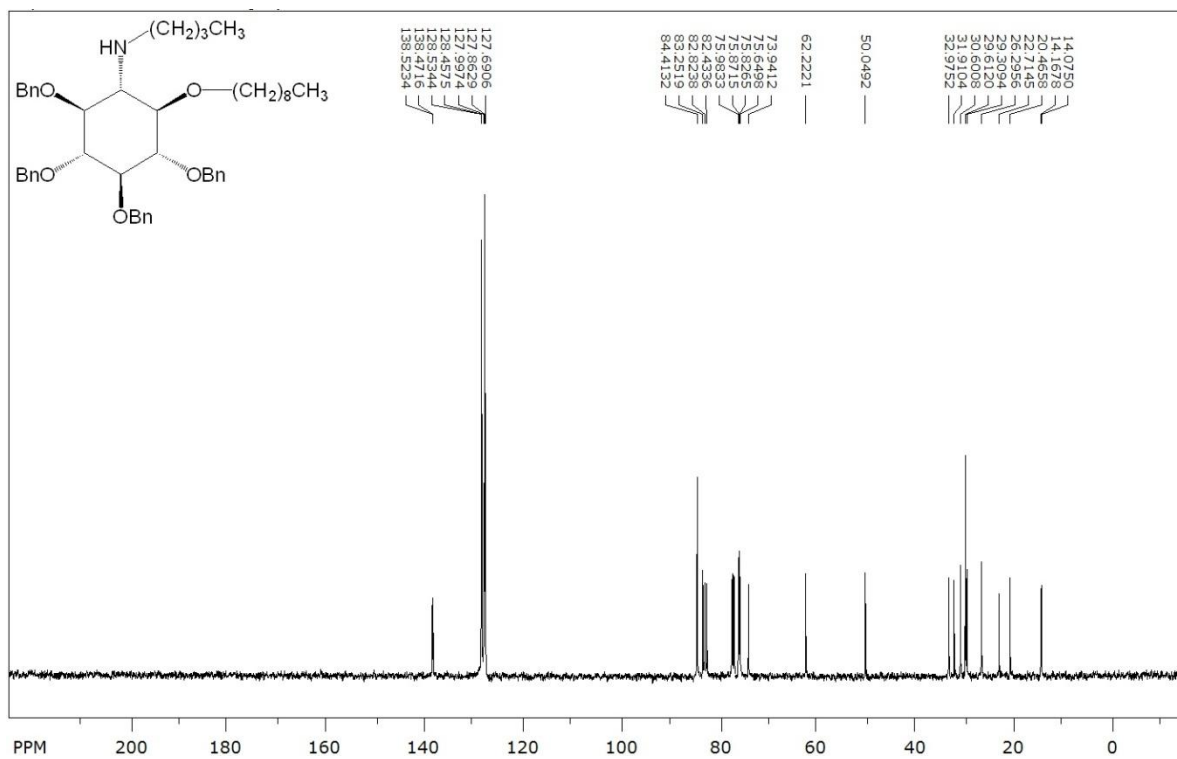
**<sup>13</sup>C NMR Spectrum (500 MHz, CDCl<sub>3</sub>) of 3.25**



**<sup>1</sup>H NMR Spectrum (500 MHz, CDCl<sub>3</sub>) of 3.26**

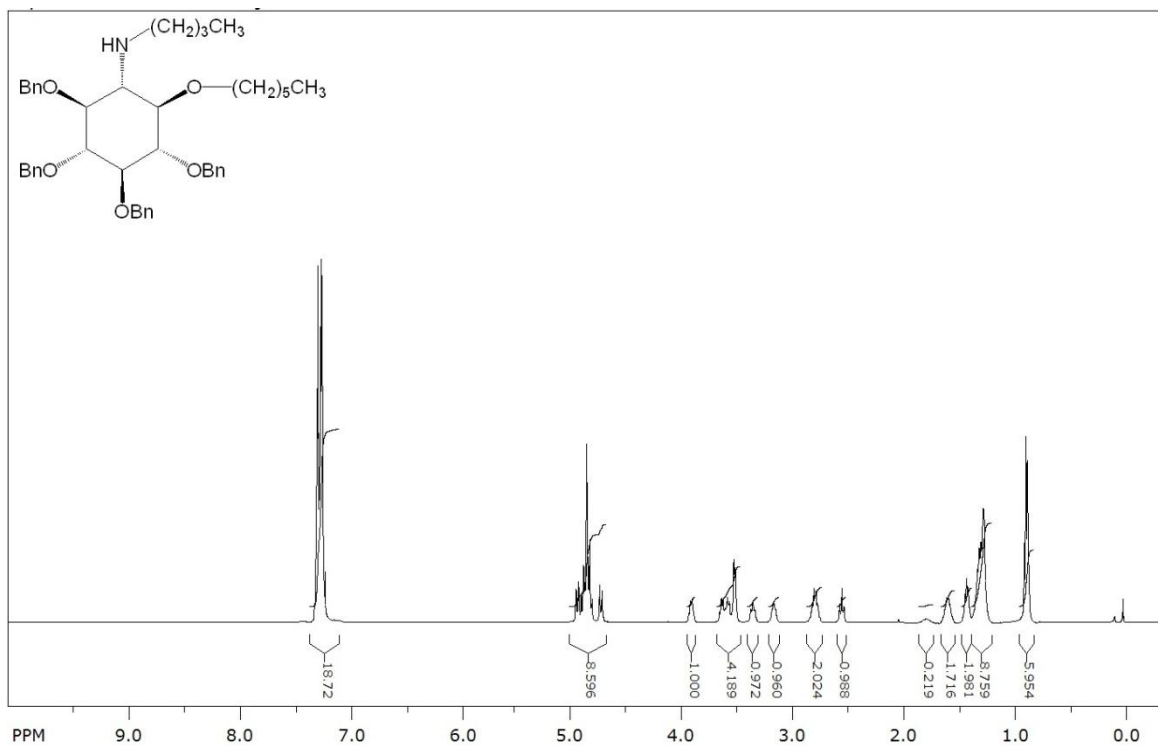


**<sup>13</sup>C NMR Spectrum (500 MHz, CDCl<sub>3</sub>) of 3.26**

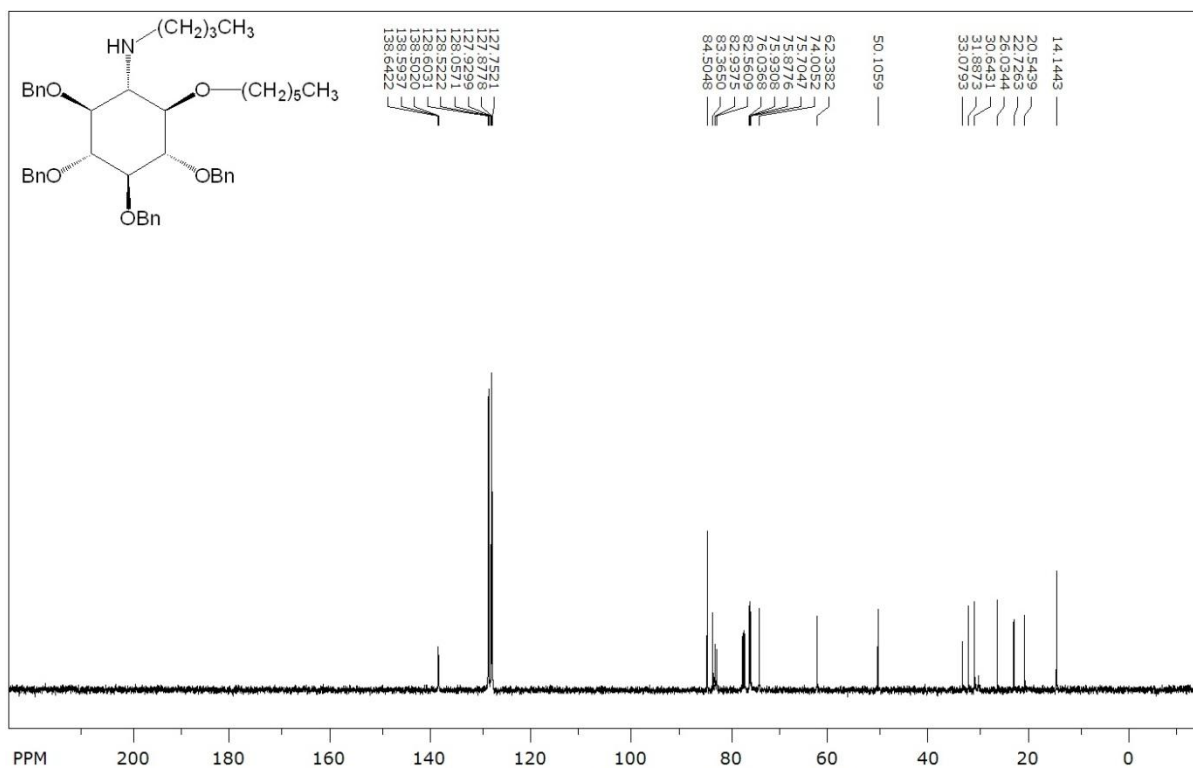




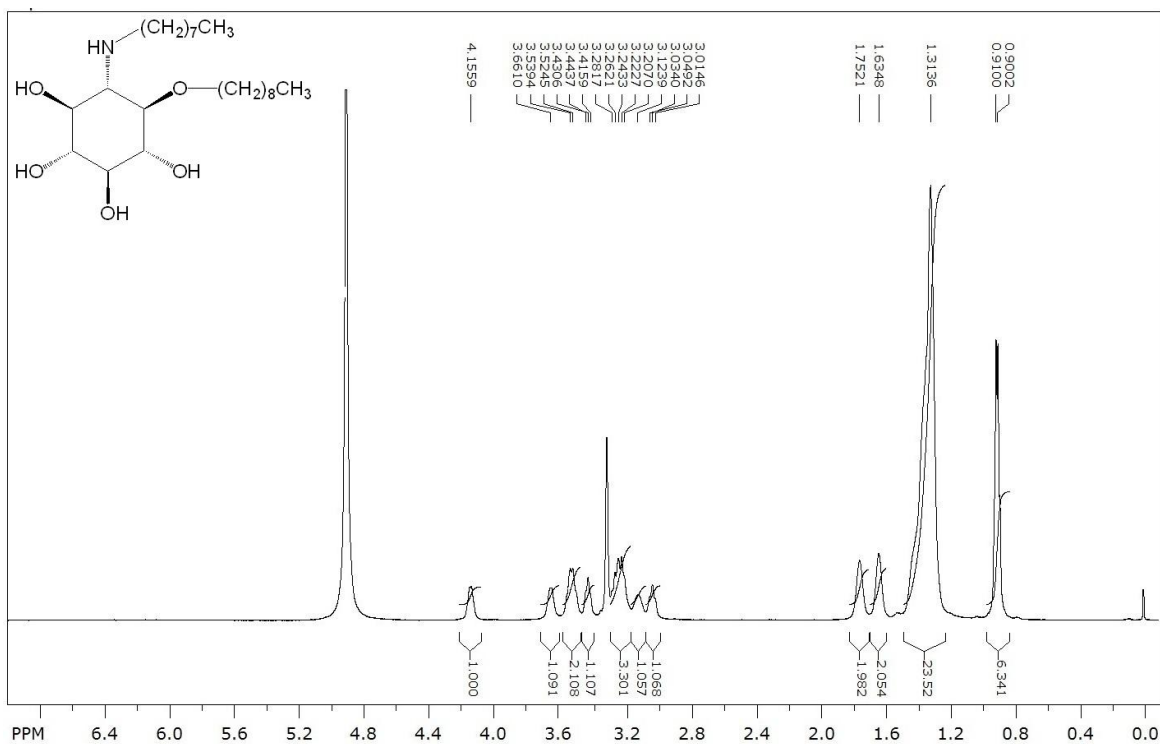
### <sup>1</sup>H NMR Spectrum (500 MHz, CDCl<sub>3</sub>) of 3.28



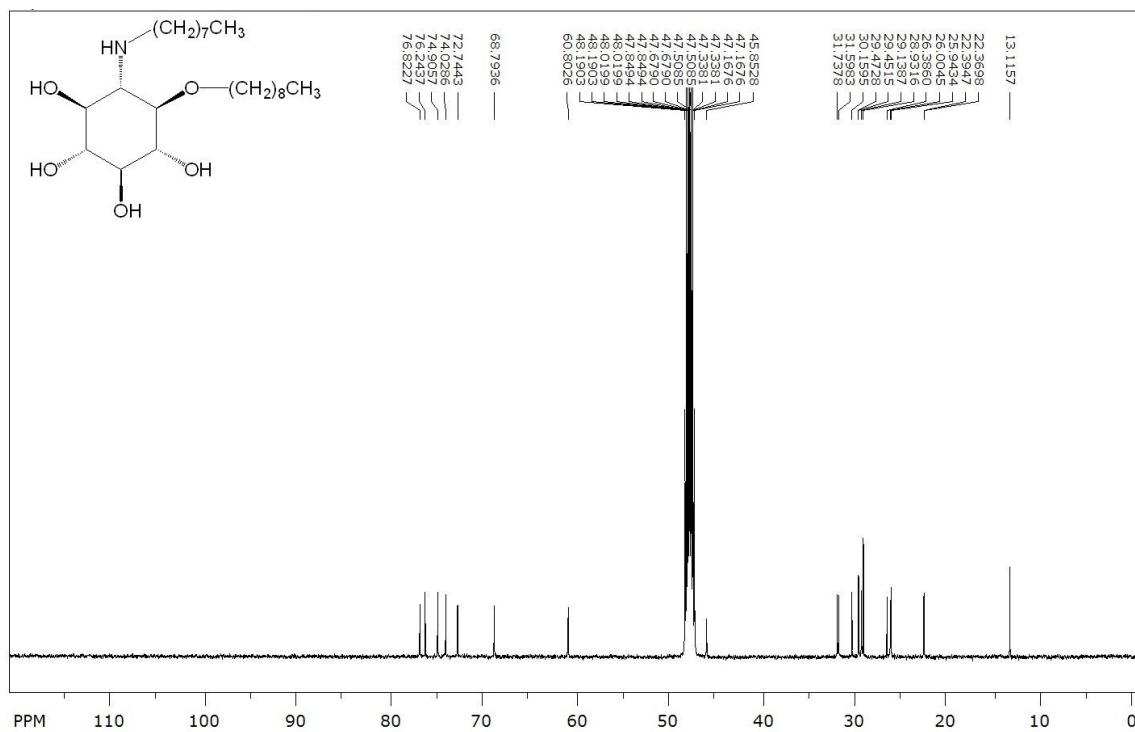
### <sup>13</sup>C NMR Spectrum (500 MHz, CDCl<sub>3</sub>) of 3.28



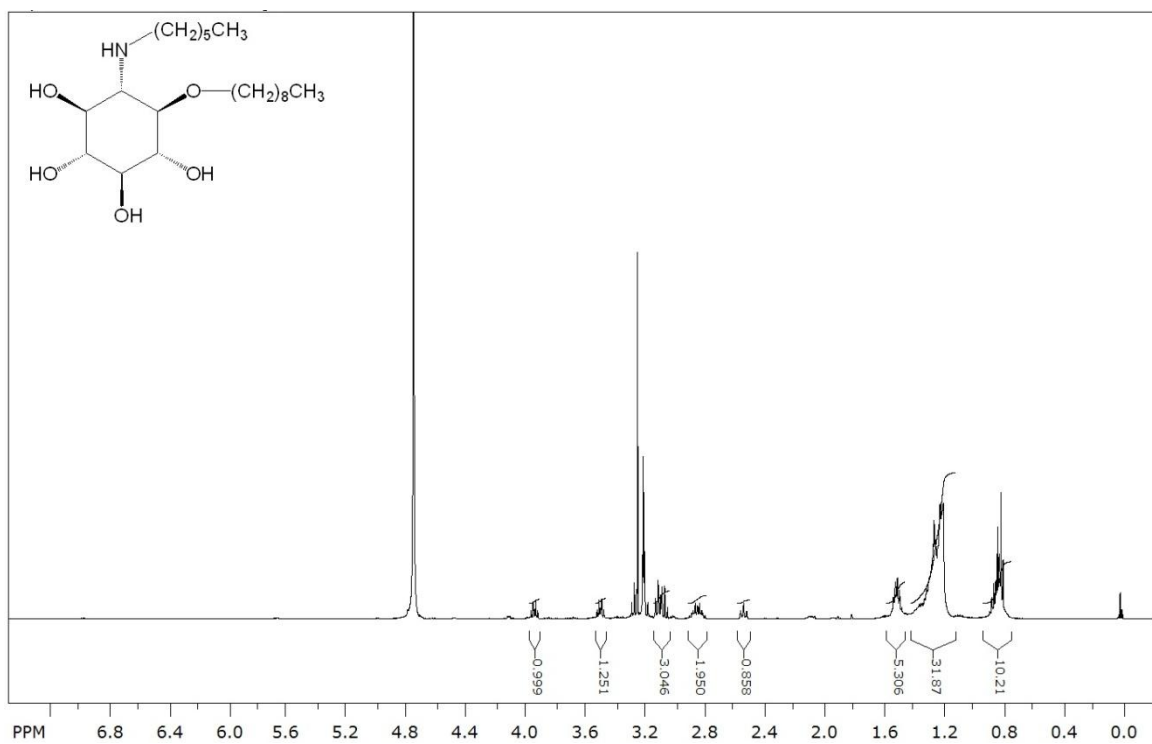
**<sup>1</sup>H NMR Spectrum (500 MHz, CD<sub>3</sub>OD) of 3.29**



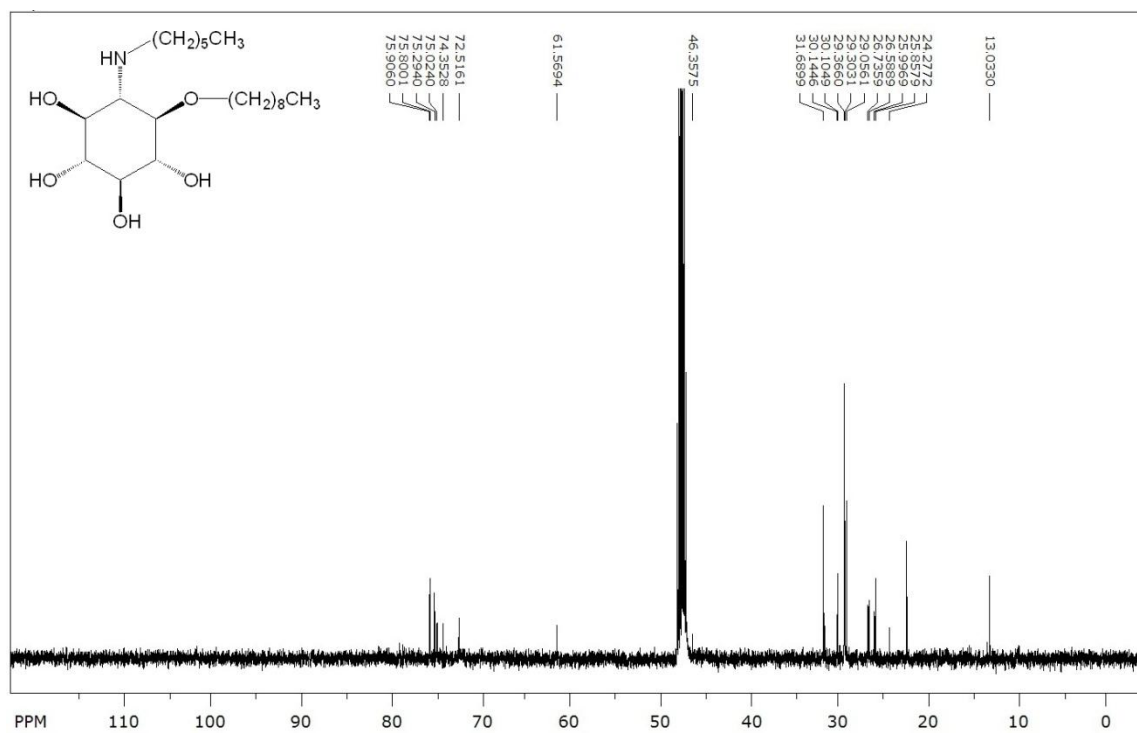
**<sup>13</sup>C NMR Spectrum (500 MHz, CD<sub>3</sub>OD) of 3.29**



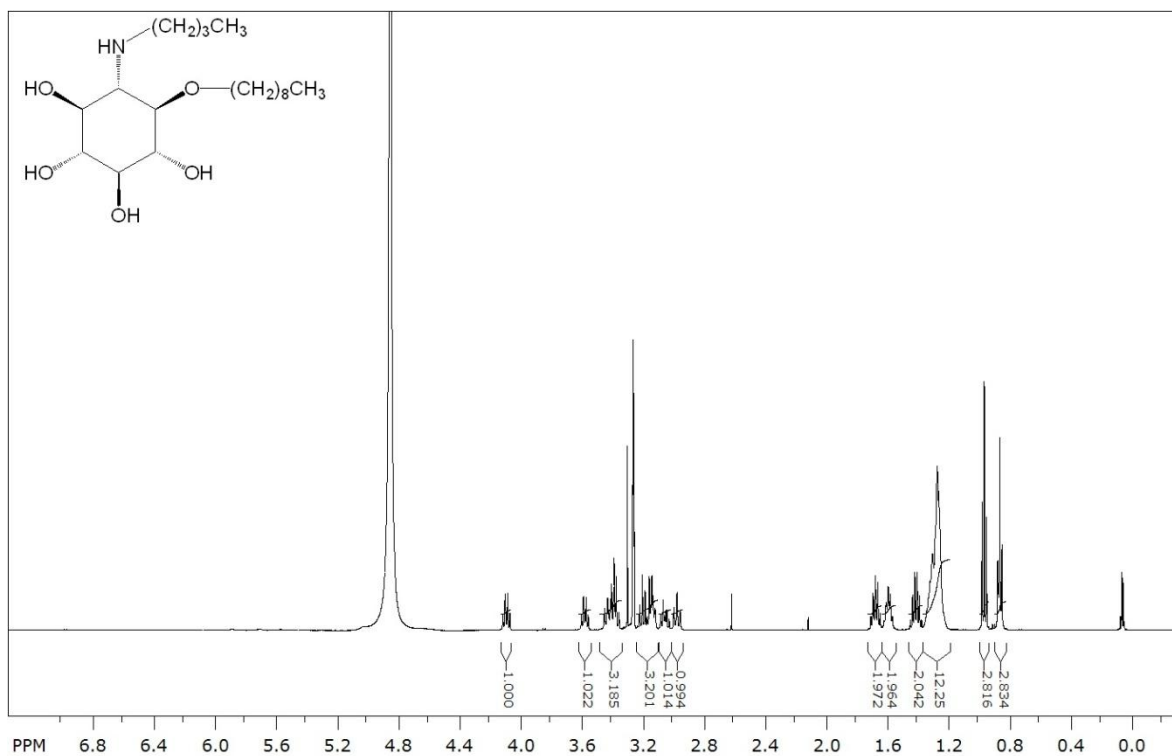
<sup>1</sup>H NMR Spectrum (500 MHz, CD<sub>3</sub>OD) of **3.30**



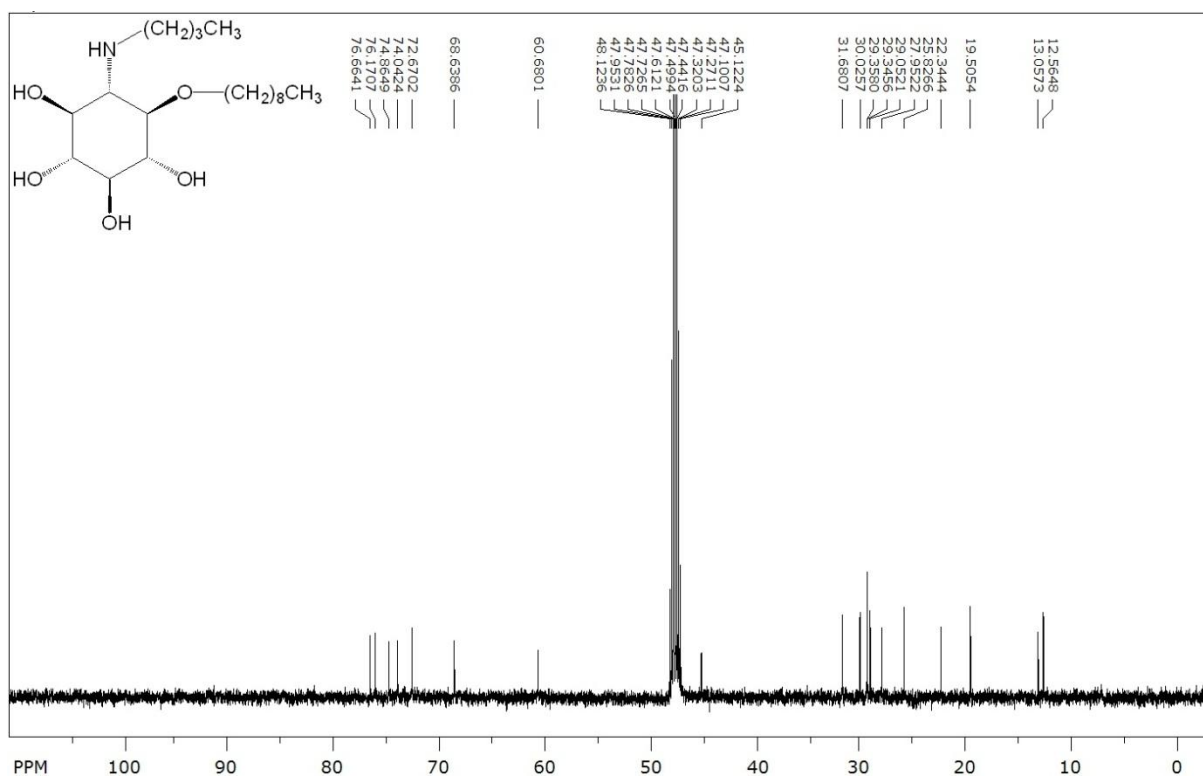
<sup>13</sup>C NMR Spectrum (500 MHz, CD<sub>3</sub>OD) of **3.30**



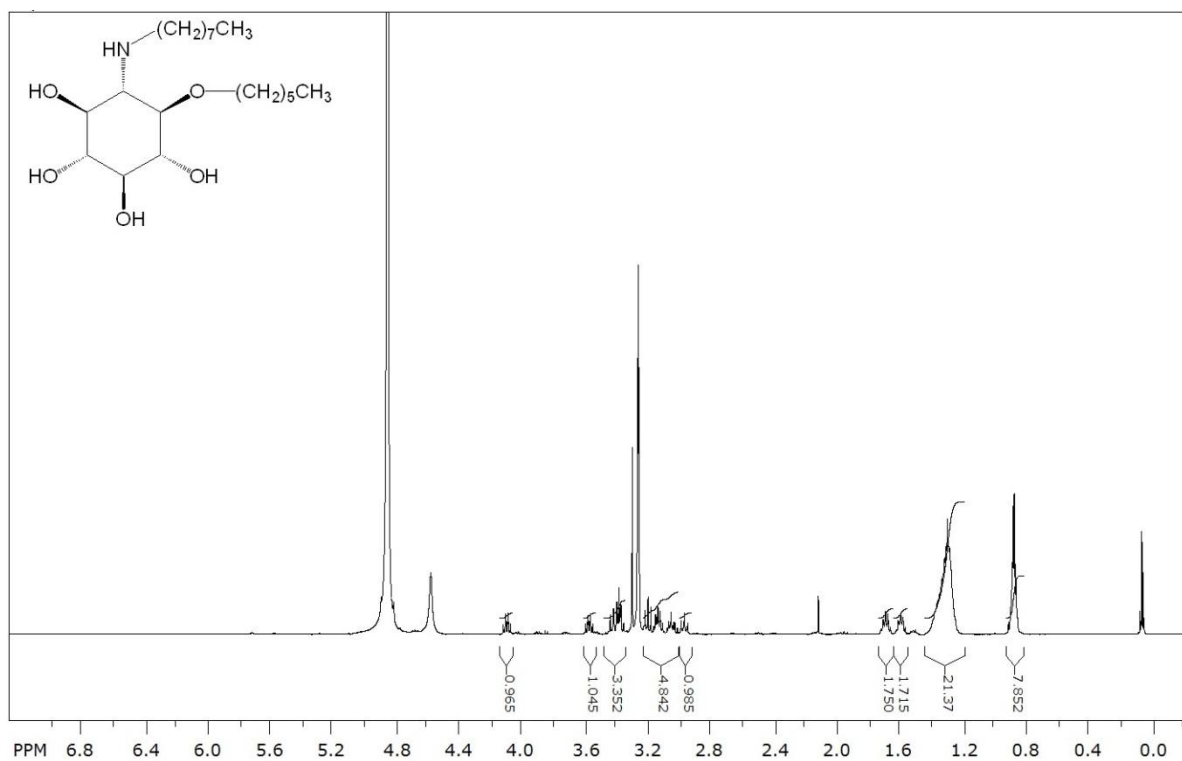
### <sup>1</sup>H NMR Spectrum (500 MHz, CD<sub>3</sub>OD) of 3.31



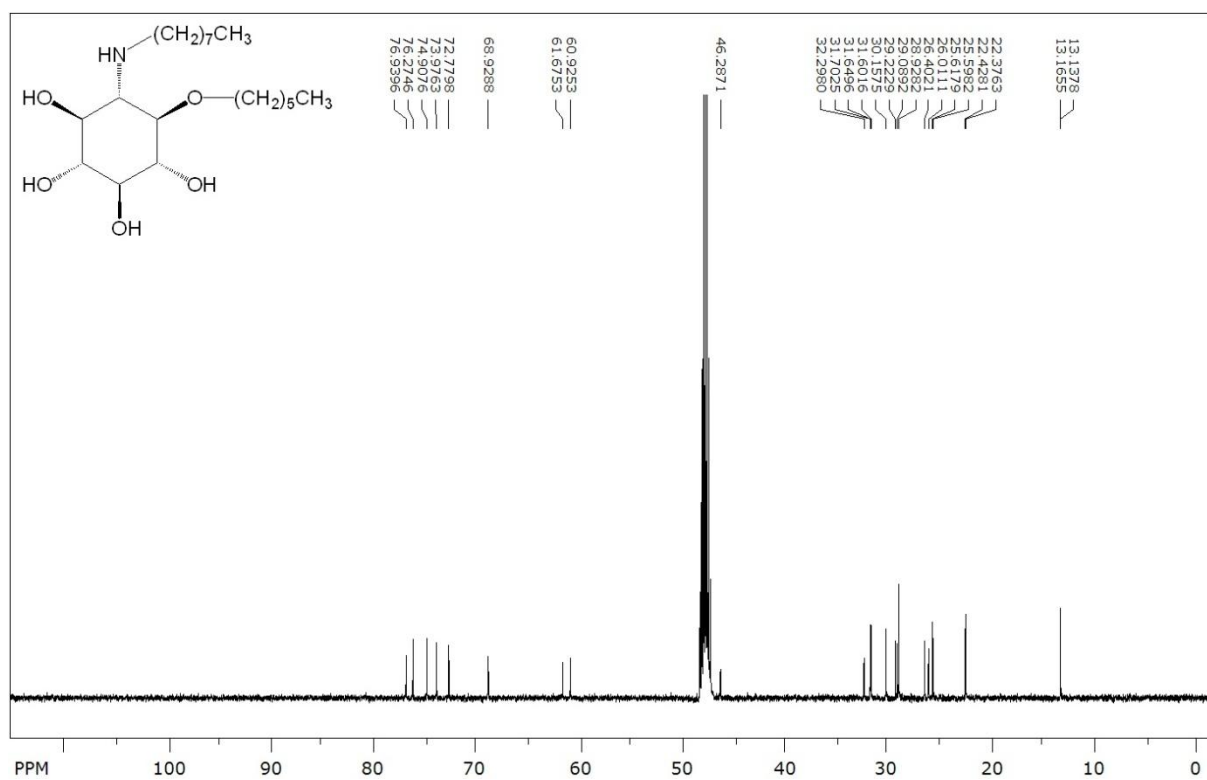
### <sup>13</sup>C NMR Spectrum (500 MHz, CD<sub>3</sub>OD) of 3.31



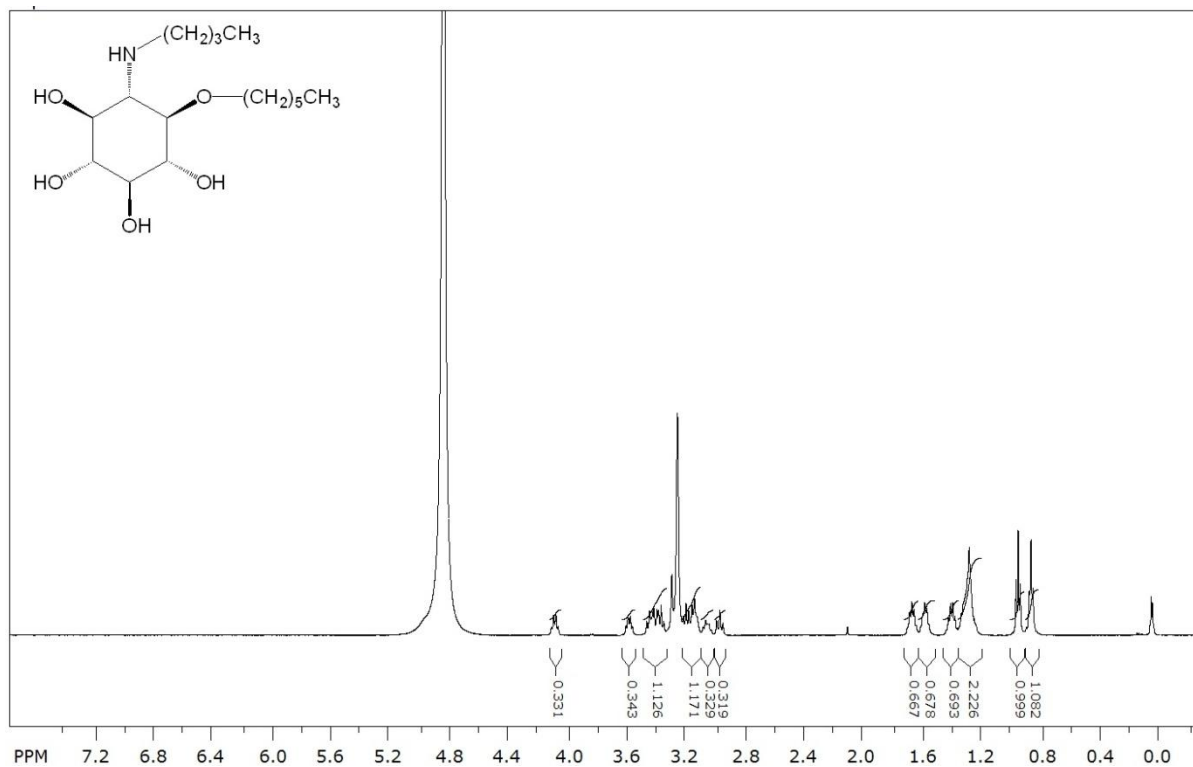
### <sup>1</sup>H NMR Spectrum (500 MHz, CD<sub>3</sub>OD) of 3.32



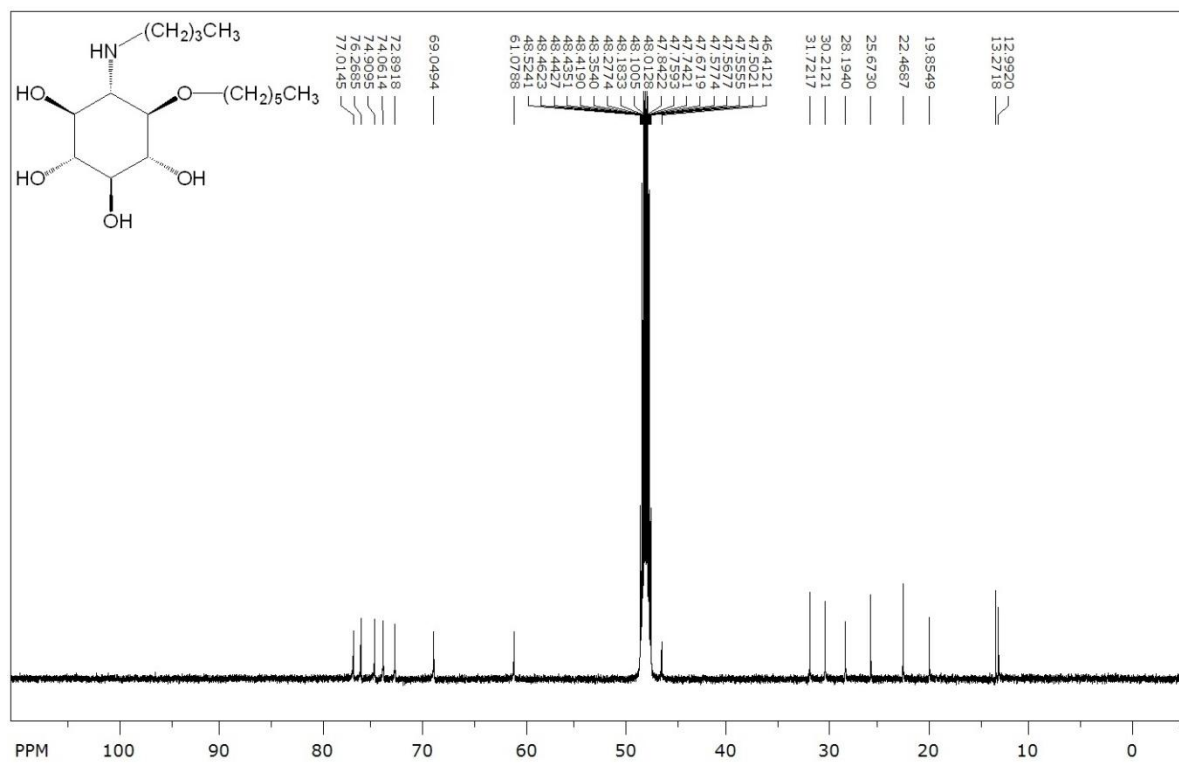
### <sup>13</sup>C NMR Spectrum (500 MHz, CD<sub>3</sub>OD) of 3.32



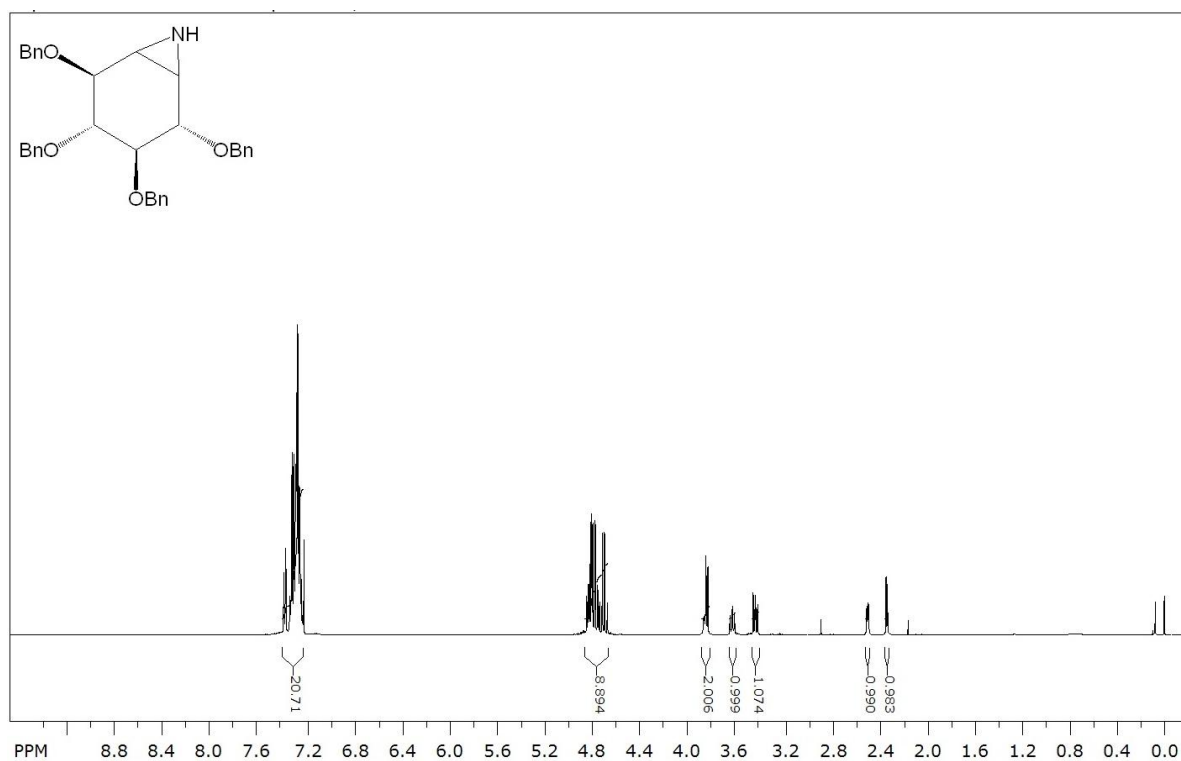
### <sup>1</sup>H NMR Spectrum (500 MHz, CD<sub>3</sub>OD) of 3.33



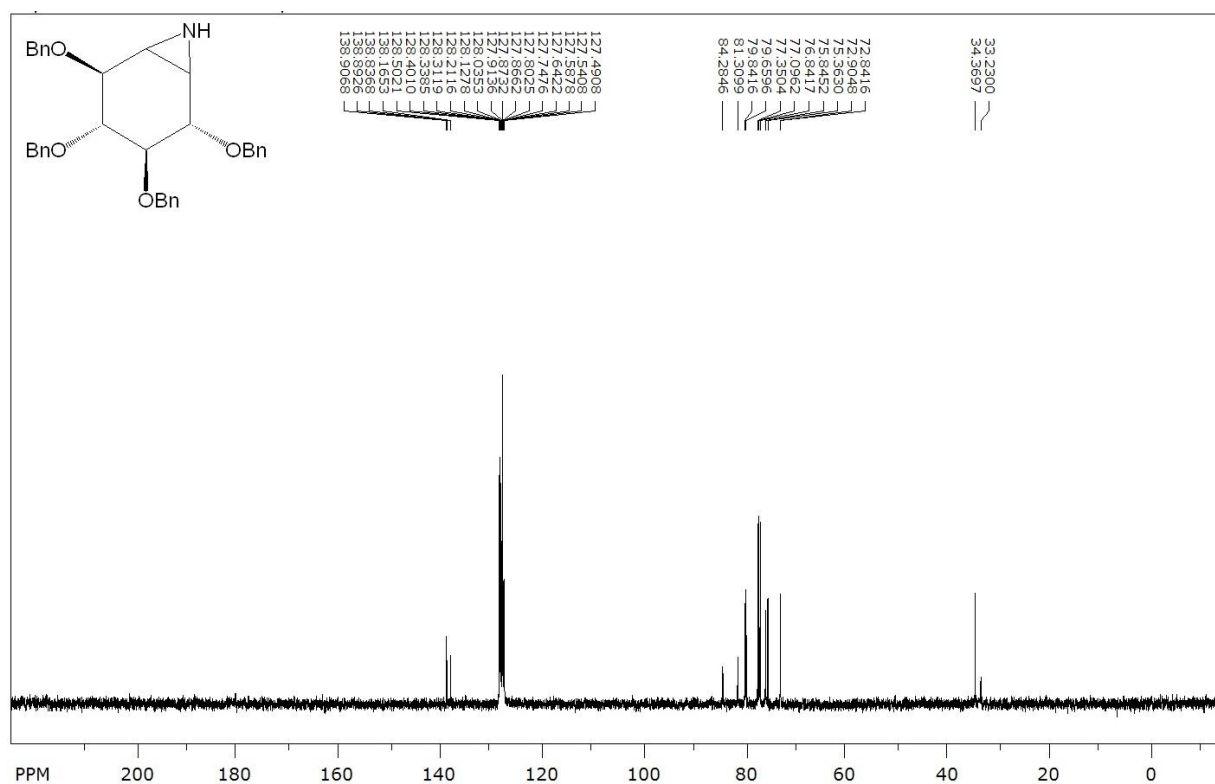
### <sup>13</sup>C NMR Spectrum (500 MHz, CD<sub>3</sub>OD) of 3.33



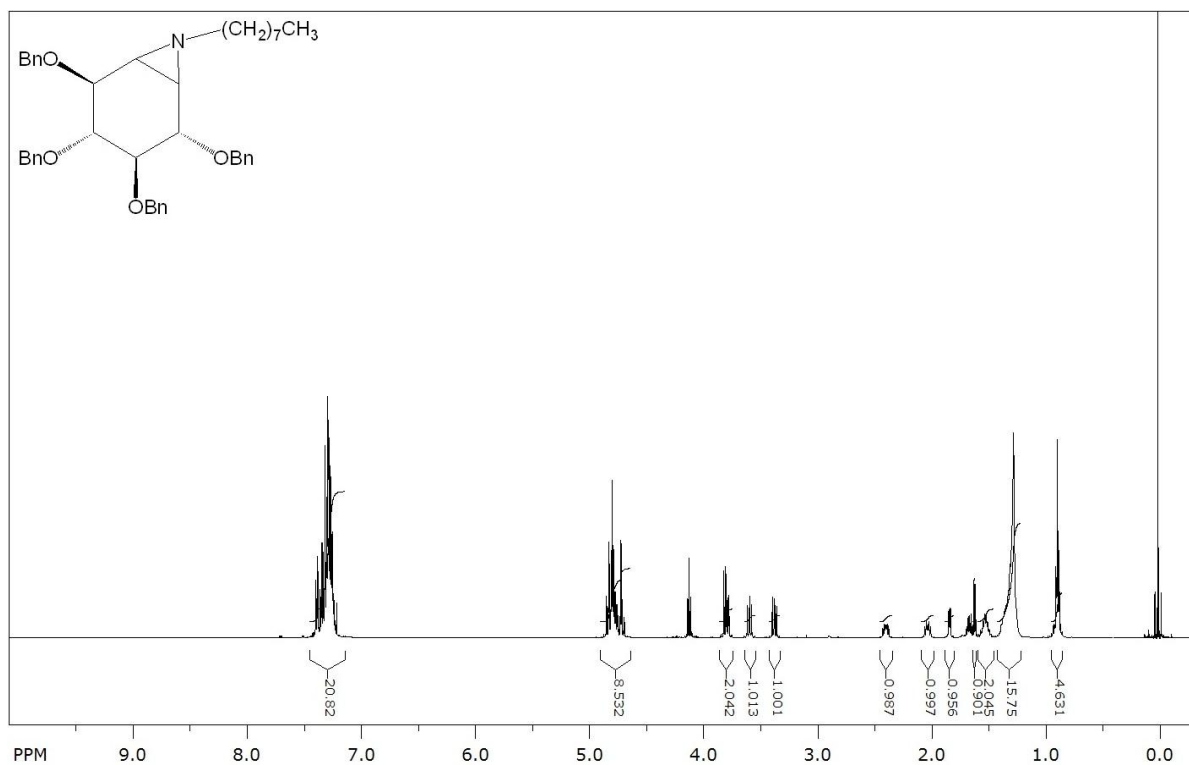
### <sup>1</sup>H NMR Spectrum (500 MHz, D<sub>2</sub>O) of 3.35



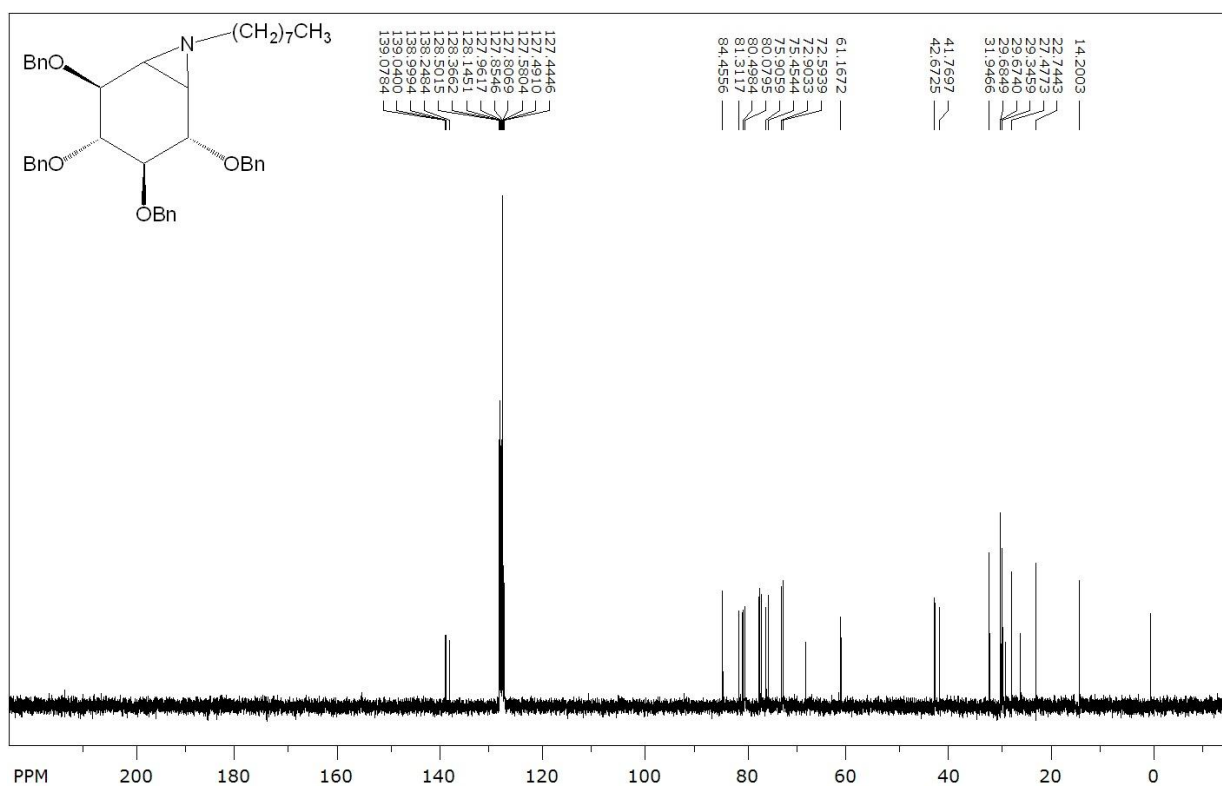
### <sup>13</sup>C NMR Spectrum (500 MHz, D<sub>2</sub>O) of 3.35



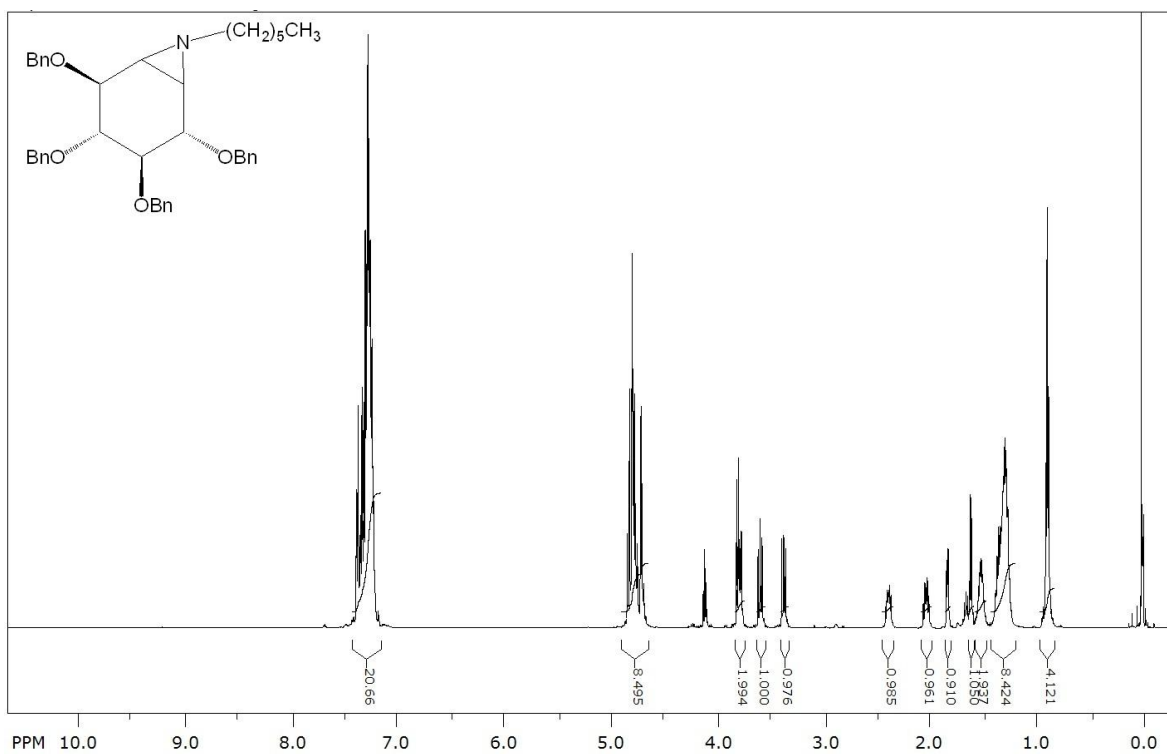
**<sup>1</sup>H NMR Spectrum (500 MHz, CDCl<sub>3</sub>) of 3.36**



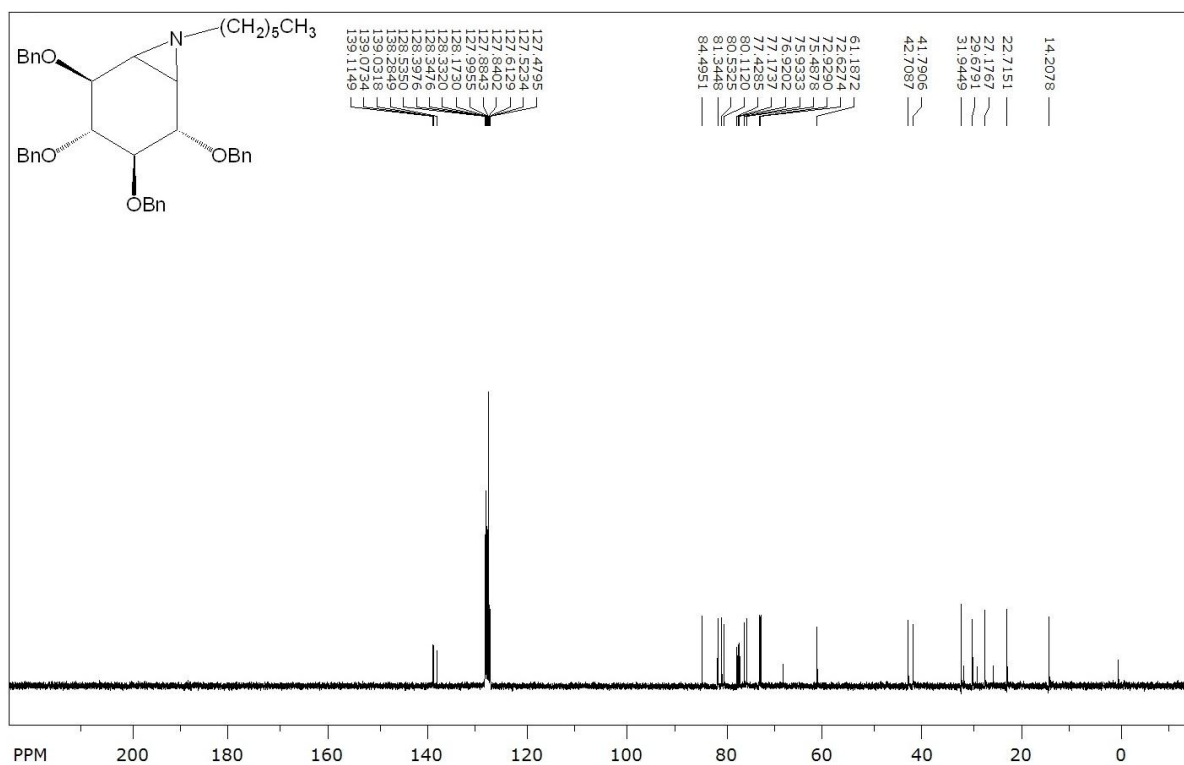
**<sup>13</sup>C NMR Spectrum (500 MHz, CDCl<sub>3</sub>) of 3.36**



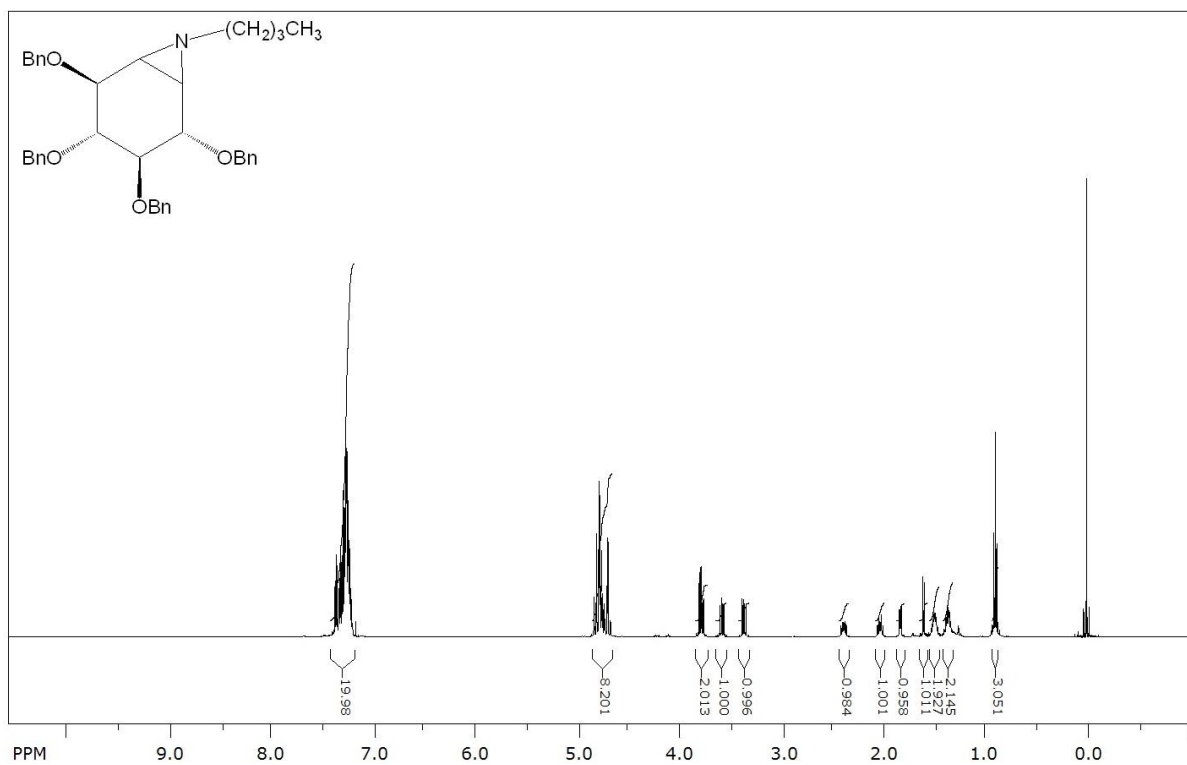
**<sup>1</sup>H NMR Spectrum (500 MHz, CDCl<sub>3</sub>) of 3.37**



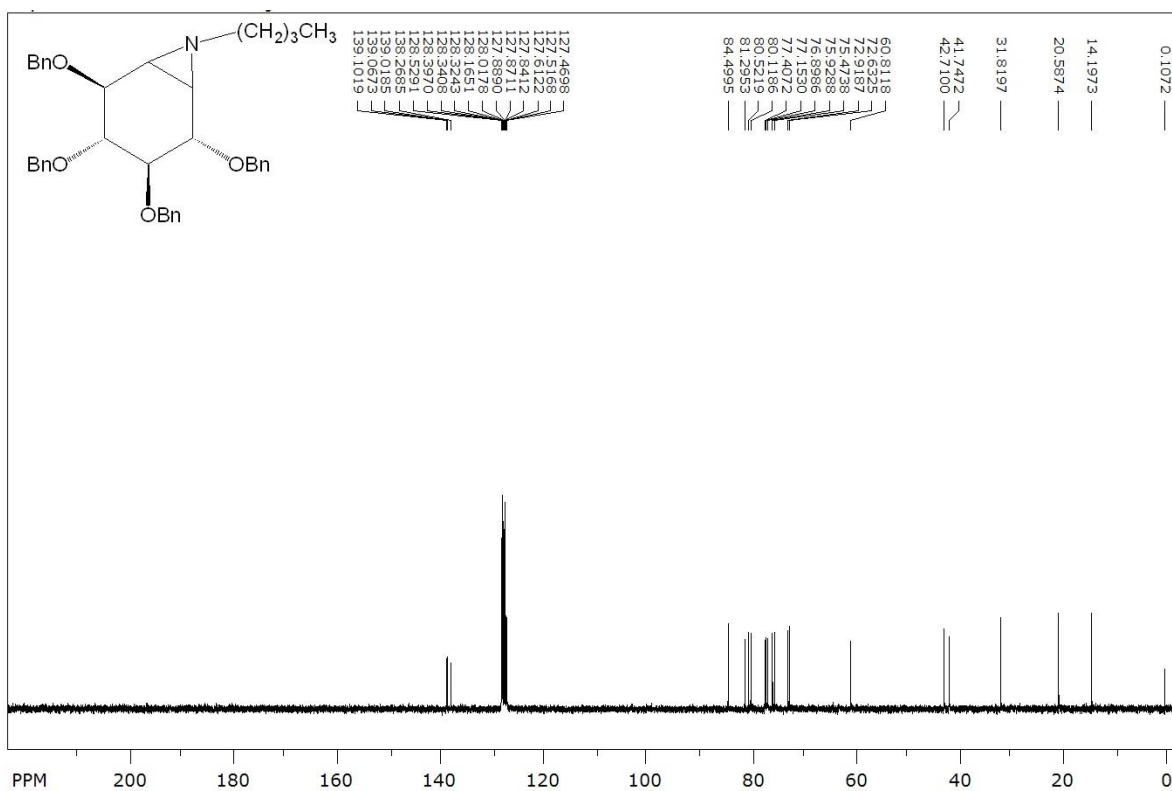
**<sup>13</sup>C NMR Spectrum (500 MHz, CDCl<sub>3</sub>) of 3.37**



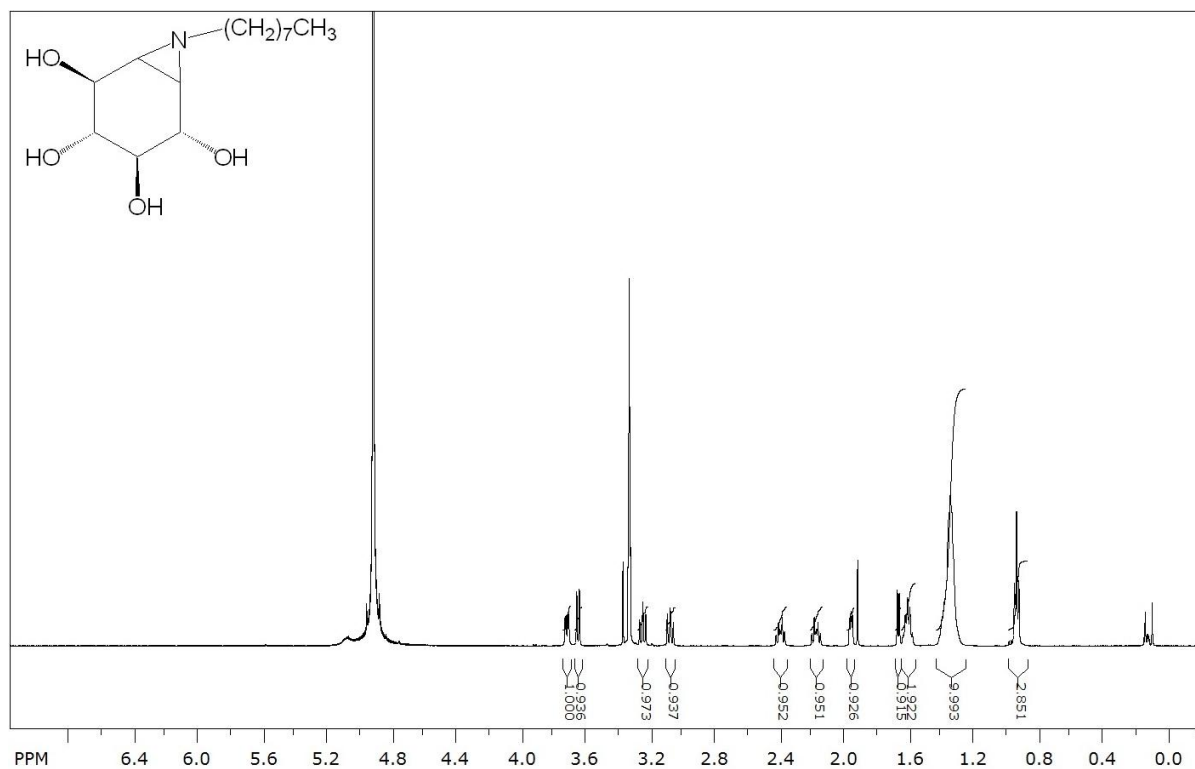
### <sup>1</sup>H NMR Spectrum (500 MHz, CDCl<sub>3</sub>) of 3.38



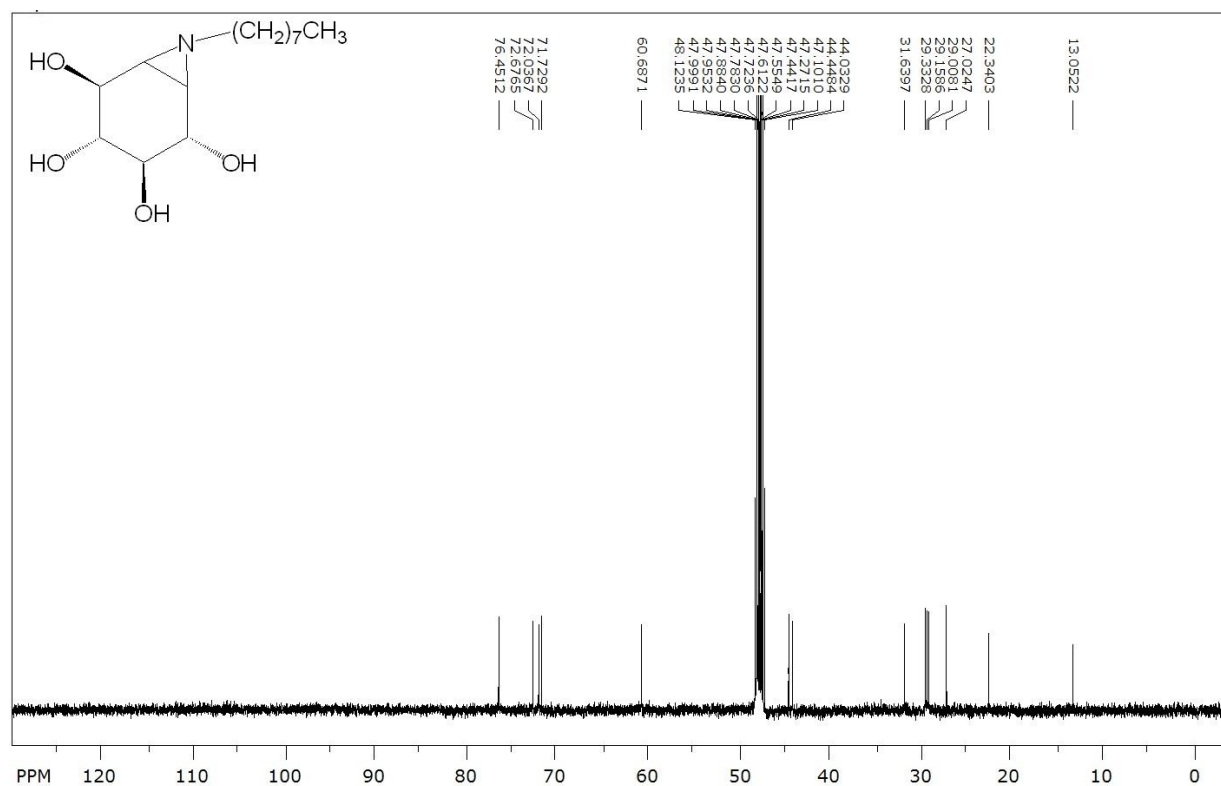
### <sup>13</sup>C NMR Spectrum (500 MHz, CDCl<sub>3</sub>) of 3.38



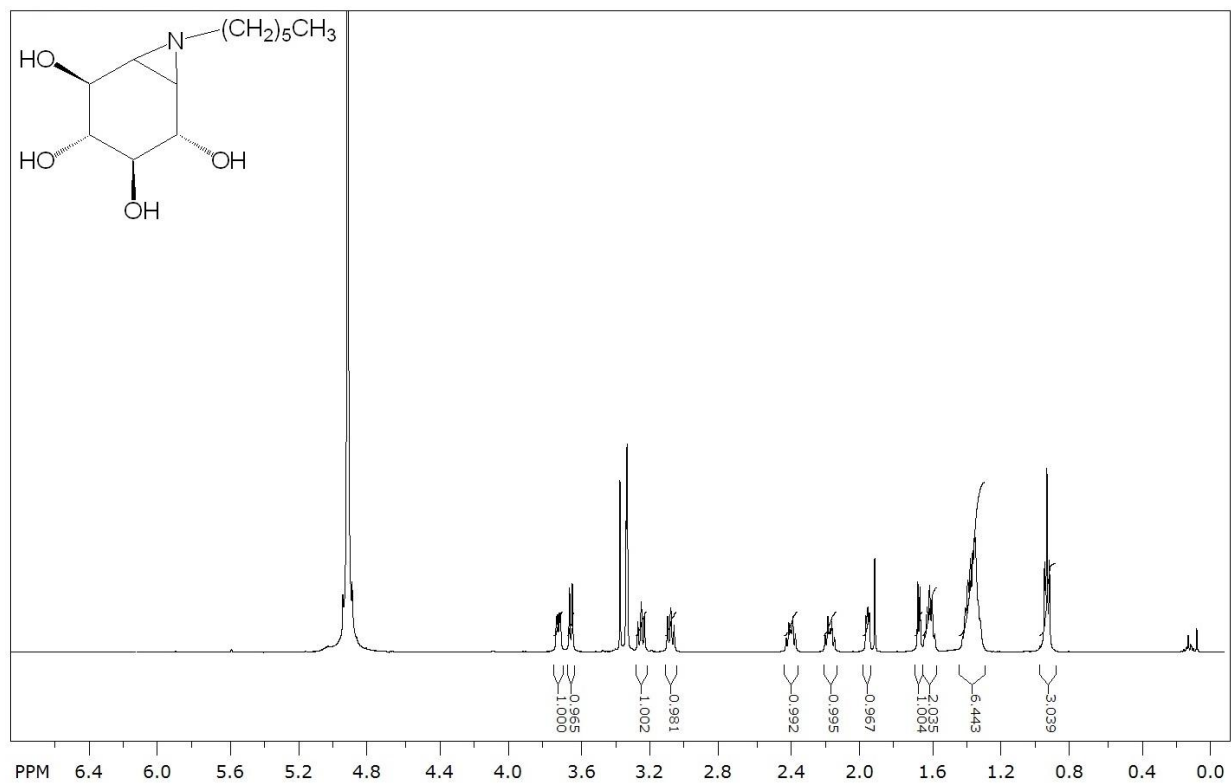
### <sup>1</sup>H NMR Spectrum (500 MHz, CD<sub>3</sub>OD) of 3.39



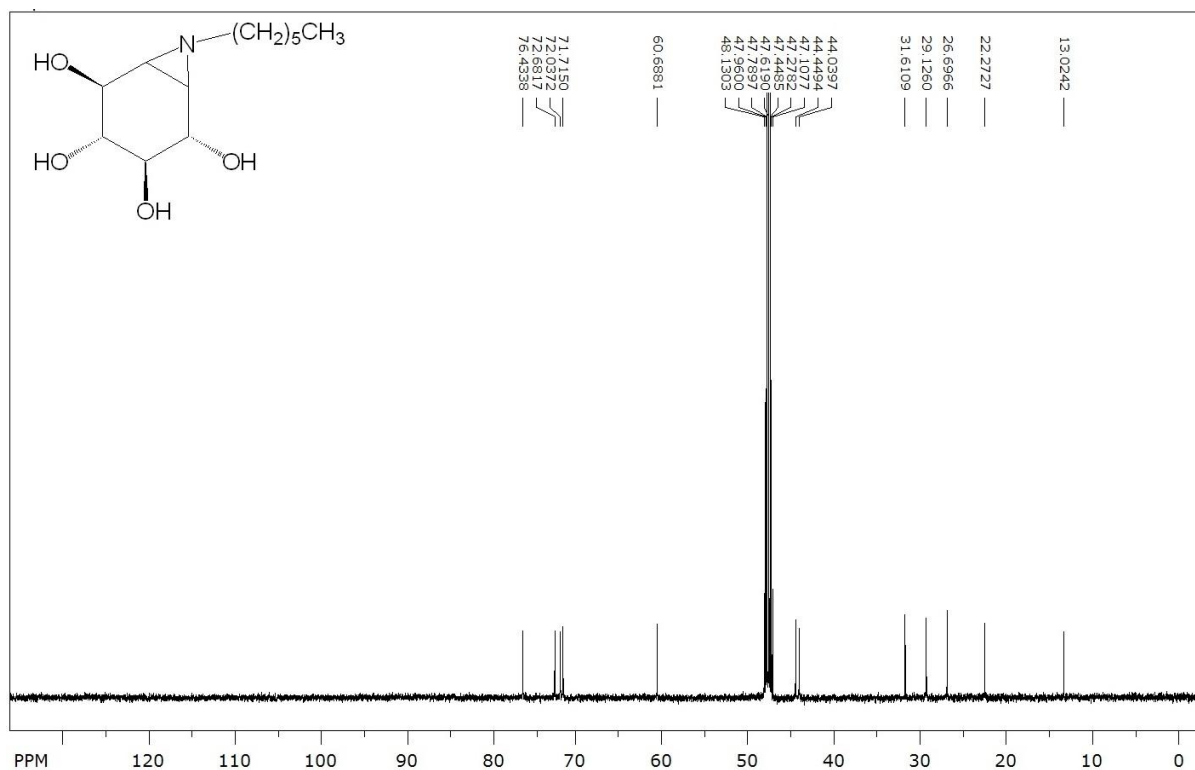
### <sup>13</sup>C NMR Spectrum (500 MHz, CD<sub>3</sub>OD) of 3.39



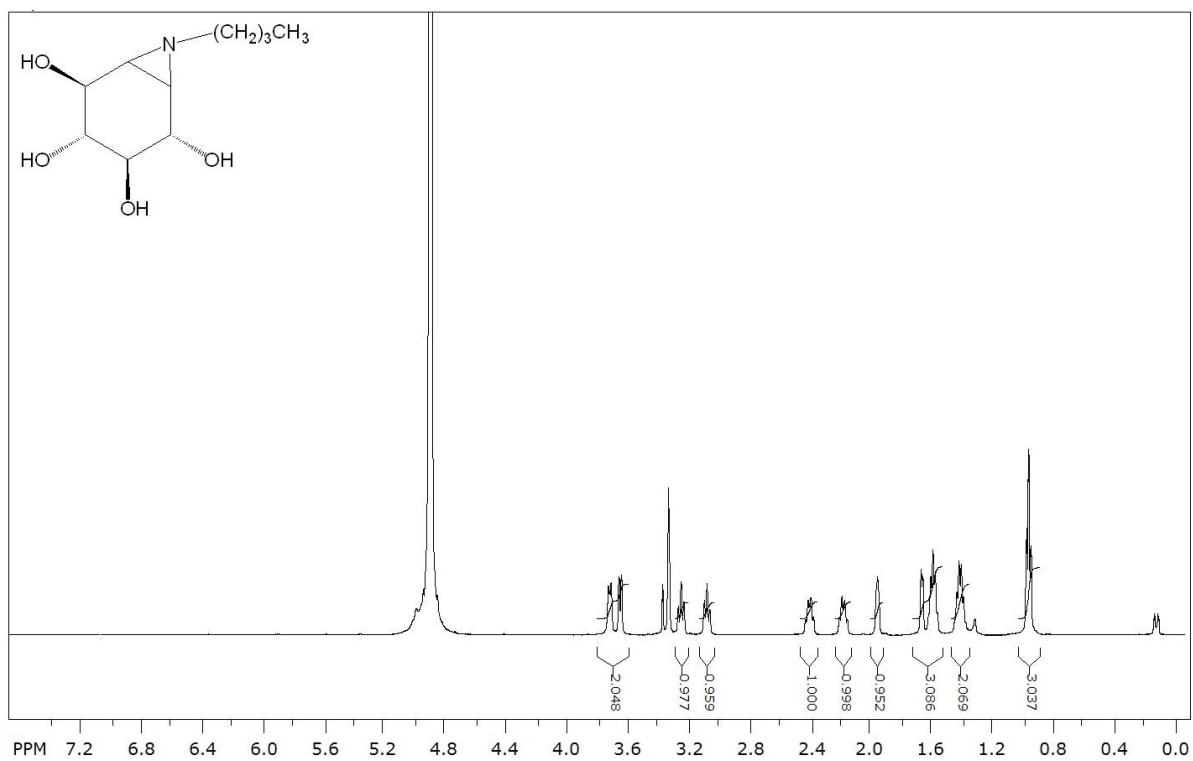
**<sup>1</sup>H NMR Spectrum (500 MHz, CD<sub>3</sub>OD) of 3.40**



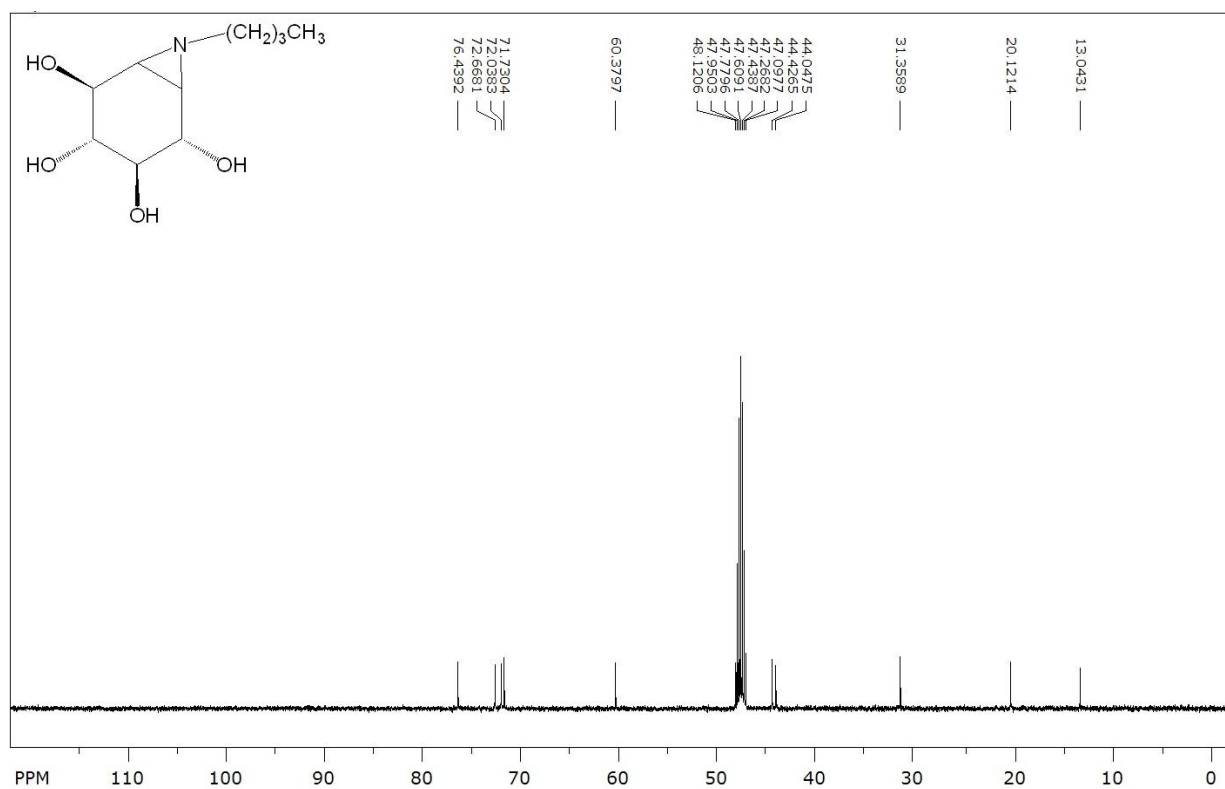
**<sup>13</sup>C NMR Spectrum (500 MHz, CD<sub>3</sub>OD) of 3.40**



### <sup>1</sup>H NMR Spectrum (500 MHz, CD<sub>3</sub>OD) of 3.41



### <sup>13</sup>C NMR Spectrum (500 MHz, CD<sub>3</sub>OD) of 3.41



## References

1. (a) McDonald, A. G.; Boyce, S.; Moss, G. P.; Dixon, H. B. F.; Tipton, K. F., ExplorEnz: a MySQL database of the IUBMB enzyme nomenclature. *BMC biochemistry* 2007, *8*; (b) McDonald, A. G.; Boyce, S.; Tipton, K. F., ExplorEnz: the primary source of the IUBMB enzyme list. *Nucleic Acids Research* 2009, *37*, D593-D597.
2. Cantarel, B. L.; Coutinho, P. M.; Rancurel, C.; Bernard, T.; Lombard, V.; Henrissat, B., The Carbohydrate-Active EnZymes database (CAZy): an expert resource for Glycogenomics. *Nucleic Acids Research* 2009, *37*, D233-D238.
3. Davies, G.; Henrissat, B., STRUCTURES AND MECHANISMS OF GLYCOSYL HYDROLASES. *Structure* 1995, *3* (9), 853-859.
4. (a) Wolfenden, R.; Lu, X. D.; Young, G., Spontaneous hydrolysis of glycosides. *Journal of the American Chemical Society* 1998, *120* (27), 6814-6815; (b) Zechel, D. L.; Withers, S. G., Glycosidase mechanisms: Anatomy of a finely tuned catalyst. *Accounts of Chemical Research* 2000, *33* (1), 11-18.
5. Vuong, T. V.; Wilson, D. B., Glycoside Hydrolases: Catalytic Base/Nucleophile Diversity. *Biotechnology and Bioengineering* 2010, *107* (2), 195-205.
6. Koshland, D. E., STEREOCHEMISTRY AND THE MECHANISM OF ENZYMATIC REACTIONS. *Biological Reviews* 1953, *28* (4), 416-436.
7. Phillips, D. C., THE HEN EGG-WHITE LYSOZYME MOLECULE. *Proceedings of the National Academy of Sciences* 1967, *57* (3), 483-495.
8. Sinnott, M. L., CATALYTIC MECHANISMS OF ENZYMATIC GLYCOSYL TRANSFER. *Chemical Reviews* 1990, *90* (7), 1171-1202.
9. Vocadlo, D. J.; Davies, G. J.; Laine, R.; Withers, S. G., Catalysis by hen egg-white lysozyme proceeds via a covalent intermediate. *Nature* 2001, *412* (6849), 835-838.
10. Withers, S. G.; Rupitz, K.; Street, I. P., 2-DEOXY-2-FLUORO-D-GLYCOSYL FLUORIDES - A NEW CLASS OF SPECIFIC MECHANISM-BASED GLYCOSIDASE INHIBITORS. *Journal of Biological Chemistry* 1988, *263* (17), 7929-7932.
11. (a) Asano, N.; Nash, R. J.; Molyneux, R. J.; Fleet, G. W. J., Sugar-mimic glycosidase inhibitors: natural occurrence, biological activity and prospects for therapeutic application. *Tetrahedron-Asymmetry* 2000, *11* (8), 1645-1680; (b) Lillelund, V. H.; Jensen, H. H.; Liang, X. F.; Bols, M., Recent developments of transition-state analogue glycosidase inhibitors of non-natural product origin. *Chemical Reviews* 2002, *102* (2), 515-553; (c) Gloster, T. M.; Davies, G. J., Glycosidase inhibition: assessing mimicry of the transition state. *Organic & Biomolecular Chemistry* 2010, *8* (2), 305-320.
12. Asano, N., Glycosidase inhibitors: update and perspectives on practical use. *Glycobiology* 2003, *13* (10), 93R-104R.

13. (a) Meany, D.; Chan, D., Aberrant glycosylation associated with enzymes as cancer biomarkers. *Clinical Proteomics* 2011, 8 (1), 7; (b) Bernacki, R. J.; Niedbala, M. J.; Korytnyk, W., GLYCOSIDASES IN CANCER AND INVASION. *Cancer and Metastasis Reviews* 1985, 4 (1), 81-101.
14. (a) Beck, M., New therapeutic options for lysosomal storage disorders: enzyme replacement, small molecules and gene therapy. *Human Genetics* 2007, 121 (1), 1-22; (b) Desnick, R. J., Enzyme replacement and enhancement therapies for lysosomal diseases. *Journal of Inherited Metabolic Disease* 2004, 27 (3), 385-410; (c) Parenti, G., Treating lysosomal storage diseases with pharmacological chaperones: from concept to clinics. *Embo Molecular Medicine* 2009, 1 (5), 268-279.
15. Gieselmann, V., LYSOSOMAL STORAGE DISEASES. *Biochimica Et Biophysica Acta-Molecular Basis of Disease* 1995, 1270 (2-3), 103-136.
16. Moser, H. W., *Basic Neurochemistry, Molecular, Cellular and Medical Aspects: Lysosomal and Peroxisomal Diseases*. 7 ed.; Elsevier Academic Press: 2006.
17. Butters, T. D.; Dwek, R. A.; Platt, F. M., Inhibition of glycosphingolipid biosynthesis: Application to lysosomal storage disorders. *Chemical Reviews* 2000, 100 (12), 4683-+.
18. Futerman, A. H.; van Meer, G., The cell biology of lysosomal storage disorders. *Nature Reviews Molecular Cell Biology* 2004, 5 (7), 554-565.
19. Fan, J. Q., A contradictory treatment for lysosomal storage disorders: inhibitors enhance mutant enzyme activity. *Trends in Pharmacological Sciences* 2003, 24 (7), 355-360.
20. van Gelder, C. M.; Vollebregt, A. A. M.; Plug, I.; van der Ploeg, A. T.; Reuser, A. J. J., Treatment options for lysosomal storage disorders: developing insights. *Expert Opinion on Pharmacotherapy* 2012, 13 (16), 2281-2299.
21. Sawkar, A. R.; Adamski-Werner, S. L.; Cheng, W. C.; Wong, C. H.; Beutler, E.; Zimmer, K. P.; Kelly, J. W., Gaucher disease-associated glucocerebrosidases show mutation-dependent chemical chaperoning profiles. *Chemistry & Biology* 2005, 12 (11), 1235-1244.
22. Hruska, K. S.; LaMarca, M. E.; Scott, C. R.; Sidransky, E., Gaucher disease: Mutation and polymorphism spectrum in the glucocerebrosidase gene (GBA). *Human Mutation* 2008, 29 (5), 567-583.
23. Grabowski, G. A., Lysosomal storage disease 1 - Phenotype, diagnosis, and treatment of Gaucher's disease. *Lancet* 2008, 372 (9645), 1263-1271.
24. Meikle, P. J.; Hopwood, J. J.; Clague, A. E.; Carey, W. F., Prevalence of lysosomal storage disorders. *Jama-Journal of the American Medical Association* 1999, 281 (3), 249-254.
25. Boot, R. G.; Verhoek, M.; Donker-Koopman, W.; Strijland, A.; van Marle, J.; Overkleeft, H. S.; Wennekes, T.; Aerts, J., Identification of the non-lysosomal glucosylceramidase as beta-glucosidase 2. *Journal of Biological Chemistry* 2007, 282 (2), 1305-1312.

26. Liou, B.; Kazimierczuk, A.; Zhang, M.; Scott, C. R.; Hegde, R. S.; Grabowski, G. A., Analyses of variant acid beta-glucosidases - Effects of Gaucher disease mutations. *Journal of Biological Chemistry* 2006, *281* (7), 4242-4253.
27. Alattia, J. R.; Shaw, J. E.; Yip, C. M.; Prive, G. G., Molecular imaging of membrane interfaces reveals mode of beta-glucosidase activation by saposin C. *Proceedings of the National Academy of Sciences of the United States of America* 2007, *104* (44), 17394-17399.
28. Beutler, E.; Beutler, L.; West, C., Mutations in the gene encoding cytosolic beta-glucosidase in Gaucher disease. *Journal of Laboratory and Clinical Medicine* 2004, *144* (2), 65-68.
29. (a) Hayashi, Y.; Okino, N.; Kakuta, Y.; Shikanai, T.; Tani, M.; Narimatsu, H.; Ito, M., Klotho-related protein is a novel cytosolic neutral beta-glycosylceramidase. *Journal of Biological Chemistry* 2007, *282* (42), 30889-30900; (b) Daniels, L. B.; Coyle, P. J.; Chiao, Y. B.; Glew, R. H.; Labow, R. S., PURIFICATION AND CHARACTERIZATION OF A CYTOSOLIC BROAD SPECIFICITY BETA-GLUCOSIDASE FROM HUMAN-LIVER. *Journal of Biological Chemistry* 1981, *256* (24), 3004-3013; (c) Dekker, N.; Voorn-Brouwer, T.; Verhoek, M.; Wennekes, T.; Narayan, R. S.; Speijer, D.; Hollak, C. E. M.; Overkleeft, H. S.; Boot, R. G.; Aerts, J., The cytosolic beta-glucosidase GBA3 does not influence type 1 Gaucher disease manifestation. *Blood Cells Molecules and Diseases* 2011, *46* (1), 19-26.
30. Deegan, P. B.; Cox, T. M., Imiglucerase in the treatment of Gaucher disease: a history and perspective. *Drug Design Development and Therapy* 2012, *6*.
31. (a) Delgado, A.; Casas, J.; Llebaria, A.; Abad, J. L.; Fabrias, G., Inhibitors of sphingolipid metabolism enzymes. *Biochimica Et Biophysica Acta-Biomembranes* 2006, *1758* (12), 1957-1977; (b) Lieberman, R. L.; D'Aquino, J. A.; Ringe, D.; Petsko, G. A., Effects of pH and Iminosugar Pharmacological Chaperones on Lysosomal Glycosidase Structure and Stability. *Biochemistry* 2009, *48* (22), 4816-4827.
32. (a) Egado-Gabas, M.; Serrano, P.; Casas, J.; Llebaria, A.; Delgado, A., New aminocyclitols as modulators of glucosylceramide metabolism. *Organic & Biomolecular Chemistry* 2005, *3* (7), 1195-1201; (b) Egado-Gabas, M.; Canals, D.; Casas, J.; Llebaria, A.; Delgado, A., Aminocyclitols as pharmacological chaperones for glucocerebrosidase, a defective enzyme in Gaucher disease. *Chemmedchem* 2007, *2* (7), 992-994; (c) Diaz, L.; Casas, J.; Bujons, J.; Llebaria, A.; Delgado, A., New Glucocerebrosidase Inhibitors by Exploration of Chemical Diversity of N-Substituted Aminocyclitols Using Click Chemistry and in Situ Screening. *Journal of Medicinal Chemistry* 2011, *54* (7), 2069-2079; (d) Trapero, A.; Gonzalez-Bulnes, P.; Butters, T. D.; Llebaria, A., Potent Aminocyclitol Glucocerebrosidase Inhibitors are Subnanomolar Pharmacological Chaperones for Treating Gaucher Disease. *Journal of Medicinal Chemistry* 2012, *55* (9), 4479-4488.
33. Jespersen, T. M.; Bols, M.; Sierks, M. R.; Skrydstrup, T., SYNTHESIS OF ISOFAGOMINE, A NOVEL GLYCOSIDASE INHIBITOR. *Tetrahedron* 1994, *50* (47), 13449-13460.
34. Dong, W. L.; Jespersen, T.; Bols, M.; Skrydstrup, T.; Sierks, M. R., Evaluation of isofagomine and its derivatives as potent glycosidase inhibitors. *Biochemistry* 1996, *35* (8), 2788-2795.

35. (a) Walker, M. S.; Walker, J. B., Enzymic studies on the biosynthesis of streptomycin. Transamidation of inosamine and streptamine derivatives. *The Journal of biological chemistry* 1966, 241 (6); (b) DeJongh, D. C.; Hribar, J. D.; Hanessian, S.; Woo, P. W., Mass spectrometric studies on aminocyclitol antibiotics. *Journal of the American Chemical Society* 1967, 89 (13); (c) Rinehart, K. L., Jr., Comparative chemistry of the aminoglycoside and aminocyclitol antibiotics. *The Journal of infectious diseases* 1969, 119 (4).
36. Horii, S.; Fukase, H.; Matsuo, T.; Kameda, Y.; Asano, N.; Matsui, K., SYNTHESIS AND ALPHA-D-GLUCOSIDASE INHIBITORY ACTIVITY OF N-SUBSTITUTED VALIOLAMINE DERIVATIVES AS POTENTIAL ORAL ANTIDIABETIC AGENTS. *Journal of Medicinal Chemistry* 1986, 29 (6), 1038-1046.
37. Ogawa, S.; Washida, K., Synthesis and glycosidase inhibitory activity of five stereoisomers of 5-amino-5-C-methyl-1,2,3,4-cyclopentanetetrol. *European Journal of Organic Chemistry* 1998, (9), 1929-1934.
38. Rodriguez-Perez, T.; Lavandera, I.; Fernandez, S.; Sanghvi, Y. S.; Ferrero, M.; Gotor, V., Novel and efficient chemoenzymatic synthesis of D-glucose 6-phosphate and molecular modeling studies on the selective biocatalysis. *European Journal of Organic Chemistry* 2007, (17), 2769-2778.
39. Ekholm, F. S.; Polakova, M.; Pawlowicz, A. J.; Leino, R., Synthesis of Divalent 2,2'-Linked Mannose Derivatives by Homodimerization. *Synthesis-Stuttgart* 2009, (4), 567-576.
40. Damager, I.; Numao, S.; Chen, H. M.; Brayer, G. D.; Withers, S. G., Synthesis and characterisation of novel chromogenic substrates for human pancreatic alpha-amylase. *Carbohydrate Research* 2004, 339 (10), 1727-1737.
41. Morris, W. J.; Shair, M. D., Stereoselective Synthesis of 2-Deoxy-beta-glycosides Using Anomeric O-Alkylation/Arylation. *Organic Letters* 2009, 11 (1), 9-12.
42. Desai, T.; Gigg, J.; Gigg, R.; Martinzamora, E.; Schnetz, N., THE SYNTHESIS AND RESOLUTION OF (+/-)-1,4-DI-O-BENZYL-2,3-O-ISOPROPYLIDENE-MYO-INOSITOL. *Carbohydrate Research* 1994, 258, 135-144.
43. Martin, S. F.; Josey, J. A.; Wong, Y. L.; Dean, D. W., GENERAL-METHOD FOR THE SYNTHESIS OF PHOSPHOLIPID DERIVATIVES OF 1,2-O-DIACYL-SN-GLYCEROLS. *Journal of Organic Chemistry* 1994, 59 (17), 4805-4820.
44. Crombez-Robert, C.; Benazza, M.; Frechou, C.; Demailly, G., Tin-mediated regioselective etherification and esterification of unprotected xylitol. *Carbohydrate Research* 1998, 307 (3-4), 355-359.
45. Rudolf, M. T.; Dinkel, C.; Traynor-Kaplan, A. E.; Schultz, C., Antagonists of myo-inositol 3,4,5,6-tetrakisphosphate allow repeated epithelial chloride secretion. *Bioorganic & Medicinal Chemistry* 2003, 11 (15), 3315-3329.

46. Danishefsky, S.; Hungate, R., TOTAL SYNTHESIS OF OCTOSYL ACID-A - A NEW DEPARTURE IN ORGANOSTANNYLENE CHEMISTRY. *Journal of the American Chemical Society* 1986, *108* (9), 2486-2487.
47. Nagashima, N.; Ohno, M., SELECTIVE MONOALKYLATION OF ACYCLIC DIOLS BY MEANS OF DIBUTYLTIN OXIDE AND FLUORIDE SALTS. *Chemical & Pharmaceutical Bulletin* 1991, *39* (8), 1972-1982.
48. Zhou, Y. X.; Li, J. Y.; Zhan, Y. J.; Pei, Z. C.; Dong, H., Halide promoted organotin-mediated carbohydrate benzylation: mechanism and application. *Tetrahedron* 2013, *69* (13), 2693-2700.
49. Brown, C. J.; Kirby, A. J., Efficiency of proton transfer catalysis. Intramolecular general acid catalysis of the hydrolysis of dialkyl acetals of benzaldehyde. *Journal of the Chemical Society-Perkin Transactions 2* 1997, (6), 1081-1093.
50. AbdelMagid, A. F.; Carson, K. G.; Harris, B. D.; Maryanoff, C. A.; Shah, R. D., Reductive amination of aldehydes and ketones with sodium triacetoxyborohydride. Studies on direct and indirect reductive amination procedures. *Journal of Organic Chemistry* 1996, *61* (11), 3849-3862.
51. Surfraz, M. B. U.; Akhtar, M.; Allemann, R. K., Bis-benzyl protected 6-amino cyclitols are poisonous to Pd/C catalysed hydrogenolysis of benzyl ethers. *Tetrahedron Letters* 2004, *45* (6), 1223-1226.
52. Schoffers, E.; Gurung, S. R.; Kohler, P. R. A.; Rossbach, S., Chemical synthesis of scyllo-inosamine and catabolism studies in *Sinorhizobium meliloti*. *Bioorganic & Medicinal Chemistry* 2008, *16* (16), 7838-7842.
53. Lee, H.; Lee, J. W.; Kim, D. Y.; Park, J.; Seo, Y. T.; Zeng, H.; Moudrakovski, I. L.; Ratcliffe, C. I.; Ripmeester, J. A., Tuning clathrate hydrates for hydrogen storage. *Nature* 2005, *434* (7034), 743-746.
54. Trapero, A.; Llebaria, A., The myo-1,2-Diaminocyclitol Scaffold Defines Potent Glucocerebrosidase Activators and Promising Pharmacological Chaperones for Gaucher Disease. *Acs Medicinal Chemistry Letters* 2011, *2* (8), 614-619.
55. (a) Wang, Q.; Trimbur, D.; Graham, R.; Warren, R. A. J.; Withers, S. G., IDENTIFICATION OF THE ACID/BASE CATALYST IN AGROBACTERIUM-FAECALIS BETA-GLUCOSIDASE BY KINETIC-ANALYSIS OF MUTANTS. *Biochemistry* 1995, *34* (44), 14554-14562; (b) Kempton, J. B.; Withers, S. G., MECHANISM OF AGROBACTERIUM BETA-GLUCOSIDASE - KINETIC-STUDIES. *Biochemistry* 1992, *31* (41), 9961-9969; (c) Withers, S. G.; Rupitz, K.; Trimbur, D.; Warren, R. A. J., MECHANISTIC CONSEQUENCES OF MUTATION OF THE ACTIVE-SITE NUCLEOPHILE GLU-358 IN AGROBACTERIUM BETA-GLUCOSIDASE. *Biochemistry* 1992, *31* (41), 9979-9985.
56. Rempel, B. P. Synthesis and Enzymatic Evaluation of Activated Fluorosugars as Inactivators of Lysosomal Enzymes. University of British Columbia, Vancouver, 2009.
57. Cornish-Bowden, A., *Fundamentals of Enzyme Kinetics*. Third ed.; Portland Press Ltd.: London UK, 2004.

58. Harvey Motulsky, A. C., *Fitting Models to Biological Data Using Linear and Nonlinear Regression: A Practical Guide to Curve Fitting*. Oxford University Press, Inc.: 198 Madison Avenue, New York, New York, 2004.
59. Haefner, J. W., *Modeling Biological Systems: Principles and Applications*. 2nd ed.; Springer Science+Business Media, Inc.: 233 Spring Street, New York, New York, 2005.
60. Ludewig, S.; Kossner, M.; Schiller, M.; Baumann, K.; Schirmeister, T., Enzyme Kinetics and Hit Validation in Fluorimetric Protease Assays. *Current Topics in Medicinal Chemistry* 2010, 10 (3), 368-382.
61. Rempel, B. P.; Withers, S. G., Covalent inhibitors of glycosidases and their applications in biochemistry and biology. *Glycobiology* 2008, 18 (8), 570-586.
62. Miao, S. C.; McCarter, J. D.; Grace, M. E.; Grabowski, G. A.; Aebersold, R.; Withers, S. G., IDENTIFICATION OF GLU(340) AS THE ACTIVE-SITE NUCLEOPHILE IN HUMAN GLUCOCEREBROSIDASE BY USE OF ELECTROSPRAY TANDEM MASS-SPECTROMETRY. *Journal of Biological Chemistry* 1994, 269 (15), 10975-10978.
63. Phenix, C. P.; Rempel, B. P.; Colobong, K.; Doudet, D. J.; Adam, M. J.; Clarke, L. A.; Withers, S. G., Imaging of enzyme replacement therapy using PET. *Proceedings of the National Academy of Sciences* 2010, 107 (24), 10842-10847.
64. Witte, M. D.; van der Marel, G. A.; Aerts, J.; Overkleeft, H. S., Irreversible inhibitors and activity-based probes as research tools in chemical glycobiology. *Organic & Biomolecular Chemistry* 2011, 9 (17), 5908-5926.
65. Caron, G. Synthesis of Cyclitol-based Glucoside Inhibitors. University of British Columbia, 1988.
66. Furmeier, S.; Metzger, J. O., Fat-derived aziridines and their N-substituted derivatives: Biologically active compounds based on renewable raw materials. *European Journal of Organic Chemistry* 2003, (4), 649-659.
67. Caron, G.; Withers, S. G., CONDURITOL AZIRIDINE - A NEW MECHANISM-BASED GLUCOSIDASE INACTIVATOR. *Biochemical and Biophysical Research Communications* 1989, 163 (1), 495-499.
68. Hackl, K. A.; Falk, H., THE SYNTHESIS OF N-SUBSTITUTED UREAS .1. THE N-ALKYLATION OF UREAS. *Monatshefte Fur Chemie* 1992, 123 (6-7), 599-606.
69. Padwa, A., 1.01 - Aziridines and Azirines: Monocyclic. In *Comprehensive Heterocyclic Chemistry III*, Editors-in-Chief: Alan, R. K.; Christopher, A. R.; Eric, F. V. S.; Richard, J. K. T., Eds. Elsevier: Oxford, 2008; pp 1-104.
70. Roll, M.; Shtelzer, S.; Stark, A. A.; Blum, J., STRUCTURE-ACTIVITY-RELATIONSHIPS IN MUTAGENICITY AND IN NUCLEOPHILIC RING-OPENING OF N-(ARYLMETHYL)PHENANTHRENE 9,10-IMINES. *Mutagenesis* 1990, 5 (1), 25-30.

71. Fusco, R.; Garanti, L.; Zecchi, G., INTRAMOLECULAR 1,3-DIPOLAR CYCLOADDITIONS OF ARYL AZIDES BEARING ALKENYL, ALKYNYL, AND NITRILE GROUPS. *Journal of Organic Chemistry* 1975, 40 (13), 1906-1909.
72. Dye, J. L.; Cram, K. D.; Urbin, S. A.; Redko, M. Y.; Jackson, J. E.; Lefenfeld, M., Alkali metals plus silica gel: Powerful reducing agents and convenient hydrogen sources. *Journal of the American Chemical Society* 2005, 127 (26), 9338-9339.
73. Nandi, P.; Dye, J. L.; Jackson, J. E., Birch Reductions at Room Temperature with Alkali Metals in Silica Gel (Na<sub>2</sub>K-SG(I)). *Journal of Organic Chemistry* 2009, 74 (16), 5790-5792.
74. Goddard-Borger, E. D.; Tropak, M. B.; Yonekawa, S.; Tysoe, C.; Mahuran, D. J.; Withers, S. G., Rapid Assembly of a Library of Lipophilic Iminosugars via the Thiol-Ene Reaction Yields Promising Pharmacological Chaperones for the Treatment of Gaucher Disease. *Journal of Medicinal Chemistry* 2012, 55 (6), 2737-2745.
75. Rempel, B. P.; Tropak, M. B.; Mahuran, D. J.; Withers, S. G., Tailoring the Specificity and Reactivity of a Mechanism-Based Inactivator of Glucocerebrosidase for Potential Therapeutic Applications. *Angewandte Chemie-International Edition* 2011, 50 (44), 10381-10383.
76. Tatsuta, K., Total synthesis and chemical design of useful glycosidase inhibitors. *Pure and Applied Chemistry* 1996, 68 (6), 1341-1346.
77. Kallemeijn, W. W.; Li, K. Y.; Witte, M. D.; Marques, A. R. A.; Aten, J.; Scheij, S.; Jiang, J. B.; Willems, L. I.; Voorn-Brouwer, T. M.; van Roomen, C.; Ottenhoff, R.; Boot, R. G.; van den Elst, H.; Walvoort, M. T. C.; Florea, B. I.; Codee, J. D. C.; van der Marel, G. A.; Aerts, J.; Overkleeft, H. S., Novel Activity-Based Probes for Broad-Spectrum Profiling of Retaining beta-Exoglucosidases In Situ and In Vivo. *Angewandte Chemie-International Edition* 2012, 51 (50), 12529-12533.
78. Peters, S. P.; Coyle, P.; Glew, R. H., DIFFERENTIATION OF BETA-GLUCOCEREBROSIDASE FROM BETA-GLUCOSIDASE IN HUMAN TISSUES USING SODIUM TAUROCHOLATE. *Archives of Biochemistry and Biophysics* 1976, 175 (2), 569-582.
79. (a) Briggs GE, H. J., A Note on the Kinetics of Enzyme Action. *Biochemical Journal* 1925, 19 (2), 338-339; (b) Michaelis L, M. M., Die Kinetik der Invertinwirkung. *Biochemische Zeitschrift* 1913, 49, 333-369; (c) Johnson, K. A.; Goody, R. S., The Original Michaelis Constant: Translation of the 1913 Michaelis-Menten Paper. *Biochemistry* 2011, 50 (39), 8264-8269.

## Chapter 8: Appendix

### 8.1 Equations for Fundamental Enzyme Kinetics

#### 8.1.1 Michaelis-Menten Kinetics

The current form of enzyme kinetics was proposed by Leonor Michaelis and Maud Leonora Menten in 1913 and refined by George Briggs and John Burdon Sanderson Haldane in 1925.<sup>79</sup> The final Michaelis-Menton (M-M) equation relies on a number of assumptions to allow for its derivation and they are as follows:

A1) In the initial stages of the reaction  $[P] \approx 0$ .

A2) Throughout the reaction, ES is in a steady state therefore  $[ES]$  is constant

A3) The enzyme only exists as  $[E]$  and  $[ES]$  with no  $[EP]$ .

A4) The catalytic step (formation of  $E + P$ ) is slower than the binding step (ES formation) and dissociation step (ES into  $E + S$ )

A5)  $[S] \gg [E]_0$  so that S forming ES is negligible and  $[S]$  remains constant throughout the reaction

Free enzyme (E) combines with free substrate (S) to form an enzyme-substrate complex (ES) that reacts to produce free enzyme and free product (P). All steps are in equilibrium with rate constants  $k_1$  and  $k_{-1}$  for the formation of ES and  $k_2$  and  $k_{-2}$  for the formation of product shown in the scheme below.



If we use the first assumption (A1) that  $[P]$  is very small like in the initial stages of the reaction where velocity is measured then the reverse rate  $k_{-2}$  is minimal thus the scheme becomes:



Under the assumption of steady state conditions (A2) where [ES] remains constant we have:

$$\frac{\partial[ES]}{\partial t} = k_1[E][S] - k_{-1}[ES] - k_2[ES] = 0 \quad (1)$$

Following assumption (A3), the total concentration of enzyme present in the reaction  $[E]_0$  is the sum of [E] and [ES]:

$$[E]_0 = [E] + [ES] \quad (2)$$

Substituting (2) into (1) and solving for [ES] we get:

$$[ES] = \frac{([E]_0[S])}{\left([S] + \frac{k_{-1} + k_2}{k_1}\right)} \quad (3)$$

If we assume the catalysis is rate limiting (A4) so that  $k_2 < k_{-1}$  and  $k_1$  then:

$$V_0 = k_2[ES] \quad (4)$$

We can then express  $V_0$  with measurable values by substituting (3) into (4):

$$V_0 = k_2[ES] = \frac{k_2([E]_0[S])}{\left([S] + \frac{k_{-1} + k_2}{k_1}\right)} \quad (5)$$

The rate constants  $(k_{-1} + k_2)/k_1$  can be grouped into a single term  $K_m$  known as the Michaelis constant.

Additionally, if  $[S] \gg K_m$  then enzyme bound with substrate approaches total enzyme or  $[E]_0 \approx ES$ , which corresponds with the maximal velocity ( $V_{max}$ ) using equation (4). Substituting these into (5) we derive the Michaelis-Menten equation:

$$V_0 = \frac{V_{max}[S]}{[S] + K_m} \quad (6)$$

When  $[S] = K_m$ , then:

$$V_0 = \frac{V_{max}[S]}{2[S]} = \frac{V_{max}}{2}$$

Therefore we can determine  $V_{max}$  and  $K_m$  from a single M-M plot of velocity versus time. An example of the M-M plot is shown in **Figure A1** below.

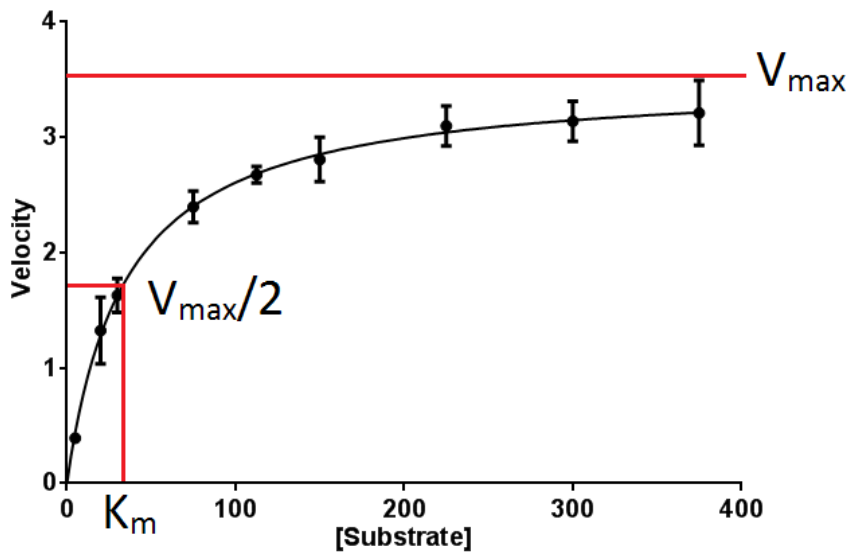


**Figure A1:** A general plot displaying M-M enzyme kinetics

### 8.1.2 Enzyme Kinetics with a Reversible Inhibitor

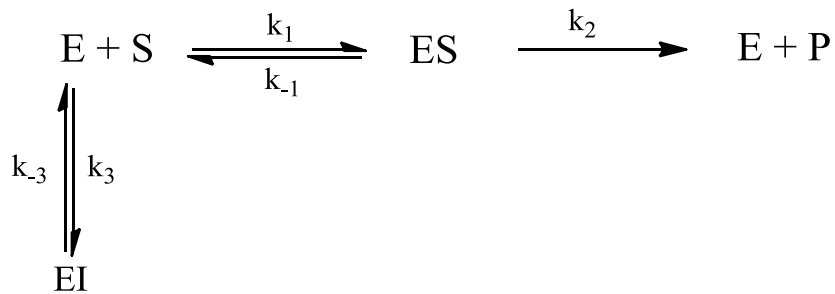
Michaelis-menten kinetics can be applied to the enzyme kinetics in the presence of a competitive inhibitor. The same assumptions apply but with the additions of:

A3\*) The enzyme only exists as  $[E]$ ,  $[ES]$ , and  $[EI]^*$  with no  $[EP]$ .

A6) Throughout the reaction  $EI$  is in a steady state therefore  $[EI]$  is constant

A7)  $[I] \gg [E]_0$  so that  $I$  forming  $EI$  is negligible and  $[I]$  remains constant throughout the reaction

Like with regular M-M kinetics, free enzyme (E) combines with free substrate (S) to form an enzyme-substrate complex (ES) that reacts to produce free enzyme and free product (P), but there is also free enzyme that combines with inhibitor (I) to form an enzyme-inhibitor complex (EI). All steps are in equilibrium with rate constants  $k_1$  and  $k_{-1}$  for the formation of ES and  $k_2$  and  $k_{-2}$  for the formation of product and  $k_3$  and  $k_{-3}$  for the formation of EI shown in the scheme below.



If we follow assumptions A2 and A6 where ES and EI are in steady state then:

$$\frac{\partial[ES]}{\partial t} = k_1[E][S] - k_{-1}[ES] - k_2[ES] = 0 \quad (1)$$

$$\frac{\partial[EI]}{\partial t} = k_3[E][I] - k_{-3}[EI] = 0 \quad (7)$$

Rearranging (1) to define [E] gives:

$$[E] = \frac{(k_{-1}+k_2)[ES]}{k_1[S]} = \frac{K_m[ES]}{[S]} \quad (8)$$

Substituting (8) into (7) and rearranging to define [EI] and simplifying  $k_3/k_{-3} = K_i$  gives:

$$\frac{\partial[EI]}{\partial t} = k_3 K_m [ES][I]/[S] - k_{-3}[EI] = 0$$

$$[EI] = \frac{k_3 K_m [ES][I]}{[S]k_{-3}} = \frac{K_i K_m [ES][I]}{[S]} \quad (9)$$

Following assumption A3\* total enzyme concentration is:

$$[E]_0 = [E] + [ES] + [EI] \quad (10)$$

Substituting (9) and (8) into (10):

$$E_0 = \frac{K_m [ES]}{[S]} + [ES] + \frac{K_m [I][ES]}{K_i [S]} = [ES] \left( \frac{K_m}{[S]} + 1 + \frac{K_m [I]}{K_i [S]} \right) \quad (11)$$

Solving for [ES] gives:

$$[ES] = \frac{[E]_0 [S]}{[S] + K_m \left( 1 + \frac{[I]}{K_i} \right)} \quad (12)$$

Substituting (12) into (4) gives us the velocity:

$$V_0 = k_2 [ES] = \frac{k_2 [E]_0 [S]}{[S] + K_m \left( 1 + \frac{[I]}{K_i} \right)} \quad (12)$$

When  $[S] \gg K_m$  then enzyme bound with substrate approaches total enzyme or  $[E]_0 \approx ES$ , which corresponds with the maximal velocity ( $V_{max}$ ) Therefore  $V_{max} = k_2 [E]_0$  and the equation enters its M-M form:

$$V_0 = k_2 [ES] = \frac{V_{Max} [S]}{[S] + K_m \left( 1 + \frac{[I]}{K_i} \right)} \quad (13)$$

### 8.1.3 Enzyme Kinetics with a Mechanism-Based Inactivator

The kinetics of a mechanism-based inhibitor resembles M-M kinetics, retaining the many of the same assumptions. However, instead of the assumptions made with substrate it is with inhibitor. The scheme of an irreversible mechanism-based inhibitor is shown in the scheme below:



Where  $E \cdot I$  is intact inhibitor bound to the enzyme active site but free to dissociate and  $E-I$  is enzyme covalently inactivated by the inhibitor. If we replace  $[S]$  with  $[I]$  and define  $k_i = k_2$  and  $K_i = (k_{-1}/k_1)$  then equation (5) becomes:

$$V_0 = \frac{k_i[E][I]}{[I] + K_i + \left(\frac{K_m k_i}{k_{-1}}\right)} \quad (14)$$

Where we see pseudo first-order kinetics with respect to  $[E]$ .

If we assume  $k_{-1} \gg k_2$  or the rate of dissociation is much faster than the rate of inactivation then:

$$V_0 = \frac{k_i[E][I]}{[I] + K_i} = K_{Obs}[E] \quad (15)$$

Where:

$$K_{Obs} = \frac{k_i[I]}{[I] + K_i} \quad (16)$$

If  $K_i \gg [I]$  which is the case when the inhibitor rapidly inactivates the enzyme at low concentrations then the equation becomes:

$$K_{Obs} = \frac{k_i[I]}{K_i} \quad (17)$$

$K_{\text{obs}}$  is the observed rate constant for the loss of enzyme activity which can be obtained from fitting the enzyme activity to an exponential decay equation.